Mechanisms of Contaminant Migration from Buried Concrete Structures

Danielle Charlotte Tompkins

Submitted in accordance with the requirements for the degree of Doctor of Philosophy

The University of Leeds

School of Earth and Environment

October 2023

The candidate confirms that the work submitted is their own, except where work which has formed part of jointly authored publications has been included. The contribution of the candidate and the other authors to this work has been explicitly indicated below. The candidate confirms that appropriate credit has been given within the thesis where reference has been made to the work of others.

The work in Chapter 4 has been extended from the following publication:

Tompkins, D.C., Stewart, D.I., Graham, J.T. and Burke, I.T. 2022. In situ disposal of crushed concrete waste as void fill material at UK nuclear sites: Leaching behavior and effect of pH on trace element release. *Journal of Hazardous Materials Advances.* **5**, 100043.

The paper had a recent correction (corrigendum) published due to discovering a calculation error. Chapter 4 is not a replication of the manuscript as it contains additional data (in Table 4.1, 4.2 and 4.4 and Figures 4.4, 4.8 and 4.9) and text.

Candidate's contribution – all experimental work, preparing samples for XRD and SEM/EDX analysis, collection and analysis of SEM data, writing the manuscript and producing all figures and tables. Douglas Stewart – provided extensive manuscript review. James Graham – provided comments on the manuscript. Ian Burke - initial concept, assistance with particle size distribution figure (now in Method section 3.1) and provided extensive manuscript review. Magnox – for access to the samples used and site characterisation data.

The work in Chapter 5 of the thesis is being prepared for publication:

Tompkins, D.C., Stewart, D.I., Graham, J.T. and Burke, I.T. Dissolution kinetics of crushed concrete waste: effect of pH on leaching behaviour.

Candidate's contribution – all experimental work, preparing samples for SEM-EDS analysis and BET, collection and analysis of SEM data, writing the manuscript and producing all figures and tables. Douglas Stewart – provided extensive manuscript review. James Graham – provided comments on the manuscript. Ian Burke – initial concept, assistance with figure layout for: leachate chemistry, mass loss/BET and SEM-EDS spot analyses, advice with calculating leaching rates and provided extensive manuscript review. Magnox – for access to the samples used.

Acknowledgements

Thank you to my supervisors Ian Burke, Doug Stewart and James Graham for all your help and encouragement during this time. Thank you for dealing with my many (many) emails and worries. Thank you for your suggestions and advice on how to improve my work throughout these last few years, I have learnt a lot. Thank you to Andy Bray for explaining how to use the flow-through reactors, to Andy Connelly for all your help in the lab when I was first getting started and to Andy Hobson for your help and advice with laboratory life and writing up. Thanks to Fiona Gill for advice on managing PhD life.

A huge thank you to the many technicians who helped me and who without none of this work would have been possible: Stephen Reid with ICP help and answering my many questions, Lesley Neve for X-ray help, Fiona Keay for help with BET, lovely chats and answering my questions about ion chromatography. Thank you to Harry for walking me through the process for preparing samples for SEM analysis, and for the initial assistance with cutting blocks of concrete in my first year – great fun! Thank you to Richard for help with the SEM-EDS.

To those in Cohen Geochem: Josie, you have supported me through the some of the hardest times and provided essential moral support and motivation. Thank you to Emma for your help with my endless questions. Thank you Chiara for all our lovely chats, walks and support. Thanks to Georgia and Alba for our chats too.

To my dear family and friends who have supported me through this journey. Thank you to my Mum, your unwavering support throughout probably the hardest time of my life will forever be appreciated. Dad, I will forever be grateful for your unconditional love and support of whatever I chose to do with my life, as well as all my moans every Sunday. I wish you could have seen me finally finish this. Thank you to all my family for your love and support: Megan, Ann-Marie, Sharni & Kayla. Special thanks to my two dear nans, our regular calls helped keep me sane.

Special thanks to dear friends who have supported me through this journey: Lyd, Matilya, Poppy, Liv, Jahnavi, Jenna. HK.

Thank you to the Language Zone team who have supported me through this last year of juggling writing whilst working, always providing a welcome ear for me to vent – thank you Kate, Carolin, Anna, Sabina, Dwi, Eva and Aminah.

This project was funded by doctoral training award (EP/R513258/1) from the U.K. Engineering and Physical Science Research Council in partnership with National Nuclear Laboratory Ltd. Thank you to Magnox for providing access to the samples and site characterisation data that was used in this thesis.

Copyright permissions

In Chapter 2, the following figures and tables have been used with the following permissions:

Table 2.1 and Figure 2.4: courtesy of Svensk Kärnbränslehantering AB (SKB).

Table 2.2, Table 2.3 and Figure 2.7: Reprinted and adapted with permission from Sustainable Construction Materials, Ravindra K. Dhir, Jorge de Brito, Rui V. Silva, Chao Qun Lye, 13 - Environmental Impact, Case Studies and Standards and Specifications, p495-583., Copyright (2019), with permission from Elsevier.

Figure 2.5: Used with permission of TAYLOR & FRANCIS GROUP LLC from Leaching Processes and Evaluation Tests for Inorganic Constituent Release from Cement-Based Matrices, Andrew C. Garrabrants and David S. Kosson, in Stabilization and Solidification of Hazardous, Radioactive, and Mixed Wastes, 1st Edition, 2004; permission conveyed through Copyright Clearance Center, Inc.

Figure 2.6: Used with permission of TAYLOR & FRANCIS GROUP LLC from Leaching Processes and Evaluation Tests for Inorganic Constituent Release from Cement-Based Matrices, Andrew C. Garrabrants and David S. Kosson, in Stabilization and Solidification of Hazardous, Radioactive, and Mixed Wastes, 1st Edition, 2004; permission conveyed through Copyright Clearance Center, Inc.

Reprinted from Comparison of the characteristic leaching behavior of cements using standard (EN 196-1) cement mortar and an assessment of their long-term environmental behavior in construction products during service life and recycling, 30, H.A van der Sloot, Cement and Concrete Research, 1079-1096, Copyright (2000) with permission from Elsevier.

Abstract

Crushed concrete waste (CCW) will be generated in significant proportions as decommissioning of UK nuclear sites proceeds in the coming decades. An option to deal with this waste is on-site disposal, which avoids the environmental impacts and economic costs associated with off-site disposal to limited landfill capacity. However, there are concerns with the production of high pH leachates and the leaching of trace metal contaminants, which could lead to environmental contamination. This study used concrete that was crushed during demolition without further size reduction for leaching tests (so that element release is not overestimated). The propensity for high pH leachate generation and metal leaching from long-term stockpiled materials (>10 years) has been studied as a function of size fraction (gravel, sand and fines) and weathering in pH-dependent batch experiments, finding that the material at the surface (0-0.1 m) of the stockpiles produces lower pH leachates (pH 8-9.6) than the material from the subsurface (2.5-2.7m; pH 10-11.3), attributed to carbonation and weathering. Leaching between the size fractions was found to be generally similar (except for some scatter from the gravel fraction and higher Cu from surface fines at pH>11) and likely under equilibrium control, however the pH decreased with decreasing size fraction. Element release was generally similar between the surface and subsurface particles; however Cr, V and S release was slightly lower in the surface fractions, a positive effect of weathering during stockpiling. Under far-from-equilibrium conditions, the dissolution kinetics of the sand fraction was low for all elements ($<1 \times 10^{-10}$ mol m^{-2} s^{-1}) across pH 3-13, especially for trace metal contaminants Al, Cr, Pb, V, Mn, As and Cu, some of which were below detection. CCW has a low metal leaching potential under static and flow-through leaching conditions, and the results are relevant to environmental safety assessments for on-site disposal.

Table of Contents

List of Figures

List of Tables

Abbreviations

AA-EQS	Annual Average Environmental Quality Standard
ANC	Acid neutralisation capacity
BET	Brunauer-Emmet-Teller
BSE	Backscattered electron
BSI	British Standards Institute
CCW	Crushed concrete waste
CDW	Construction and Demolition Waste
CEN	European Committee for Standardisation
DEFRA	The Department for Environment, Food and Rural Affairs
DIW	Deionised water
DWS	Drinking water standards
GBq	Giga becquerel
GRR	Guidelines for Regulatory Release
HCl	Hydrochloric acid
HOAc	Acetic acid
IAEA	International Atomic Energy Agency
IARC	International Agency for Research on Cancer
IPCS	International Programme on Chemical Safety
ICP-MS	Inductively Coupled Plasma Optical Emission Mass Spectrometry
ICP-OES	Inductively Coupled Plasma Optical Emission Spectroscopy
L/S	Liquid to solid ratio
LEAF	Leaching Environmental Assessment Framework
LLW	Low Level Waste
LOD	Limit of detection
LOQ	Limit of quantification
MAC-EQS	Maximum allowable concentration-Environmental Quality Standard
MCL	Maximum contaminant level
NDA	Nuclear Decommissioning Authority
PPM/B	Parts per million/billion
RCA	Recycled Concrete Aggregate
RCM	Recycled Concrete Material
RSD	Relative standard deviation
SCM	Supplementary cementitious materials
SD	Standard deviation

SE	Secondary electron
SEM-EDS	Scanning electron microscopy energy dispersive x-ray spectroscopy
US EPA	United States Environmental Protection Agency
VLLW/LLW	Very Low-Level Waste/Low-Level Waste
WRAP	Waste and Resource Action Programme
XRD	X-ray powder Diffraction
XRF	X-ray Fluorescence

Cement chemistry abbreviations

AFm	Calcium monosulpoaluminate
AFt	Calcium trisulphate aluminate (ettringite)
C-(A)-S-H	Calcium aluminate silicate hydrate
C-S-H	Calcium silicate hydrate
C_2S	Belite
C_3A	Aluminate
C_3S	Alite
C_4AF	Ferrite
Cc	Calcium carbonate
CH	Portlandite
Hc/Mc	Hemicarbonate/Monocarbonate
OPC	Ordinary Portland Cement
S-H	Silica gel

Chapter 1 Introduction

1.1 Project context

CCW will be produced in significant volumes as the decommissioning of nuclear sites proceeds in the coming decades (Foy et al., 2019; Nuclear Decommissioning Authority [NDA], 2020; 2022). The majority of this waste will be inactive, uncontaminated or lightly contaminated. The conventional waste disposal option is disposal to landfill which is the least environmentally and economically sustainable approach when managing waste (International Atomic Energy Agency [IAEA], 2008; NDA, 2016; 2020). The nuclear industry is considering alternative waste management approaches such as the on-site disposal of CCW (Foy et al., 2019), in scenarios like those given in the Guidelines for Regulatory Release (GRR) which apply to radioactively contaminated waste (Guidelines for Regulatory Release [GRR], 2018; Foy et al., 2019). On-site disposal involves the burial of CCW in existing subsurface facilities, as void fill in site restoration work (e.g. landscaping) or placing CCW in-situ (Foy et al., 2019; NDA, 2021; Department for Energy Security & Net Zero, 2023a; GRR, 2018). This approach would reduce the negative effects of off-site disposal to already limited landfill space, as well as reduce the need to import natural aggregate materials for site restoration work (NDA, 2021). This is similar to approaches in the construction and demolition waste (CDW) industry (Dhir et al., 2019), however on nuclear sites the scale at which reuse is expected to be much larger, and the CCW may be stockpiled for much longer periods of time (Foy et al., 2019). The reuse of CCW raises environmental concerns on the production of high pH alkaline leachates, as they have already been measured at some nuclear sites and they can represent an environmental hazard if they discharge to sensitive environments (Foy et al., 2019). In addition, there are concerns over the leaching of trace metal contaminants such as Cr, V, Pb or Cu which may be present in CCW and lead to environmental contamination if they are mobilised. Therefore, it is essential to understand the propensity for high pH leachate generation and contaminant release before this material may be used on-site.

As the CCW will be produced many years to decades before its final use as void fill or backfill, the material may be stockpiled for long periods of time. During stockpiling, CCW will be weathered from exposure to air and rainfall, which may affect the leachate produced. Therefore, there is a need to understand how long-term stockpiling can affect concrete waste chemistry, as it is known that weathering processes such as carbonation can reduce leachate pH, and therefore contaminant metal release.

Stockpiled CCW samples used in this project have been aged and exposed to weathering processes for over a decade, providing unique material for this study.

This project seeks to address some of the gaps in concrete waste chemistry from using long-term stockpiled CCW from a representative UK nuclear site to generate valuable data that can be used in environmental risk assessments for on-site burial of CCW. This knowledge is necessary to reduce unnecessary transport of waste off-site. As it is expected that CCW buried at the near surface will come into contact with meteoric or groundwater over time (dependent on the structural designs), it is essential to investigate leaching behaviour and different leaching mechanisms under different conditions relevant to expected field scenarios. Therefore, this project will use static and dynamic leaching experiments using different pH leachants to provide useful information for risk assessments relevant to on-site disposal. Usually, laboratory experiments use fresh crushed material, but this overestimates the concentration of the constituents released because surface area is increased, and this is unlikely to occur in field conditions. This project will use CCW fractions recovered from site stockpiles to provide realistic data on CCW leachates. In addition, the reuse of the finer fraction is usually avoided in CDW industries and instead consigned as waste for disposal due to expected enhanced leaching, so this study will also assess the influence of size fraction on leaching.

1.2 Research objectives

It is the aim of this work to contribute to the technical understanding of the evolution of CCW leachate composition in the context of on-site reuse of CCW on UK nuclear sites, either as void fill or backfill. This data will be beneficial for preparing safety assessments and evaluating the suitability of on-site disposal options.

This aim will be achieved through the following four research objectives:

1. Determine the alkalinity generating potential of stockpiled crushed concrete wastes from a representative UK nuclear site as a function of size fraction and weathering after long-term stockpiling (Chapter 4)
2. Determine the potential for release of major elements and trace contaminants from stockpiled crushed concrete wastes as a function of pH and size fraction under batch equilibrium conditions (Chapter 4)
3. Investigate the release mechanisms of major elements and trace contaminants from stockpiled CCW under far-from-equilibrium conditions (Chapter 5)

4. Determine the short-term dissolution kinetics of CCW as a function of pH under far-from-equilibrium conditions (Chapter 5)

Objectives 1 and 2 are addressed in Chapter 4 and objectives 3 and 4 are addressed in Chapter 5. The objectives are discussed in relation to the chapter conclusions in Chapter 6.

1.3 Thesis structure

This thesis contains six chapters. Following the introduction, a literature review on the reuse of CCW and a relevant summary of leaching behaviour of CCW is presented, identifying where environmental concerns arise. The third chapter describes the methods used in this thesis in additional to the theoretical background of the analytical techniques used. Chapter 4 and Chapter 5 are the results chapters. Chapter 4 (In situ disposal of crushed concrete waste as void fill material at UK nuclear sites: Leaching behaviour and effect of pH on trace element release) provides characterisation data and the results of acid neutralisation and pH-dependent batch tests. Chapter 5 (Dissolution kinetics of crushed concrete waste: Effect of pH on leaching behaviour) contains results of major and trace element leaching from CCW in flow-through reactors along with dissolution kinetics of CCW at pseudo-steady state conditions. Chapter 6 presents a synthesis of the results chapters in light of the objectives, along with the implications and scope for further work. The appendix contains the limit of detection values used in Chapters 4 and 5, as well as additional data for Table 5.3 in Chapter 5.

1.4 References

Department for Energy Security & Net Zero, D. 2023a. *Consultation: Part I UK policy proposals for managing radioactive substances and nuclear decommissioning.* [Online]. [Accessed 10/05/2023]. Available from: https://assets.publishing.service.gov.uk/government/uploads/system/uploads/attachment_data/file/1139242/part_I_policy_proposals_managing_radioactive_substances_and_nuclear_decommissioning.pdf

Dhir, R.K., de Brito, J., Silva, R.V. and Lye, C.Q. 2019. 13 - Environmental Impact, Case Studies and Standards and Specifications. In: Dhir, R.K., et al. eds. *Sustainable Construction Materials.* Woodhead Publishing, pp.495-583.

Foy, J., Jones, G., Sephton, M. and Gaitonde, R. 2019. *Managing On-site Stockpiling and Use of High Volumes of Concrete-based Demolition Material.* Cumbria, UK: AECOM on behalf of the Nuclear Decommissioning Authority.

GRR. 2018. *Management of Radioactive Waste from Decommissioning of Nuclear Sites: Guidance on Requirements for Release from Radioactive Substances Regulation Version 1.0.* [Online].

IAEA. 2008. *Managing Low Radioactivity Material from the Decommissioning of Nuclear Facilities.* Vienna, Austria: International Atomic Energy Agency.

NDA. 2016. *UK Strategy for the Management of Solid Low Level Waste from the Nuclear Industry.* [Online]. Department of Energy & Climate Change. [Accessed 10/05/2023]. Available from: https://www.gov.uk/government/consultations/consultation-on-an-update-of-the-uk-strategy-for-the-management-of-solid-low-level-radioactive-waste-from-the-nuclear-industry

NDA. 2020. *Concrete example of dealing with decommissioning rubble.* [Online]. [Accessed 05/07/21]. Available from: https://www.gov.uk/government/case-studies/concrete-example-of-dealing-with-decommissioning-rubble

NDA. 2021. *Strategy.* [Online]. Cumbria, UK: NDA. [Accessed 14/05/2023]. Available from: https://assets.publishing.service.gov.uk/government/uploads/system/uploads/attachment_data/file/973438/NDA_Strategy_2021_A.pdf

NDA. 2022. *2022 UK Radioactive Waste Inventory.* [Online]. Cumbria, UK: NDA. [Accessed 14/05/2023]. Available from: https://ukinventory.nda.gov.uk/wp-content/uploads/2023/02/2022-Waste-Report-010223.pdf

Chapter 2 Literature Review

2.1 Management of concrete-based demolition wastes and associated challenges

In the UK, the NDA are responsible for the decommissioning and clean-up of 17 nuclear sites and their release from regulation for beneficial reuse (NDA, 2021). It is estimated that decommissioning will take over 100 years to complete at a cost of over £120 billion (NDA, 2021). A significant challenge for the NDA is that substantial quantities of concrete-based demolition wastes will be generated from decommissioning activities in the coming decades (IAEA, 2008; NDA, 2020). The majority of radioactive waste is generated by the nuclear power industry, with smaller amounts generated by defence activities, research establishments, medical and industry uses (NDA, 2022). In the 2022 UK Radioactive Waste Inventory (NDA, 2022) the total volume of UK radioactive waste (including present and future arisings) is estimated to be nearly 4.5 million m^3. More than 94% of this waste will be categorised as Low-Level Waste (LLW) or Very Low-Level Waste (VLLW), the majority of which will be concrete building demolition materials generated from the dismantling of nuclear reactor facilities, and a smaller amount of excavated soil from construction and demolition activities (NDA, 2022). LLW is defined as having <4 GBq per tonne of alpha activity or 12 GBq per tonne of beta/gamma activity, whilst VLLW is a subcategory of LLW with low total radioactivity (NDA, 2022). High volume VLLW has a maximum of 4 MBq per tonne of total activity (NDA, 2022). Many nuclear sites also have subsurface structures that may be lightly contaminated (NDA, 2021). It would be overly conservative to clear every concrete structure as potentially hazardous (Nuclear Energy Agency, 2017). Typically, the conventional disposal option for LLW is LLW repositories, whilst VLLW can typically be disposed at conventional landfill sites (NDA, 2016; 2020). The majority of concrete rubble waste will be out of scope with respect to the Radioactive Substances Regulation and therefore ‘non-radioactive’ (The Department for Environment, Food and Rural Affairs [DEFRA], 2011; Foy et al., 2019) and resemble conventional demolition material that can also be disposed at permitted landfill sites (DEFRA, 2018; NDA, 2020; 2022). The management of significant volumes of VLLW, LLW and out of scope material represents a significant challenge for the NDA, as solid LLW/VLLW must be managed in accordance with the waste hierarchy as well as environmental and radiological regulations (Figure 2.1) (NDA, 2021).

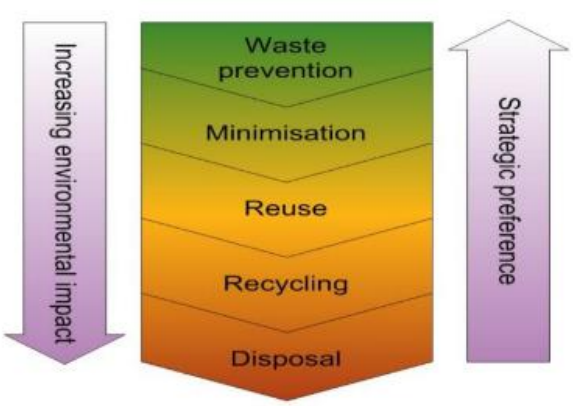

Figure 2.1 Waste management hierarchy (NDA, 2016)

Although the removal of subsurface structures on nuclear sites undergoing decommissioning could allow for faster release from nuclear regulation and therefore immediate availability for reuse of the site, excavation (for disposal elsewhere) would contribute to the generation of huge volumes of concrete demolition waste that would be consigned for off-site disposal to landfill (NDA, 2021). The excavation of these structures as well as the off-site transport has several negative impacts on people and the environment including increased traffic, the use of limited landfill capacity, health and safety risks from exposure to workers and the import of new materials required for void-filling (NDA, 2020; 2021). Disposal to landfill is the least favoured approach and the last resort on the waste hierarchy (Figure 2.1), so there are significant environmental and economic imperatives to seek out sustainable options in alignment with higher levels of the waste hierarchy (IAEA, 2008). Following the waste hierarchy, an alternative and perhaps more beneficial approach to off-site disposal is on-site disposal, and the NDA commissioned a report in 2019 (Foy et al., 2019) to investigate this potential option. On-site disposal involves leaving subsurface structures (that may be contaminated) in-situ, and using concrete demolition wastes as void fill for redundant structures, within trench caps and in voids across the site (GRR, 2018; Foy et al., 2019; NDA, 2021; Department for Energy Security & Net Zero, 2023a). The requirements for on-site disposal of radioactively contaminated waste on nuclear sites are outlined in the GRR (2018), and the potential scenarios available are shown in Figure 2.2 (GRR, 2018).

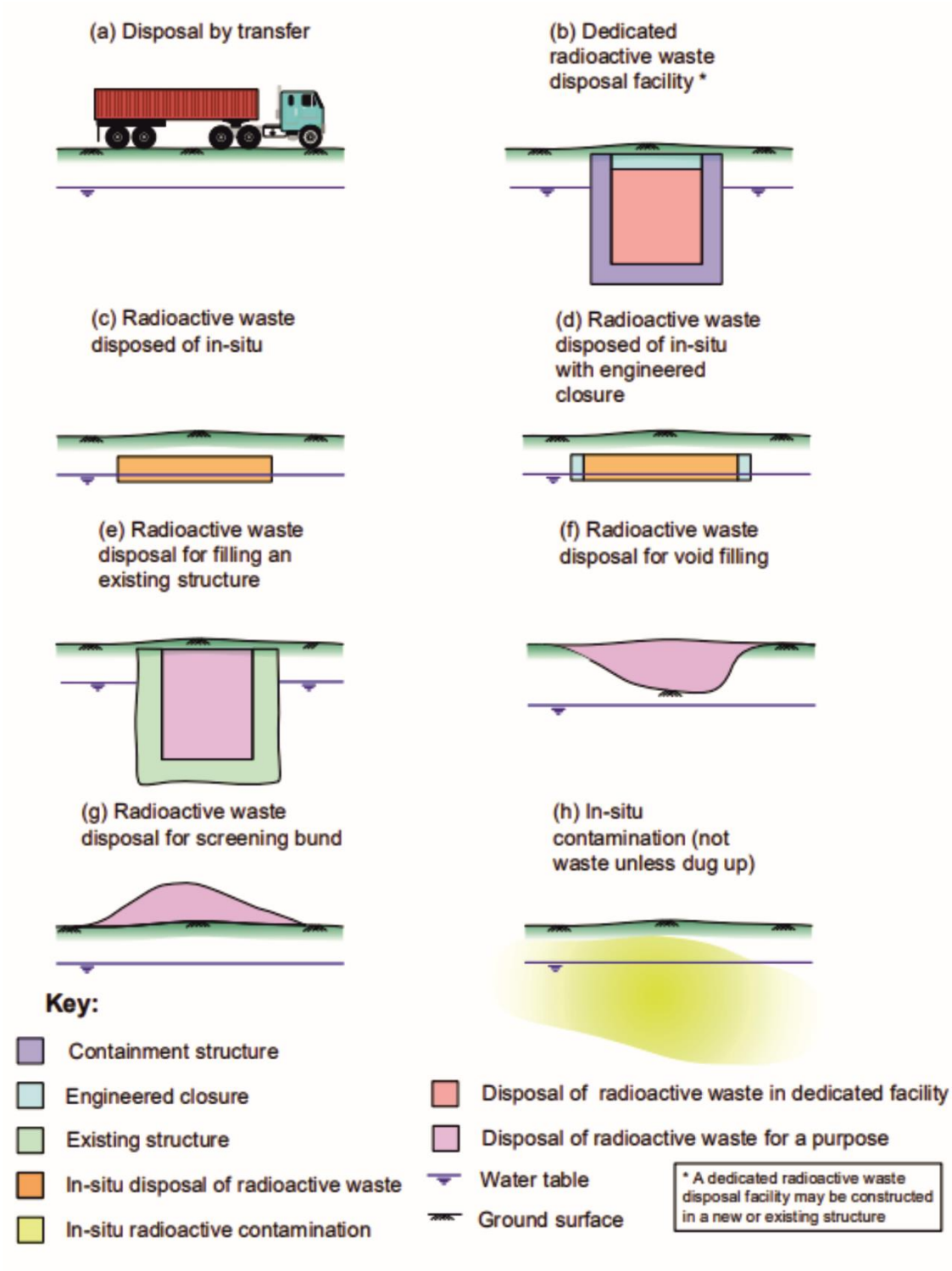

Figure 2.2 Management options for radioactively contaminated waste generated during the decommissioning of nuclear sites (GRR, 2018). It is noted in the figure that the position of the water table in the figure is illustrative only and does not indicate that radioactive waste disposals in the saturated zone would always be authorised (GRR, 2018).

The reuse of concrete demolition wastes as void fill is a common approach in the CDW industry (Foy et al., 2019; NDA, 2020). Concrete demolition waste is crushed, producing CCW which is used in landscaping, void fill or as aggregate (Coudray et al., 2017; NDA, 2020). In the CDW sector, concrete demolition waste is mechanically processed by the separation of undesirable fractions and crushed to produce new materials referred to as recycled aggregates (Diotti et al., 2020), recycled concrete aggregates (RCA) or recycled concrete material (RCM) (Foy et al., 2019), which are all types of CCW. In this thesis, concrete-based demolition wastes will be referred to as CCW.

In the CDW industry, CCW is often used in geotechnical applications (pavement construction, road sub-base, backfill, embankments) (Engelsen et al., 2006; 2012; 2017; Rahman, M. et al., 2014; Coudray et al., 2017; Dhir et al., 2019; Wright et al., 2023) or as aggregate in new concrete (Townsend et al., 2004; Galvín et al., 2014a; Coudray et al., 2017; Dhir et al., 2019). Concerning the reuse of CCW as backfill, this usually occurs shortly after CCW is generated, and in relatively small volumes in comparison with what is anticipated in the nuclear industry (Foy et al., 2019; NDA, 2020). However, in the nuclear industry concrete demolition wastes are likely to be generated decades before use is required as backfill in much larger voids and redundant structures on-site (Foy et al., 2019). Moreover, on-site disposal is subject to regulatory control, and planning permission from local government authorities may be required (NDA 2021). Current regulation requires stockpiling and reuse within 12 months, unless additional licenses, permits or planning permission are obtained, which is not always possible (Foy et al., 2019). This represents a challenge for the nuclear industry (Foy et al., 2019). Long-term stockpiling is not addressed in the new policy proposals (Department for Energy Security & Net Zero, 2023a;b) but is something that is important to consider. Long-term stockpiling (>12 months) and the reuse of concrete demolition wastes requires approval from the environmental regulator, and usually the specific end use must be agreed on at the time of stockpiling, which is not always known (Foy et al., 2019). This is a significant regulatory challenge, which possibly makes off-site disposal a preferred option for nuclear sites (Foy et al., 2019).

On-site disposal of concrete demolition wastes must be shown to be beneficial to the site end state (NDA, 2021). There are several benefits associated with on-site disposal. Firstly, in-situ disposal has the benefit of utilising extant subsurface structures and avoiding the risks associated with their excavation, in addition to diverting concrete demolition waste from landfill and saving disposal capacity elsewhere (Nuclear Energy

Agency, 2017; Foy et al., 2019). Secondly, concrete demolition material could also have a beneficial use in site restoration work through void filling and landscaping, which has environmental and economic benefits from the usual requirement to import new virgin materials from elsewhere (NDA, 2021). Currently, on-site reuse or disposal of cementitious waste materials at nuclear sites is undertaken on a site-specific case-by-case basis (IAEA, 2008). On-site reuse of crushed concrete waste materials has occurred in Sweden, Spain, Italy, Belgium, Germany, Japan, the United States and the UK (Nuclear Energy Agency, 2017). For example, in the UK crushed concrete has been reused in infrastructure works at Sellafield, and as bulk fill around containers at the UK Low Level Waste Repository (Nuclear Energy Agency, 2011). Outside of the UK, at Vandellos-1 nuclear power plant in Spain, 77,000 tonnes of concrete from buildings together with 1,900 tonnes of concrete that was outside the scope of radioactive regulations has been reused onsite for land restoration purposes (Nuclear Energy Agency, 2017). It is hoped that the regulatory environment can be made more favourable to promote on-site disposal where it is safe to do so, and this is apparent in the current policy amendment framework put forth by the UK government, which is currently under public consultation (Department for Energy Security & Net Zero, 2023a).

CCW is classified as inert under EU waste legislation and the Waste and Resource Action Programme (WRAP) Quality Protocol. Inert is defined as “waste that does not undergo any significant physical, chemical or biological transformations. Inert waste will not dissolve, burn or otherwise physically or chemically react, biodegrade or adversely affect other matter with which it comes into contact in a way likely to give rise to environmental pollution or harm human health. The total leachability and pollutant content of the waste and the ecotoxicity of the leachate must be insignificant, and in particular not endanger the quality of surface water and/or groundwater” (Council Directive 1999/31/EC (1999), p.2). Despite this designation, there are valid concerns over the environmental impacts of using CCW in the subsurface environment, both in the nuclear industry (WRAP, 2013; Foy et al., 2019) and in the CDW industry as it has the potential to contaminate surface water or groundwaters through the generation of high pH leachates and may release inorganic contaminants of concern such as As, Ba, Cd, Cr, Cu, Hg, Mn, Mo, Ni, Pb, Ti, V, Zn and sulphates (Kang et al., 2011; Chen, J. et al., 2012; 2013; Somasundaram et al., 2014; Bestgen et al., 2016a; Gupta et al., 2018; Kluge et al., 2018; Dhir et al., 2019; Foy et al., 2019; Chen, Y. and Zhou, 2020;

Oliveira, F.D. et al., 2020; Wright et al., 2023). Organic pollutants may also be a concern (Bestgen et al., 2016a; Kriech and Osborn, 2022).

High pH leachate readings were detected from CCW placed as backfill in below ground concrete structures (that were continuously saturated) for more than 10 years since placement on an NDA site (Foy et al., 2019). Therefore, there are valid concerns that on-site disposal could cause high pH leachates (Foy et al., 2019). As the material for on-site disposal must be demonstrated to comply with environmental permits and suitable end states, concerns over high pH leachate generation and leaching of metals must be addressed prior to on-site disposal.

The concerns over high pH leachate generation and contaminant release have been covered in the CDW literature in the context for assessing leaching behaviour (Delay et al., 2007; Wehrer and Totsche, 2008; Butera et al., 2014; 2015a; Oliveira, M.L.S. et al., 2019), environmental risk and/or suitability for reuse of CCW in geotechnical or structural applications (Engelsen et al., 2002; 2003; 2006; 2009; 2010; 2012; 2017; Kang et al., 2011; Chen, J. et al., 2012; 2013; Rahman, M. et al., 2014; Galvín et al., 2018; Gupta et al., 2018; Cabrera et al., 2019; Dhir et al., 2019; Oliveira, F.D. et al., 2020) or from stockpiles of CCW (Sadecki et al., 1996). Concern has also been raised for the production of alkaline plumes from cementitious repositories (Braney et al., 1993; Chen, X. et al., 2015). Although, CCW may produce lower pH leachates than those expected from cementitious repositories because the cement phases will have been degraded to varying degrees. In addition, this may be due to dilution because concrete contains less cement than cementitious backfill. Typically, there is variation between studies based on whether CCW is suitable for a given application, usually based on whether pollutant leachate concentrations meet specific local criteria for the intended application (e.g. backfill material, (Rahman, M. et al., 2014), unrestricted use (Butera et al., 2015a), regulatory limits such as waste acceptance criteria (e.g. inert, non-hazardous or hazardous (Butera et al., 2014; 2015a)) or comparisons to surface water, ground water and/or drinking water quality standards (Chen, J. et al., 2013; Gupta et al., 2018).

The concerns surrounding reuse of CCW are the same in the CDW industry and nuclear industry. Previous studies in the CDW sector have focused on the leaching of constituents and leaching and alkalinity generation from CCW in geotechnical applications. However, there is a gap in the literature on using CCW that have arisen from nuclear sites. It is important to characterise CCW before reuse because of the natural heterogeneity in the CCW (Diotti et al., 2021). As CCW are predominantly

composed of cementitious materials, the composition of concrete is reviewed in the following section.

2.2 Mineralogical and chemical composition of concrete

Concrete is a hardened composite material composed of a cement binder material, fine and coarse aggregate) and water (Ochs et al., 2015). The cement binder accounts for around 10% of concrete mass (Habert et al., 2020) whilst aggregate dominates concrete by volume/mass (Ekström, 2001). The aggregate is usually crushed rocks such as sand (quartz) or gravel from silicate or calcareous rocks (Ochs et al., 2015). Ordinary Portland Cement (OPC) is the most common cement binder and is widely used across the world in construction (Taylor, 1997; Ochs et al., 2015). Admixtures or supplementary cementitious materials (SCM) may be mixed in with Portland cement and include fly-ash, metakaolin or slag, forming blended cements (Richardson et al., 2016), although Foy et al (2019) notes that the admixture of concrete used on the NDA estate is unknown. OPC is formed through the heating of limestone and clay in a cement kiln at 1450 °C, and this product is then mixed with gypsum to produce clinker (Taylor, 1997). The four main clinker phases of OPC (and their respective cement notation) are alite (C_3S), belite (C_2S), aluminate (C_3A) and ferrite (C_4AF). Cement chemistry notation refers to: CaO = C; SiO_2 = S; Al_2O_3 = A; Fe_2O_3 = F; H = H_2O (Neville, 2011), and is used in this thesis. When OPC is mixed with water, typically at a water/cement ratio of 0.3-0.6, the clinker phases undergo a series of complex hydration reactions which set and harden the cement (Taylor, 1997). According to Berner (1992), hydrated cement (with cement chemistry notation) is composed of (by weight): calcium silicate hydrate (C-S-H; 40-50%), portlandite (CH; 20-25%), calcium monosulphate aluminate and trisulphate aluminate phases (respectively AFm and AFt; 10-20%), minor hydroxides (e.g. NaOH, KOH, $Mg(OH)_2$; 0-5%) and a pore solution (10-20%). The range for composition varies by cement blends but C-S-H is the dominant constituent of cement paste (Marty et al., 2015) and most important for the durability of concrete. It is reported by Lagerblad (2001) that some cement clinker, particularly C_2S and C_4AF, can remain unhydrated, even after 90 years in water. Similarly, Diamond (2004) reports that unhydrated clinker is retained in nearly all Portland cements. Generally, during hydration alite and belite form CH and C-S-H, whilst aluminate and ferrite react with water to form AFt (e.g. ettringite) or AFm (Ochs et al., 2015; Richardson et al., 2016). Detailed studies on cement hydration are ubiquitous and some key papers include Richardson (2000), Bullard et al. (2011) and Scrivener and Nonat (2011). The cement pore solution, which originates from the excess water not

used in hydration, is in equilibrium with the cement phases and contains Na^+, K^+, Ca^{2+} and OH^- ions from the dissolution of Na and K hydroxides, causing high pH (>13) and high ionic strength (Ekström, 2001; Rothstein et al., 2002; Deissmann et al., 2006; Hidalgo et al., 2007). Although, the use of SCM's usually result in concrete with a lower pore solution pH of 12.5-13 (Engelsen, 2020). In fresh cement pastes, it is the C-S-H gel, CH and alkalis that determine the chemical composition of the pore solution (Hidalgo et al., 2007).

C-S-H is the main, dominant binding phase in all cement pastes and is referred to as a poorly crystalline gel that is highly variable in composition, non-stoichiometric and nearly amorphous (Taylor, 1986; Berner, 1992; Richardson, 1999; Harris et al., 2002; Lothenbach et al., 2011; Rossen et al., 2015). The hyphens in C-S-H indicate that the stoichiometry is variable (Richardson, 1999). The nanoscale structure of C-S-H is likened to that of the rare natural minerals, 1.4-nm tobermorite ($C_5S_6H_9$) and jennite ($C_9S_6H_{11}$), which each have a Ca/Si ratio of ~0.8 and ~1.5 respectively (Taylor, 1986; Chen, J.J. et al., 2004; Richardson, 2004). Tobermorite and jennite have layers of calcium oxide sheets connected by linear silicate "dreierkette" chains, which means that Ca ions are coordinated to silicate tetrahedra after every third silicate tetrahedra (Richardson, 2004; Nonat, 2004). At the atomic level, it is thought that the C-S-H structure mostly resembles a defective tobermorite with variable Ca/Si ratios accounted for by missing silicate tetrahedra at high Ca/Si ratios (Richardson, 2004; Lothenbach and Nonat, 2015; Rossen et al., 2015). There are also interlayers between the Ca-silicate sheets that contain varying amounts of Ca ions, water molecules, alkalis and other ions (Tits et al., 2011; Rossen et al., 2015). The Ca/Si ratio of C-S-H in Portland cement is usually around 1.5 to 2 (Taylor, 1986; Zhang, X.Z. et al., 2000; Lothenbach and Nonat, 2015; Rossen et al., 2015). The Ca/Si variation is due to cement composition, for example the SCM content often results in lower Ca/Si ratios (Lothenbach et al., 2011; Berodier and Scrivener, 2015; Richardson et al., 2016). As C-S-H compositional data is usually obtained from SEM-EDS, Richardson (1999) notes that the interaction volume is usually larger (several μm^3) than the cement phases, which means the composition of C-S-H can often only be estimated after considering that other phases (e.g. CH) may be intermixed with the C-S-H (Richardson, 1999). This is something that is usually taken into consideration. Further, as C-S-H in Portland cement is not phase pure, it may be referred to as calcium (alumino) silicate hydrate (C-(A)-S-H) as Al can enter the structure and substitute for Si (Richardson, 1999; L'Hôpital et al., 2015; 2016; Lothenbach and Nonat, 2015). Other ions can also enter

the structure of C-S-H, for example Mg can replace Ca in C-S-H and Al, S and Fe can replace Si (Rayment and Majumdar, 1982). A significant proportion of all surface area in cement paste is attributed to C-S-H, which has a high porosity (Hidalgo et al., 2007).

2.3 Leaching mechanisms

Leaching is a diffusion-based process that occurs when an aqueous solution (the leachant) is in contact with a solid matrix (the solid-water interface) that releases chemical species into solution (Garrabrants and Kosson, 2004). The fundamental mechanisms that determine the release of constituents from solid material into the solution are chemical (dissolution, sorption, availability) and physical (diffusion, advection, surface wash-off) in nature (Garrabrants and Kosson, 2004; van der Sloot and Dijkstra, 2004; Cabrera et al., 2019). The release of constituents is usually described in terms of (chemical) equilibrium control or (physical) mass-transport control (Kosson et al., 2002; Garrabrants and Kosson, 2004).

2.3.1 Solubility control

Solubility control occurs when a solution in contact with a solid is saturated with respect to the constituent species and is determined by dissolution and desorption of phases which determine the absolute maximum concentration of constituents (Kosson et al., 1996; Appelo and Postma, 2005). This leaching mechanism usually occurs at low liquid-solid ratios (L/S) ratios in the field where percolation processes dominate (Kosson et al., 1996). Dissolution and desorption are strongly pH-dependent processes that occur at the solid-water interface and affect constituent solubility at particle surfaces (Garrabrants and Kosson, 2004; van der Sloot and Dijkstra, 2004; Appelo and Postma, 2005).

When the solid is in equilibrium with the leachant solution, constituent release will depend on the solubility of the solid, which is affected by the pH of the solution, temperature and ionic composition of the leachant (Kosson et al., 2002; Garrabrants and Kosson, 2004). pH is crucial to solubility behaviour; at acidic pH, dissolution and desorption processes dominate, whilst under high pH conditions precipitation may occur which reduces solubility (Bestgen et al., 2016a). Solubility is also affected by the composition of the leachant (presence of other ions or organic matter may result in complexation) and redox conditions (van der Sloot, 1996; Garrabrants and Kosson, 2004). In aqueous solution, ions can interact and form aqueous complexes or ion pairs (Appelo and Postma, 2005). Aqueous complexes are associations between a cation (metal ion) and anion or neutral molecule in water (Langmuir, 1997). An example is

$CaOH^+$ or heavy metal complexes $CdCl^+$ and $PbOH^+$ (Appelo and Postma, 2005). Complexes are either inner-sphere complexes, which form largely covalent or ionic bonds between a metal ion and a ligand (an anion or neural molecule that donates an electron), or outer-sphere complexes which are transient ion pairs formed by a cation and anion separated by one or more water molecules and held by long-range electrostatic forces (Stumm and Morgan, 1996; Langmuir, 1997). Complexing of dissolved species can increase the solubility of the mineral containing that species (Langmuir, 1997; Appelo and Postma, 2005). For example, Cl^- is a complexing agent (Appelo and Postma, 2005). Heavy metals tend to complex with humic substances in waters and soil (organic matter), which can potentially increase their solubility (van der Sloot and Dijkstra, 2004).

Sorption to active sites on solid surfaces control the release of elements with sorptive affinity (Bestgen et al., 2016a). Cations (e.g. Cu^{2+}) that are not controlled by mineral dissolution may show affinity for adsorption to negatively charged surfaces such as oxides or organic matter (van der Sloot and Dijkstra, 2004). Metal ions may sorb to cement hydrate products such as C-S-H and calcium (sulfo) aluminate hydrates (e.g. AFt (ettringite) and AFm (monosulphate), which have large surface areas, or to surface sites on oxides, oxyhydroxides and organic matter (McBride, 1994; Baur and Johnson, 2003; Garrabrants and Kosson, 2004; Bestgen et al., 2016a). Sorption of cations and anions to C-S-H gel occurs, although the mechanism is not always known (Ochs et al., 2015). The change in pH may affect the surface charge of cement phases, which can affect the adsorbed metal ions (Garrabrants and Kosson, 2004). The ionic composition of the leachant is also important as ions (e.g. Na^+, K^+, Ca^{2+} and H^+) can compete with metal ions for sorption to negatively charged surfaces (Garrabrants and Kosson, 2004).

2.3.2 Availability control

The availability of a constituent in the solid phase is the maximum fraction available for leaching under particular chemical conditions and is usually defined at maximum release conditions (Garrabrants and Kosson, 2004). Availability-limited leaching is when the solid phase determines the release potential of constituents (van der Sloot, 1996). At high L/S ratios, availability-limited control may be observed, especially for very soluble ions such as Na^+, K^+ and Cl^- (Garrabrants and Kosson, 2004). Thus, the total composition of constituents is not necessarily an indicator for leachability; van der Sloot (2000) found lower leachability of Cr was observed when total Cr content was highest in cement mortars. Instead, most major reactions are controlled by surface reactions (dissolution and desorption) and mass-transport mechanisms.

2.3.3 Mass-transport control

Mass-transport mechanisms include diffusion, advection and surface wash-off (Garrabrants and Kosson, 2004; van der Sloot and Dijkstra, 2004). The driving force for the reactions is the renewal of the leachant, which disturbs the attainment of chemical equilibrium and introduces kinetic controls on leaching.

Diffusion occurs solely from the random movement of molecules from an area of high concentration to an area of low concentration, in the absence of flow and is time-dependent (van der Sloot and Dijkstra, 2004). The rate of diffusion will depend on the concentration gradient between two regions. Diffusion can lead to increased dissolution of solid phases when a material is contact with a leachant, as constituents in equilibrium with solids will leach from the pore solution and into the surrounding leachant, which will drive further dissolution and desorption processes (Garrabrants and Kosson, 2004). Diffusion of ions occurs inside the solid matrix, from the inner regions to the surface, and out into the leachant, and this is relevant for monoliths (Garrabrants and Kosson, 2004).

Advection is the movement of constituents in a fluid by bulk fluid flow, driven by pressure gradients (e.g. through percolation by rainwater in the field) (Garrabrants and Kosson, 2004; van der Sloot and Dijkstra, 2004). This can lead to increased leaching as constituents are transported away, driving further dissolution and desorption processes (Garrabrants and Kosson, 2004).

Surface-wash off is often observed in the initial phases of dynamic experiments and is attributed to the leaching of highly soluble salts and/or trace metals at particle surfaces (Wehrer and Totsche, 2008). After the initial wash-off, other mass-transport mechanisms will dominate release behaviour (van der Sloot and Dijkstra, 2004).

Whether mass-transport (e.g. diffusion) or surface reactions (e.g. dissolution, desorption) control constituent release depends on the rate-limiting reaction; if surface reactions are faster than diffusion of constituents from the solid matrix, then the reaction is transport-controlled (Schott et al., 2009). If transport of constituents from the surface is fast, then dissolved species do not build up at the solid-liquid interface and the reaction rate becomes diffusion-controlled (Schott et al., 2009). Moreover, the mechanisms controlling release may change with time; for example, long-term leaching studies have found an initial fast reaction period followed by slower release rates (Krishnamoorthy et al., 1993; Garrabrants and Kosson, 2004). This is also similar to the

surface wash-off initially causing high constituent release, after which diffusion may become the rate-limiting step (Wehrer and Totsche, 2008).

2.3.4 Leaching tests

Leaching tests are essential to investigate the leaching behaviour and mechanisms controlling contaminant release as CCW will interact with surface waters, rainwater and groundwater in the environment. Laboratory leaching tests may be categorised as: basic characterisation tests (batch tests that vary chemical and physical parameters to characterise leaching over the short or long-term), compliance tests with specified reference values or regulatory limits (e.g. in England for waste acceptance criteria to inert, non-hazardous or hazardous landfill, standards BS EN 12457 part 1, 2, 3 or 4 are used to measure compliance of granular materials), or on-site verification tests (performed on-site where waste was generated and ensures waste is the same as previous compliance tests undertaken (BSI, 2002a; van der Sloot and Dijkstra, 2004).

Characterisation tests are beneficial for investigating constituent release mechanisms from crushed concrete by varying chemical and physical parameters relevant to field conditions such as pH, L/S, time, leachant contact and renewal, and leachant composition. They are divided into closed system (batch) experiments and open system (dynamic) system experiments, based on whether leachant is kept constant or exchanged. Open system experiments include dynamic leach tests, which investigate kinetics of release as a function of time (upflow column or down-flow lysimeter and tank or diffusion test) (van der Sloot and Dijkstra, 2004). There are a multitude of different leaching tests that are similar but specific to individual countries such as pH-dependent batch tests are under BS EN 14429 in the UK (British Standards Institute, 2015) and LEAF1313 in the USA (Kosson et al., 2017), but leaching tests broadly address similar leaching mechanisms.

An important distinction in leaching tests is whether the material is monolithic or granular, as the major leaching mechanisms vary between the two forms (van der Sleet et al., 1997). Leaching from monoliths is governed mainly by diffusion (from the inner matrix as solid-phase diffusion, and from the surface into the leachant) and surface wash-off, whereas leaching from granular materials is usually dominated by percolation (van der Sloot and Dijkstra, 2004). Leaching of monolithic materials are typically studied using diffusion tank tests, where the monolith is immersed in a tank of water and the leachant is exchanged periodically, whilst the release mechanisms from granular materials are studied using batch and column tests (van der Sloot and

Dijkstra, 2004). As discussed in van der Sloot (2004), it is beneficial to use leaching tests that focus on the key chemical and physical mechanisms that control inorganic constituent release.

Key factors affecting all leaching tests that may be varied include pH, leachant composition, particle size, L/S, mode of water contact (static, dynamic and/or intermittent) and temperature (van der Sloot, 1996; Garrabrants and Kosson, 2004; Maia et al., 2018) to understand material leaching characteristics across different conditions.

Of relevance to the disposal of CCW in the subsurface are leaching tests that resemble field leaching conditions, such as batch equilibrium tests for slow-flow percolation conditions (solubility-control) and dynamic leach tests (e.g., columns, flow-through reactors) for faster flow conditions (mass-transport control, or solubility-control for slower conditions). Whilst columns are useful for slow flow conditions, there is a lack in experiments incorporating faster flow conditions in the CCW literature, nor any focus on dissolution kinetics for CCW.

2.3.4.1 Batch tests (closed system)

Batch tests are usually closed-system reactors as the leachant solution is not replenished (static) and therefore leaching is under chemical control, and reactions tend toward chemical equilibrium (Schott et al., 2009). Therefore, the underlying assumption with batch tests is that an equilibrium condition is achieved at the end of the test (Chandler et al., 1997). Although, true chemical equilibrium may not be achieved for some species with slow reaction kinetics (Engelsen, 2020), pseudo-equilibrium conditions may be established (Lopez Meza et al., 2008). Under equilibrium conditions, leaching is under geochemical control by the solid and the chemistry of the solution, rather than the contact time (van der Sloot, 2002; Garrabrants and Kosson, 2004; Lopez Meza et al., 2008; Galvín et al., 2012). Agitation is often used to reach equilibrium as soon as possible, using shaker tables, stirring or tumbling (Chandler et al., 1997; Garrabrants and Kosson, 2004). At equilibrium, constituent leaching is controlled by solubility and sorption which determine leaching (Mahedi and Cetin, 2023). Solubility determines leaching when the constituents are at saturation with respect to the minerals of the constituents and sorption to surfaces, oxides, oxy-hydroxides and organic matter may occur (Komonweeraket et al., 2015; Mahedi and Cetin, 2023).

Batch experiments are useful for simulating slow-flow (percolation) or stagnant conditions in the field where reactions are likely to be equilibrium-controlled, as solubility and sorption are key leaching mechanisms. In these conditions dissolution and desorption will depend on the solubility of the solid matrix in the leachant and the saturation of the species (Engelsen, 2020). To investigate the phases controlling solubility, geochemical modelling can be undertaken using input data from pH-dependent batch tests (Engelsen et al., 2009; 2010; Mahedi and Cetin, 2023).

pH is a critical factor that affects constituent solubility and therefore pH-dependent batch tests are often carried out to evaluate leaching behaviour across a range of pH values (usually pH 2 to 14). Environmentally relevant pH values will be field site dependent however they are usually between pH 4 (representing peat soils) to neutral (most soils) and alkaline pH (>10) (such as concrete in water where flow is limited) (van der Sloot, 2000). A L/S ratio of 10:1 is typically used in batch tests because constituent release has been identified as solubility-controlled over this range for pH values that are encountered in the field (van der Sloot, 2000; Kosson et al., 2002; Mahedi and Cetin, 2020). The results of batch tests are usually displayed in terms of mg/kg of dry residue to estimate constituent release (van der Sloot, 2000).

Other leaching tests include one or two step batch tests which measure leaching as a function of L/S and tests which vary leachant composition by using simulated acid rainwaters or municipal waste leachates (Bestgen et al., 2016a; Mahedi and Cetin, 2020). The former tests may be used to characterise material leaching behaviour or to assess compliance to standards such as landfills, whilst the latter tests are only relevant for specific field scenarios.

Other closed system experiments include acid neutralisation tests and availability tests. Acid neutralisation tests measure the ability of the solid to resist a decrease in pH and are used for estimating the buffering capacity (Garrabrants and Kosson, 2004). These tests are relevant as waters in contact with CCW in the field will likely contain some acidity. In particularly weathered concrete that has lost portlandite, acid buffering ability and acid resistance is provided by the decalcification of C-S-H over time (Garrabrants and Kosson, 2004). Availability tests are sequential batch tests that assess the total mass available for leaching and minimise solubility control by using very finely ground material (<125 μm) at L/S = 100 and measuring leached constituents at pH 4 and 7 (van der Sloot, 1996). These conditions are not representative of typical use of coarser size fractions in the field and so provide conservative results specific to the test condition and so are less useful for applications of CCW in the field when taken alone.

They are useful for providing values on the absolute maximum leaching concentrations, but for actual leaching conditions dynamic leach tests would be more beneficial for investigating leaching behaviour and mechanisms.

2.3.4.2 Dynamic tests (open system)

Dynamic tests involve the renewal of leachant with time in the laboratory, introduce kinetics controls on constituent release and are used to investigate mass-transport controlled release mechanisms (diffusion, advection, surface wash-off) (van der Sleet et al., 1997). They are referred to as open system as the leachant is renewed. Open system experiments include semi-dynamic tank tests, up-flow columns, down flow columns (lysimeters), and flow-through leaching tests. Diffusion tank tests use cement monoliths or granular materials to measure leaching by diffusion from the solid matrix into solution and are semi-dynamic batch style tests with regular leachant renewal designed to maintain the diffusive driving force (Garrabrants and Kosson, 2004; van der Sloot and Dijkstra, 2004). When investigating the mass-transport controls on granular materials, usually column or percolation tests are used.

Up-flow column experiments involve continuous leachant renewal which maintains saturation of the column, and a variety of flow rates may be used. Equilibrium conditions may be established with slower flow rates (Garrabrants and Kosson, 2004) or advection as a function of time (Lopez Meza et al., 2008). They are used to study leaching as a function of L/S, which approximates both short-term and long-term leaching conditions (Kosson et al., 2002; Wehrer and Totsche, 2008). The smaller L/S ratios established in the beginning of column tests are considered representative of percolation conditions occurring in the field.

Lysimeters are down-flow columns that simulate field conditions where percolation is expected. They are usually much larger than up-flow column experiments conducted in the laboratory and are rarely saturated. The leachates collected, like in field studies, are subject to carbonation and neutralisation as the collection tanks are typically not isolated from the air (van der Sloot, 1996; Delay et al., 2007). Therefore, leachate concentrations are relevant for the leachate pH after equilibrium with atmospheric CO_2, which neutralises high pH leachates (van der Sloot, 1996).

Flow-through leaching experiments are conducted either through monoliths (Poon and Chen, 1999; Garrabrants and Kosson, 2004) or with granular materials (Trapote-Barreira et al., 2014; Marty et al., 2015; 2017). Flow-through leaching experiments are similar to up-flow column tests in terms of the flow direction of the leachant solution.

However, flow-through leaching with granular material varies from column tests as the material is not compacted, and leaching will be under equilibrium control or mass-transport control, depending on the flow-rate (Garrabrants and Kosson, 2004). Flow-through leaching tests tend toward steady-state conditions with time (Steefel, 2008) and are used to measure dissolution kinetics of various minerals (Oelkers and Devidal, 2001; Wolff-Boenisch et al., 2004; Bray et al., 2014; 2015), and on C-S-H, AFm and mortar (Trapote-Barreira et al., 2014; Marty et al., 2015; 2017) but the use of crushed concrete demolition waste has not yet been covered in the literature. This could be beneficial for investigating release rates of contaminants.

In dynamic tests, time is an important variable. In column tests, leaching test results are reported in terms of L/S, which is related to the rate of infiltration and timescale for leaching (van der Sloot, 1996). The initial leachates represent low L/S ratios. At L/S = 10, the results can be compared to batch tests conducted at L/S = 10 (Kosson et al., 2002; Mahedi and Cetin, 2020). Column tests are usually carried out for compacted granular materials whilst diffusion tank tests are used for monoliths (van der Sloot, 1996).

The units of mass-transport tests may be presented as mg/L or as mg/kg. Data presented as mg/L is used for comparing concentrations to compliance values and reflects solubility control and the influence of leachant pH on constituent solubility (van der Sloot, 1996). However, release displayed as mg/kg reflect constituent release, and enables comparison with leachate concentrations in batch tests (van der Sloot, 1996). Furthermore, mass-transport rate tests may also use cumulative release (mg/m^2) or constituent flux (mg/m^2 s), such as in tank leach tests (Garrabrants and Kosson, 2004). In dissolution kinetic studies, rates are usually normalised by mineral stoichiometry that is reported in moles per unit of surface area (e.g. mol m^2 s^{-1}) (Brantley et al., 2008; Trapote-Barreira et al., 2014).

2.3.4.3 Field tests

Field tests offer the best route for investigating leaching mechanisms in the field expected for CCW as backfill or void-fill. Field investigations on using crushed concrete waste materials have been conducted in the context of using the material as hydraulically unbound void fill in road pavement construction (Engelsen et al., 2012;2017), unbound base course, (Chen, J. et al., 2013) or as backfill in a utility trench (Engelsen et al., 2002; 2003; Dhir et al., 2019). They are specific to the intended

use but provide insight into use of CCW will affect the surrounding soil environment with time in terms of constituent release and pH of leachates.

2.4 Concrete leaching behaviour

Concrete is known for its great durability and slow leaching kinetics over time, with leaching occurring by around a few centimetres over 100 years (Gérard et al., 2002; Kamali et al., 2003; Yokozeki et al., 2004). Several leaching and degradation studies have been conducted on concrete (Yokozeki et al., 2004; Beddoe and Dorner, 2005; Glasser et al., 2008; Hartwich and Vollpracht, 2017; Beddoe et al., 2022), cement-based waste forms (Sanchez et al., 2002; Garrabrants and Kosson, 2004; Garrabrants et al., 2004; Gervais et al., 2004), CCW in demolition waste (Butera et al., 2014; 2015a;b; Delay et al., 2007; Del Rey et al., 2015; Diotti et al., 2020; 2021; Wehrer and Totsche, 2008), RCA (Engelsen et al., 2009; 2010; Chen, J. et al., 2012; 2013), shotcrete in underground tunnels (Galan et al., 2019), or degradation of concrete or cement used in nuclear waste repositories (Adenot and Buil, 1992; Faucon et al., 1997; 1998; Haga et al., 2005; Trapote-Barreira et al., 2014; 2016; Ferreira et al., 2019; Jacques et al., 2021). The important factor with leaching studies is particle size; as large concrete structures (essentially monoliths) have a low surface area to volume ratio, whereas crushed concrete (resembling granular materials) has a large reactive surface that may be in contact with lower volumes of water so leaching behaviour is relevant for evaluating the environmental risk of using CCW in the subsurface, where water contact is likely inevitable.

Concrete is dominated by aggregate (e.g. quartz), which is known to be relatively inert so its effect on leaching is often expected to be insignificant relative to leaching from the cement paste. For example, leaching of natural rock materials (Ca, K and S) may occur by up to 10% relative to the total composition of the solid when using availability tests (Tossavainen and Forssberg, 1999), but this occurred under conditions that cement leaching studies of interest are not usually carried out at nor relevant to realistic leaching conditions in the field (i.e. rock materials crushed to <125 μm, L/S = 100) (Engelsen et al., 2009). Therefore, in leaching studies on concrete conducted under conditions relative to field conditions (i.e. lower L/S, not highly acidic conditions), the contribution to leaching from aggregates is usually not considered and is deemed insignificant. Moreover, Atkinson et al. (1988) reports that silica aggregate reaction rate with CH (important for pore solution pH) is really slow so can be ignored when considering effect of cement on leachate pH. Instead, it is the dissolution and degradation of cement paste that is the focus of leaching studies as it is least inert part

of concrete and source of high pH, alkaline leachates as well as leaching of major, minor and trace constituents (Engelsen, 2020). It is therefore useful to review studies on concrete and fresh cement paste to understand the cement paste composition as it ages, as this will impact the leaching behaviour of crushed concrete. Although the kinetics of concrete leaching are very slow, there are concerns over long-term environmental risks (Cabrera et al., 2019).

2.5 Degradation of cement

As cementitious materials are not in geochemical equilibrium with their surroundings, they will slowly degrade with time (Jacques et al., 2021). The renewal of water is most destructive to concrete and cement chemistry because of the diffusive concentration gradients set up between the concrete interior solution with the leachant (Adenot and Buil, 1992; Faucon et al., 1996; Mainguy et al., 2000). Therefore, there are a plethora of experimental and modelling studies on the dissolution and degradation behaviour of cement pastes, most notably from Adenot and Buil (1992), Faucon et al. (1996; 1997; 1998), Berner (1992), Moranville et al. (2004), Atkinson et al. (1985; 1989), Mainguy et al. (2000), Kamali et al. (2003; 2008), Haga et al. (2002; 2005) and Trapote-Barreira et al. (2014). A detailed review of decalcification and concrete degradation reactions is available in Glasser et al. (2008).

Hydrated cement paste is composed of solid phases that are stable at very basic pH levels, and these phases are in local chemical equilibrium with the pore solution described in section 2.2.1. When water with a pH lower than the pore solution is in contact with concrete, this disturbs the equilibrium and concentration gradients are set up between the pore solution constituents and the attacking water which drive the leaching of cement paste hydrates by dissolution and diffusion (Adenot and Buil, 1992; Faucon et al., 1997; 1998; Gérard et al., 2002). Degradation of cement hydrates typically follow a sequential order based on changes in the pore solution induced by concentration gradients between the pore solution and the attacking water (Figure 2.3, after Baston et al. (2012)). In general, there are four stages of long-term pH evolution identified from leaching experiments and modelling studies (Jacques et al., 2010; Baston et al., 2012). The dissolution of cement paste occurs at the solid-solution interface and begins with the leaching of Na, K and Ca hydroxides which produces a highly alkaline leachate pH of ~13 (Faucon et al., 1998) (Figure 2.3). The leaching of calcium ions from the pore solution drives the dissolution of portlandite (Stage 2), which is the most soluble hydrate and therefore first to dissolve (Segura et al., 2013). The dissolution of portlandite drives a progressive drop in the pore solution pH from

equilibrium with portlandite (pH 12.5) to pH 10, when the pore solution composition will be buffered by AFt, AFm and C-S-H phases (Stage 3) (Gérard et al., 2002; Jacques et al., 2010). As pH drops below 12.5, calcium sulphoaluminates such as AFm (e.g. monosulphate) and AFt (ettringite) will also dissolve at pH 11.6 and 10.7 respectively (Gabrisová et al., 1991; Jacques et al., 2010). The degradation process forms a degraded surface layer surrounding an intact core, and aluminate and sulphate species from AFm and ettringite may diffuse inward and react with Ca ions from portlandite or calcite dissolution, forming secondary precipitations of AFm and ettringite (Faucon et al., 1997; 1998). Calcite can also precipitate in this inner degraded region (Faucon et al., 1997; 1998). As the pH drops from 12.5 to 10, decalcification of C-S-H occurs, and as a result the Ca/Si ratio of the C-S-H decreases from the surface layer to core (Berner, 1988; Adenot and Buil, 1992; Carde et al., 1996; Faucon et al., 1997; Trägårdh and Lagerblad, 1998). Aluminium and iron are reported to enter the structure of lower Ca/Si ratio C-S-H gel during decalcification from water leaching (Faucon et al., 1998).

Many experimental and modelling studies have investigated the leaching behaviour of C-S-H gels, which will control the long-term behaviour of concrete chemistry (Berner, 1988; Hidalgo et al., 2007; Baston et al., 2012; Trapote-Barreira et al., 2014; Walker et al., 2016; Jin et al., 2022), as it is expected the geochemical environment in both geological and near surface disposal systems will be controlled by C-S-H phases (Berner, 1988; Jacques et al., 2021). During the dissolution of C-S-H phases (Equation 2.1; Bonen and Sarkar (1995)), calcium ions are leached from C-S-H, producing dissolved $Ca(OH)_2$, which leads to a drop in the molar Ca/Si ratio of the C-S-H (Berner, 1988; 1992; Trägårdh and Lagerblad, 1998; Harris et al., 2002).

$$\boldsymbol{x}\mathbf{CaO{\cdot}SiO_2{\cdot}}\ \boldsymbol{n}\mathbf{H_2O} + \boldsymbol{y}\mathbf{H_2O} \rightarrow (\boldsymbol{x}-\boldsymbol{y})\mathbf{CaO{\cdot}SiO_2}\cdot\boldsymbol{n}\mathbf{H_2O} + \boldsymbol{y}\mathbf{Ca(OH)_2} \quad \textbf{(Equation 2.1)}$$

When C-S-H is progressively (dynamically) leached by deionised or pure water, higher Ca/Si ratio C-S-H phases dissolve first by incongruent dissolution where the Ca/Si ratio of the leachate is higher than that in the solid phase, and the Ca/Si ratio of the remaining C-S-H gel declines (Atkinson et al., 1985; Berner, 1988; 1992; Harris et al., 2002; Hidalgo et al., 2007; Baston et al., 2012; Segura et al., 2013; Walker et al., 2016). During this stage, dissolution of C-S-H gels produces trace amounts of dissolved SiO_2 as it is Ca which is preferentially leached (Berner, 1992; Faucon et al., 1998). Baston et al (2012) divided stage 3 into 3a and 3b (Figure 2.3), where incongruent dissolution of C-S-H controls the decline in pH from 12.5 to ~9.8 (Stage

3a), with continued leaching of C-S-H phases (Baston et al., 2012). Decalcification and incongruent leaching of C-S-H gels proceed until the Ca/Si ratio of the solid C-S-H is around ~0.8 to 0.9, after which it dissolves congruently (Stage 3b), meaning the Ca/Si ratio of the aqueous phase is equal to that in the solid phase (Berner, 1992; Harris et al., 2002). Congruent leaching at Ca/Si = 0.8 is the same as the natural composition of tobermorite (Berner, 1992). A comprehensive review of C-S-H solubility data at near-equilibrium can be found in Walker et al. (2016) and recent model developments on the durability of cement in the context of radioactive waste disposal can be found in Jacques et al. (2021).

After all C-S-H, AFm and AFt phases have been leached out, calcite and any aggregates plus the groundwater composition will control the pore solution composition (Figure 2.3 Stage 4) (Jacques et al., 2010; Baston et al., 2012). However, this entire degradation process (particularly by water) occurs very slowly and is highly dependent on the cement composition and groundwater composition (Andersson et al., 1989). For example, Atkinson et al. (1988) calculated that cement in a radioactive waste repository leached with a synthetic groundwater would likely maintain pH above 10.5 for several hundred thousand years, but when leached with deionised water it would be on the order of million years where a low flow rate is expected.

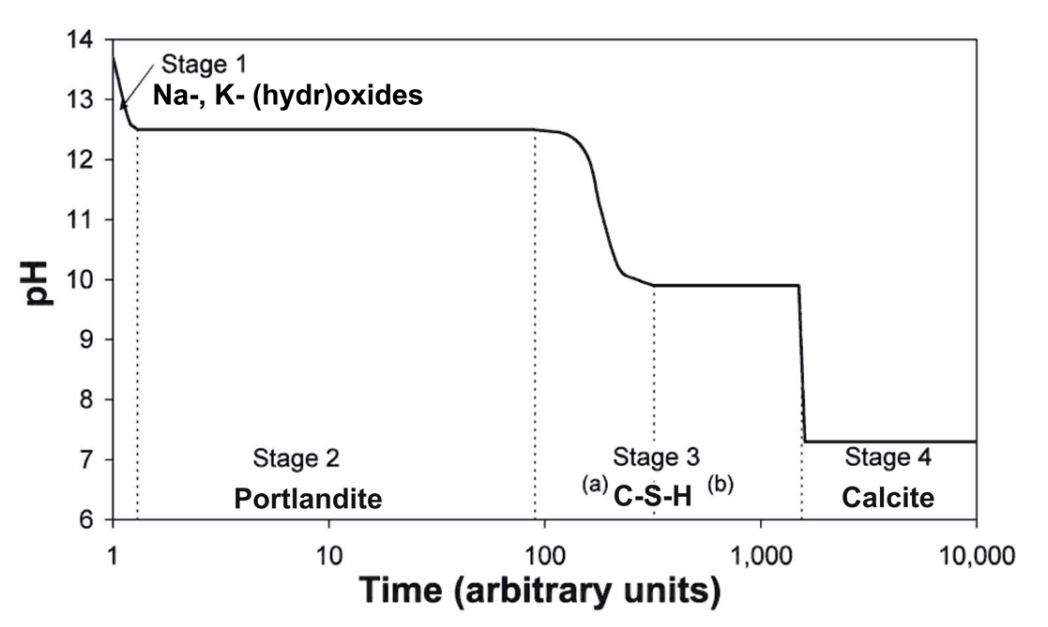

Figure 2.3 Stages of long-term pH evolution of cement leached by water, adapted from Baston et al. (2012) based on information in Wang et al. (2009), Lagerblad (2005) and Jacques et al. (2010). Stage 1 is controlled by Na and K (hydr)oxides with pH above 12.5; Stage 2 is controlled by portlandite at pH 12.5; Stage 3 is buffered by the dissolution of C-S-H phases, first by incongruent leaching (Stage 3a) from pH 12.5 to ~9.8, and secondly by congruent dissolution of C-S-H (Stage 3b) at pH ~9.8. Stage 4 is controlled by dissolution of calcite and the groundwater composition.

Generally, the sequence of the cement degradation reactions (Figure 2.3) are not affected by the composition of the attacking water, but the duration of the stages are strongly dependent on the composition of the attacking water (Jacques et al., 2010). Often, leaching experiments use pure water (Faucon et al., 1996; 1997; 1998; Gérard et al., 2002), mineralised water (Berner, 1992; Moranville et al., 2004) or acidic leachants such as ammonium nitrate in order to accelerate the leaching process (Moranville et al., 2004). In many studies it is found that pure water is more aggressive than mineralised water (Faucon et al., 1998; Moranville et al., 2004; Hartwich and Vollpracht, 2017). This is because carbonate ions present in mineralised water react with Ca ions leached from the cement phases which precipitate as calcite on the concrete surface, which protects the core of the concrete from further dissolution (Hartwich and Vollpracht, 2017). This reaction is known as carbonation, which is well-known degradation process affecting cementitious phases.

2.5.1 Carbonation

Carbonation is the reaction of atmospheric CO_2 with cement hydrate phases in the presence of moisture, as gaseous CO_2 cannot react directly with the phases (Neville, 1995). It is a common reaction that contributes to the degradation stages of cement described above in Figure 2.3 (Section 2.5), driving calcium leaching from CH, C-S-H and AFt or AFm phases, which ultimately lowers the alkalinity of the pore solution (Neville, 1995; Morandeau et al., 2014; Šavija and Luković, 2016).

When in contact with air, carbonation begins with the dissolution of atmospheric CO_2 into cement pore water according to Equation 2.2 and 2.3, controlled by the inward diffusion of gaseous CO_2 and carbonate ions (Lagerblad, 2005). The carbonate species present depends on the pH of the water. At neutral pH, carbonic acid will dissociate into bicarbonate, but in the pore solution of (non-carbonated) concrete, bicarbonate will dissociate into carbonate ions (Equation 2.4) as pH is high (above pH 10).

$$\mathbf{CO_2 + H_2O \rightleftharpoons H_2CO_3} \qquad \textbf{(Equation 2.2)}$$

$$\mathbf{H_2CO_3 \rightleftharpoons H^+ + HCO_3^-} \quad \mathbf{pK_a = 6.35} \qquad \textbf{(Equation 2.3)}$$

$$\mathbf{HCO_3^- \rightleftharpoons H^+ + CO_3^{2-}} \quad \mathbf{pK_a = 10.33} \qquad \textbf{(Equation 2.4)}$$

The carbonate ions react with the calcium ions in the pore solution (Equation 2.5), precipitating calcium carbonate either as an amorphous form or one of the polymorphs calcite, vaterite or aragonite (Groves et al., 1991; Taylor, 1997; Ekström, 2001; Glasser et al., 2008; Šavija and Luković, 2016). Usually, calcite is the main product formed over time (Lagerblad, 2005).

$$\mathbf{Ca^{2+} + CO_3^{2-} = CaCO_3} \qquad \textbf{(Equation 2.5)}$$

The precipitation of calcium carbonate can drive the dissolution of portlandite where carbonate ions are present in excess (Equation 2.6), forming more calcium carbonate (Lagerblad, 2005). The dissolution of portlandite (and precipitation of calcium carbonate in the presence of carbonate ions) typically occurs before decalcification of C-S-H (Glasser and Matschei, 2007; Morandeau et al., 2014). Calcium carbonate typically covers portlandite crystals, which can slow the carbonation rate with time (Groves et al., 1991). It is known that a carbonation layer is formed at the surface which will grow inwards, and the process becomes diffusion controlled as carbonate species must diffuse through the carbonated layer to reach the material interior

(Neville, 1995; Engelsen et al., 2012). The precipitation of calcium carbonate causes pore blocking due to its low solubility, which reduces the porosity and permeability of concrete and can reduce further degradation of cement pastes (Taylor, 1997; Johannesson and Utgenannt, 2001; Moranville et al., 2004; Hartwich and Vollpracht, 2017).

$$Ca(OH)_2 + H^+ + HCO_3^- \rightleftharpoons CaCO_3 + 2H_2O \qquad \textbf{(Equation 2.6)}$$

Once all CH is consumed, the pH and the concentration of calcium ions in the pore solution drop which drives the dissolution and decalcification of C-S-H (Equation 2.7) (Bonen and Sarkar, 1995; Taylor, 1997; Ekström, 2001; Lagerblad, 2005). The decalcification of C-S-H gel (Equation 2.7) reduces its Ca/Si ratio, much like degradation by water, and produces calcium hydroxide which is carbonated to form calcite like in Equation 2.6 (Garrabrants et al., 2004; Lagerblad, 2005). When the Ca ion concentration and pore solution pH declines, Ca-containing phases AFm will decompose at pH 11.6 forming ettringite and aluminate, followed by the decomposition of ettringite at pH 10.5, releasing aluminium hydroxide and sulphate ions that can diffuse inwards and precipitate as gypsum, new ettringite or metal hydroxides in the carbonated regions (Lagerblad, 2005) (Table 2.1; Figure 2.4).

$$x\text{CaO.SiO}_2\text{.H}_2\text{O} + y\text{H}_2\text{O} \rightarrow (x\text{-}y)\text{CaO.SiO}_2\text{.}\ n\text{H}_2\text{O} + y\text{Ca(OH}_2\text{)} \qquad \textbf{(Equation 2.7)}$$

The final products of carbonation (Equation 2.8) transform C-S-H gel into an amorphous, Ca-poor silica gel, calcium carbonate and water (Bonen and Sarkar, 1995). Some Ca ions will remain in the silica gel (Lagerblad, 2005). Fully carbonated concrete has a pore solution pH below 9, which can be as low as 8.3, indicating a calcite-controlled system (Papadakis et al., 1992; van der Sloot, 2000; Šavija and Luković, 2016). According to Lagerblad (2005), the Ca/Si ratio of C-S-H is around 0.85 when pH is <9.2 (as indicated by phenolphthalein colour change) (Engelsen et al., 2005).

$$\text{C-S-H} + HCO_3^- \rightarrow CaCO_3 + SiO_{2(gel)} + H_2O \qquad \textbf{(Equation 2.8)}$$

CCW is likely to be carbonated to varying degrees, during the service life of the concrete prior to crushing, or after crushing (Engelsen et al., 2009; Chen, J. et al., 2012; Butera et al., 2014). Carbonation will mostly occur after crushing, due to increased surface area as well as exposure of uncarbonated concrete (Engelsen et al., 2005; Lagerblad, 2005; Butera et al., 2014). When CCW is used as backfill or infill for

subsurface structures, it will be subject to carbonation with time through interaction with carbonated water from groundwater percolation and surface rain infiltration (Bonen and Sarkar, 1995). Carbonation and leaching occur intermittently in the field (Van Gerven et al., 2006). In the field, carbonation will depend on whether concrete is saturated in water or intermittently wetted, as CO_2 diffuses around 10,000 times faster in air than in water, so carbonation occurs faster in partially filled pores (van der Sleet et al., 1997).

In summary, carbonation affects the composition of cementitious phases responsible for controlling the pore solution composition, pH and leachant composition with time. Table 2.1 summarises the phase changes caused by carbonation, similar to stages in Figure 2.3 describing leaching with time. Figure 2.4 shows the solubility of cement phase hydrates and metal hydroxides with decreasing pH.

Table 2.1 Phase changes in the carbonation process using cement notation. The pore solution is buffered by CH, AFm and AFt which decompose through the stages. C-S-H releases CH, resulting in a progressively lower Ca/Si ratio indicated by C-S-H (1), (2) and (3) where increasing number indicates decreasing Ca/Si ratio, which is linked to a lower pH (Chen, J.J. et al., 2004). After Lagerblad (2005), courtesy of Svensk Kärnbränslehantering AB (SKB).

Intact concrete	**Stage 1**	**Stage 2**	**Stage 3**	**Carbonated**
CH	……..	……..	……..	……..
C-S-H (1)	C-S-H (1)	C-S-H (2)	C-S-H (3)	S-H (with some CaO)
	CC	CC	CC	CC
AFm	AFm	AFt/$Al(OH)_3$	$Al(OH)_3$	$Al(OH)_3$
AFt	AFt	AFt	$Fe(OH)_3$	$Fe(OH)_3$
pH >12.5	pH <12.5	pH <11.6	pH <10.5	pH <10

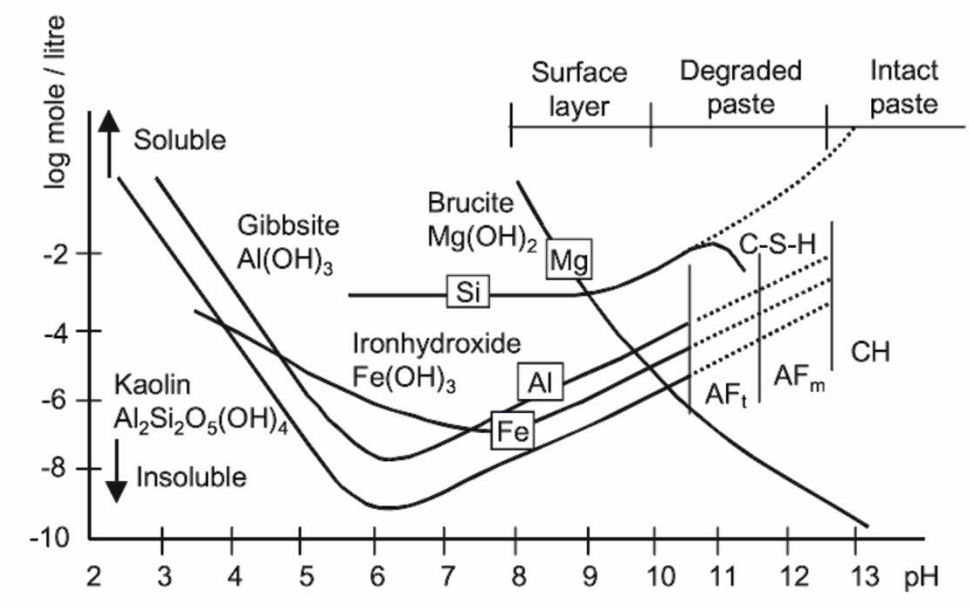

Figure 2.4 Solubility of cement paste hydrates and metal hydroxides with decreasing pH. After Lagerblad (2001), courtesy of SKB.

The degradation of cement paste by carbonation and water leaching causes the formation of compositional regions in monolithic cement paste: a carbonated surface layer rich in silica and depleted in portlandite, followed by a partly carbonated and degraded front where the inner region may have secondary precipitations of ettringite, AFm and calcite and an outer region where these secondary precipitations dissolve (Faucon et al., 1997; 1998; Glasser et al., 2008). The partly carbonated/degraded zone surrounds an inner uncarbonated matrix with higher Ca and possibly CH still intact (Bonen and Sarkar, 1995; Carde et al., 1996; Garrabrants et al., 2004; Gervais et al., 2004; Van Gerven et al., 2006). There is also a gradient of decalcified C-S-H from a low Ca/Si ratio C-S-H at the surface to higher Ca/Si ratios in the inner unleached/intact region (Carde et al., 1996; Faucon et al., 1997; 1998; Glasser et al., 2008).

2.6 Chemical composition of crushed concrete leachates

The chemical composition of crushed concrete leachates is dependent upon the composition and solubility of the cement phases, the pH of the pore solution, as well as parameters that can affect leaching. The composition of water in contact with crushed concrete surfaces will depend on the solubility of the phases at the solid-water interface. In the environment, constituents in groundwater (carbonate, sulphate, chloride, magnesium) will react with cement hydrates and induce a series of dissolution and precipitation reactions (Lagerblad, 2001; Walker et al., 2016). Therefore, investigation into material leaching behaviour is conducted in laboratory tests to gain

an understanding of how crushed concrete produces high pH leachates and what effect this can have on element release. Although the use of deionised water in laboratory experiments is more aggressive than conditions expected in the field (Hartwich and Vollpracht, 2017), it is useful for comparing leaching behaviour between different studies, and how this compares to field test conditions.

Several studies have covered the leaching behaviour and chemical composition of crushed concrete material in the context for evaluating the environmental behaviour and suitability for reuse in geotechnical applications such as road and pavement construction (Engelsen et al., 2009; 2010; 2012; 2017; 2020; Kang et al., 2011; Chen, J. et al., 2013; Roque et al., 2016; Gupta et al., 2018; Zhang, Y. et al., 2018; Dhir et al., 2019; Oliveira, F.D. et al., 2020) and backfilling (Engelsen et al., 2006; Rahman, M. et al., 2014; Coudray et al., 2017; Liu et al., 2020). Studies on CDW are also valuable resources for studying leaching behaviour as they are usually dominated by CCW (Delay et al., 2007; Wehrer and Totsche, 2008; Butera et al., 2014; 2015a).

2.6.1 pH of crushed concrete leachates

The pH of crushed concrete leachates is determined by the material composition, which may vary based on the source of the concrete, cement composition, cement additives (e.g. fly ash, steel slag) and weathering of the crushed concrete during storage in stockpiles (Butera et al., 2014; Natarajan et al., 2019).

In laboratory investigations using deionised water, the pH of crushed concrete leachates is reported to range between 7.7 and 13 (Steffes, 1999; Townsend et al., 1999; Lopez Meza et al., 2008; Engelsen et al., 2009; Mulugeta et al., 2011; Chen, J. et al., 2013; Butera et al., 2014; Galvín et al., 2014b; Abbaspour et al., 2016a; Bestgen et al., 2016a; Coudray et al., 2017; Saca et al., 2017; Gupta et al., 2018; Natarajan et al., 2019; Mahedi and Cetin, 2020; Sanger et al., 2020), depending on the extent of carbonation in the crushed material. In non-carbonated, freshly crushed concrete waste, the leachate pH is above pH ~12, and can be as high as pH 13 (Butera et al., 2014; Bestgen et al., 2016a; Abbaspour et al., 2016b), whilst carbonated concrete produces a pH from 7.7 to 11.9 (Sanchez et al., 2002; Garrabrants et al., 2004; Engelsen et al., 2009; Mulugeta et al., 2011; Chen, J. et al., 2013; Butera et al., 2014; Galvín et al., 2014a; Abbaspour et al., 2016a; Bestgen et al., 2016a; Natarajan et al., 2019; Mahedi and Cetin, 2020). Crushed concrete may be stockpiled for as long as 5 years in the CDW sector (Chen, J. et al., 2013) and during this time it may be weathered and carbonated, according to whether dissolved CO_2 is saturated (i.e. in

equilibrium with) the water in contact with the CCW. Carbonated concrete is associated with lower pH leachates as carbonation neutralises OH^-, reducing leachate alkalinity whilst the least carbonated material is associated with alkaline leachates (Engelsen et al., 2009; Mulugeta et al., 2011; Chen, J. et al., 2013; Bestgen et al., 2016b).

Crushing and atmospheric exposure have a significant influence on leachate pH (Engelsen et al., 2005; Mulugeta et al., 2011; Bestgen et al., 2016a; Mahedi and Cetin, 2020). The particle size of crushed concrete used in laboratory investigations can impact leachate pH, dependent on whether the material is crushed for laboratory experiments. When size fractions are not crushed for experiments, leachate pH has been reported to be slightly lower for finer size fractions due to the increased number of reaction surfaces on which carbonation may occur, producing lower pH leachates (Zhang, Y. et al., 2018; Natarajan et al., 2019). On the other hand, the opposite trend may occur where pH is highest for finer particles (when they are uncarbonated) which have a greater surface area available for leaching relative to the coarser particles (Coudray et al., 2017). When the material is further crushed for experiments, the pH obtained is typically higher than non-crushed material because crushing exposes non-carbonated cement phases responsible for high pH leachates (van der Sloot, 1996; Lee et al., 2012; Butera et al., 2015a; Abbaspour et al., 2016a). Moreover, Engelsen et al. (2009) found cement paste concentrated in finer size fractions and found that smaller particle sizes had a lower material pH than coarser grain sizes, attributable to carbonation. On the contrary, a particle size effect on leachate pH is not always found; when CCW was fractionated, Bestgen et al. (2016a) found pH was stable across nine different size fractions, and instead concluded pH was more dependent on the material composition rather than the particle size. As leaching in the field will use different particle sizes that are not crushed to fine fractions, leachate pH will likely be lower than that measured in laboratory tests using samples that have been crushed. Overall, the particle size effect on pH will vary depending on the material composition and the extent of carbonation, which will be affected by stockpiling.

The pH of crushed concrete leachates may also vary between different laboratory methodologies including batch tests (Engelsen et al., 2009; 2010; Butera et al., 2014; Abbaspour et al., 2016a), up-flow column tests (Chen, J. et al., 2013; Gupta et al., 2018) or lysimeters (Delay et al., 2007; Lopez Meza et al., 2008; 2010; Butera et al., 2015a). The leachate pH in batch and up-flow column tests are usually in the same range (pH 10-12.5) with variation typically attributed to carbonation at particle surfaces and particle size effects, although increasing L/S may lead to declines in leachate pH in

column tests (e.g. Delay et al. (2007)) or batch tests that vary L/S (Gupta et al., 2018). In column tests, pH is reported to either stay high (maintained between pH 10.8 and 12 for 100 pore volumes of flow, (Chen, J. et al., 2013)) or slightly decrease with time (from pH 12.5 to 11.5 with increasing L/S up to L/S=20, (Delay et al., 2007)). Contrary to batch and up-flow column tests, lysimeters usually produce relatively lower pH leachates (around pH 7-9.5) as slower leachate collection times from percolation results in longer contact with carbon dioxide in the air causing neutralisation of alkalinity and possible precipitations which reduce Ca leachate concentrations, which are correlated with leachate pH (Delay et al., 2007; Butera et al., 2015a; Roque et al., 2016). Similarly, in unsaturated down-flow column tests leachate pH is lower than under saturated conditions because carbonation of cement phases at particle surfaces can occur (Lopez Meza et al., 2009; Sanger et al., 2020). However, Butera et al. (2015a) found that it was the particle size difference between up-flow columns (crushed, <4 mm) and down-flow lysimeters (not crushed, <40 mm) along with different flow patterns and the 3-day pre-equilibration period for up-flow columns that caused a lower leachate pH in the lysimeters. Overall, leachate pH variation between laboratory leaching tests may be attributed to the water contact time, exposure of the leachate to atmospheric CO_2 (which reduces pH) and particle size.

In the field, the leachate pH of crushed concrete used as road sub-base has been recorded to initially be high (12.6; the same pH as the material pH) which then progressively lowered to near-neutral pH (7.3 to 8.7) after one to ten years (Mulugeta et al., 2011; Engelsen et al., 2012; 2017). Other authors found that pH was consistently maintained at near-neutral values (pH 6.6 to 8) initially, after seven months (Chen, J. et al., 2013) and after eight years (Natarajan et al., 2019). The initial material pH of the field samples was conducted in batch experiments and was consistently above pH 11 (Engelsen et al., 2012; Chen, J. et al., 2013), so the lower leachate pH is attributed to weathering and carbonation occurring from percolating water (Chen, J. et al., 2013; Engelsen et al., 2017). However, this trend is not always the case as Chen, J. et al. (2013) also found that crushed concrete stockpiled for 5 years had a material pH between 10.9 to 11.8 (depending on particle size, with decreasing pH associated with decreasing particle size) that in another field test site produced a low pH leachate initially (pH 7.3, presumed controlled by surface carbonate layers) that rose upward to pH 12.1 after 2 pore volumes of flow). The authors attribute this high pH leachate to water residence time, surface area and saturation (Engelsen et al., 2012; Chen, J. et al., 2013). This study indicates the heterogeneity in crushed concrete material

composition, even when stockpiled and carbonated. Fundamentally, the pH of crushed concrete leachates in field applications will depend on neutralisation reactions, primarily from carbonation reactions with atmospheric CO_2, soil vapour CO_2 and soil acidity (Gupta et al., 2018; Oliveira, F.D. et al., 2020).

Whether experiments are conducted in the laboratory or in the field determines the leachate pH, and laboratory experiments are associated with higher pH leachate generation for extended periods of time whilst field investigations usually show an initial high pH that progressively declines to near neutral over time. Field investigations are promising because this alleviates concerns with long-term high pH generation from CCW. Typically, the laboratory pH of the same crushed concrete source is higher than measured in corresponding field studies. Chen, J. et al. (2013) and Natarajan et al. (2019) undertook laboratory investigations on the same CCW that was used in the field as road sub-base and found that column laboratory pH measurements (pH 10.8 to 12.5) were always higher than those taken in the field. It is hypothesised that this discrepancy is due to percolating water causing carbonation and preferential flow patterns (Chen, J. et al., 2013), as well as agitation what may have removed the protective carbonate covering, exposing non-carbonated surfaces in laboratory experiments (Natarajan et al., 2019). Differences between field and laboratory experiments may also be due to redox conditions, as Kosson et al. (2014) found that field is likely to be mildly to strongly reducing, whilst laboratory conditions are usually more oxidised (Butera et al., 2015a).

Overall, the pH recorded is influenced by the material composition (affected by stockpiling conditions, weathering and carbonation, possibly particle size) as well as experimental methodology (experiment type – batch, dynamic/column) and varying factors (e.g., L/S, saturation). Ultimately, the main factor determining the pH of crushed concrete leachates is the presence of cement hydrate phases, which vary due to carbonation and degradation processes.

2.6.2 Major and trace element composition

The major constituents of leachates from crushed concrete are calcium, aluminium, iron, sulphates, carbonates, potassium, silica and hydroxide ions, which are derived from the dissolution of the cement hydrate phases (Tränkler et al., 1996; Limbachiya et al., 2007; Engelsen et al., 2009; van der Sloot et al., 2009; Coudray et al., 2017).

Trace elements such as As, Ba, Cd, Co, Cr, Cu, Li, Mn, Mo, Ni, P, Pb, Sb, Se, Sr, V and Zn may be present in crushed concrete leachates because they are found in

cement hydration products (Vollpracht and Brameshuber, 2016), cement additives such as slag or fly ash that are known to leach heavy metals (Cetin et al., 2012; Müllauer et al., 2012; 2015; Aydilek, 2015b; Gupta et al., 2018; Eštoková and Oravec, 2021) or they may be introduced by demolition and recycling processes that could introduce contaminants (Gupta et al., 2018). Regarding cement additives, which replace the amount of cement used, the contribution to the leachate composition may be negligible or enhanced (Müllauer et al., 2015; Nagataki et al., 2002; Yu et al., 2005). For example, increased fly ash content, which can contain more alkalis and trace metals (e.g., V, Cr, Pb, Cd, V), increases the total metal composition of concrete, but this can have varying effects on leachate composition. Cements with an increased fly ash content and water to binder ratio have been shown to generally leach higher heavy metal concentrations in Nagataki et al. (2002) and Yu et al. (2005). However, Müllauer et al. (2015) found that whilst V release was enhanced, Cr release was not, so the effect on leachate composition varies. Although, it is noted that the heavy metal concentrations leached are generally small overall (Nagataki et al., 2002), with Müllauer et al. (2015) finding that only 2% of the total V concrete composition was released in tank leaching tests. This was attributed to low solubility of V at the pH conditioned by the concrete (pH 11.5 ±0.3; Müllauer et al., 2015). Also, alkali release may be lower when cement is replaced by fly ash as fly ash can densify the concrete microstructure and reduce release (Mullauer et al., 2015). Rebar, which is present in reinforced concrete, would be likely removed from concrete (for recycling) prior to use in backfilling operations; for example, a uranium processing facility in Ranstad, Sweden submitted planned to use building rubble with rebar and the lining removed for backfilling voids on-site (Nuclear Energy Agency, 2017). However, if rebar was present, the passive iron film (ferrous oxide) that covers the steel would degrade once the pore solution lowers below 9.5 (Huet et al., 2005; Green, 2020; Šavija and Luković, 2016). Therefore, it could be assumed that rebar would contribute to the concentration of Fe in crushed concrete leachate where the alkalinity of the pore solution, which maintains the passivity of steel, was depleted due to degradation processes which can lower pore solution pH (i.e. carbonation and leaching). However, this would only be the case if rebar was present.

Contaminants can leach directly from the dissolution of phases at concrete surfaces and/or diffuse from the pore solution to concrete surfaces (Müllauer et al., 2012; Kovalcikova and Estokova, 2014). The release of contaminants depends on their solubility in cement hydrate phases, the formation of aqueous complexes and

precipitation of phases that limit solubility (Müllauer et al., 2012; Kovalcikova and Estokova, 2014). The release of oxyanion-forming elements (e.g., As, Cr, Mo, Se, V) can occur in CCW and CDW leachates, and primarily Cr and Se are problematic (Engelsen et al., 2010; Butera et al., 2014; 2015a;b). Oxyanions are formed by a covalent bond between oxygen and the metal, and oxyanions form when elements are close to oxygen in electronegativity (the ability of an element to attract shared electrons) such as Cr and Mo respectively forming CrO_4^{2-} and MoO_4^{2-} (Shriver and Atkins, 1999; Engelsen et al., 2010).

The relative proportions and concentrations of each element leached will vary based on the cement composition and the extent of degradation and carbonation of the cement, therefore there will be variations between studies as CCW is heterogeneous (Mahedi and Cetin, 2020). In CDW studies, the relative concentrations will also vary based on other CDW materials that may be mixed in with the crushed concrete such as masonry and ceramics (Del Rey et al., 2015).

2.6.3 Factors affecting element release

During the service life of concrete, metals are not leached to significant degrees, but they may be leached after concrete is crushed and used in secondary applications such as unbound aggregate, which warrants leaching investigations prior to reuse (van der Sloot, 2000; Johnson, 2004). The major and trace element composition of CCW leachates have been studied in various laboratory tests including batch tests which may vary parameters such as L/S and particle size (Chen, J. et al., 2012; Galvín et al., 2012; Butera et al., 2015a; Bestgen et al., 2016a;b; Coudray et al., 2017; Zhang, Y. et al., 2018; Natarajan et al., 2019), pH-dependent batch tests which evaluate solubility controlling phases (often with geochemical speciation modelling) (Engelsen et al., 2009; 2010; Galvín et al., 2012; Mahedi and Cetin 2023) and column tests which investigate leaching mechanisms associated with leachant renewal, L/S, contact time and saturation (Steffes, 1999; Delay et al., 2007; Lopez Meza et al., 2008; 2009; 2010; Chen, J. et al., 2013; Del Rey et al., 2015; Butera et al., 2015a; Saca et al., 2017; Gupta et al., 2018).

When crushed concrete is in contact with water, the pH of the leachate and leachant, and extent of carbonation are significant factors that determine element release (van der Sloot, 1996; Natarajan et al., 2019). Major element chemistry is an important factor that dictates contaminant release, as major elements control the pore solution composition and the pH (van der Sloot, 1996). Precipitation and dissolution of Ca and

Mg have a significant influence on leachate pH (Izquierdo and Querol, 2012; Bestgen et al., 2016a; Mahedi and Cetin, 2020). Although pH is a significant factor affecting leaching behaviour, other experimental factors also affect leaching (Diotti et al., 2020). The leachate composition is affected by the factors that control and affect element release: chemical, (e.g pH, buffer capacity, chemical speciation), physical (permeability, particle size, porosity), and experimental parameters (e.g leachant renewal, L/S) (Figure 2.5). Factors affecting release of all elements are shown in Figure 2.5, although not all factors are equally significant (van der Sloot and Dijkstra, 2004). A review of the significant factors relevant to the laboratory investigations is provided below on carbonation, pH variation and L/S ratio and particle size. The pH is the most significant due to pH-dependent processes controlling solubility, and the extent of carbonation varying between CCW, which changes the pore solution pH and mineralogy of CCW. pH significantly impacts the leaching of heavy metals (Galvín et al., 2012).

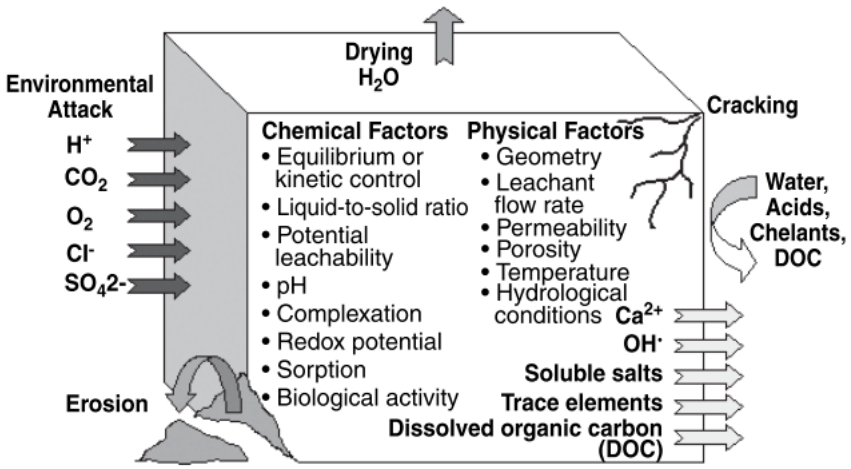

Figure 2.5 Factors affecting leaching rates from solid materials. After Garrabrants and Kosson (2004) and information in van der Sloot and Dijkstra (2004), reproduced with permission.

Often, the total composition of crushed concrete is reported alongside leachate concentrations, however there are not conclusive relationships between total content and leachability, with some studies reporting a positive correlation between Al, S, Ca and Si leachability (Limbachiya et al., 2007) and others not finding any correlation with Cr (van der Sloot, 2000) in mortar or Cu in RCA/CCW (Bestgen et al., 2016a). Therefore, the total content is not necessarily a reliable indicator of the chemical composition of crushed concrete leachates and this was found by several studies (van

der Sloot, 2000; Kosson et al., 2002; van der Sloot and Dijkstra, 2004; Chen, J. et al., 2012; Bestgen et al., 2016a; Zhang, Y. et al., 2018; Eckbo et al., 2022). Therefore, leaching tests are essential to investigate release behaviour as a function of different chemical and physical factors.

2.6.3.1 Carbonation and release at material pH

Studies at the material pH are defined as the pH obtained using deionised water as the leachant, usually at a L/S of 10, which is specified in different leaching test frameworks such as EN 12457-2 (BSI 2002b), CEN/TS 14429 (CEN, 2015), or EPA method 1313 (Kosson et al.,1997). The release of elements at material pH is strongly affected by the carbonation of cement phases. Carbonation is the most significant leaching parameter as it affects pH, and generally all solubility-controlled reactions are pH-dependent, which is relevant for the establishment of equilibrium conditions in laboratory experiments. The effect of carbonation on element release at material pH (using deionised water) has been studied by several authors using CCW, which has a lower material pH than fresh concrete and is often sourced from stockpiles, often comparing it to freshly crushed concrete waste (Mahedi and Cetin, 2020; 2023), freshly produced concrete (Engelsen et al., 2009; 2010), or artificially carbonated CCW (Mulugeta et al., 2011). As CCW is often carbonated to varying degrees, the effect of carbonation on material pH and element is inherent in studies utilising CCWs (Engelsen et al., 2009; 2010; Mulugeta et al., 2011; Chen, J. et al., 2012; 2013; Butera et al., 2014; Bestgen et al., 2016a; Natarajan et al., 2019; Mahedi and Cetin, 2020). Therefore, it is important to consider how carbonation affects element release.

At material pH, the composition of the leachate will depend on the solubility of the cement phases. Lowest leaching for Ca, Mg, S and Si is observed at material pH, relative to other pH values, as cement phase hydrates are stable (Engelsen et al., 2009). The composition of major elements is determined by the cement phases. S and Si release is known to be greater at material pH for carbonated samples (Engelsen et al., 2009; Butera et al., 2015a; Mahedi and Cetin, 2023). As the major elements determine the composition of the leachate, this will largely control trace element leachability (van der Sloot, 1996). For example, the precipitation and dissolution of Ca and Mg has been shown to dictate the leachate pH, which therefore impacts the solubility of contaminant metals (Mahedi and Cetin, 2020; 2023). Leaching of trace element contaminants will depend on pH-dependent processes such as mineral precipitation and dissolution, sorption to Fe and Al hydroxides, and complexation with humic substances (e.g., for Cu) (Engelsen et al., 2010; 2017; Gupta et al., 2018).

Higher calcium carbonate contents in CCW are associated with lower Ca leaching and lower leachate pH, indicating carbonated cements release lower concentrations of Ca (Mahedi and Cetin, 2020). In the leachate of carbonated cements, the solubility of calcium is lower as calcite is insoluble at higher pH values (above pH 10) and is far less soluble than portlandite in non-carbonated cements (Garrabrants et al., 2004; Butera et al., 2014; Komonweeraket et al., 2015; Mahedi and Cetin, 2020). On the contrary, higher Ca concentrations in leachates are associated with higher leachate pH (Cetin et al., 2012; Bestgen et al., 2016a; Mahedi and Cetin, 2020) and alkalinity as dissociation of CaO and portlandite increases Ca release and leachate pH (Mahedi and Cetin, 2020). The release of sodium and potassium is also lower in carbonated cement leachates relative to non-carbonated cement leachates (Garrabrants et al., 2004). This was also observed in Butera et al. (2014), who found that carbonated concrete leachates (pH between 10.5 and 11.9) had a lower release of Ca, Sr, Ba, Na and K relative to lesser carbonated CCW leachates. The release of Si in carbonated leachates is typically higher than non-carbonated leachates because C-S-H is transformed into a silica gel through carbonation, and silica gel is soluble at alkaline pH so enhanced Si release occurs (Engelsen et al., 2009; 2012; Chen, J. et al., 2013).

The trace element concentrations of carbonated concrete vary based on the leachate pH dictated by the concrete as well as the material composition. As the pH of highly alkaline material is lowered (e.g., by carbonation) release of oxyanionic species are found to increase because of high solubility at mild alkaline to neutral pH (van der Sloot, 2000; 2002; Mulugeta et al., 2011). When pH approaches neutral, the surface charge of concrete will become more negative due to carbonation of C-(A)-S-H/C-S-H, which can lead to the incorporation of aluminium originating from the decalcification of AFm and AFt phases (Saillio et al. 2014) and the transformation of C-S-H into a silica gel, which is negatively charged (Langmuir, 1997). Calcite, which may be present on the surfaces of carbonated concrete (Lagerblad, 2005), could have a positive charge if the solution is saturated with respect to calcium carbonate and in contact with atmospheric CO_2 at neutral pH (Zachara et al., 1990; Heberling et al., 2014). Otherwise, the surface charge of calcite is likely to be negative across pH 5-11 (according to surface complexation models reported in Al Mahrouqi et al. (2017)), which encompass the pH range of carbonated cement leachates (Lagerblad, 2005; Section 2.5.1 on carbonation). The speciation of oxyanion-forming elements As, Cr, Mo, Sb, Se and V in carbonated CCW leachates was studied by Mulugeta et al. (2011), where they reportedly had an enhanced release and predominantly existed as

oxyanions in solution. In fresh concrete (non-carbonated) samples, the same elements were also found predominantly in their anionic form at neutral pH (Mulugeta et al., 2010a). This suggests the net surface charge of concrete is indeed negative as pH is lowered, as a higher solubility of oxyanions in solution implies repulsion from similarly negatively charged surfaces.

Mulugeta et al. (2011) compared the oxyanion composition of material pH leachates using CCW from a stockpile (several years old; pH 11.5) and from a recycling facility (pH 11.9), with four freshly made concrete samples (pH 12.4-12.5), and a portion of each fresh concrete sample was artificially carbonated (pH 10.3-11.8). In the carbonated leachates, oxyanion release was enhanced, particularly for the artificially carbonated samples, relative to the non-carbonated leachates (Mulugeta et al., 2011). The authors (Mulugeta et al., 2011) report that their study results finding enhanced solubility of oxyanions are in agreement with existing works that show enhanced release from carbonated cementitious materials for As (Venhuis and Reardon, 2001; Sanchez et al., 2002; Garrabrants et al., 2004), Cr (Macias et al., 1997; Alba et al., 2001; Van Ginneken et al., 2004) and Mo, Sb and V (Van Ginneken et al., 2004). Mahedi and Cetin (2020;2023) also found higher release of Cr in carbonated CCW leachates. The solubility of oxyanions is greater in carbonated leachates, which have a lower pH relative to non-carbonated leachates, most likely because of the degradation of cement phases such as C-S-H (Halim et al., 2004) and ettringite containing the anionic species substituted for silicate or SO_4^{2-} respectively in their structures (Mulugeta et al. (2011), and references within). Enhanced sulphate release in highly carbonated CCW leachates also correlated with high Cr and Ca release and was attributed to the dissolution of AFm and ettringite phases as the material pH was below the respective equilibrium pH of 11.6 and 10.6 respectively (Komonweeraket et al., 2015; Engelsen et al., 2017; Mahedi and Cetin, 2020). Cr release was also found to be sensitive to Ca concentrations and was attributed to the dissolution of chromate-ettringite solid solutions (Leisinger et al., 2010; Mahedi and Cetin, 2020).

As oxyanion-forming elements are present in carbonated CCW leachates, this would be relevant to radioactively contaminated land, which may have chromium present in low and intermediate level radioactive wastes (Rahman, Z. et al., 2023; IAEA, 2002; Cattant et al., 2008). Whilst this would have implications for the fate of carbonated CCW leachates on contaminated land, this is currently unknown and beyond the scope of this thesis, which is focused on non-active CCW.

2.6.3.2 Variation with pH

The pH of the leachant will impact the chemical composition of crushed concrete leachates. pH is a critical parameter that affects element release (Zhang, Y. et al., 2018) and can affect metal solubility by several orders of magnitudes as pH is varied (van der Sloot et al., 2008; Hartwich and Vollpracht, 2017). As such, pH-dependent tests are widely used for characterising how release behaviour may change over a wide range of pH values (Engelsen et al., 2009; 2010; Mulugeta et al., 2011). Investigations often compare freshly crushed (non- or partially carbonated) concrete to carbonated concrete (from increased atmospheric exposure after crushing in laboratory conditions or in stockpiles outside), as the pH-dependent leaching behaviour will depend on carbonation (Engelsen et al., 2009; 2010). pH-dependent batch tests are conducted under equilibrium conditions, which are dominated by solubility processes (Kosson et al., 2002; Bestgen et al., 2016a). The factors affecting metal release at equilibrium as pH is varied are displayed in Figure 2.6. Many leaching studies often use laboratory-based pH-dependent tests and geochemical speciation modelling to identify solubility-controlling phases (Engelsen et al., 2009; 2010; van der Sloot, 2002; Chen, J. et al. 2012; Butera et al., 2015a; Chen, Y. and Zhou, 2020). The leaching of major elements is controlled by the solubility of the cement paste hydrates (Engelsen et al., 2009) that are present (CH, C-(A)-S-H/C-S-H, calcium sulphoaluminates, alkalis Na and K if they’re not already leached out). However, there are notable differences between carbonated concretes with freshly produced concretes as pH is altered outside the material pH range (Engelsen et al., 2009; 2010).

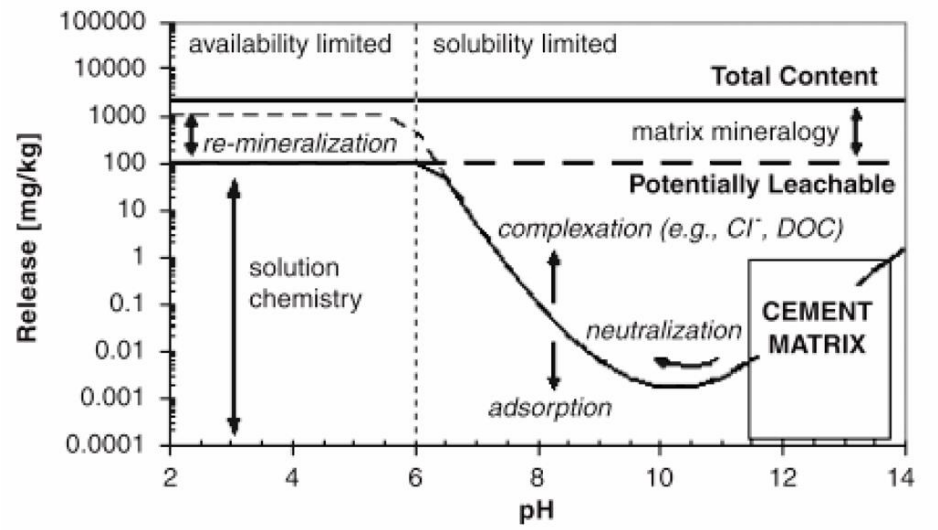

Figure 2.6 Factors controlling the leaching of metals at equilibrium conditions in different chemical environments. After Garrabrants and Kosson (2004) modified from van der Sloot (2000), reproduced with permission.

Acid neutralising tests are usually conducted alongside pH-dependent tests (e.g. Engelsen et al. (2009), Chen, J. et al. (2012; 2013); Natarajan et al. (2019); Mahedi and Cetin (2023)). The acid neutralising capacity (ANC) of CCW is crucial to release behaviour because it determines the ability of the CCW to maintain high pH alkaline conditions over time (van der Sleet et al., 1997). Highly carbonated CCW has been shown to have a lower ANC between pH 6 and 12, whilst lesser carbonated samples had a higher resistance to acid addition attributed to the presence of intact cement phases (Engelsen et al., 2009; Mahedi and Cetin, 2023). A plateau between pH 5 and 6 is usually observed in carbonated CCWs, indicating a higher buffering capacity in this pH range (Mahedi and Cetin, 2023). Major buffering for highly carbonated samples is only found below pH 8 (Engelsen et al., 2009), and at pH 5-6, where highly carbonated samples show the greatest ANC, indicating presence of calcium carbonate and absence of intact cement hydrate (Engelsen et al., 2009). This trend was also seen in Natarajan et al. (2019) and Chen, J. et al. (2012) in the fines (<0.075mm) which was shown to be the most carbonated size fraction.

When pH is raised above or lowered below the material pH range, the release of major, minor and trace constituents will vary. The leaching behaviour of metal cations and elements that form oxyanions will differ (Engelsen et al., 2010). Table 2.2 and 2.3 show how the maximum and minimum leaching of major and trace elements changes as pH is varied, along with the dominant oxidation state in CCW leachates and expected reduced species present in field conditions. Typical leaching patterns are shown in

Figure 2.7. K and Na may be considered as minor constituents in fresh concrete, but in CCW they may be leached out as they are highly soluble. In addition, K and Na often exhibit pH-independent leaching behaviour (Engelsen et al., 2009; 2010).

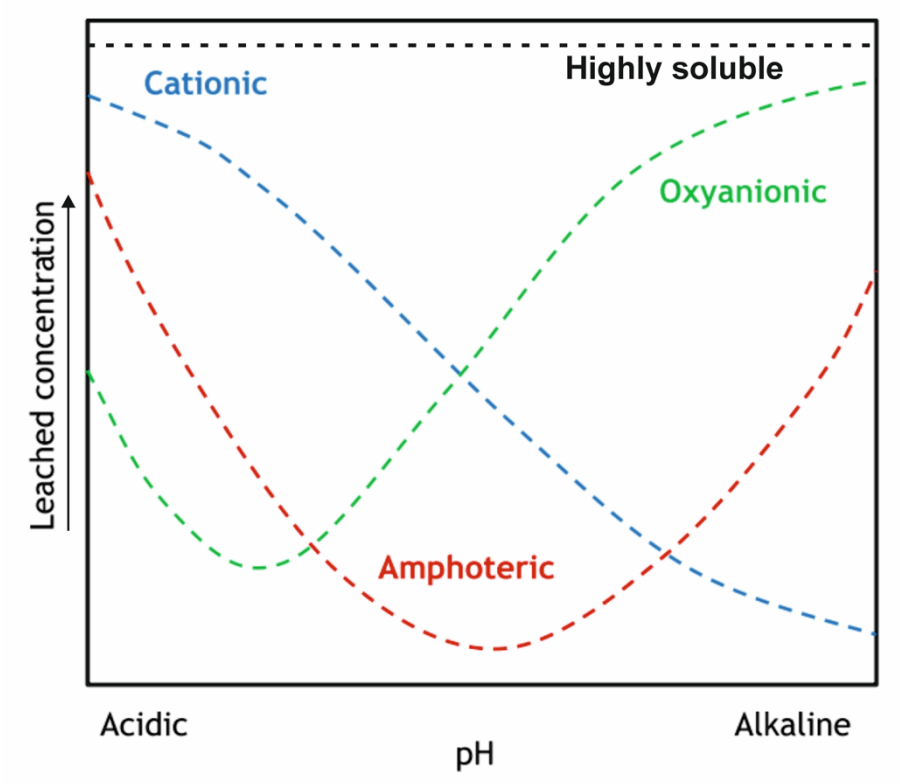

Figure 2.7 Conceptual diagram displaying broad leaching patterns (cationic, oxyanionic, amphoteric) as a function of pH. pH-independent leaching of highly soluble ions (e.g., Na^+, K^+) is indicated by a straight line. Adapted from Dhir et al. (2019) with permission.

Table 2.2 Dominant species of major elements and the leaching pattern as a function of pH in CCW laboratory leachates under oxic conditions (adapted from Dhir et al. (2019) and Daiber (2023) with permission). The laboratory experiments were conducted without atmospheric control and conditions are naturally oxidising (Butera et al., 2015a). As field conditions are expected to be mildly to strongly reducing (Butera et at al., 2015), reduced species are also indicated.

Dominant species in oxic CCW leachates	**Leaching pattern**	**pH where leaching is**		**Species produced in reducing conditions**	**References**
		Highest	**Lowest**		
Al(III)	Amphoteric; cationic	2-4; 13	5-9	Not reported	Abbaspour et al. (2016a), Butera et al. (2015a), Cho and Yeo (2004), Engelsen et al. (2009)
Ca(II)	Cationic	1-6	13-14	Not redox sensitive	Abbaspour et al. (2016a); Butera et al. (2015a;b), Engelsen et al. (2009), Lewis et al. (2015), Mahedi and Cetin (2023)
Fe(III)	Cationic	1-2	7-12	Reduced to Fe^{2+}	Abbaspour et al. (2016a), Bestgen et al. (2016a;b), Butera et al. (2015a), Cho and Yeo (2004), , Engelsen et al. (2009)
Mg(II)	Cationic	1-5	12-13	Not redox sensitive	Abbaspour et al. (2016a), Butera et al. (2015a), Engelsen et al. (2009), Mahedi and Cetin (2023)
Si(IV) as amorphous SiO_2	Cationic	1-3	11-13	Not reported	Butera et al. (2015a), Engelsen et al. (2009)
S(VI) as SO_4^{2-}	Cationic	2-6	11-13	Reduced to S(-II) **[1]**	Mahedi and Cetin (2023), Engelsen et al. (2009)

[1] O'Loughlin et al. (2021)

Table 2.3 Dominant species of trace elements and the leaching pattern as a function of pH in CCW laboratory leachates under oxic conditions (adapted from Dhir et al. (2019) and Daiber (2023) with permission). The laboratory experiments were conducted without atmospheric control and conditions are naturally oxidising (Butera et al., 2015a). As field conditions are expected to be mildly to strongly reducing (Butera et at al., 2015), reduced species are also indicated. The table is continued on the next page.

Dominant species in oxic CCW leachates	**Leaching pattern**	**pH where leaching is**		**Species produced in reducing conditions**	**References**
		Highest	**Lowest**		
As(V)	Constant Cationic	n/a 2-10	n/a 12 (material pH)	Reduction of As(V) to As (III) **[1]**	Butera et al. (2015a) Zhang, Y. et al. (2018); Chen et al. (2012)
Ba(II)	Cationic	2-4	12-13	Not reported	Butera et al. (2015a); Mahedi and Cetin, (2023)
Cd(II)	Cationic	1-3	>7	Not reported	Engelsen et al. (2010); Butera et al. (2015a)
Co	Amphoteric	3-4; 11-13	8-10	Not reported	Butera et al. (2015a)
Cr(VI); Cr(III)	Amphoteric; oxyanionic	1-3; 9-13	5-6.5	Cr(VI) reduced to Cr(III) **[2]**	Aydilek, (2015a);Butera et al. (2015a); Engelsen et al. (2010); Chen, J. et al. (2012); Edil et al. (2012); Bestgen et al., (2016a;b)
Cu(II)	Amphoteric; cationic	1-3; 13	7-10	Cu(II) reduced to Cu(I) or Cu(0) **[3]**	Chen, J. et al. (2012); Edil et al. (2012); Aydilek, (2015a); Abbaspour et al. (2016a); Bestgen et al.(2016a;b);Engelsen et al. (2010); Lewis et al. (2015)
Li(I)	Cationic	4-6	13	Not reported	Butera et al. (2015a)
Mn(II)	Cationic	1-3	10-12	Already in the most reduced form. **[4]**	Cho and Yeo (2004); Engelsen et al. (2010); Butera et al. (2015a)

[1] Kosson et al. (2017)
[2] Eckbo et al. (2022). Kosson et al. (2014).
[3] Lockwood et al. (2015); Fulda et al. (2013); Weber et al. (2009).
[4] Garrabrants and Kosson (2014); Rumsby et al. (2014)

Table 2.3 Continued

Dominant species in oxic CCW leachates	Leaching pattern	pH where leaching is		Species produced in reducing conditions	References
		Highest	Lowest		
Mo(VI)	Amphoteric; oxyanionic	1-2; 6-11	4	Reduction of Mo (VI) to Mo(V) and Mo(VI) species **[5]**	Engelsen et al. (2010); Butera et al. (2015a)
Ni(II)	Cationic	1-6	10-13	Ni(II) stable over different redox conditions, but can sorb to redox-sensitive species e.g. Mn, Fe so indirectly affected **[6]**	Engelsen et al. (2010); Butera et al. (2015a)
Pb(II)	Cationic	1-3	6-12	Not reported	Engelsen et al. (2010); Butera et al. (2015a)
Se(IV), Se(VI)	Constant	n/a	n/a	Se(VI) is not easily reduced to Se(IV) and solid phase speciation is maintained **[7]**	Butera et al. (2015a)
Sr(II)	Cationic	4-5	11-13	Not reported	Butera et al. (2015a)
V(V)	Amphoteric; oxyanionic	1-2; 9-11	4-7	Reduction of V(V) to V(IV) and V(III) **[7]**	Engelsen et al. (2010); Butera et al. (2015a);
Zn(II)	Amphoteric; cationic	1-3; 13	8-12	Not reported	Cho and Yeo (2004); Engelsen et al. (2010); Chen, J. et al. (2012); Edil et al. (2012), Lewis et al. (2015); Aydilek (2015a); Butera et al (2015a); Bestgen et al. (2016a;b)

[5] Torres et al. (2014); Wang (2012)

[6] Lockwood et al. (2015); Rinklebe and Shaheen (2017)

[7] Mulugeta et al. (2010b); Bye and Lund (1988); O'Loughlin et al. (2021)

Maximum leaching for all major elements (Al, Ca, Fe, Mg, S and Si) occurs when pH is most acidic, and at this pH leaching is similar for carbonated and non-carbonated (freshly produced concrete) (Engelsen et al., 2009; 2010; Lewis et al., 2015; Zhang, Y. et al., 2018). When pH is lowered below the material pH, major element concentrations rise as cement hydrate phases are dissolved and sorption is reduced (Engelsen et al.,

2009; Lewis et al., 2015; Mahedi and Cetin, 2023). Ca concentrations increase rapidly as dissolution of cement hydrates and calcite proceed (Bestgen et al., 2016a; Zhang, Y. et al., 2018). For example, Ca concentrations were around 2-3 x 10^4 mg/L from pH 2 to 12, which rapidly decreased above pH 12 (Zhang, Y. et al., 2018). Mg release patterns were similar, rapidly dropping from 2 x 10^4 mg/L from pH 2-9, to 10 mg/L at pH 12 (Zhang, Y. et al., 2018). Mahedi and Cetin (2023) found a prominent difference between highly carbonated and least carbonated CCW in the release of Ca and Mg at neutral to alkaline pH, with the highly carbonated phases having the lowest leaching across this pH range. When pH was between 4 and 10, Si release was constant and geochemical modelling showed concentrations were close to the saturation index of amorphous silica, indicating amorphous silica as the controlling solubility phase (Engelsen et al., 2009). Al release is controlled by the dissolution and precipitation of hydroxide minerals across all pH values measured (Zhang, Y. et al., 2018), as Al release patterns are different to the other major elements, exhibiting minimum solubility across neutral pH (Engelsen et al., 2009). Minimum release of Al (around 5 mg/L) is at pH 9, whilst maximum release (3-5 x 10^5 mg/L) at pH 2 and 13 occurred (Zhang, Y. et al., 2018). The Fe release pattern was similar to Al release, with minimum release at pH 9 (50 mg/L) (Zhang, Y. et al., 2018). SO_4^{2-} release was highest below pH 7, and lowest under high pH conditions (Engelsen et al., 2009; Mahedi and Cetin, 2023) and carbonation affected release behaviour (Mahedi and Cetin, 2023). At low pH, the less carbonated CCW leached more SO_4^{2-}, but above and at the material pH there was greater release from carbonated CCW (Mahedi and Cetin, 2023).

Above material pH, release is determined by the cement paste hydrates and varies based on carbonation. The leaching of major elements is distinctly different in the alkaline pH region (Engelsen et al., 2009; Mahedi and Cetin, 2023). Carbonated cements release lower Ca concentrations relative to uncarbonated cements because portlandite is present in uncarbonated cements and has a greater solubility than C-S-H and calcite (Garrabrants et al., 2004; Engelsen et al., 2009; Müllauer et al., 2012; Butera et al., 2015a; Bestgen et al., 2016a). Higher pH conditions are associated with precipitation and sorption, resulting in lower constituent leaching of major elements (Komonweeraket et al., 2015; Mahedi and Cetin, 2023). Carbonated cementitious materials typically release higher Si as they contain amorphous silica gel, which is stable at neutral pH but soluble at high pH (Van Gerven et al., 2003; 2006; Müllauer et al., 2012; Butera et al., 2015a). Al release is also higher for carbonated materials as pH was raised above pH 11, attributed to the formation of Al (hydr)oxide complexes

(Appelo and Postma, 2005; Engelsen et al., 2009). In addition, higher Al and SO_4^{2-} release from carbonated CCW is attributed to enhanced solubility of AFt and AFm at high pH (Engelsen et al., 2009; Butera et al., 2015a).

Trace contaminant leaching is greatest at acidic pH due to dissolution of the cement hydrate phases (Engelsen et al., 2010; Chen, J. et al., 2012; Bestgen et al., 2016a). Under equilibrium conditions, the release of trace metals is attributed to the dissolution of cement hydrate phases (Engelsen et al., 2010; Mulugeta et al., 2011) and sorption processes (Kosson et al., 2002). The leaching of cations (Cd, Cu, Mn, Ni, Pb, Zn) is low between pH 7 and 10 and is usually attributed to metal hydroxides that are insoluble across this pH range or sorption processes (Engelsen et al., 2010; Chen, J. et al., 2012; Lewis et al., 2015). Differences in metal cation release between carbonated and fresh concrete have been reported in the near-neutral to alkaline pH range (Engelsen et al., 2010). The solubility minimum for Cu (pH 6-10) was lower for non-carbonated concrete by orders of magnitude, attributed to complexation of Cu with humic substances causing enhanced release in carbonated samples-(Engelsen et al., 2010).

At mildly alkaline pH, leaching is generally at a minimum (Dhir et al., 2019)(Table 2.3). At high pH, it is established that Cr, Zn and Cu leach into solution (Engelsen et al., 2010; Chen, J. et al., 2012). Zn and Cu leached at greater concentrations in CCW (carbonated) than for non-carbonated concrete (Engelsen et al., 2010). This is attributed to greater retention in the (intact) cement hydrate phases in fresh samples, and different phases controlling release, such as calcium zincate controlling Zn release at high pH (Engelsen et al., 2010). Although, the increase in Cr release when pH was raised above the material pH was more noticeable in non-carbonated samples in Engelsen et al. (2010) and was attributed to greater solubility of ettringite present.

Highly alkaline environments can promote the leaching of toxic elements (Dhir et al., 2019), although leaching behaviour is not always consistent between studies. The release of oxyanion-forming metals Cr, Mo and V increased as pH was lowered below the material pH and is greatest at neutral pH to mildly alkaline pH (van der Sloot, 2002; Engelsen et al., 2010). The leaching of oxyanion-forming metals Cr, Mo and V have a solubility minimum at pH 4-6 and solubility maximum from pH 8-11 and <3 (Engelsen et al., 2010). This amphoteric pattern was similar but at different pH values in a study by Chen, J. et al. (2012), where it was found that Cr leaching was at a maximum at pH <2 and >12, and at a minimum between pH 5 and 6.5, similar to van der Sloot (2002). This release behaviour is in agreement with other CCW studies that showed enhanced

oxyanion (e.g. As, Cr, Mo, Sb, Se, V) release in carbonated cement leachates that have a lower material pH caused by natural and artificial carbonation (i.e. between pH 10.8 and 11.9) (Mulugeta et al., 2011; Mahedi and Cetin, 2023). Conversely, Bestgen et al. (2016a) found minimum Cr release at pH 10.5, and Mahedi and Cetin (2023) found that highly carbonated samples had a concentration plateau between pH 7 and 10.5 that increased at pH 13. In less carbonated samples, Cr release was slightly lower than the highly carbonated samples and leaching decreased up to pH 12, before slightly increasing at pH 13 (Mahedi and Cetin, 2023). The differences were attributed to carbonation, as the samples referred to as highly carbonated had higher CaO contents (measured by XRF) from higher $CaCO_3$ contents (measured by thermogravimetric analyses) (Mahedi and Cetin, 2023). Overall, Cr release was greater for carbonated samples (Mahedi and Cetin, 2023). As mentioned in the previous section, the increase in release of oxyanion-forming metals with lower pH is attributed to the degradation of cement hydrates phases such as ettringite or C-S-H that contained the anionic species (e.g. Cr(VI)) substituted in their structures (Engelsen et al., 2010; Leisinger et al., 2010; 2014; Mulugeta et al., 2011).

The leaching of As was found to be constant (500 µg/L) from pH <2 to 10, after which leaching was sensitive to pH and dropped to a minimum release (10 µg/L) at the material pH (~12), which was the same as the United States Environmental Protection Agency (US EPA) maximum contaminant level (MCL) in drinking water at 10 µg/L (Zhang, Y. et al., 2018). This implies the release of As represents an environment risk, especially as pH will likely reduce with time due to carbonation of cement phases.

2.6.3.3 Liquid to solid ratio (L/S): batch and column tests

The L/S will affect the leachate composition (van der Sloot, 1996) and may be varied in batch experiments to investigate the influence of saturation on element release (Galvín et al., 2012; Butera et al., 2015a; Bestgen et al., 2016b) or investigated during column tests, where L/S is associated with time (Delay et al., 2007; Lopez Meza et al., 2008; 2010; Butera et al., 2015a). Conflicting information exist on whether an increase in L/S ratio causes enhanced (Townsend et al., 2003; Galvín et al., 2012; Saca et al., 2017) or reduced leaching (Bestgen et al., 2016b).

The effect of L/S ratio on leachate concentrations is varied when using batch experiments, with some studies reporting lower concentrations attributed to dilution as L/S increases (using L/S of 5, 10, 15 and 20) (Bestgen et al., 2016a), and others reporting rising concentrations (Galvín et al., 2012; 2013; Mahedi and Cetin, 2020). For

example, higher L/S produced lower Ca, Cr, Cu and Fe concentrations, attributed to dilution of the leachate (Bestgen et al., 2016a). Lower Cr concentrations are presumed due to sorption of Cr to ettringite or hydrous ferric oxide, whilst decreasing Fe concentrations are likely due to the presence of insoluble Fe precipitates such as $FeCO_3$ or $Fe(OH)_3$, as these precipitates are insoluble above pH 10, and leachate pH was consistently above 10.5 (Bestgen et al., 2016a). On the contrary, an increase in L/S generally caused higher leaching concentrations for heavy metals (Cu, As, Mo, Cd, Sb, Ba, Hg, Pb) from a two-step batch test (at L/S = 2 and then L/S = 10) on CCW (Jiménez et al., 2012; Saca et al., 2017), indicating higher L/S ratios can increase aqueous phase concentrations, in agreement with Townsend et al. (2003). Similarly, Galvín et al. (2012) also report an increase in leached metal concentrations (As, Ba, Ni, Sb, Se and Cu) in similar experiments which increase in line with rising L/S from 2 to 10.

Column tests on CCW have been conducted by many authors (Delay et al., 2007; Lopez Meza et al., 2008; 2009; 2010; Schiopu et al., 2009; Chen, J. et al., 2012; 2013; Butera et al., 2015a; Eckbo et al., 2022) to investigate release behaviour with L/S. In column tests, early leachates are represented by low L/S ratios, and usually during these early stages leaching is highest due to dissolution and surface-wash off processes (Delay et al., 2007; Lopez Meza et al., 2008; 2010; Chen, J. et al., 2013; Eckbo et al., 2022). The concentrations of major (Ca, Na, K, SO_4^{2-}) and trace (Cr, Cu) elements decreased with increasing L/S in up-flow column tests (Delay et al., 2007; Chen, J. et al., 2013; Eckbo et al., 2022). In Delay et al. (2007), Cu and Cr leaching were critically high for Cu (866 µg/L) and Cr (440 µg/L) in early leachates (up to L/S=3), exceeding the total Cr and total Cu thresholds (of the Federal German Soil protection and Contaminated Sites Ordinance) by a factor of at least 10. If Cr is present as Cr(VI), which is the dominant chromium species at high pH (Brookins, 1988), this meant the threshold was exceeded by a factor of 50 (Delay et al., 2007). Although Cr concentrations declined to around 11 ± 1 µg/L at L/S 10.5 L/kg, the initial leachate concentrations are still an environmental concern (Delay et al., 2007). A similar pattern was observed in column leach tests (Chen, J. et al., 2013; Eckbo et al., 2022). For example, in Eckbo et al. (2022) there was an initial high release of Cr (~38 µg/L at L/S 0.3) that stabilised with time (~10-15 µg/L from L/S 0.9 to 2.4) and pH remained above 12. The initial high release is attributed to a first flush effect and preferential flow paths (Eckbo et al., 2022). The first flush occurs when a large volume of water leads to enhanced contaminant release initially (Deletic, 1998; Kayhanian and Streenstrom,

2005), and preferential flow paths occur where water movement is easiest and fastest so that Cr release is high (Hendrickx and Flury, 2001; Gerke, 2006; Eckbo et al., 2022).

Column experiments may be continuously saturated or intermittently unsaturated, and this may affect leachate pH and constituent release. When up-flow columns are saturated, Cr leaching has been reported as around an order of magnitude greater than under unsaturated conditions (Eckbo et al., 2022). However, Lopez Meza et al. (2009) did not find any significant difference in constituent release (Ba, Ca, Na, Fe, Sr, Pb), pH or conductivity between intermittent unsaturated and saturated flow conditions, except higher initial salt concentrations in the unsaturated conditions at low L/S ratios (<2).

When leaching from batch and column tests are compared, Lopez Meza et al. (2008) found no significant differences between the tests for most elements except for As, identified as a contaminant of concern. The release of As by carbonated concrete was underestimated by batch tests relative to column tests, therefore it is useful to use different leaching tests for evaluating release behaviour of contaminant metals (Lopez Meza et al., 2008), especially as percolating conditions will prevail in field conditions (Kosson et al., 1996). Similarly, Butera et al. (2015a) compared up-flow columns (unsaturated and saturated) and (down-flow) lysimeters and found that major (Al, Mg, Si) and trace element (As, Ba, Cd, Cu, Mn, Ni, P, Pb, Sb, Se, Zn) leaching of CDW was different in early leachates (up to L/S = 5), with reasonable agreement of cumulative release at L/S = 10 for most elements except Ba, Mg, Zn and Pb which showed significant differences. Differences were attributed to different leachate pH associated with particle size reduction that occurred in up-flow columns, preferential flow paths in lysimeters and non-equilibrium conditions in lysimeters (Butera et al., 2015a). These studies indicate the need to study leaching behaviour under different leaching conditions to evaluate release behaviour.

In percolation (down-flow) column tests, Galvín et al. (2014b) investigated the effect of compaction on release behaviour and found that the highest levels of leaching of Cr and SO_4^{2-} were associated with compaction. It was also found that release of pollutants (Cr, SO_4^{2-}) was greatest in the finer particle size fractions, attributed to a decreased distance for pollutants to travel from particle centre to surface and release into the aqueous phase (van der Sloot and Dijkstra, 2004; Galvín et al., 2014b). This is relevant to use in the field as compaction may be suggested as a way to reduce leaching from the fines fraction, which are considered to cause high pH leachates (Foy et al., 2019). However, as discussed previously (Section 2.6.1) the generation of high pH leachates

from the fines fraction is not necessarily true if the fines fraction is taken from stockpiled CCW rather than using after immediately crushing, so this could impact constituent release dependent on the leachate pH.

2.6.3.4 Particle size

Particle size is an important factor that influences leaching, as the particle size controls the available surface area for reaction and therefore rate of leaching (Law and Evans, 2013; Dhir et al., 2019). Smaller particles ($<10^{-4}$ cm) have a larger proportion of their atoms at particle surfaces, which increases reactive surface area, causing an increase in the solubility of the particle (Stumm and Morgan, 1996). Smaller grain sizes are associated with fast reactions and transport, whilst coarser grain sizes are usually limited by diffusion (van der Sloot and Dijkstra, 2004; Mahedi and Cetin, 2020). Leaching is usually greater for smaller size fractions, as leaching occurs mainly by diffusion (Van Gerven et al., 2007) so smaller fractions have a greater surface area where diffusion from solid to solution can occur. Therefore, decreasing particle size is associated with an increase in particle surface area, which increases the surface area available for leaching (Langmuir, 1997; Garrabrants and Kosson, 2004).

The effect of particle size on leaching has been studied by several authors (Chen, J. et al., 2012; Bestgen et al., 2016a;b; Coudray et al., 2017; Zhang, Y. et al., 2018; Natarajan et al., 2019; Mahedi and Cetin, 2020). Several studies report an increase in leaching with reduced particle size (Bestgen et al., 2016b; Coudray et al., 2017; Zhang, Y. et al., 2018; Natarajan et al., 2019; Mahedi and Cetin, 2020; Eckbo et al., 2022; Chen, J. et al 2012). However, sometimes this effect is only seen for finer particles at very low pH values (<2) (Zhang, Y. et al., 2018). Some studies explore the effect of particle size on leaching but crush the fractionated portions for laboratory experiments (Engelsen et al., 2009; 2010) to decrease the time taken to reach equilibrium conditions, but this does not represent realistic release behaviour and instead overestimates leaching (van der Sloot, 2000; Kosson et al., 2002; Butera et al., 2015a).

Particle size effects are not always found, instead differences in leaching behaviour may be attributed to variations in the cement paste composition (Bestgen et al., 2016a). Therefore, the particle size distribution and size-reduction for experiments or field applications are important parameters to consider when investigating the leaching behaviour of crushed concrete.

2.7 Environmental impact of CCW leachates

The concern with the use of CCW in the environment lies with the impact of high pH alkaline leachates and the leaching of potentially harmful elements that may contaminate surface and ground waters (Dhir et al., 2019) and migrate to sensitive ecological receptors (Foy et al., 2019). Although CCW is generally regarded as inert for construction applications, there are valid concerns raised in the literature about the leaching behaviour of toxic trace elements and alkalinity, which can affect water quality. CCW has the propensity to produce high pH leachates, which depends on the extent of carbonation and may be harmful to the environment when considering reuse applications in the field.

High pH alkaline leachates from concrete may impact groundwaters, and ecosystems in surface waters at drainage locations and cause harmful impacts (Gupta et al., 2018). When alkali leachates raise the pH of fresh water, it can become toxic to fish through injuring the skin and gills, which interferes with respiration (Law and Evans, 2013). Even a rise in pH from 7 to 8 can cause a tenfold increase in the toxicity of ammonia to fish (Doudoroff and Katz, 1950; Alabaster and Lloyd, 1980; Law and Evans, 2013). Above pH 10, fish may become stressed and die (Wurts and Durborow, 1992). In ecotoxicological tests, highly alkaline CCW leachates (pH 11.6-12.3) caused the death of test organisms freshwater invertebrates *Daphnia magna* and freshwater plant duckweed, and toxic harm to freshwater algae (Mocová et al., 2019). Highly alkaline waters can cause the acceleration of $CaCO_3$ precipitation, which consumes alkalinity and is ecologically harmful as calcite precipitation can form a layer over water and smother benthic habitats downstream (Mayes and Younger, 2006; Mayes et al., 2009). Moreover, high pH leachates can also disturb the carbonate equilibria of naturally acidic waters and cause algal blooms during periods of rapid photosynthesis induced by the release of carbonate from dissociation of bicarbonate (Wurts and Durborow, 1992; Kluge et al., 2018). However, as alkaline CCW leachate moves through and interacts with the surrounding subsurface soil environment it will be neutralised to some extent (Gupta et al., 2018; Chen, J. et al., 2019; Oliveira, F.D. et al., 2020). Neutralisation of the leachate will occur by interaction with soil acidity and carbon dioxide from biological activity in the soil (Gupta et al., 2018; Chen, J. et al., 2019; Oliveira, F.D. et al., 2020). Moreover, dilution in local groundwater will reduce the concentration of OH^- further and through reaction with groundwater acidity (Gupta et al., 2018; Oliveira, F.D. et al., 2020). Nevertheless, there may be impacts to biota in the immediate vicinity of where CCW is emplaced prior to dilution. Therefore, proximity to

sensitive ecological receptors will determine the potential impact of CCW leachates, so investigation of CCW leaching behaviour is important. The extent of high pH and alkalinity attenuation will depend on local environmental conditions (mineral composition and dissolution, carbonation) and interaction with the surrounding soil environment (Gupta et al., 2018; Chen, J. et al., 2019; Oliveira, F.D. et al., 2020).

When in contact with water, CCW leachates can impact water quality and represent an environmental risk through the leaching of non-hazardous elements, trace contaminants and heavy metals. As several of the metals that may leach from CCW are identified in the Water Framework Directive as freshwater specific pollutants (As, Cl^-, Cr (III), Cr (VI), Co, Cu, Fe, Mn, SO_4^{2-}, V, Zn) and freshwater priority substances (Hg, Pb, Ni) in the UK (Environment Agency, 2022), it is necessary to understand release behaviour of these substances from that may be present in CCW. The dominant species that may leach will depend on the composition of the CCW and additives such as fly ash or steel slag. Fly ash and steel slag can contain very high concentrations of oxyanion forming elements (As, Cr, Mo, Sb, Se, V); for example, steel slag can contain up to 30,000 mg/kg of Cr and 10,000 mg/kg V (Cornelis et al., 2008). Environmental concerns surrounding CCW leaching exist because environmental pollutants can cause harm to biota and humans as they are toxic, carcinogenic and can accumulate in the environment for several years (Stambulska et al., 2018; Molla et al., 2021; Mitra et al., 2022). For example, Cr is a known carcinogen (Mitra et al., 2022). As, along with Mn and Cd are neurotoxic (Mitra et al., 2022). Co can cause harmful health effects from long-term exposure although it is present in trace concentrations in vegetables and fish (Kovalcikova and Estokova, 2014). Cu is essential to all living organisms, but higher doses can cause harm to human health (Kovalcikova and Estokova, 2014). Fe is an abundant and essential mineral in the human body, but acute iron poisoning can occur in children and animals (Kovalcikova and Estokova, 2014). Mn has a relatively low toxicity but can cause harm to the human nervous system from prolonged moderate exposure (Pearson and Greenway, 2005). Inorganic V (as V^{5+}) is known to be a potential carcinogen (IARC, 2006; Zwolak, 2014). In high pH concrete leachates, Cr is usually present in its hexavalent form Cr(VI) as chromate ions (CrO_4^{2-}) which are only present under alkaline (pH >10) and oxidising conditions (Townsend et al., 2004). Cr(VI) is considered a more toxic species than Cr(III), as Cr (III) in hydroxide, oxide or sulphate species is less mobile (Cervantes et al., 2001). Cr(VI) is highly soluble in water (Eštoková et al., 2016) and is hazardous to the environment and human health (World Health Organisation, 1988; Katz and Salem,

1993; Cervantes et al., 2001; International Programme on Chemical Safety [IPCS], 2013; Prasad et al., 2021). Cr(VI) accumulation from excessive exposure can negatively affect plant metabolism, pollute water and along with Ni it is known to be carcinogenic to humans (IPCS, 2013; Prasad et al., 2021).

CCW leachates have the propensity to cause ecological harm to aquatic organisms (Mocová et al., 2019; Purdy et al., 2020; Esterhuizen et al., 2022; Wright et al., 2023) and to contaminate surface and groundwaters through the migration of soluble species, colloids or metal nanoparticles via surface run-off (Oliveira, M.L.S. et al., 2019). Oliveira, M.L.S. et al. (2019) found that while acute exposure risks were minimal, consistent release from contact with rainwater may cause concerns in the long-term from leachable constituents migrating to surface and groundwaters. Although the most potentially harmful elements were not detected at the material pH, an enhanced mobility for oxyanion-forming elements (e.g. As, Mo, V and Cr) were found (Oliveira, M.L.S. et al., 2019). Therefore, investigation of the pollutant release potential from CCW is necessary for environmental risk assessments. Moreover, the particle size of the CCW is important when considering the environmental impact of CCW leachates because enhanced contaminant release from the fine fraction of CCW have been reported (Chen, J. et al., 2012; Bestgen et al., 2016b; Coudray et al., 2017; Zhang, Y. et al., 2018; Natarajan et al., 2019; Mahedi and Cetin, 2020; Eckbo et al., 2022). An ecotoxicological study by Esterhuizen et al. (2022) found that the finer fraction of concrete demolition debris (<1 mm, originally pulverised from 5cm-15cm concrete blocks) caused the most harm to oligochaetes (worms). In their comprehensive review on leaching of contaminants from CDW, Molla et al. (2021) concluded that the fine residues (<4.75 mm) should be disposed to landfill because of the potential risks to the environment and human health from enhanced contaminant release. Therefore, further study on contaminant release from finer fractions of CCW is necessary to evaluate potential environmental impacts relating to disposal and/or secondary uses of finer fractions present in CCW.

The use of CCW in the environment must be proven to be safe, meaning the chemical composition of leachates must be within acceptable limits (Engelsen, 2020). Studies tend to evaluate the leaching of contaminants from CDW through comparison of the non-hazardous and hazardous pollutant concentration to local water quality standards such as risk-based groundwater thresholds (Gupta et al., 2018), US EPA MCL for drinking water (Chen, J. et al., 2013; Bestgen et al., 2016a; Mahedi and Cetin, 2023) and local state water quality standards (e.g., review by Daiber (2022)). Recently, an

extensive report was conducted by Daiber (2022) for the Department of Ecology for the State of Washington on the leachate of RCA (CCW), which featured a review of the cationic and (oxy)anionic constituents of leachates in the literature that were then compared to local Washington state groundwater and surface water criteria. By comparing to local criteria, potential constituents of concern can be identified which are relevant to the location whereby the use of CCW in secondary applications may be undertaken. As such, a similar approach is taken in this review to identify inorganic elements of concern by using the water quality standards relevant to the UK, which are the environmental quality standards (EQS) for surface freshwaters and UK drinking water standards (DWS) (Table 2.4). A summary of the CCW literature in relation to exceedances of these thresholds at the material pH in the laboratory (deionised water only) and of field studies is provided below.

The release of anions chloride and sulphate were sometimes above the water quality standards. The leaching of chloride was always below the EQS and DWS (Table 2.4) in laboratory leach tests (Galvín et al., 2013; 2014b; Del Rey et al., 2015; Roque et al., 2016; Saca et al., 2017; López Meza et al., 2010). Chloride only largely exceeded the standards by around three times in leachate measurements from stockpiles of fine and coarse concrete over one year (Sadecki et al., 1996). Chloride is important because it can increase the solubility of metals through complexation (Daiber, 2022), and increase ionic strength, which could reduce metal ion solubility through a common ion effect. The leaching of SO_4^{2-} exceeded water quality thresholds in several laboratory studies in some CCW samples in batch and column studies (López Meza et al., 2010; Galvín et al., 2014b; Del Rey et al., 2015; Diotti et al., 2020). However, sulphate leaching was not always above the EQS-AA (Butera et al., 2014; 2015a; Roque et al., 2016; Saca et al., 2017).

The release of oxyanion-forming elements As, Cr, Se and V sometimes exceeded the water quality standards. The leaching of As was above the DWS in batch, column and field leaching tests (Sadecki et al., 1996; Engelsen et al., 2006; 2012; Butera et al., 2014; 2015a; Diotti et al., 2021) and often above the EQS-AA (Sadecki et al., 1996; Engelsen et al., 2006; Chen, J. et al., 2013). However, As release did not exceed either standard in many studies (Galvín et al., 2013; 2014b; Del Rey et al., 2015; Saca et al., 2017; Gupta et al., 2018; Diotti et al., 2020) including those using CCW and artificially carbonated concrete laboratory leachates (Mulugeta et al., 2011). However, field leachates in Mulugeta et al. (2011) did sometimes exceed the DWS for As at alkaline pH.

Table 2.4 Surface freshwater environmental quality standards (EQS) annual average (AA) and maximum allowable concentration (MAC) and groundwater (drinking water standard, DWS) threshold values (µg/L).

	µg/L	
	EQS Freshwater AA (MAC)[1]	**DWS[2]**
Al		200
As	50	10
Cd	0.08-0.25 (0.45-1.5)	5
Chloride	250000	250000
Co	3	
Cr	3.4-4.7	50
Cu	1	2000
Fe	1000	200
Hg	(0.07)	1
Mn	123	50
Ni	4 (34)	20
Pb	1.2	10
Sb		5
Se		10
Sulphate	400000	250000
V	20-60	
Zn	10.9	5000

[1]Environment Agency (2022)

[2]*The Water Supply (Water Quality) Regulations* 2016

The leaching of Cr from CCW in batch and column laboratory studies at the material pH above was often above the UK DWS for Cr in several laboratory (López Meza et al., 2010; Chen, J. et al., 2013; Galvín et al., 2013; 2014b; Butera et al., 2014; 2015a; Del Rey et al., 2015; Bestgen et al., 2016a; Gupta et al., 2018; Mahedi and Cetin, 2020; Eckbo et al., 2022; Mahedi and Cetin, 2023; Saca et al., 2017) and field studies (Sadecki et al., 1996; Engelsen et al., 2006; 2012; Mulugeta et al., 2011). Cr release was sometimes above the EQS-AA but below the DWS (Barbudo et al., 2012; Roque et al., 2016; Bestgen et al., 2016a; Saca et al., 2017; Engelsen et al., 2017).

Se leaching was sometimes above the DWS (Chen, J. et al., 2013; Butera et al., 2014; Del Rey et al., 2015; Gupta et al., 2018) but below the threshold in other studies (Mulugeta et al., 2011; Diotti et al., 2020; 2021).

V release exceeds EQS-AA in some field and laboratory studies (Sadecki et al., 1996; Engelsen et al., 2012; Diotti et al., 2020; 2021) but not others (Engelsen et al., 2010; Butera et al., 2014; 2015a; Gupta et al., 2018; Saca et al., 2017).

The release of elements that leach in the cationic pattern (Cd, Co, Cu, Hg, Mn, Ni, Pb, Zn) varied between several studies, with many often below detection or below the thresholds.

Cd was often below detection or below the DWS in laboratory and field tests (Engelsen et al., 2006; 2017; Galvín et al., 2012; 2013; Butera et al., 2014; Gupta et al., 2018) although Cd sometimes exceeded the EQS-AA in few samples (Butera et al., 20154; 2015a; Engelsen et al., 2017). Co release was sometimes above the EQS-AA (Butera et al., 2014; Diotti et al., 2020; 2021; Gupta et al., 2018) or below the thresholds (Limbachiya et al., 2007; Gupta et al., 2018). Cu was above the EQS-AA but below the DWS in many studies (Engelsen et al., 2006; 2012; Limbachiya et al., 2007; López Meza et al., 2010; Galvín et al., 2013; 2014b; Butera et al., 2014; 2015a; Del Rey et al., 2015; Roque et al., 2016; Bestgen et al., 2016a; Saca et al., 2017; Gupta et al., 2018).

Hg was rarely detected in CCW leachates (Sadecki et al., 1996; Barbudo et al., 2012; Galvín et al., 2013; Galvín et al., 2014b) or was at the threshold for DWS (Diotti et al., 2020) or below the EQS-MAC for Hg (Saca et al., 2017). Mn release was below the water quality standards when measured (Limbachiya et al., 2007; Engelsen et al., 2010; Butera et al., 2014; 2015a; Gupta et al., 2018). Ni leaching exceeded both standards in several laboratory studies (Limbachiya et al., 2007; Galvín et al., 2013; Butera et al., 2014; Saca et al., 2017) or only the EQS-AA but below the EQS-MAC (Del Rey et al., 2015; Saca et al., 2017; Gupta et al., 2018; Diotti et al., 2020). Ni

leaching was below either threshold in other studies (Barbudo et al., 2012; Butera et al., 2015a; Roque et al., 2016).

Pb was not always detected in laboratory or field studies due to low solubility in the material pH range of CCW (Engelsen et al., 2012; 2017; Galvín et al., 2014b; Del Rey et al., 2015; Gupta et al., 2018) or regarded as negligible in laboratory leaching tests (Barbudo et al., 2012; Galvín et al., 2013). Pb release exceeded the EQS-AA but was mostly just below the DWS in some laboratory studies and field leachates (Chen, J. et al., 2013; Gupta et al., 2018; Saca et al., 2017; Butera et al., 2014), although it exceeded both standards in one study where the L/S was 50 (Limbachiya et al., 2007). Zn was above the EQS-AA in some studies but below the DWS (Butera et al., 2014; 2015a; Del Rey et al., 2015; Bestgen et al., 2016a). However, Zn concentrations were reported below detection in many studies (Barbudo et al., 2012; Galvín et al., 2013; 2014a; Gupta et al., 2018).

The leaching of generally non-hazardous elements such as sulphate, iron and sodium can impact water quality by exceeding groundwater or drinking water standards and therefore raise an environmental concern (Townsend et al., 1999). Although, it is also said that iron release may not represent an environmental concern (Daiber, 2022) as concentrations released are below the standards (Gupta et al., 2018) or occasionally above the DWS (Sadecki et al., 1996; Bestgen et al., 2016a).

Leachate concentrations exceeding these standards may represent environmental concerns, particularly for sensitive ecological receptors, or impact on the quality of surface and groundwater where alkali leachates may discharge to. However, the exceedance of risk thresholds do not necessarily prevent beneficial reuse, but rather are used to indicate appropriate and suitable reuse applications (Kluge et al., 2018). In addition, contaminant thresholds are not always exceeded and vary with the CCW as it is naturally heterogenous. Moreover, comparison to these drinking water or groundwater quality standards is not always appropriate because of dilution and attenuation that can occur in the waste disposal scenarios once leachates reach surface or groundwaters (van der Sloot et al., 2009; Engelsen, 2020). Moreover, interaction with organic matter may prove to reduce any harmful metal concentrations in the field; for example, Cr is reported to be immobilised by organic matter in soils during column tests (Eckbo et al., 2022). Although studies in the literature indicate what metals may be of concern, they are specific to the study because of the variation in material composition of CCW. Nevertheless, if this material is to be used on a large-scale, such as backfill on nuclear sites, detailed characterisations of leaching

behaviour are necessary for environmental risk assessments. Therefore, it is important to characterise the leaching behaviour of CCW prior to field applications because of potential harmful environmental and ecological impacts associated with the leaching of CCW. This includes studies on the dissolution kinetics and leaching mechanisms of contaminants with a range of leachants to represent the range of environmental conditions that are relevant to the on-site disposal of CCW – from acidic pH (peats), neutral to slightly basic (most groundwaters), to alkaline (co-disposal with other CCW wastes).

In summary, CCW has the propensity to contaminate surface and ground waters due to the production of high pH leachates and the leaching of potentially harmful contaminants. This may cause harmful environmental impacts. As established in Section 2.5 and 2.6, this propensity is strongly dependent on the material composition of the CCW and the extent of weathering and carbonation, which determines leachate pH. Thus, the propensity for high pH leachate production is dependent on the extent of carbonation. As high pH leachates can impact surface waters and groundwaters, it is important to establish the degree to which CCW is carbonated and the leaching behaviour of CCW, as leaching of non-hazardous elements and trace metal contaminants can contaminate surface and groundwater quality. Exceedances of water quality criteria may imply an environment concern. The leaching of contaminants is highly variable based on CCW material composition, the presence of cement additives (e.g., fly ash or slag) that can enhance heavy metal content (Section 2.6.2), and the extent of degradation and carbonation of cement phases. As mentioned in Section 2.6.3.1, oxyanion-forming contaminants (e.g. Cr) may be associated with cement phases (e.g., C-(A)-S-H, ettringite) through incorporation or sorption to ettringite or hydrous ferric oxide (Bestgen et al., 2016). As pH is lowered through carbonation this destabilises and degrades cement phases, leading to contaminant release. There are also valid concerns around the particle size of CCW, as finer fractions are associated with higher contaminant leaching and ecotoxicity (Esterhuizen et al. 2022; Molla et al., 2021). It is apparent from comparison with the UK EQS and DWS that CCW is varied in composition as almost all pollutants exceeded at least one standard in the referenced studies, particularly oxyanion forming elements and frequently Cr, but this did vary from study to study. This indicates the importance of investigating leaching behaviour of CCW samples prior to reuse as void fill onsite, especially those with proximity to sensitive ecological receptors.

2.8 References

Abbaspour, A., Tanyu, B. and Cetin, B. 2016a. Impact of aging on leaching characteristics of recycled concrete aggregate. **23**.

Abbaspour, A., Tanyu, B., Cetin, B. and Brown, M.C. 2016b. Stockpiling Recycled Concrete Aggregate: Changes in Physical Properties and Leachate Characteristics Due to Carbonation and Aging. *Geo-Chicago 2016.* pp.73-82.

Adenot, F. and Buil, M. 1992. Modeling of the corrosion of the cement paste by deionized water. *Cement and Concrete Research.* **22**(2-3), pp.489-496.

Alabaster, J.S. and Lloyd, R. 1980. *Water quality criteria for freshwater fish.* London: Butterworth [for] the Food and Agriculture Organization of the United Nations.

Alba, N., Vazquez, E., Gasso, S. and Baldasano, J.M. 2001. Stabilization/solidification of MSW incineration residues from facilities with different air pollution control systems. Durability of matrices versus carbonation. *Waste Management.* **21**(4), pp.313-323.

Al Mahrouqi, D., Vinogradov, J. and Jackson, M.D. 2017. Zeta potential of artificial and natural calcite in aqueous solution. *Advances in Colloid and Interface Science.* **240**, pp.60-76.

Andersson, K., Allard, B., Bengtsson, M. and Magnusson, B. 1989. Chemical composition of cement pore solutions. *Cement and Concrete Research.* **19**(3), pp.327-332.

Appelo, C.A.J. and Postma, D. 2005. *Geochemistry, groundwater and pollution.* 2nd ed. Leiden ;: A.A. Balkema.

Atkinson, A. 1985. *The time dependence of pH within a repository for radioactive waste disposal.* UKAEA Atomic Energy Research Establishment.

Atkinson, A., Everitt, N.M. and Guppy, R.M. 1988. Time Depndence of pH in a Cementitious Repository. *MRS Online Proceedings Library.* **127**(1), pp.439-446.

Atkinson, A., Goult, D.J. and Hearne, J.A. 1985. An Assessment of the Long-Term Durability of Concrete in Radioactive Waste Repositories. *MRS Online Proceedings Library.* **50**(1), pp.239-246.

Atkinson, A., Hearne, J.A. and Knights, C.F. 1989. Aqueous chemistry and thermodynamic modelling of CaO–SiO2–H2O gels. *Journal of the Chemical Society, Dalton Transactions.* (12), pp.2371-2379.

Aydilek, A.H. 2015a. *Development of Design Guidelines for Proper Selection of Graded Aggregate Base in Maryland State Highways - Environmental Suitability of Recycled Concrete Aggregate in Highways.* MD, USA: University of Maryland, College Park.

Aydilek, A.H. 2015b. *Environmental suitability of recycled concrete aggregate in highways.* Baltimore, MD: Maryland State Highway Administration.

Barbudo, A., Galvín, A.P., Agrela, F., Ayuso, J. and Jiménez, J.R. 2012. Correlation analysis between sulphate content and leaching of sulphates in recycled aggregates from construction and demolition wastes. *Waste Management.* **32**(6), pp.1229-1235.

Baston, G.M.N., Clacher, A.P., Heath, T.G., Hunter, F.M.I., Smith, V. and Swanton, S.W. 2012. Calcium silicate hydrate (C-S-H) gel dissolution and pH buffering in a cementitious near field. *Mineralogical Magazine.* **76**(8), pp.3045-3053.

Baur, I. and Johnson, C.A. 2003. Sorption of Selenite and Selenate to Cement Minerals. *Environmental Science & Technology.* **37**(15), pp.3442-3447.

Beddoe, R.E. and Dorner, H.W. 2005. Modelling acid attack on concrete: Part I. The essential mechanisms. *Cement and Concrete Research.* **35**(12), pp.2333-2339.

Beddoe, R.E., Mullauer, W. and Heinz, D. 2022. On leaching mechanisms of major and trace elements from concrete-Carbonation, exposure to deicing salt and external sulphates. *Journal of Building Engineering.* **45**, article no: 103435 [no pagination].

Berner, U.R. 1988. Modelling the Incongruent Dissolution of Hydrated Cement Minerals. *Radiochimica Acta.* **44-45**(2), pp.387-394.

Berner, U.R. 1992. Evolution of pore water chemistry during degradation of cement in a radioactive waste repository environment. *Waste Management.* **12**(2), pp.201-219.

Berodier, E. and Scrivener, K. 2015. Evolution of pore structure in blended systems. *Cement and Concrete Research.* **73**, pp.25-35.

Bestgen, J.O., Cetin, B. and Tanyu, B.F. 2016a. Effects of extraction methods and factors on leaching of metals from recycled concrete aggregates. *Environmental Science and Pollution Research.* **23**(13), pp.12983-13002.

Bestgen, J.O., Hatipoglu, M., Cetin, B. and Aydilek, A.H. 2016b. Mechanical and Environmental Suitability of Recycled Concrete Aggregate as a Highway Base Material. *Journal of materials in civil engineering.* **28**(9).

Bonen, D. and Sarkar, S.L. 1995. The effects of simulated environmental attack on immobilization of heavy metals doped in cement-based materials. *Journal of hazardous materials.* **40**(3), pp.321-335.

Braney, M.C., Haworth, A., Jefferies, N.L. and Smith, A.C. 1993. A study of the effects of an alkaline plume from a cementitious repository on geological materials. *Journal of Contaminant Hydrology.* **13**(1), pp.379-402.

Brantley, S.L., Kubicki, J.D. and White, A.F. 2008. Kinetics of mineral dissolution. *Kinetics of water-rock interaction.* New York: Springer Verlag.

Bray, A.W., Benning, L.G., Bonneville, S. and Oelkers, E.H. 2014. Biotite surface chemistry as a function of aqueous fluid composition. *Geochimica et Cosmochimica Acta.* **128**, pp.58-70.

Bray, A.W., Oelkers, E.H., Bonneville, S., Wolff-Boenisch, D., Potts, N.J., Fones, G. and Benning, L.G. 2015. The effect of pH, grain size, and organic ligands on biotite weathering rates. *Geochimica et Cosmochimica Acta.* **164**, pp.127-145.

British Standards Institute (BSI). 2002a. EN 12457-3:2002. *Characterisation of waste-leaching-compliance test for leaching of granular waste materials and sludges. Part 3.* London: BSI.

British Standards Institute (BSI). 2002b. EN 12457-2:2002. *Characterisation of waste. Leaching. Compliance test for leaching of granular waste materials and sludges. One stage batch test at a liquid to solid ratio of 10 l/kg for materials with particle size below 4 mm (without or with size reduction) Part 2.* London: BSI.

British Standards Institute (BSI). 2015. BS EN14429. *Characterization of waste — Leaching behaviour test — Influence of pH on leaching with initial acid / base addition.* London: BSI.

Brookins, D.G. 1988. *Eh-PH diagrams for geochemistry.* Berlin: Springer.

Bullard, J.W., Jennings, H.M., Livingston, R.A., Nonat, A., Scherer, G.W., Schweitzer, J.S., Scrivener, K.L. and Thomas, J.J. 2011. Mechanisms of cement hydration. *Cement and Concrete Research.* **41**(12), pp.1208-1223.

Butera, S., Christensen, T.H. and Astrup, T.F. 2014. Composition and leaching of construction and demolition waste: Inorganic elements and organic compounds. *Journal of Hazardous Materials.* **276**, pp.302-311.

Butera, S., Hyks, J., Christensen, T.H. and Astrup, T.F. 2015a. Construction and demolition waste: Comparison of standard up-flow column and down-flow lysimeter leaching tests. *Waste Management.* **43**, pp.386-397.

Butera, S., Trapp, S., Astrup, T.F. and Christensen, T.H. 2015b. Soil retention of hexavalent chromium released from construction and demolition waste in a road-base-application scenario. *Journal of Hazardous Materials.* **298**, pp.361-367.

Bye, R. and Lund, W. 1988. Optimal conditions for the reduction of selenate to selenite by hydrochloric acid. *Fresenius' Zeitschrift für analytische Chemie.* **332**(3), pp.242-244.

Cabrera, M., Galvín, A.P. and Agrela, F. 2019. 12 - Leaching issues in recycled aggregate concrete. In: de Brito, J. and Agrela, F. eds. *New Trends in Eco-efficient and Recycled Concrete.* Woodhead Publishing, pp.329-356.

Carde, C., François, R. and Torrenti, J.-M. 1996. Leaching of both calcium hydroxide and C-S-H from cement paste: Modeling the mechanical behavior. *Cement and Concrete Research.* **26**(8), pp.1257-1268.

Cattant, F., Crusset, D. and Féron, D. 2008. Corrosion issues in nuclear industry today. *Materials Today.* **11**(10), pp.32-37.

CEN. 2015. *Characterization of waste - Leaching behaviour test - Influence of pH on leaching with initial acid/base addition.* Brussels: CEN.

Cervantes, C., Campos-García, J., Devars, S., Gutiérrez-Corona, F., Loza-Tavera, H., Torres-Guzmán, J.C. and Moreno-Sánchez, R. 2001. Interactions of chromium with microorganisms and plants. *FEMS microbiology reviews.* **25**(3), pp.335-347.

Cetin, B., Aydilek, A.H. and Guney, Y. 2012. Leaching of trace metals from high carbon fly ash stabilized highway base layers. *Resources, Conservation and Recycling.* **58**, pp.8-17.

Chandler, A.J., Eighmy, T.T., Hartlén, J., Hjelmar, O., Kosson, D.S., Sawell, S.E., van der Sloot, H.A. and Vehlow, J. 1997. Chapter 14 - Leaching tests. In: Chandler, A.J., et al. eds. *Studies in Environmental Science.* Elsevier, pp.579-606.

Chen, J., Sanger, M., Ritchey, R., Edil, T. and Ginder-Vogel, M. 2019. Neutralization of High pH and Alkalinity Effluent from Recycled Concrete Aggregate (RCA) by Common Subgrade Soil. *Journal of Environmental Quality.*

Chen, J., Tinjum, J.M. and Edil, T.B. 2013. Leaching of Alkaline Substances and Heavy Metals from Recycled Concrete Aggregate Used as Unbound Base Course. *Transportation Research Record.* **2349**(1), pp.81-90.

Chen, J., Bradshaw, S., Benson, C.H., Tinjum, J.M. and Edil, T.B. 2012. pH-Dependent Leaching of Trace Elements from Recycled Concrete Aggregate. *GeoCongress 2012.* pp.3729-3738.

Chen, J.J., Thomas, J.J., Taylor, H.F.W. and Jennings, H.M. 2004. Solubility and structure of calcium silicate hydrate. *Cement and Concrete Research.* **34**(9), pp.1499-1519.

Chen, X., Thornton, S.F. and Small, J. 2015. Influence of Hyper-Alkaline pH Leachate on Mineral and Porosity Evolution in the Chemically Disturbed Zone Developed in the Near-Field Host Rock for a Nuclear Waste Repository. *Transport in Porous Media.* **107**(2), pp.489-505.

Chen, Y. and Zhou, Y. 2020. The contents and release behavior of heavy metals in construction and demolition waste used in freeway construction. *Environmental Science and Pollution Research.* **27**(1), pp.1078-1086.

Cho, Y.-H. and Yeo, S.-H. 2004. Application of recycled waste aggregate to lean concrete subbase in highway pavement. *Canadian Journal of Civil Engineering.* **31**(6), pp.1101-1108.

Cornelis, G., Johnson, C.A., Gerven, T.V. and Vandecasteele, C. 2008. Leaching mechanisms of oxyanionic metalloid and metal species in alkaline solid wastes: A review. *Applied Geochemistry.* **23**(5), pp.955-976.

Coudray, C., Amant, V., Cantegrit, L., Le Bocq, A., Thery, F., Denot, A. and Eisenlohr, L. 2017. Influence of Crushing Conditions on Recycled Concrete Aggregates (RCA) Leaching Behaviour. *Waste and Biomass Valorization.* **8**(8), pp.2867-2880.

Daiber, E. 2022. *Recycled Concrete Aggregate Leachate: A Literature Review.* Publication 22-03-003 ed. [Online]. Olympia: Washington State Department of Ecology. [Accessed 16/05/2023]. Available from: https://apps.ecology.wa.gov/publications/SummaryPages/2203003.html

DEFRA. 2018. *UK Statistics on Waste.* London: Government Statistical Service.

Deissmann, G., Bath, A., Jefferis, S., Thierfeldt, S. and Wörlen, S. 2006. Development and application of knowledge-based source-term models for radionuclide mobilisation from contaminated concrete. *MRS Online Proceedings Library.* **932**(991).

Del Rey, I., Ayuso, J., Galvín, A.P., Jiménez, J.R., López, M. and García-Garrido, M.L. 2015. Analysis of chromium and sulphate origins in construction recycled materials based on leaching test results. *Waste Management.* **46**, pp.278-286.

Delay, M., Lager, T., Schulz, H.D. and Frimmel, F.H. 2007. Comparison of leaching tests to determine and quantify the release of inorganic contaminants in demolition waste. *Waste Management.* **27**(2), pp.248-255.

Deletic, A. 1998. The first flush load of urban surface runoff. *Water Research.* **32**(8), pp.2462-2470.

Department for Energy Food and Rural Affairs. 2011. *Environmental Permitting Guidance Radioactive Substances Regulation.* [Online]. London, UK: Department for Energy, Food and Rural Affairs. [Accessed 15/05/2023].

Department for Energy Security & Net Zero, D. 2023a. *Consultation: Part I UK policy proposals for managing radioactive substances and nuclear decommissioning.* [Online]. [Accessed 10/05/2023]. Available from: https://assets.publishing.service.gov.uk/government/uploads/system/uploads/attachment_data/file/1139242/part_I_policy_proposals_managing_radioactive_substances_and_nuclear_decommissioning.pdf

Department for Energy Security & Net Zero, D. 2023b. *Consultation: Part II Draft UK policy framework for managing radioactive substances and nuclear decommissioning.* [Online]. [Accessed 10/05/2023]. Available from: https://assets.publishing.service.gov.uk/government/uploads/system/uploads/attachment_data/file/1139248/part_II_draft_policy_managing_radioactive_substances_and_nuclear_decommissioning.pdf

Dhir, R.K., de Brito, J., Silva, R.V. and Lye, C.Q. 2019. 13 - Environmental Impact, Case Studies and Standards and Specifications. In: Dhir, R.K., et al. eds. *Sustainable Construction Materials.* Woodhead Publishing, pp.495-583.

Diamond, S. 2004. The microstructure of cement paste and concrete—a visual primer. *Cement and Concrete Composites.* **26**(8), pp.919-933.

Diotti, A., Galvín, A.P., Piccinali, A., Plizzari, G. and Sorlini, S. 2020. Chemical and Leaching Behavior of Construction and Demolition Wastes and Recycled Aggregates. **12**(24), p10326.

Diotti, A., Plizzari, G. and Sorlini, S. 2021. Leaching Behaviour of Construction and Demolition Wastes and Recycled Aggregates: Statistical Analysis Applied to the Release of Contaminants. *Applied Sciences-Basel.* **11**(14), article no: 6265 [no pagination].

Doudoroff, P. and Katz, M. 1950. Critical Review of Literature on the Toxicity of Industrial Wastes and Their Components to Fish: I. Alkalies, Acids, and Inorganic Gases. *Sewage and Industrial Wastes.* **22**(11), pp.1432-1458.

Eckbo, C., Okkenhaug, G. and Hale, S.E. 2022. The effects of soil organic matter on leaching of hexavalent chromium from concrete waste: Batch and column experiments. *Journal of Environmental Management.* **309**, p114708.

Edil, T., Tinjum, J. and Benson, C. 2012. *Recycled Unbound Materials.* Madison, WI, USA: Department of Civil and Environmental Engineering, University of Wisconsin.

Ekström, T. 2001. *Leaching of concrete: experiments and modelling.* Lund University.

Engelsen, C.J. 2020. Leaching performance of recycled aggregates. In: Pacheco-Torgal, F., et al. eds. *Advances in Construction and Demolition Waste Recycling.* Woodhead Publishing, pp.439-451.

Engelsen, C.J., Lund, O., Hansen, E. and Hansesveen, H. 2002. Leaching of harmful substances from recycled aggregates in laboratory and field site. In: *Proceedings of the Third International Conference on Sustainable Building, Oslo, Norway*. p.7

Engelsen, C.J., Lund, O., Hansen, E. and Hansesveen, H. 2003. Leaching characteristic of unbound recycled aggregates: preliminary study and ongoing research. In: *Wascon 2003 Progress on the Road to Sustainability, San Sebastian, Spain* pp.117-187.

Engelsen, C.J., Mehus, J., Pade, C. and Sæther, D.H. 2005. *Carbon dioxide uptake in demolished and crushed concrete.* Oslo, Norway: Norwegian Building Research Institute.

Engelsen, C.J., van der Sloot, H., Petkovic, G., Wibetoe, G., Stoltenberg-Hansson, E. and Lund, W. 2006. *Constituent release predictions for recycled aggregates at field site in Norway.* Oslo, Norway: SINTEF Building and Infrastructure.

Engelsen, C.J., van der Sloot, H.A. and Petkovic, G. 2017. Long-term leaching from recycled concrete aggregates applied as sub-base material in road construction. *Science of The Total Environment.* **587-588**, pp.94-101.

Engelsen, C.J., van der Sloot, H.A., Wibetoe, G., Justnes, H., Lund, W. and Stoltenberg-Hansson, E. 2010. Leaching characterisation and geochemical modelling of minor and trace elements released from recycled concrete aggregates. *Cement and Concrete Research.* **40**(12), pp.1639-1649.

Engelsen, C.J., van der Sloot, H.A., Wibetoe, G., Petkovic, G., Stoltenberg-Hansson, E. and Lund, W. 2009. Release of major elements from recycled concrete aggregates and geochemical modelling. *Cement and Concrete Research.* **39**(5), pp.446-459.

Engelsen, C.J., Wibetoe, G., van der Sloot, H.A., Lund, W. and Petkovic, G. 2012. Field site leaching from recycled concrete aggregates applied as sub-base material in road construction. *Science of The Total Environment.* **427-428**, pp.86-97.

Environment Agency. 2022. [Online]. [Accessed 31/08/2023]. Available from: https://www.gov.uk/guidance/surface-water-pollution-risk-assessment-for-your-environmental-permit

Esterhuizen, M., von Wolff, M.A., Kim, Y.J. and Pflugmacher, S. 2022. Ecotoxicological implications of leachates from concrete demolition debris on oligochaetes: survival and oxidative stress status. *Heliyon.* **8**(10), pe11237.

Eštoková, A. and Oravec, J. 2021. Analyzing the leachability of selected heavy metals from cement composites by long-term and cyclic tests. *Selected Scientific Papers - Journal of Civil Engineering.* **16**(1), pp.105-115.

Eštoková, A., Palaščáková, L. and Kovalčíková, M. 2016. Chromium-Leaching Study of Cements in Various Environments. *World Academy of Science, Engineering and Technology, International Journal of Civil, Environmental, Structural, Construction and Architectural Engineering.* **10**, pp.727-730.

Faucon, P., Adenot, F., Jacquinot, J.F., Petit, J.C., Cabrillac, R. and Jorda, M. 1998. Long-term behaviour of cement pastes used for nuclear waste disposal: review of physico-chemical mechanisms of water degradation. *Cement and Concrete Research.* **28**(6), pp.847-857.

Faucon, P., Adenot, F., Jorda, M., Cabrillac, R.J.M. and Structures. 1997. Behaviour of crystallised phases of Portland cement upon water attack. **30**(8), pp.480-485.

Faucon, P., Le Bescop, P., Adenot, F., Bonville, P., Jacquinot, J.F., Pineau, F. and Felix, B. 1996. Leaching of cement: Study of the surface layer. *Cement and Concrete Research.* **26**(11), pp.1707-1715.

Ferreira, E.G.A., Marumo, J.T., Franco, M.K.K.D., Yokaichiya, F. and Vicente, R. 2019. 10000 years cement – Can hydrated cement last as much as long-lived radionuclides? *Cement and Concrete Composites.* **103**, pp.339-352.

Foy, J., Jones, G., Sephton, M. and Gaitonde, R. 2019. *Managing On-site Stockpiling and Use of High Volumes of Concrete-based Demolition Material.* Cumbria, UK: AECOM on behalf of the Nuclear Decommissioning Authority.

Fulda, B., Voegelin, A., Ehlert, K. and Kretzschmar, R. 2013. Redox transformation, solid phase speciation and solution dynamics of copper during soil reduction and reoxidation as affected by sulfate availability. *Geochimica et Cosmochimica Acta.* **123**, pp.385-402.

Gabrisová, A., Havlica, J. and Sahu, S. 1991. Stability of calcium sulphoaluminate hydrates in water solutions with various pH values. *Cement and Concrete Research.* **21**(6), pp.1023-1027.

Galan, I., Baldermann, A., Kusterle, W., Dietzel, M. and Mittermayr, F. 2019. Durability of shotcrete for underground support– Review and update. *Construction and Building Materials.* **202**, pp.465-493.

Galvín, A.P., Agrela, F., Ayuso, J., Beltrán, M.G. and Barbudo, A. 2014a. Leaching assessment of concrete made of recycled coarse aggregate: Physical and environmental characterisation of aggregates and hardened concrete. *Waste Management.* **34**(9), pp.1693-1704.

Galvín, A.P., Ayuso, J., Agrela, F., Barbudo, A. and Jiménez, J.R. 2013. Analysis of leaching procedures for environmental risk assessment of recycled aggregate use in unpaved roads. *Construction and Building Materials.* **40**, pp.1207-1214.

Galvín, A.P., Ayuso, J., Barbudo, A., Cabrera, M., López-Uceda, A. and Rosales, J. 2018. Upscaling the pollutant emission from mixed recycled aggregates under compaction for civil applications. *Environmental Science and Pollution Research.* **25**(36), pp.36014-36023.

Galvín, A.P., Ayuso, J., García, I., Jiménez, J.R. and Gutiérrez, F. 2014b. The effect of compaction on the leaching and pollutant emission time of recycled aggregates from construction and demolition waste. *Journal of Cleaner Production.* **83**, pp.294-304.

Galvín, A.P., Ayuso, J., Jiménez, J.R. and Agrela, F. 2012. Comparison of batch leaching tests and influence of pH on the release of metals from construction and demolition wastes. *Waste Management.* **32**(1), pp.88-95.

Garrabrants, A.C. and Kosson, D.S. 2004. *Leaching Processes and Evaluation Tests for Inorganic Constituent Release from Cement-Based Matrices.* Boca Raton: CRC Press.

Garrabrants, A.C., Sanchez, F. and Kosson, D.S. 2004. Changes in constituent equilibrium leaching and pore water characteristics of a Portland cement mortar as a result of carbonation. *Waste Management.* **24**(1), pp.19-36.

Gérard, B., Le Bellego, C. and Bernard, O. 2002. Simplified modelling of calcium leaching of concrete in various environments. *Materials and Structures.* **35**(10), pp.632-640.

Gerke, H.H. 2006. Preferential flow descriptions for structured soils. *Journal of Plant Nutrition and Soil Science.* **169**(3), pp.382-400.

Gervais, C., Garrabrants, A.C., Sanchez, F., Barna, R., Moszkowicz, P. and Kosson, D.S. 2004. The effects of carbonation and drying during intermittent leaching on the release of inorganic constituents from a cement-based matrix. *Cement and Concrete Research.* **34**(1), pp.119-131.

Glasser, F.P., Marchand, J. and Samson, E. 2008. Durability of concrete — Degradation phenomena involving detrimental chemical reactions. *Cement and Concrete Research.* **38**(2), pp.226-246.

Glasser, F.P. and Matschei, T. 2007. Interactions between Portland cement and carbon dioxide. In: *Proceedings of the ICCC Conference*.

Groves, G.W., Brough, A., Richardson, I.G. and Dobson, C.M. 1991. Progressive changes in the structure of hardened C_3S cement pastes due to carbonation. *Journal of the American Ceramic Society.* **74**(11), pp.2891-2896.

Green, W.K. 2020. Steel reinforcement corrosion in concrete – an overview of some fundamentals. *Corrosion Engineering, Science and Technology.* **55**(4), pp.289-302.

GRR. 2018. *Management of Radioactive Waste from Decommissioning of Nuclear Sites: Guidance on Requirements for Release from Radioactive Substances Regulation Version 1.0.* [Online]. [Accessed 20/05/2023]. Available from: https://www.sepa.org.uk/media/365893/2018-07-17-grr-publication-v1-0.pdf

Gupta, N., Kluge, M., Chadik, P.A. and Townsend, T.G. 2018. Recycled concrete aggregate as road base: Leaching constituents and neutralization by soil Interactions and dilution. *Waste Management.* **72**, pp.354-361.

Habert, G., Miller, S.A., John, V.M., Provis, J.L., Favier, A., Horvath, A. and Scrivener, K.L. 2020. Environmental impacts and decarbonization strategies in the cement and concrete industries. *Nature Reviews Earth & Environment.* **1**(11), pp.559-573.

Haga, K., Shibata, M., Hironaga, M., Tanaka, S. and Nagasaki, S. 2002. Silicate Anion Structural Change in Calcium Silicate Hydrate Gel on Dissolution of Hydrated Cement. *Journal of Nuclear Science and Technology.* **39**(5), pp.540-547.

Haga, K., Shibata, M., Hironaga, M., Tanaka, S. and Nagasaki, S. 2005. Change in pore structure and composition of hardened cement paste during the process of dissolution. *Cement and Concrete Research.* **35**(5), pp.943-950.

Halim, C.E., Amal, R., Beydoun, D., Scott, J.A. and Low, G. 2004. Implications of the structure of cementitious wastes containing Pb(II), Cd(II), As(V), and Cr(VI) on the leaching of metals. *Cement and Concrete Research.* **34**(7), pp.1093-1102.

Harris, A.W., Manning, M.C., Tearle, W.M. and Tweed, C.J. 2002. Testing of models of the dissolution of cements—leaching of synthetic CSH gels. *Cement and Concrete Research.* **32**(5), pp.731-746.

Hartwich, P. and Vollpracht, A. 2017. Influence of leachate composition on the leaching behaviour of concrete. *Cement and Concrete Research.* **100**, pp.423-434.

Heberling, F., Bosbach, D., Eckhardt, J.-D., Fischer, U., Glowacky, J., Haist, M., Kramar, U., Loos, S., Müller, H.S., Neumann, T., Pust, C., Schäfer, T., Stelling, J., Ukrainczyk, M., Vinograd, V., Vučak, M. and Winkler, B. 2014. Reactivity of the calcite–water-interface, from molecular scale processes to geochemical engineering. *Applied Geochemistry.* **45**, pp.158-190.

Hendrickx, J.M. and Flury, M. 2001. *Uniform and preferential flow Mechanisms in the vadose zone.* Washington D. C: National Academy Press.

Hidalgo, A., Petit, S., Domingo, C., Alonso, C. and Andrade, C. 2007. Microstructural characterization of leaching effects in cement pastes due to neutralisation of their alkaline nature: Part I: Portland cement pastes. *Cement and Concrete Research.* **37**(1), pp.63-70.

Huet, B., L'Hostis, V., Miserque, F. and Idrissi, H. 2005. Electrochemical behavior of mild steel in concrete: Influence of pH and carbonate content of concrete pore solution. *Electrochimica Acta.* **51**(1), pp.172-180.

IARC. 2006. *Cobalt in hard metals and cobalt sulfate, gallium arsenide, indium phosphide and vanadium pentoxide. IARC monographs on the evaluation of carcinogenic risks to humans* Lyon, France: International Agency for Research on Cancer.

IAEA. 2002. *Management of low and intermediate level radioactive wastes with regard to their chemical toxicity.* Vienna, Austria: International Atomic Energy Agency.

IAEA. 2008. *Managing Low Radioactivity Material from the Decommissioning of Nuclear Facilities.* Vienna, Austria: International Atomic Energy Agency.

IPCS. 2013. *Concise international chemical assessment document 78 inorganic-chromium(VI) compounds.* Geneva, Switzerland: World Health Organisation.

Izquierdo, M. and Querol, X. 2012. Leaching behaviour of elements from coal combustion fly ash: An overview. *International Journal of Coal Geology.* **94**, pp.54-66.

Jacques, D., Phung, Q.T., Perko, J., Seetharam, S.C., Maes, N., Liu, S., Yu, L., Rogiers, B. and Laloy, E. 2021. Towards a scientific-based assessment of long-term durability and performance of cementitious materials for radioactive waste conditioning and disposal. *Journal of Nuclear Materials.* **557**, p153201.

Jacques, D., Wang, L., Martens, E. and Mallants, D. 2010. Modelling chemical degradation of concrete during leaching with rain and soil water types. *Cement and Concrete Research.* **40**(8), pp.1306-1313.

Jiménez, J.R., Ayuso, J., Agrela, F., López, M. and Galvín, A.P. 2012. Utilisation of unbound recycled aggregates from selected CDW in unpaved rural roads. *Resources, Conservation and Recycling.* **58**, pp.88-97.

Jin, M., Ma, Y.F., Li, W.W., Huang, J.L., Zeng, H.Y., Lu, C., Zhang, J. and Liu, J.P. 2022. Degradation of C-S-H(I) at different decalcification degrees. *Journal of Materials Science.* **57**(41), pp.19260-19279.

Johannesson, B. and Utgenannt, P. 2001. Microstructural changes caused by carbonation of cement mortar. *Cement and Concrete Research.* **31**(6), pp.925-931.

Johnson, C.A. 2004. Cement stabilization of heavy-metal-containing wastes. *Geological Society, London, Special Publications.* **236**(1), pp.595-606.

Kamali, S., Gérard, B. and Moranville, M. 2003. Modelling the leaching kinetics of cement-based materials—influence of materials and environment. *Cement & Concrete Composites.* **25**, pp.451-458.

Kamali, S., Moranville, M. and Leclercq, S. 2008. Material and environmental parameter effects on the leaching of cement pastes: Experiments and modelling. *Cement and Concrete Research.* **38**(4), pp.575-585.

Kang, D.-H., C. Gupta, S., R. Bloom, P., Ranaivoson, A., Roberson, R. and Siekmeier, J. 2011. *Recycled Materials as Substitutes for Virgin Aggregates in Road Construction: II. Inorganic Contaminant Leaching.*

Katz, S.A. and Salem, H. 1993. The toxicology of chromium with respect to its chemical speciation: a review. *Journal of Applied Toxicology.* **13**(3), pp.217-224.

Kayhanian, M. and Streenstrom, M.K. 2005. *First Flush Phenomenon Characterization.* California, Los Angeles. .

Kluge, M., Gupta, N., Watts, B., Chadik, P.A., Ferraro, C. and Townsend, T. 2018. Characterisation and management of concrete grinding residuals. *Waste Manag Res.* **36**(2), pp.149-158.

Komonweeraket, K., Cetin, B., Aydilek, A.H., Benson, C.H. and Edil, T.B. 2015. Effects of pH on the leaching mechanisms of elements from fly ash mixed soils. *Fuel (Guildford).* **140**, pp.788-802.

Kosson, D.S., Garrabrants, A.C., Thorneloe, S., Fagnant, D., Helms, G., Connolly, K. and Rodgers, M. 2017. Leaching Environmental Assessment Framework (LEAF) How-To Guide. [Online]. [Accessed 14/01/2023]. Available from: https://www.epa.gov/sites/default/files/2019-05/documents/final_leaching_environmental_assessment_framework_leaf_how-to_guide.pdf

Kosson, D.S., van der Sloot, H., Garrabrants, A. and Seignette, P.F.A.B. 2014. *Leaching Test Relationships, Laboratory-to- Field Comparisons and Recommendations for Leaching Evaluation using the Leaching Environmental Assessment Framework D.S. Kosson, H.A. van der Sloot, A.C. Garrabrants and P.F.A.B. Seignette EPA-600/R-14/061 2014.*

Kosson, D.S., van der Sloot, H.A. and Eighmy, T.T. 1996. An approach for estimation of contaminant release during utilization and disposal of municipal waste combustion residues. *Journal of Hazardous Materials.* **47**(1), pp.43-75.

Kosson, D.S., van der Sloot, H.A., Sanchez, F. and Garrabrants, A.C. 2002. An Integrated Framework for Evaluating Leaching in Waste Management and Utilization of Secondary Materials. **19**(3), pp.159-204.

Kovalcikova, M. and Estokova, A. 2014. Monitoring of heavy metal concentrations in concrete leachates. In: *9th International Conference on Environmental Engineering (ICEE), May 22-23, Vilnius, LITHUANIA*.

Kriech, A.J. and Osborn, L.V. 2022. Review of the impact of stormwater and leaching from pavements on the environment. *Journal of Environmental Management.* **319**, p115687.

Krishnamoorthy, T.M., Joshi, S.N., Doshi, G.R. and Nair, R.N. 1993. Desorption kinetics of radionuclides fixed in cement matrix. *Nuclear Technology.* **104**(3), pp.351-357.

L'Hôpital, E., Lothenbach, B., Scrivener, K. and Kulik, D.A. 2016. Alkali uptake in calcium alumina silicate hydrate (C-A-S-H). *Cement and Concrete Research.* **85**, pp.122-136.

L'Hôpital, E., Lothenbach, B., Le Saout, G., Kulik, D. and Scrivener, K. 2015. Incorporation of aluminium in calcium-silicate-hydrates. *Cement and Concrete Research.* **75**, pp.91-103.

Lagerblad, B. 2001. *Leaching performance of concrete based on studies of samples from old concrete constructions.* Stockholm, Sweden: Swedish Cement and Concrete Research Institute.

Lagerblad, B. 2005. *Carbon dioxide uptake during concrete life cycle - State of the art.* [Online]. Stockholm, Sweden: Swedish Cement and Concrete Research Institute.

Langmuir, D. 1997. *Aqueous environmental geochemistry.* Upper Saddle River, N.J: Prentice Hall.

Law, D. and Evans, J. 2013. Effect of Leaching on pH of Surrounding Water. *Magazine of Concrete Research.* **110**, pp.291-296.

Lee, J.-C., Song, T.-H. and Lee, S.-H. 2012. Leaching behavior of toxic chemicals in recycled aggregates and their alkalinity. *Journal of Material Cycles and Waste Management.* **14**(3), pp.193-201.

Leisinger, S.M., Bhatnagar, A., Lothenbach, B. and Johnson, C.A. 2014. Solubility of chromate in a hydrated OPC. *Applied Geochemistry.* **48**, pp.132-140.

Leisinger, S.M., Lothenbach, B., Le Saout, G., Kagi, H., Wehrli, B. and Johnson, C.A. 2010. Solid Solutions between CrO4- and SO4-Ettringite Ca-6(Al(OH)(6))(2)-(CrO4)(x)(SO4)(1-x) (3)*26 H2O. *Environmental Science & Technology.* **44**(23), pp.8983-8988.

Lewis, J., Cetin, B. and Aydilek, A.H. 2015. Effect of pH on the Leaching of Elements from Highway Base Layers Built with Recycled Concrete Aggregates. *IFCEE 2015.* pp.2758-2766.

Limbachiya, M.C., Marrocchino, E. and Koulouris, A. 2007. Chemical–mineralogical characterisation of coarse recycled concrete aggregate. *Waste Management.* **27**(2), pp.201-208.

Liu, H., Zhang, J., Li, B., Zhou, N., Xiao, X., Li, M. and Zhu, C. 2020. Environmental behavior of construction and demolition waste as recycled aggregates for backfilling in mines: Leaching toxicity and surface subsidence studies. *Journal of Hazardous Materials.* **389**, p121870.

Lockwood, C.L., Stewart, D.I., Mortimer, R.J.G., Mayes, W.M., Jarvis, A.P., Gruiz, K. and Burke, I.T. 2015. Leaching of copper and nickel in soil-water systems contaminated by bauxite residue (red mud) from Ajka, Hungary: the importance of soil organic matter. *Environmental Science and Pollution Research.* **22**(14), pp.10800-10810.

Lopez Meza, S., Garrabrants, A.C., van der Sloot, H. and Kosson, D.S. 2008. Comparison of the release of constituents from granular materials under batch and column testing. *Waste Management.* **28**(10), pp.1853-1867.

López Meza, S., Kalbe, U., Berger, W. and Simon, F.-G. 2010. Effect of contact time on the release of contaminants from granular waste materials during column leaching experiments. *Waste Management.* **30**(4), pp.565-571.

Lopez Meza, S., van der Sloot, H.A. and Kosson, D.S. 2009. The Effects of Intermittent Unsaturated Wetting on the Release of Constituents from Construction Demolition Debris. *Environmental Engineering Science.* **26**(3), pp.463-469.

Lothenbach, B. and Nonat, A. 2015. Calcium silicate hydrates: Solid and liquid phase composition. *Cement and Concrete Research.* **78**, pp.57-70.

Lothenbach, B., Scrivener, K. and Hooton, R.D. 2011. Supplementary cementitious materials. *Cement and Concrete Research.* **41**(12), pp.1244-1256.

Macias, A., Kindness, A. and Glasser, F.P. 1997. Impact of carbon dioxide on the immobilization potential of cemented wastes: Chromium. *Cement and Concrete Research.* **27**(2), pp.215-225.

Mahedi, M. and Cetin, B. 2020. Carbonation based leaching assessment of recycled concrete aggregates. *Chemosphere.* **250**, p126307.

Mahedi, M. and Cetin, B. 2023. Effects of Carbonation and Saturation on the Leaching Characteristics of Recycled Concrete Aggregates. *Geotechnical Testing Journal.*

Maia, M.B., Brito, J.d., Martins, I.M. and Silvestre, J.D. 2018. Toxicity of Recycled Concrete Aggregates: Review on Leaching Tests. *The Open Construction and Building Technology Journal.*

Mainguy, M., Tognazzi, C., Torrenti, J.-M. and Adenot, F. 2000. Modelling of leaching in pure cement paste and mortar. *Cement and Concrete Research.* **30**(1), pp.83-90.

Marty, N.C.M., Grangeon, S., Lerouge, C., Warmont, F., Rozenbaum, O., Conte, T. and Claret, F. 2017. Dissolution kinetics of hydrated calcium aluminates (AFm-Cl) as a function of pH and at room temperature. *Mineralogical Magazine.* **81**(5), pp.1245-1259.

Marty, N.C.M., Grangeon, S., Warmont, F. and Lerouge, C. 2015. Alteration of nanocrystalline calcium silicate hydrate (C-S-H) at pH 9.2 and room temperature: a combined mineralogical and chemical study. *Mineralogical Magazine.* **79**(2), pp.437-458.

Mayes, W.M., Batty, L.C., Younger, P.L., Jarvis, A.P., Kõiv, M., Vohla, C. and Mander, U. 2009. Wetland treatment at extremes of pH: A review. *Science of The Total Environment.* **407**(13), pp.3944-3957.

Mayes, W.M. and Younger, P.L. 2006. Buffering of Alkaline Steel Slag Leachate across a Natural Wetland. *Environmental Science & Technology.* **40**(4), pp.1237-1243.

McBride, M.B. 1994. *Environmental Chemistry of Soils.* Oxford University Press.

Mitra, S., Chakraborty, A.J., Tareq, A.M., Emran, T.B., Nainu, F., Khusro, A., Idris, A.M., Khandaker, M.U., Osman, H., Alhumaydhi, F.A. and Simal-Gandara, J. 2022. Impact of heavy metals on the environment and human health: Novel therapeutic insights to counter the toxicity. *Journal of King Saud University - Science.* **34**(3), p101865.

Mocová, K., Sackey, L. and Renkerová, P. 2019. Environmental impact of concrete and concrete-based construction waste leachates. In: *IOP Conference Series: Earth and Environmental Science*: IOP Publishing, p.012023.

Molla, A.S., Tang, P., Sher, W. and Bekele, D.N. 2021. Chemicals of concern in construction and demolition waste fine residues: A systematic literature review. *Journal of Environmental Management.* **299**, p113654.

Morandeau, A., Thiery, M. and Dangla, P. 2014. Investigation of the carbonation mechanism of CH and C-S-H in terms of kinetics, microstructure changes and moisture properties. *Cement and Concrete Research.* **56**, pp.153-170.

Moranville, M., Kamali, S. and Guillon, E. 2004. Physicochemical equilibria of cement-based materials in aggressive environments—experiment and modeling. *Cement and Concrete Research.* **34**(9), pp.1569-1578.

Müllauer, W., Beddoe, R.E. and Heinz, D. 2012. Effect of carbonation, chloride and external sulphates on the leaching behaviour of major and trace elements from concrete. *Cement and Concrete Composites.* **34**(5), pp.618-626.

Müllauer, W., Beddoe, R.E. and Heinz, D. 2015. Leaching behaviour of major and trace elements from concrete: Effect of fly ash and GGBS. *Cement and Concrete Composites.* **58**, pp.129-139.

Mulugeta, M., Engelsen, C.J., Wibetoe, G. and Lund, W. 2011. Charge-based fractionation of oxyanion-forming metals and metalloids leached from recycled concrete aggregates of different degrees of carbonation: A comparison of laboratory and field leaching tests. *Waste Management.* **31**(2), pp.253-258.

Mulugeta, M., Wibetoe, G., Engelsen, C.J. and Lund, W. 2010a. Overcoming matrix interferences in ion-exchange solid phase extraction of As, Cr, Mo, Sb, Se and V species from leachates of cement-based materials using multiple extractions. *Talanta.* **82**(1), pp.158-163.

Mulugeta, M., Wibetoe, G., Engelsen, C.J. and Lund, W. 2010b. Speciation analysis of As, Sb and Se in leachates of cementitious construction materials using selective solid phase extraction and ICP-MS. *Journal of Analytical Atomic Spectrometry.* **25**(2), pp.169-177.

Nagataki, S., Yu, Q. and Hisada, M. 2002. Effect of leaching conditions and curing time on the leaching of heavy metals in fly ash cement mortars. *Advances in Cement Research.* **14**(2), pp.71-83.

Natarajan, B.M., Kanavas, Z., Sanger, M., Rudolph, J., Ginder-Vogel, M., Edil, T., Chen, J. and Tuncer. 2019. *Characterization of Recycled Concrete Aggregate after Eight Years of Field Deployment.*

NDA. 2016. *UK Strategy for the Management of Solid Low Level Waste from the Nuclear Industry.* [Online]. Department of Energy & Climate Change. [Accessed 10/05/2023]. Available from: https://www.gov.uk/government/consultations/consultation-on-an-update-of-the-uk-strategy-for-the-management-of-solid-low-level-radioactive-waste-from-the-nuclear-industry

NDA. 2020. *Concrete example of dealing with decommissioning rubble.* [Online]. [Accessed 05/07/21]. Available from: https://www.gov.uk/government/case-studies/concrete-example-of-dealing-with-decommissioning-rubble

NDA. 2021. *Strategy.* [Online]. Cumbria, UK: NDA. [Accessed 14/05/2023]. Available from: https://assets.publishing.service.gov.uk/government/uploads/system/uploads/attachment_data/file/973438/NDA_Strategy_2021_A.pdf

NDA. 2022. *2022 UK Radioactive Waste Inventory.* [Online]. Cumbria, UK: NDA. [Accessed 14/05/2023]. Available from: https://ukinventory.nda.gov.uk/wp-content/uploads/2023/02/2022-Waste-Report-010223.pdf

Neville, A.M. 1995. *Properties of concrete.* Longman London.

Nonat, A. 2004. The structure and stoichiometry of C-S-H. *Cement and Concrete Research.* **34**(9), pp.1521-1528.

Nuclear Energy Agency. 2011. *Decontamination and Demolition of Radioactive Concrete Structures.* Organisation for Economic Co-operation and Development.

Nuclear Energy Agency. 2017. *Reycling and Re-use of Materials Arising From the Decommissioning of Nuclear Facilities.* Co-operative Programme on Decommissioning.

Ochs, M., Mallants, D. and Wang, L. 2015. Cementitious Materials and Their Sorption Properties. *Radionuclide and Metal Sorption on Cement and Concrete. Topics in Safety, Risk, Reliability and Quality.* [Online]. Springer, Cham.

Oelkers, E. and Devidal, J.L. 2001. On the interpretation of closed system mineral dissolution experiments: comment on “Mechanism of kaolinite dissolution at room temperature and pressure part II: kinetic study” by. *Geochimica et Cosmochimica Acta.* **65**, pp.4429-4432.

Oliveira, F.D., Gupta, N., Kluge, M., Finizio, C.M., Spreadbury, C.J., Chadik, P., Laux, S.J. and Townsend, T. 2020. pH attenuation by soils underlying recycled concrete aggregate road base. *Resources, Conservation and Recycling.* **161**, p104987.

Oliveira, M.L.S., Izquierdo, M., Querol, X., Lieberman, R.N., Saikia, B.K. and Silva, L.F.O. 2019. Nanoparticles from construction wastes: A problem to health and the environment. *Journal of Cleaner Production.* **219**, pp.236-243.

O’Loughlin, E.J., Boyanov, M.I. and Kemner, K.M. 2021. Reduction of Vanadium(V) by Iron(II)-Bearing Minerals. *Minerals.* **11**(3).

World Health Organisation. 1988. *Chromium (Environmental Health Criteria 61).* Geneva: World Health Organisation.

Papadakis, V.G., Fardis, M.N. and Vayenas, C.G. 1992. Effect of composition, environmental factors and cement-lime mortar coating on concrete carbonation. *Materials and Structures.* **25**(5), pp.293-304.

Pearson, G.F. and Greenway, G.M. 2005. Recent developments in manganese speciation. *TrAC Trends in Analytical Chemistry.* **24**(9), pp.803-809.

Poon, C.-S. and Chen, Z.Q. 1999. Comparison of the characteristics of flow-through and flow-around leaching tests of solidified heavy metal wastes. *Chemosphere.* **38**(3), pp.663-680.

Prasad, S., Yadav, K.K., Kumar, S., Gupta, N., Cabral-Pinto, M.M.S., Rezania, S., Radwan, N. and Alam, J. 2021. Chromium contamination and effect on environmental health and its remediation: A sustainable approaches. *Journal of Environmental Management.* **285**, p112174.

Purdy, K., Reynolds, J.K. and Wright, I.A. 2020. Potential water pollution from recycled concrete aggregate material. *Marine and freshwater research.* **72**(1), pp.58-65.

Rahman, M.A., Imteaz, M., Arulrajah, A. and Disfani, M.M. 2014. Suitability of recycled construction and demolition aggregates as alternative pipe backfilling materials. *Journal of Cleaner Production.* **66**, pp.75-84.

Rahman, Z., Thomas, L., Chetri, S.P.K., Bodhankar, S., Kumar, V. and Naidu, R. 2023. A comprehensive review on chromium (Cr) contamination and Cr(VI)-resistant extremophiles in diverse extreme environments. *Environmental Science and Pollution Research.* **30**(21), pp.59163-59193.

Rayment, D.L. and Majumdar, A.J. 1982. The composition of the C-S-H phases in portland cement pastes. *Cement and Concrete Research.* **12**(6), pp.753-764.

Richardson, I.G. 1999. The nature of C-S-H in hardened cements. *Cement and Concrete Research.* **29**(8), pp.1131-1147.

Richardson, I.G. 2000. The nature of the hydration products in hardened cement pastes. *Cement & Concrete Composites.* **22**(2), pp.97-113.

Richardson, I.G. 2004. Tobermorite/jennite- and tobermorite/calcium hydroxide-based models for the structure of C-S-H: applicability to hardened pastes of tricalcium silicate, β-dicalcium silicate, Portland cement, and blends of Portland cement with blast-furnace slag, metakaolin, or silica fume. *Cement and Concrete Research.* **34**(9), pp.1733-1777.

Richardson, I.G., Girão, A.V., Taylor, R. and Jia, S. 2016. Hydration of water- and alkali-activated white Portland cement pastes and blends with low-calcium pulverized fuel ash. *Cement and Concrete Research.* **83**, pp.1-18.

Richardson, I.G. and Groves, G.W. 1992. Microstructure and microanalysis of hardened cement pastes involving ground granulated blast-furnace slag. *Journal of Materials Science.* **27**(22), pp.6204-6212.

Richardson, I.G. and Groves, G.W. 1993. Microstructure and microanalysis of hardened ordinary Portland cement pastes. *Journal of Materials Science.* **28**(1), pp.265-277.

Rinklebe, J. and Shaheen, S.M. 2017. Redox chemistry of nickel in soils and sediments: A review. *Chemosphere.* **179**, pp.265-278.

Roque, A.J., Martins, I.M., Freire, A.C., Neves, J.M. and Antunes, M.L. 2016. Assessment of Environmental Hazardous of Construction and Demolition Recycled Materials (C&DRM) from Laboratory and Field Leaching Tests Application in Road Pavement Layers. *Procedia Engineering.* **143**, pp.204-211.

Rossen, J.E., Lothenbach, B. and Scrivener, K.L. 2015. Composition of C-S-H in pastes with increasing levels of silica fume addition. *Cement and Concrete Research.* **75**, pp.14-22.

Rothstein, D., Thomas, J.J., Christensen, B.J. and Jennings, H.M. 2002. Solubility behavior of Ca-, S-, Al-, and Si-bearing solid phases in Portland cement pore solutions as a function of hydration time. *Cement and Concrete Research.* **32**(10), pp.1663-1671.

Rumsby, P., Rockett, L., Clegg, H., Jonsson, J., Benson, V., Harman, M., Doyle, T., Rushton, L., Wilkinson, D. and Warwick, P. 2014. *Speciation of manganese in drinking water.*

Saca, N., Dimache, A., Radu, L.R. and Iancu, I. 2017. Leaching behavior of some demolition wastes. *Journal of Material Cycles and Waste Management.* **19**(2), pp.623-630.

Sadecki, R.W., Busacker, G., Moxness, K., Faruq, K. and Allen, L. 1996. *An investigation of water quality in runoff from stockpiles of salvaged concrete and bituminous paving.* St Paul, Minnesota: Minnesota Department of Transportation.

Saillio, M., Baroghel-Bouny, V. and Barberon, F. 2014. Chloride binding in sound and carbonated cementitious materials with various types of binder. *Construction and Building Materials.* **68**, pp.82-91.

Sanchez, F., Gervais, C., Garrabrants, A.C., Barna, R. and Kosson, D.S. 2002. Leaching of inorganic contaminants from cement-based waste materials as a result of carbonation during intermittent wetting. *Waste Management.* **22**(2), pp.249-260.

Sanger, M., Natarajan, B.M., Wang, B., Edil, T. and Ginder-Vogel, M. 2020. Recycled concrete aggregate in base course applications: Review of field and laboratory investigations of leachate pH. *J Hazard Mater.* **385**, p121562.

Šavija, B. and Luković, M. 2016. Carbonation of cement paste: Understanding, challenges, and opportunities. *Construction and Building Materials.* **117**, pp.285-301.

Schiopu, N., Tiruta-Barna, L., Jayr, E., Méhu, J. and Moszkowicz, P. 2009. Modelling and simulation of concrete leaching under outdoor exposure conditions. *Science of The Total Environment.* **407**(5), pp.1613-1630.

Schott, J., Pokrovsky, O.S. and Oelkers, E.H. 2009. 6. The Link Between Mineral Dissolution/Precipitation Kinetics and Solution Chemistry. In: Eric, H.O. and Jacques, S. eds. *Thermodynamics and Kinetics of Water-Rock Interaction.* Berlin, Boston: De Gruyter, pp.207-258.

Scrivener, K.L. and Nonat, A. 2011. Hydration of cementitious materials, present and future. *Cement and Concrete Research.* **41**(7), pp.651-665.

Segura, I., Molero, M., Aparicio, S., Anaya, J.J. and Moragues, A. 2013. Decalcification of cement mortars: Characterisation and modelling. *Cement and Concrete Composites.* **35**(1), pp.136-150.

Shriver, D.F. and Atkins, P.W. 1999. *Inorganic chemistry.* Third edition. ed. Oxford: Oxford University Press.

Somasundaram, S., Jeon, T.-W., Kang, Y.-Y., Kim, W.-I.L., Jeong, S.-K., Kim, Y.-J., Yeon, J.-M. and Shin, S.K. 2014. Characterization of wastes from construction and demolition sector. *Environmental Monitoring and Assessment.* **187**(1), p4200.

Stambulska, U.Y., Bayliak, M.M. and Lushchak, V.I. 2018. Chromium(VI) Toxicity in Legume Plants: Modulation Effects of Rhizobial Symbiosis. *BioMed Research International.* **2018**, p8031213.

Steefel, C.I. 2008. Geochemical Kinetics and Transport. In: Brantley, S.L., et al. eds. *Kinetics of Water-Rock Interaction.* New York, NY: Springer New York, pp.545-589.

Steffes, R. 1999. *Laboratory Study of the Leachate From Crushed Portland Cement Concrete Base Material.* Iowa: Iowa Department of Transportation.

Stumm, W. and Morgan, J.J. 1996. *Aquatic chemistry: chemical equilibria and rates in natural waters.* Third edition. ed. New York: Wiley.

Taylor, H.F.W. 1986. Proposed structure for calcium silicate hydrate gel. *Journal of the American Ceramic Society.* **69**(6), pp.464-467.

Taylor, H.F.W. 1997. *Cement chemistry.* 2nd ed. London: Thomas Telford.

The Water Supply (Water Quality) Regulations 2016. (614). London: The Stationary Office.

Tits, J., Geipel, G., Macé, N., Eilzer, M. and Wieland, E. 2011. Determination of uranium(VI) sorbed species in calcium silicate hydrate phases: A laser-induced luminescence spectroscopy and batch sorption study. *Journal of Colloid and Interface Science.* **359**(1), pp.248-256.

Torres, J., Gonzatto, L., Peinado, G., Kremer, C. and Kremer, E. 2014. Interaction of Molybdenum(VI) Oxyanions with +2 Metal Cations. *Journal of Solution Chemistry.* **43**(9), pp.1687-1700.

Tossavainen, M. and Forssberg, E. 1999. The potential leachability from natural road construction materials. *Science of The Total Environment.* **239**(1), pp.31-47.

Townsend, T., Jang, Y.-C., Tolaymat, T. and Jambeck, J. 2003. Leaching tests for evaluating risk in solid waste management decision making. *Florida Center for Solid and Hazardous Waste Management. Report.* (03-01).

Townsend, T., Tolaymat, T., Leo, K. and Jambeck, J. 2004. Heavy metals in recovered fines from construction and demolition debris recycling facilities in Florida. *Science of The Total Environment.* **332**(1), pp.1-11.

Townsend, T., Jang, Y. and Thurn, L.G. 1999. Simulation of Construction and Demolition Waste Leachate. *Journal of Environmental Engineering.* **125**(11), pp.1071-1081.

Trägårdh, J. and Lagerblad, B. 1998. *Leaching of 90-year old concrete mortar in contact with stagnant water.*

Tränkler, J.O.V., Walker, I. and Dohmann, M. 1996. Environmental impact of demolition waste — An overview on 10 years of research and experience. *Waste Management.* **16**(1), pp.21-26.

Trapote-Barreira, A., Cama, J. and Soler, J.M. 2014. Dissolution kinetics of C-S-H gel: Flow-through experiments. **70**, pp.17-31.

Trapote-Barreira, A., Cama, J., Soler, J.M. and Lothenbach, B. 2016. Degradation of mortar under advective flow: Column experiments and reactive transport modeling. *Cement and Concrete Research.* **81**, pp.81-93.

van der Sleet, H.A., Heasman, L. and Quevauviller, P. 1997. Chapter 2: General principles for the leaching and extraction of materials. In: van der Sleet, H.A., et al. eds. *Studies in Environmental Science.* Elsevier, pp.13-39.

van der Sloot, H.A. 1996. Developments in evaluating environmental impact from utilization of bulk inert wastes using laboratory leaching tests and field verification. *Waste Management.* **16**(1), pp.65-81.

van der Sloot, H.A. 2000. Comparison of the characteristic leaching behavior of cements using standard (EN 196-1) cement mortar and an assessment of their long-term environmental behavior in construction products during service life and recycling. *Cement and Concrete Research.* **30**(7), pp.1079-1096.

van der Sloot, H.A. 2002. Characterization of the leaching behaviour of concrete mortars and of cement–stabilized wastes with different waste loading for long term environmental assessment. *Waste Management.* **22**(2), pp.181-186.

van der Sloot, H.A. and Dijkstra, J.J. 2004. *Development of horizontally standardized leaching tests for construction materials: a material based or release based approach? Identical leaching mechanisms for different materials.* Energy Research Center of the Netherland.

van der Sloot, H.A., Meeussen, J.C.L., Garrabrants, A.C. and Kosson, D.S. 2009. *Review of the Physical and Chemical Aspects of Leaching Assessment.* IAEA.

van der Sloot, H.A., van Zomeren, A., Stenger, R., Schneider, M., Spanka, G., Stoltenberg-Hansson, A. and Dath, P. 2008. Environmental CRIteria for CEMent based products, ECRICEM.

Van Gerven, T., Cornelis, G., Vandoren, E. and Vandecasteele, C. 2007. Effects of carbonation and leaching on porosity in cement-bound waste. *Waste Management.* **27**(7), pp.977-985.

Van Gerven, T., Cornelis, G., Vandoren, E., Vandecasteele, C., Garrabrants, A.C., Sanchez, F. and Kosson, D.S. 2006. Effects of progressive carbonation on heavy metal leaching from cement-bound waste. *AIChE Journal.* **52**(2), pp.826-837.

Van Gerven, T., Van Baelen, D., Dutré, V. and Vandecasteele, C. 2003. Influence of carbonation and carbonation methods on leaching of metals from mortars. *Cement and Concrete Research.* **34**(1), pp.149-156.

Van Ginneken, L., Dutré, V., Adriansens, W. and Weyten, H. 2004. Effect of liquid and supercritical carbon dioxide treatments on the leaching performance of a cement-stabilised waste form. *The Journal of Supercritical Fluids.* **30**(2), pp.175-188.

Venhuis, M.A. and Reardon, E.J. 2001. Vacuum method for carbonation of cementitious wasteforms. *Environmental Science & Technology.* **35**(20), pp.4120-4125.

Vollpracht, A. and Brameshuber, W. 2016. Binding and leaching of trace elements in Portland cement pastes. *Cement and Concrete Research.* **79**, pp.76-92.

Walker, C.S., Sutou, S., Oda, C., Mihara, M. and Honda, A. 2016. Calcium silicate hydrate (C-S-H) gel solubility data and a discrete solid phase model at 25 °C based on two binary non-ideal solid solutions. *Cement and Concrete Research.* **79**, pp.1-30.

Wang, D. 2012. Redox chemistry of molybdenum in natural waters and its involvement in biological evolution. *Frontiers in microbiology.* **3**, p427.

Wang, L., Martens, E., Jacques, D., De Cannière, P., Berry, J.A. and Mallants, D. 2009. *Review of sorption values for the cementitious near field of a near surface radioactive waste disposal facility, project near surface disposal of category A waste at Dessel. ONDRAF/NIRAS.*

Weber, F-A., Voegelin, A. and Kretzschmar, R. 2009. Multi-metal contaminant dynamics in temporarily flooded soil under sulfate limitation. *Geochimica et Cosmochimica Acta.* **73**(19), pp.5513-5527

Wehrer, M. and Totsche, K.U. 2008. Effective rates of heavy metal release from alkaline wastes--quantified by column outflow experiments and inverse simulations. *Journal of contaminant hydrology.* **101**(1-4), pp.53-66.

Wolff-Boenisch, D., Gislason, S.R., Oelkers, E.H. and Putnis, C.V. 2004. The dissolution rates of natural glasses as a function of their composition at pH 4 and 10.6, and temperatures from 25 to 74°C. *Geochimica et Cosmochimica Acta.* **68**(23), pp.4843-4858.

WRAP. 2013. *Quality Protocol. Aggregates from inert waste.* [Online]. Oxford, UK: Environmental Agency. [Accessed 10/05/2023]. Available from: https://assets.publishing.service.gov.uk/government/uploads/system/uploads/attachment_data/file/296499/LIT_8709_c60600.pdf

Wright, I.A., Nettle, H., Franklin, M.J.M. and Reynolds, J.K. 2023. Recirculating Water through Concrete Aggregates Rapidly Produced Ecologically Hazardous Water Quality. *Water.* **15**(9), article no: 1705 [no pagination].

Wurts, W. and Durborow, R. 1992. Interactions of pH, Carbon Dioxide, Alkalinity and Hardness in Fish Ponds. *Southern Regional Aquaculture Center Publication.* **464**.

Yokozeki, K., Watanabe, K., Sakata, N. and Otsuki, N. 2004. Modeling of leaching from cementitious materials used in underground environment. *Applied Clay Science.* **26**(1), pp.293-308.

Yu, Q., Nagataki, S., Lin, J., Saeki, T. and Hisada, M. 2005. The leachability of heavy metals in hardened fly ash cement and cement-solidified fly ash. *Cement and Concrete Research.* **35**(6), pp.1056-1063.

Zhang, X.Z., Chang, W.Y., Zhang, T.J. and Ong, C.K. 2000. Nanostructure of calcium silicate hydrate gels in cement paste. *Journal of the American Ceramic Society.* **83**(10), pp.2600-2604.

Zhang, Y., Chen, J., Ginder-Vogel, M. and Edil, T. 2018. Effect of pH and Grain Size on the Leaching Mechanism of Elements from Recycled Concrete Aggregate. pp.325-334.

Zachara, J.M., Cowan, C.E. and Resch, C.T. 1990. *Metal Cation/Anion Adsorption on Calcium Carbonate: Implications to metal ion concentrations in groundwater.* USA: Pacific Northwest Laboratory.

Zwolak, I. 2014. Vanadium carcinogenic, immunotoxic and neurotoxic effects: a review of in vitro studies. *Toxicol Mech Methods.* **24**(1), pp.1-12.

Chapter 3 Methodology

This chapter contains information on the source of crushed concrete and preparation of samples, the theoretical underpinning of the instruments used in the experimental chapters, and experimental design and rationale, which describes the reagents used and analysis quality control. Specific details of the experiments described can be found in data chapters 4 and 5.

3.1 Sample materials

3.1.1 Source of the crushed concrete

Crushed concrete from the demolition of various buildings across a UK nuclear licensed site was produced between 1997 and 2012. Subsequently this was stockpiled on site with the intention to use it as backfill in future site restoration activities. Characterisation work carried out by the site managers involved excavation of twenty-one trial pits at nineteen different locations at across the rubble stockpile, of which material from two trial pits (RS1 and RS4) where made available for this study (Figure 3.1). Four samples outside the scope of nuclear regulations (total activity <0.4 Bq g^{-1}; ~25 kg each) were obtained from the surface (0 – 0.1 m) and subsurface (2.5 – 2.7 m) of each trial pit. Preliminary on-site processing involved spreading of the samples on benches and removal of foreign object debris, such as metals, wood and electrical cable, leaving only cementitious and soil waste materials. Particle size analysis was carried out by an independent construction material testing laboratory, Celtest, in accordance with their standard operating procedures and BS EN 933-1:2012 using the sieving method. Although there were variations between samples recovered from different trial pits, particle size analysis (Figure 3.2) indicated that on average particles >20 mm accounted for ~50% of the total sample mass, which were not further characterised in this study. The proportions of the stockpiled material in the smaller sizes were, ~25% between 6.3 – 20 mm, ~20% between 0.6 – 6.3 mm and ~5% < 0.6 mm (size fractionation is described below), and these size fractions were chosen for study. Approximately 50% of the samples were not used because of their large particle size, which is unsuitable for laboratory experiments. In addition, most of the surface area that will contribute to leaching is found in the smaller size fractions, which is why the smaller fractions are used in this project.

Scale 1:800

Figure 3.1 Aerial photograph of four crushed concrete stockpiles (SP1-4) present on a UK Nuclear site. Each of four stockpiles are distinguished by different border colours. Yellow circles indicate the location of 21 trial pits where samples where recovered. Samples for this study were recovered from both surface and subsurface layers from trial pits RS1 and RS4 on SP1. The stockpiles are around 3 metres high.

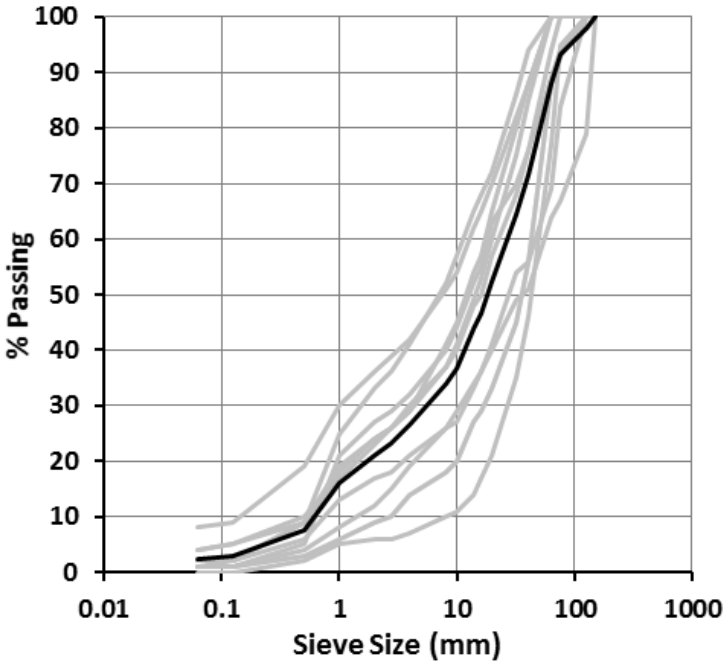

Figure 3.2 Particle size distribution curves of stockpiled concrete wastes collected from an average depth of 1.8 ±0.6 m below surface level from ten trial pits on stockpile 1 (Figure 3.1). Grey lines represent the individual samples, and the black line is mean of all samples.

3.1.2 Preparation of crushed concrete samples

For each of the four samples of crushed concrete obtained, 1.2 – 2 kg sub-samples were randomly taken from the bulk (~25 kg) sample to be used for laboratory experiments and dried at 40 °C overnight to remove moisture prior to fractionating using test sieves of 20 mm, 6.3 mm and 0.6 mm.

The size fractions chosen are based on ISO 14688-1:2017 (International Organization for Standardization, 2017) which assigns:

- 6.3 – 20 mm: medium gravel (Gravel)
- 0.63 – 6.3 mm: fine gravel and coarse sand (Sand)
- < 0.63 mm: medium and fine sand (Fines)

These size-fractions were then dried again at 40°C overnight, and double-bagged in polyethylene self-seal bags, and stored in 2 L airtight glass jars. In preparation for the batch experiments, the coarse gravel fractions were washed in a 25% w/w methanol-water suspension to remove any fines adhered to their surfaces. This suspension was used based on CH_3OH-water vapor-liquid equilibrium data (e.g. on page 337 in Felder

et al (2018)) as the drying time for materials wetted in this mixture is much shorter than if pure water was used.

3.2 Sample characterisation techniques

3.2.1 X-ray powder Diffraction (XRD)

The mineralogical composition of a sample can be determined using XRD, which is a non-destructive technique using an x-ray beam (Leng, 2008; Dutrow and Clark, 2023). X-rays are used because they have a short wavelength (10^{-10} m) that is on the same order of magnitude as the distance between atoms in crystalline solids (Battey, 1975; Stanjek and Häusler, 2004). When a beam of x-rays at a fixed wavelength and certain angle strikes the atoms in a crystal, the x-rays are diffracted according to the arrangement of atoms (Leng, 2008; Henry et al., 2018). Scattered x-rays interfere constructively when the phase difference between two waves travelling in the same direction are an integer multiple of the wavelength (Stanjek and Häusler, 2004; Leng, 2008). This constructive interference leads to diffracted x-rays exiting the crystal at the same angle as the incident x-ray beam (Henry et al., 2018). Diffraction is described by Bragg's Law, which relates the angle of diffraction to the atomic spacing between crystal planes at a specific wavelength (Leng, 2008; Henry et al., 2018; Dutrow and Clark, 2023) according to:

$$n\lambda = 2d \sin\theta$$

where n is an integer, λ is the wavelength, d is the inter-atomic spacing between crystal planes and θ is the angle of the incident x-ray.

Diffraction patterns are produced and are used to 'fingerprint' minerals by comparing the pattern to an X-ray diffraction database (Leng, 2008).

XRD was carried out on a Bruker D8 X-ray diffractometer with powder samples that were first crushed using a steel pestle and mortar and Agate Tema barrel mill to <120 µm. Samples were placed on silicon slides and scanned between 2 and 70 2θ using Cu K-alpha radiation.

3.2.2 X-ray Fluorescence (XRF)

XRF provides information on the elemental composition of a powder sample using x-rays and is a non-destructive technique (Brouwer, 2010). An x-ray beam (typically from an x-ray tube) irradiates the sample, and x-ray photons and electrons with sufficiently high energy (that can overcome the binding energy of the electron) cause the ejection

of inner shell electrons (Brouwer, 2010). This leaves a vacant electron site, so outer shell electrons at a higher energy level fall to replace ejected inner shell electrons (Brouwer, 2010). During this process, fluorescent radiation is emitted characteristic to that specific atom, allowing identification of the element (Brouwer, 2010).

XRF was carried out on powder samples (crushed, as described in previous section 3.2.1) to determine the major and minor elemental composition using Olympus Innovex X-5000.

3.2.3 Brunauer-Emmet-Teller (BET) specific surface area

The specific surface area (m^2/g) of a material can be measured using the BET theory (Brunauer et al., 1938) which extends the Langmuir theory of monolayer adsorption to include multilayer molecular absorption of gases on particle surfaces (Gregg and Sing, 1967; Ościk, 1982). The BET surface area is calculated using gas adsorption isotherm data obtained at different relative pressures, usually from p/p0 = 0.05 to 0.3 (Sing, 1985). Samples are first degassed with an inert gas at a constant temperature to remove any physisorbed species from particle surfaces (Sing, 1992). Samples are immersed in liquid nitrogen, and the amount of adsorbed gas (usually nitrogen) is measured using a volumetric or gravimetric method (Sing, 1985; 1992).

The surface area was measured by BET using Micrometrics Gemini VII 2390 with nitrogen gas. Before analysis, samples were degassed with nitrogen gas at 105 °C between ~19 and ~26 hours.

3.2.4 Scanning Electron Microscopy (SEM)

Scanning electron microscopes (SEM) use a beam of electrons generated from an electron gun to provide images of samples down to the nanoscale (Goldstein et al., 2003). Many systems use an electron gun with a heated tungsten filament (Zhou et al., 2007). The electron beam diameter is condensed to a small spot on the sample (1-100 nm) using electromagnetic lenses and apertures to produce high-resolution images (Sarkar et al., 2001; Zhou et al., 2007). The electron beam is scanned in a raster (x-y) pattern across the sample surface (Goldstein et al., 2003). The energy of the electron beam can be manually varied between 0.1 to 30 kilo electron volts (keV) (Goldstein et al., 2003). As electrons can interact with gases, the SEM is maintained under high vacuum conditions ($< 10^{-4}$ Pa) to reduce unwanted scattering from atoms and molecules in gases (Goldstein et al., 2003).

Images are created from the interaction of the electron beam with the sample surface, which produces various signals from the reflection or absorption of electrons (Sarkar et al., 2001). When an incident electron interacts with the sample surface, the electron beam causes the formation of the primary excitation volume (interaction volume), the size of which depends on the accelerating voltage of the microscope and the atomic number (Zhou et al., 2007). For example, the interaction volume at 15 keV is around several cubic microns (Watt, 1997). In this region, electrons collide with the atoms in the sample and produce different signals (Zhou et al., 2007). The scattering of electrons may be described as either elastic, where electrons are scattered in a different direction but there is insignificant change in electron energy, or inelastic, where beam electrons transfer energy to the sample atoms (Goldstein et al., 2003).

Secondary electrons (SE) and backscattered electrons (BSE) are produced from the reflection (scattering) of the incident electron beam and are used to image the sample (Zhou et al., 2007). SE have a relatively low energy (< 50 eV, majority below 5 eV) and are produced when sample atoms are ionised by the interaction between the electron beam and sample surface, leading to the excitation and emission of loosely bound electrons at shallow depths by inelastic scattering (typically a few nanometres of the surface) (Goldstein et al., 2003; Zhou et al., 2007). SE produce images with high resolution and are mainly used to image sample topography (Zhou et al., 2007).

BSE have a relatively high energy (> 50 eV) as these electrons are produced by elastic scattering from the interaction of the electron beam with atomic nuclei in the sample (Zhou et al., 2007). Images produced by BSE can provide topographic as well as compositional information (Zhou et al., 2007). The resolution of SE images is greater than BSE images because the region from where BSEs are produced is larger than that from SE as BSE are not adsorbed by the sample due to their high energy (Zhou et al., 2007). The brightness of images produced by BSE are related to the atomic number and material density, with higher atomic number substances producing brighter images (Sarkar et al., 2001). For example, in cement unhydrated clinker grains are brighter than C-S-H, as Fe present in clinker has a higher atomic number than calcium or aluminium (Sarkar et al., 2001).

The interaction of the electron beam and sample also produces characteristic x-rays that can provide semi-quantitative information about the chemical composition of a sample (Zhou et al., 2007). This information is obtained using Energy Dispersive X-ray spectroscopy (EDS), using detectors in the microscope (Goldstein et al., 2003). When an incident electron collides with an electron occupying the inner shell orbital, an outer

shell electron falls to takes its place and this produces x-rays photons which are characteristic of specific atoms (Goldstein et al., 2003; Zhou et al., 2007). SEM-EDS can also produce elemental maps, where elements are assigned a colour based on measured concentration (Goldstein et al., 2003).

Each SEM sample was set in epoxy resin (Huntsman Advanced Materials) and the surfaces of the resin blocks were polished using 3-, 1- and ¼-µm diamond paste (Struers) to expose cross-sections through the concrete grains. No water was used in polishing. Before analysis under the SEM, samples must be conductive therefore they were carbon coated (10-15 nm thickness) prior to analysis. BSE micrographs were taken using a Tescan VEGA3 XM equipped with an Oxford instruments X-max 150 SDD EDS using Aztec 3.3 software. Images were obtained at a working distance of 15 mm. A cobalt calibration standard was used to check drift in total detector counts between analyses of particles.

To choose the samples for analysis, initially wide field mode on the microscope was used to view the particles in the entire sample and then resolution mode was used for obtaining BSE images of individual particles. When viewing the samples under the microscope, the dominant mineral phase encountered were quartz particles. Aside from quartz, concrete particles composed the bulk of particles seen, and it was these particles that were chosen for analysis because they are the reactive phases of interest for leaching. Concrete particles were chosen at random for imaging. In Chapter 4, a total of 5 representative images (from 5 different particles) were taken from the surface and subsurface stockpile samples for elemental mapping and point counting analysis, the details of which may be found in Chapter 4. For EDS spot analysis, 9-10 particles were imaged in Chapter 4, and 5-12 particles per leached sample were imaged in Chapter 5.

3.2.4.1 Determination of C-(A)-S-H matrix composition

Cementitious phases are often smaller than the beam interaction volume, therefore it is difficult to characterise cement phases using SEM-EDS as intermixing of phases occur (Rossen and Scrivener 2017). This is especially apparent in cement blends with SCMs which makes estimation of composition difficult (Rossen and Scrivener, 2017; Scrivener et al., 2017). The usual convention to distinguish cement phases is to report EDS spot analyses as atomic ratio plots Al/Ca vs. Si/Ca as intermixing of cement phases occurs in the EDS interaction volume (1-2 μm^3 at 15 kV (Rossen and Scrivener, 2017)) whereas the composition of the C-(A)-S-H phases are reported in terms of Ca/Si

ratios (Rossen and Scrivener, 2017; Scrivener et al., 2017; Georget et al., 2021). Both approaches are used in this thesis.

To calculate the approximate Ca/Si ratio of the C-S-H/C-(A)-S-H gel matrix, which makes up the largest proportion of cement paste (Berner, 1992; Trapote-Barreira et al., 2014), a general boundary threshold (minimum) of Si/Ca = 0.5 and Al/Ca = 0.1, which corresponds to clinker phase belite (C_2S) (Georget et al., 2021) was used to exclude any cement clinker relics (which usually fall below this threshold) as well as carbonates or inter-mixed regions from the EDS spot analyses. The threshold was used because suspected unhydrated clinker relics were present in the matrix (which is common in mature cement paste samples, Diamond (2004)) and clinker that resembled belite, aluminate and ferrite (Stutzman et al., 2015) was observed in SEM images.

The assumption is that residual unreacted clinker phase relics will fall beneath the boundary values, and that any non-clinker phases with compositions below these values that were excluded are intermixed (e.g. with carbonates or hydrated aluminates such as AFt or AFm). Due to intermixing, the values are therefore only approximate using these thresholds. Spectral points with Fe >10% were not included in calculations as these visually corresponded to Fe oxides (bright spots on BSE images) which were separate from the C-(A)-S-H phases in the matrix. This was approach was taken in both Chapters 4 and 5.

3.3 Geochemical analyses

3.3.1 Inductively Coupled Plasma (ICP) spectroscopy

Inductively Coupled Plasma Optical Emission Spectroscopy (ICP-OES) and Inductively Coupled Plasma Mass Spectroscopy (ICP-MS) are analytical techniques used to measure the concentration of elements in a sample. An alternating electric current (radio-frequency field) or a direct current is used to generate a strong electrical field, which causes the ionisation of a gas (typically argon) to produce a plasma at very high temperatures (7000-15000 K)(Jeffrey et al., 1989; Hou and Jones, 2000). Under these temperatures, most elements are ionised (Hall, 1992). The sample is introduced into the centre of the hot plasma as an aerosol using a nebuliser, where it is broken down into free atoms and ions (Jeffrey et al., 1989; Boss and Fredeen, 2004). The energy from the plasma is absorbed by the atoms, causing them to enter into an excited state where electrons are elevated from lower energy orbitals to higher energy orbitals (Boss and Fredeen, 2004). The excited state is unstable, leading to the collision of atoms with

other particles, or the emission of photons of light which allow the electrons to decay to lower energy states (Thomas, 2001; Boss and Fredeen, 2004).

In ICP-OES, the intensity of the photon emission is measured at specific wavelengths to determine the elemental concentration of the sample (Boss and Fredeen, 2004). The light emitted is unique to each element. A monochromator is used to separate the emitted light into individual wavelengths, or a polychromator is used to measure emitted light at different wavelengths (Boss and Fredeen, 2004). Once the light is separated by wavelength, a photomultiplier detector is used to detect the light (Boss and Fredeen, 2004). The element concentration of a sample is obtained by comparing the calibration curve obtained using standard solutions, where the intensity of emission versus the concentration is plotted for each element (Boss and Fredeen, 2004).

ICP-MS is a high sensitivity technique capable of reaching very low detection limits (Thomas, 2001; Boss and Fredeen, 2004). In ICP-MS, the elemental concentration is determined using a quadruple mass spectrometer under a high vacuum (10^{-6} Torr), which separates atoms and/or ions of interest by their mass to charge ratio using a mass analyser (Thomas, 2001; Boss and Fredeen, 2004). Positively charged ions are measured using ICP-MS, and a lens component with applied voltages is used to prevent repulsion between ions and to move them into the mass analyser (Thomas, 2001). In the mass analyser, electrostatic fields are set up that allow ions of a specific mass to pass through and hit the negatively charged detector which attracts the positively charged ions (Thomas, 2001). The striking of the ion to the detector surface leads to emission of electrons, which are measured by an analyser (Thomas, 2001). The magnitude of electrons measured by the analyser correspond to the concentration of the element of interest (Thomas, 2001). The concentration of elements are then determined by calibration curves generated using standards (Thomas, 2001).

In this analysis, samples were filtered using a 0.22 µm polyethersulfone filter and diluted in a 1:10 ratio in 2% nitric acid before analysis on Thermo iCAP 7400 radial ion-coupled plasma optical emission spectrometer and Thermo iCAP Qc ion-coupled plasma mass spectrometer. The limit of detection (LOD) for elements was calculated using 3x the standard deviation (SD) of 6 blank measurements and can be found in the Appendix. The LOD for elements measured by ICP-OES (Al, Ca, Fe, Mg, S, Si) and ICP-MS (V, Cr, Pb, Cu, Mn) in Chapter 4 are shown in Table A1 and Table A2 respectively. The LOD for elements measured by ICP-OES (Al, Ca, K, Mg, S, Si) and ICP-MS (As, Cu, Cr, Fe, Mn, Pb, V, Zn) in Chapter 5 are shown in Table B1 and B2

respectively. The uncertainty at the 95% confidence interval for the elements measured can also be found in the aforementioned tables in Appendix A and B.

3.3.2 Ion chromatography

The ionic component (cation or anion) of a solution can be measured using ion chromatography. An eluent (the mobile phase) is pumped through the system continuously (Weiss, 2004). The sample is injected into the system and first run through a guard column that removes trace contaminants. The sample constituents are separated as it moves through the analytical column, which is packed with a resin material (called the stationary phase) (Jeffrey et al., 1989). The species in solution will move down the analytical column at different rates because of varying affinities for the resin (Jeffrey et al., 1989). As time progresses, the eluent is measured using conductivity or UV-Vis spectrometry. Quantitative data are obtained from the chromatographic signals by examining the peak area or height of the peak, as both are proportional to the species concentration (Weiss, 2004).

The concentration of chloride (Chapter 4) was measured on a Thermo Scientific ICS5000. The first injection used was Milli-Q water, followed by calibration standards (of varying concentrations) and certified standards. After every 10 samples, a calibration standard was injected to verify quality assurance. At the end, a sample used at the beginning of the run was reinjected to check for any system problems or sample changes that may have occurred as they sat in the vial. Whilst this approach is not standard practice, it was undertaken to prove that the samples can sit in the vials without decomposing or separating. It was also used to validate that any re-injected samples (of samples that required dilution) have not changed since sitting in the vials after being injected. Due to an excessive NO_3 peak in several samples, dilutions were carried out for peak shape improvement, and to bring them into calibration range. Out of 374 samples in total, the composition of 4 samples interfered with the column's chromatography, which caused poor integration and therefore these samples were excluded from analysis on the basis of being unreliable. The LOD for Cl^- in the analyses was 100 parts per billion (ppb).

3.4 Experimental design and approach

To study the leachate composition of CCW in conditions relevant to on-site disposal, characterisation leaching tests (Section 2.3.4) were used to study the fundamental leaching mechanisms of (chemical) equilibrium control and mass-transport control. Two different experimental designs (closed and open system) were used to study CCW

leaching under different flow conditions. Both designs used granular CCW, as this is relevant for the on-site disposal of non-compacted CCW. All experiments were undertaken in the laboratory under normal atmospheric conditions (CO_2 was not controlled) to represent conditions relevant for near-surface systems, where contact with air is assumed. All experiments were carried out in replicates to minimise error and improve reproducibility.

pH-dependent batch experiments were used because they represent a closed system where chemical reactions tend toward chemical equilibrium as the leachant is not exchanged and remains static (Schott et al., 2009). As reviewed in Section 2.3.4.1, batch experiments are beneficial for approximating leaching behaviour under percolation or stagnant conditions in the field. Element release from CCW was measured at different pH values to represent a range of environments that CCW may encounter in field applications. Prior to the pH-dependent batch experiments, preliminary acid neutralisation tests were used to determine the value and molarity of acid needed to change the solution pH to the required value. This data was also used to determine the acid and base neutralising capacity of the samples. Acid neutralisation tests and the pH-dependent batch tests were carried out in triplicate for each size fraction (gravel, sand and fines). Further experimental details may be found in Chapter 4.

Flow-through experiments with non-compacted granular CCW were used to represent an upflow open system whereby the leachant is constantly replenished. This design was chosen as it is relevant to the leaching of non-compacted granular CCW in on-site disposal conditions (Section 2.3.4.2). This dynamic experiment was used to examine mass-transport leaching controls and the effect of pH on element release during far-from-equilibrium steady-state conditions. In addition, this experiment was used to calculate the dissolution kinetics of CCW. Further experimental details can be found in Chapter 5.

To ensure reproducibility and the minimisation of error, all experiments were carried out in replicates. The leachants used were 0.5-5 mM hydrochloric acid (HCl), 1 mM acetic acid (HOAc) and 1-100 mM sodium hydroxide (NaOH). Each experiment was carried out in duplicate or triplicate, and the data are presented as averages and 1 SD. Like the batch tests, the flow-through experiments used different pH leachants to study the effect of pH on leaching behaviour under different flow conditions.

3.4.1 Reagents and quality control

The reagents used (and from which stock solutions were made for the experiments) in both experiments were analytical reagent grade 70% nitric acid, 37% hydrochloric acid, glacial acetic acid and sodium hydroxide pellets. In each ICP batch, a minimum of 3 blanks of nitric acid (the matrix) were run. In the batch experiments, the elemental concentrations of three blanks were below the LOD (Appendix A). However, in the flow-through experiments the same reagent as the batch experiments was used but measurements of the matrix blank (i.e. only 9 mL of 2% nitric acid) had unexpectedly high background concentrations of several elements in the acid. To remove this background concentration, a matrix correction was undertaken to ensure that only the signal from the sample remained. The matrix correction was undertaken by taking the average element concentration of the matrix blanks, and this was subtracted from the sample values. Then, the values were only accepted as valid if they were above the average plus 3xSD of the matrix blanks, and this data was used. This stringent approach was undertaken to ensure the elemental concentrations were as accurate as possible.

3.5 References

Battey, M.H. 1975. *Mineralogy for Students.* Longman.

Berner, U.R. 1992. Evolution of pore water chemistry during degradation of cement in a radioactive waste repository environment. *Waste Management.* **12**(2), pp.201-219.

Boss, C.B. and Fredeen, K.J. 2004. *Concepts, Instrumentation and Techniques in Inductively Coupled Plasma Optical Emission Spectrometry.* USA: PerkinElmer.

Brouwer, P. 2010. *Theory of XRF. Getting acquainted with the principles. .* [Online]. Netherlands: PANalytical. [Accessed 25/09/2023]. Available from: https://www.chem.purdue.edu/xray/docs/Theory%20of%20XRF.pdf

Brunauer, S., Emmett, P.H. and Teller, E. 1938. Adsorption of Gases in Multimolecular Layers. *Journal of the American Chemical Society.* **60**(2), pp.309-319.

Dutrow, B.L. and Clark, C.M. 2023. *X-ray Powder Diffraction (XRD).* [Online]. Available from: https://serc.carleton.edu/research_education/geochemsheets/techniques/XRD.html

Felder, R. M., Rousseau, R.W. and Bullard, L.G. 2016. *Elementary Principles of Chemical Processes*. Fourth edition. USA: Wiley.

Georget, F., Wilson, W. and Scrivener, K.L. 2021. edxia: Microstructure characterisation from quantified SEM-EDS hypermaps. *Cement and Concrete Research.* **141**, p106327.

Goldstein, J., Newbury, D.E., Michael, J.R., Ritchie, N.W.M., Scott, J.H.J. and Joy, D.C. 2003. *Scanning electron microscopy and x-ray microanalysis.* Third edition. ed. New York : Kluwer Academic/Plenum Publishers.

Gregg, S.J. and Sing, K.S.W. 1967. *Adsorption, surface area, and porosity.* London ;: Academic Press.

Hall, G.E.M. 1992. Inductively coupled plasma mass spectrometry in geoanalysis. *Journal of Geochemical Exploration.* **44**(1), pp.201-249.

Henry, D., Nelson, E., Goodge, J. and Mogk, D. 2018. *X-ray reflection in accordance with Bragg's Law.* [Online]. Available from: https://serc.carleton.edu/msu_nanotech/methods/BraggsLaw.html

Hou, X. and Jones, B.T. 2000. Inductively Coupled Plasma/Optical Emission Spectrometry. In: Meyers, R.A. ed. *Encyclopedia of Analytical Chemistry.* [Online]. Chichester: John Wiley & Sons Ltd, pp.9468–9485. [Accessed 26/09/2023]. Available from: https://www.unil.ch/idyst/files/live/sites/idyst/files/shared/Labos/Hou%26Jones_2000.pdf

International Organization for Standardization. 2017. *Geotechnical investigation and testing — Identification and classification of soil — Part 1: Identification and description*. ISO 14688-1:2017.

Jeffrey, G.H., Bassett, J., Mendham, J. and Denney, R.C. 1989. *Vogel's Textbook of Quantiative Chemical Analysis.* Fifth Edition ed.

Leng, Y. 2008. X-Ray Diffraction Methods. *Materials Characterization.* pp.45-77.

Ościk, J. 1982. *Adsorption.* E. Horwood.

Rossen, J.E. and Scrivener, K.L. 2017. Optimization of SEM-EDS to determine the C–A–S–H composition in matured cement paste samples. *Materials Characterization.* **123**, pp.294-306.

Sarkar, S.L., Aimin, X. and Jana, D. 2001. 7 - Scanning Electron Microscopy, X-Ray Microanalysis of Concretes. In: Ramachandran, V.S. and Beaudoin, J.J. eds. *Handbook of Analytical Techniques in Concrete Science and Technology.* Norwich, NY: William Andrew Publishing, pp.231-274.

Scrivener, K., Bazzoni, A., Mota, B. and Rossen, J.E. 2017. Electron Microscopy In: Scrivener, K., et al. eds. *A Practical Guide to Microstructural Analysis of Cementitious Materials.* [Online]. 1sts ed. Boca Raton: CRC Press. [Accessed 7/07/2023].

Sing, K.S.W. 1985. Reporting physisorption data for gas/solid systems with special reference to the determination of surface area and porosity (Recommendations 1984). *Pure and Applied Chemistry.* **57**(4), pp.603-619.

Sing, K.S.W. 1992. Adsorption Methods for Surface Area Determination. In: Stanley-Wood, N.G. and Lines, R.W. eds. *Particle Size Analysis.* The Royal Society of Chemistry, pp.13-32.

Stanjek, H. and Häusler, W. 2004. Basics of X-ray Diffraction. *Hyperfine Interactions.* **154**(1), pp.107-119.

Thomas, R. 2001. A beginner's guide to ICP-MS. *Spectroscopy.* **16**(4), pp.38-42.

Trapote-Barreira, A., Cama, J. and Soler, J.M. 2014. Dissolution kinetics of C-S-H gel: Flow-through experiments. **70**, pp.17-31.

Watt, I.M. 1997. Electron–specimen interactions: processes and detectors. In: Watt, I.M. ed. *The Principles and Practice of Electron Microscopy.* 2 ed. Cambridge: Cambridge University Press, pp.30-58.

Weiss, J. 2004. Introduction. *Handbook of Ion Chromatography.* Weinheim: Wiley-VCH, pp.1-11.

Zhou, W., Apkarian, R., Wang, Z.L. and Joy, D. 2007. Fundamentals of Scanning Electron Microscopy (SEM). In: Zhou, W. and Wang, Z.L. eds. *Scanning Microscopy for Nanotechnology: Techniques and Applications.* New York, NY: Springer New York, pp.1-40.

Chapter 4 In situ disposal of crushed concrete waste as void fill material at UK nuclear sites: Leaching behaviour and effect of pH on trace element release

Summary

The leaching behaviour of stockpiled crushed concrete waste is important in determining its suitability for in situ disposal at UK nuclear sites. Sand sized particles from surface (0–0.1 m) and subsurface (2.5–2.7 m) samples were composed of silica and calcite grains in a matrix of calcium alumina-silicate hydrate (C-(A)-S-H) with Ca/Si ratios of 0.5 ± 0.3 and 0.9 ± 0.3 respectively. Calcite content was also higher in surface samples indicating a greater degree of weathering and carbonation. This resulted in lower leachate pH for the surface samples (pH 8–9.6) compared to subsurface samples (pH 10–11.3). The waste displayed a high acid buffering capacity but low alkaline buffering capacity. Element release as a function of pH was similar for surface and subsurface samples and between different size fractions, with the exception of Cu at pH >11 for the surface fines fraction. Leaching of contaminant metals was close to minimum values at the pH values produced by the crushed concrete but increased by several orders of magnitude at pH < 5 (for Al, Pb, Cr, V, Mn and Cu) and pH > 12 (for Al, Pb and Cu). Weathering and carbonation during long-term stockpiling, therefore, has a positive impact by producing a waste with stable pH and low metal leaching potential suitable for in-situ disposal as a void fill material.

4.1 Introduction

Concrete will form a significant proportion of the waste generated during the decommissioning and clean-up of nuclear sites across the world (IAEA, 2008; GRR, 2018). Waste management options for non-contaminated and contaminated structural wastes include disposal to landfill or to a dedicated radioactive waste repository (Deissmann et al., 2006). Off-site disposal is the least favoured pathway in the UK's Waste Management Hierarchy (NDA, 2010; 2016). The majority of decommissioning waste will be non-radioactive and resembles conventional demolition materials. Therefore, leaving existing below ground structures in-situ and using concrete demolition materials to backfill voids is currently under consideration as a waste management option (Deissmann et al., 2006; IAEA, 2008; GRR, 2018). This is similar to practice in the CDW industries, where crushing of concrete monoliths produces RCM (Sanger et al., 2020) for use in landscaping, void fill or as aggregate (Coudray et al., 2017; NDA, 2020), which may also be described as CCW. On-site reuse of CCW is an

economically and environmentally advantageous route to minimizing both off-site waste transport and import of new materials for void fill and landscaping purposes (Deissmann et al., 2006; NDA, 2020).

In CDW industries, crusher fines are often removed from CCW prior to use as crushing can concentrate the alkaline cement paste in the finest fractions (Engelsen et al., 2009; Coudray et al., 2017). At nuclear sites, however, there is a desire to use CCW as backfill in much larger volumes than is common in the CDW industry, and to use it without fines removal to limit the need for off-site waste disposal (Foy et al., 2019). In addition, proposed uses of CCW at nuclear sites differ from more common RCM applications in that nuclear facilities often have deep basements that extend below the water table, and the CCW may be stockpiled for decades prior to use as void fill as it is mainly required at the end stages of decommissioning (NDA, 2020). CCW with a higher fines content would likely reduce the porosity and permeability of the backfill, leading to a decrease in water flow. However, the high surface area of the fines will increase the rate of cement phase dissolution, so there is uncertainty over whether fines inclusion will increase or decrease leaching. Further, CCW derived from the demolition of nuclear facilities will be subject to more stringent regulatory control due to the potential presence of low-level radioactivity, so there is a need to understand the leaching behaviour of CCW over multi-decadal time scales to prepare the site closure safety cases (NDA, 2010; Nuclear Energy Agency, 2017)

Although fine and coarse aggregate (sand and gravel) dominate concrete composition by volume, the hydrated cement paste is far more reactive and produces high pH leachates when immersed in water (Ekström, 2001; Deissmann et al., 2006). Hydrated cement paste is typically composed of non-stoichiometric hydrated calcium silicate gel (C-S-H, 40–50 %), portlandite (CH; 20–25%), AFm and AFt (10-20 %), minor hydroxides (e.g. KOH, NaOH; 0–5 %), and a pore solution (10–20 %) (Berner, 1992). In Portland cement-based materials, C-S-H can readily incorporate aluminium, so is best regarded as a calcium aluminosilicate hydrate (C-(A)-S-H) with variable composition, which can be described in terms of the Ca/Si and Al/Si ratios, which is relevant for leaching (Richardson, 1999; Gérard et al., 2002; L'Hôpital et al., 2015; 2016a;b).

The pore solution of hardened cement paste contains Na^+, K^+, OH^- and Ca^{2+} ions due to dissolution of Na_2O and K_2O present in cement and equilibration with the hydrated cement phases (e.g. portlandite), and usually has a pH value above 13 (van der Sloot, 2000; Ekström, 2001; Faucon et al., 1998). When water with a pH lower than the pore

solution comes into contact with cement phases, the very soluble Na- and K-hydroxides are leached out first, resulting in a decrease in the OH^- concentration (Faucon et al., 1996). Leaching by pure water results in a cascade of cement dissolution processes that in turn control the pore water composition (Figure 2.3, Chapter 2 Section 2.5). Initially, the decreasing pH value and leaching of calcium (decalcification) drives the dissolution of CH, then the other cement phases dissolve in sequence, with each in turn controlling the pore water composition (Ekström, 2001; Glasser et al., 2008; Engelsen et al., 2009). Carbonation also drives the decalcification of cement hydrates, as gaseous CO_2 dissolves into the pore solution, forming carbonate ions which react with Ca^{2+} to form calcium carbonate (Van Gerven et al., 2006; Glasser et al., 2008). During carbonation and leaching, dissolution of the higher Ca/Si ratio cement hydrates occurs first producing cements with lower Ca/Si ratios over time (Gérard et al., 2002; Segura et al., 2013). Highly alkaline leachate is produced at all stages of leaching (Figure 2.3, Chapter 2 Section 2.5), with the pore solution pH gradually decreasing from an initial pH of over 13 to around pH 9 over time (Jacques et al., 2014).

The successive changes in pore solution pH affects the stability of different cement phases and the leaching behaviour of any contaminants. Concrete can contain trace metal and other impurities, such as Ba, Cd, Co, Cr, Cu, Mn, Mo, Ni, Pb, Sb, Ti, V and Zn, which are derived from raw materials used for cement clinker production (Faucon et al., 1998; Cornelis et al., 2008; Vollpracht and Brameshuber, 2016). Oxyanion-forming contaminants (e.g. Co, Cr, Mo and V) are a particular concern, as they have enhanced solubility at the high pH values characteristic of concrete pore solutions (Gomes et al., 2016). CCW from nuclear sites may also contain radionuclides such as ^{137}Cs, ^{3}H, ^{60}Co, ^{63}Ni, U, Pu, Am and other actinide elements (Bath et al., 2003), however, this research specifically focused on alkalinity and stable element leaching from non-radioactive CCW produced during site decommissioning, which has been stockpiled for future use as void fill. Release of contaminants of potential concern from CCW is typically controlled by the dissolution of specific host cement phases, and their subsequent interactions (e.g. incorporation or sorption) with the secondary phases that form as the chemical conditions evolve during leaching (Engelsen et al., 2010; Vollpracht and Brameshuber, 2016).

There are considerable economic and environmental incentives for reuse of CCW, however in the nuclear industry such use is conditional on sufficient risk assessment, which fundamentally rests on knowledge of CCW leaching behaviour, local

hydrochemical conditions and the site conceptual model for waste disposal (IAEA, 2008). A potential concern with the scale of future backfilling operations are that highly alkaline leachate plumes may subsequently migrate laterally outside of the legacy structure, or disperse downwards into groundwater, presenting an environmental risk. Yet whether various metals will mobilise from different concrete phases and their propensity for migration within and outside these structures is unknown. Currently, there are considerable knowledge gaps surrounding the environmental behaviour of concrete rubble; firstly, concerning the leachate that will be produced by undifferentiated cement phases from stockpiled CCW that will occur with the ingress of rainwater and/or groundwater, and secondly how this leachate will evolve over long time periods. Furthermore, it is uncertain how contaminant metals will mobilise within the disposal environment.

This research investigates the leaching behaviour of non-radioactive crushed concrete that has been stockpiled at a nuclear licensed site undergoing decommissioning. Research objectives 1 and 2 are addressed in this chapter. The materials have been characterised, and pH-dependent batch leaching tests have been conducted on different size fractions from differently weathered samples from the same stockpile. These experiments are used to determine the influence of size fraction, weathering after crushing and long-term stockpiling on the evolution of the leachate chemistry and alkalinity generating potential (research objective 1), and to evaluate the leaching behaviour of selected elements (Ca, Si, Al, Mg, Fe, S, Pb, Cr, V, Cl, Cu, Mn) as function of pH (research objective 2). Material characterisation aids in the determination of the alkalinity generating potential as a function of weathering. The data produced will inform safety assessments of in-situ disposal of crushed concrete as a void-filling material at UK nuclear sites.

4.2 Materials and Methods

4.2.1 Materials and sample characterisation

Crushed concrete samples previously fractionated into gravel (6.3 – 20 mm), sand (0.6 – 6.3 mm) and fines (<0.6 mm) size fractions from the surface (0 – 0.1 m) and subsurface (2.5 – 2.7m) of trial pits RS1 and RS4 (Chapter 3, Figure 3.1) are used in this study.

Each size fraction (gravel, sand and fines) was placed on a clean polyethylene tray and homogenized before a portion was selected by coning and quartering for mineralogical and elemental characterisation. Samples for mineralogical and chemical analysis were

crushed first using a steel pestle and mortar followed by an Agate Tema barrel mill to <0.120 µm. Mineralogical analysis was undertaken using a Bruker D8 XRD with the powder samples placed on silicon slides and scanned between 2 and 70 2θ using Cu K-alpha radiation. The major and trace element composition of the analytical samples were determined by XRF using Olympus Innovex X-5000.

Portions from the sand size-fraction from the surface and subsurface samples were subjected to SEM-EDS analysis. Samples were prepared as described in Chapter 3 Section 3.2.4. Back-scatter electron micrographs were obtained using a Tescan VEGA3 XM equipped with an Oxford instruments X-max 150 SDD EDS using Aztec 3.3 software. A beam energy of 15 keV was used, at a 15 mm working distance. Elemental mapping was performed at a resolution of 2 µm. Point counting analysis was undertaken on false-colour composite EDS images of 5 representative particles from the surface and subsurface samples. Point counting analysis was completed by imposing 5 by 20 equally spaced lines on false-colour composite EDS images (see Figure 4.1 for an example). Phases were counted at the intersection between the horizontal and vertical lines. Only phases on the particle were counted and the totals were corrected where intersections were outside the particle such as in Figure 4.1. Five representative particles from the surface (0 – 0.1 m) and the subsurface (2.5 – 2.7 m) of the stockpile samples were used. For simplicity, phases were either assigned as quartz (in blue), calcite (in red) or C-(A)-S-H (in varying shades of purple – from close to blue representing a Ca-depleted gel, to darker purple representing higher Ca/Si ratios). Where there were Fe, S or Mg particles (e.g. green particles) or Al-rich regions (lighter purples and blues in the C-(A)-S-H gel), this was also included under C-(A)-S-H. This is due to the inherent heterogeneity of C-(A)-S-H, and for ease of reference. EDS spot analysis was performed on 9 particles in the surface and 10 particles in subsurface samples by randomly selecting between 10 and 30 spots per particle region. Maximum counts per second were set at 600,000 and calibration against a cobalt standard was performed regularly.

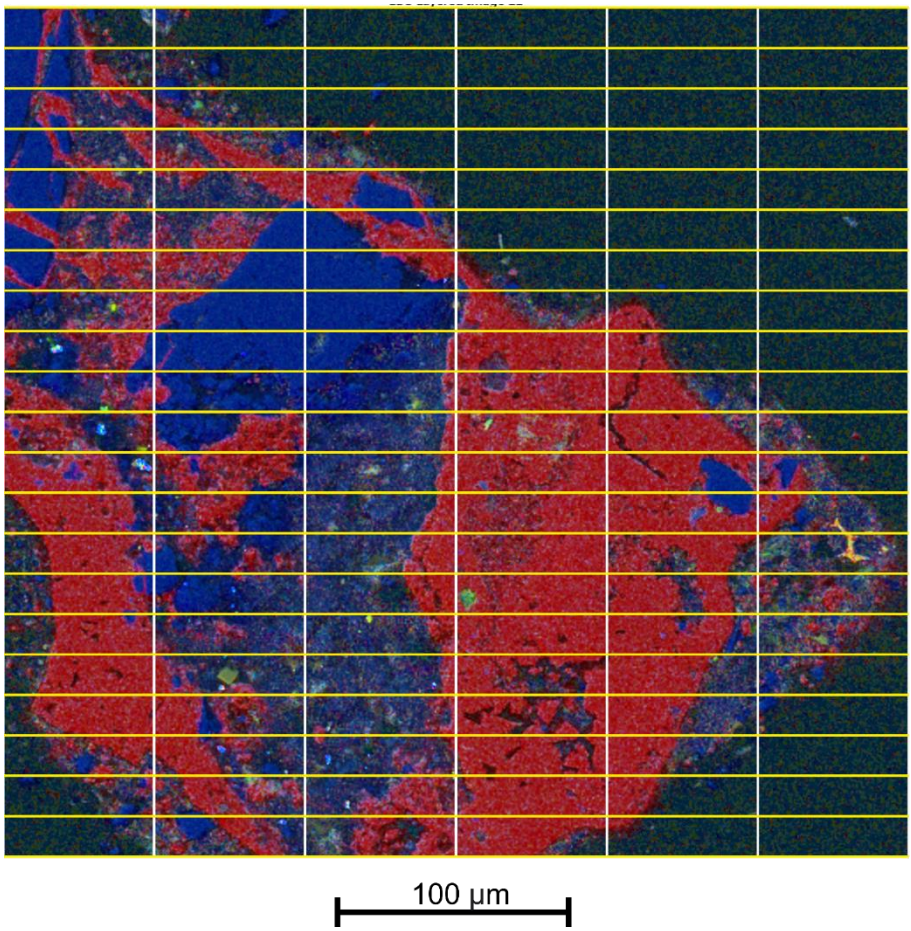

Figure 4.1 Example of grid used for point counting of false-colour composite EDS map of a sand-sized fraction from the surface 0 – 0.1 m of stockpile 1 (trial pit RS4), where Blue = Si, Red = Ca, Green = Fe, Orange = Mg, Yellow = S, Gold = Al, Magenta = Na. Area outside the particle was not included in the totals which were corrected for.

4.2.2 pH-dependent batch leaching experiments

Batch experiments were carried out on each of the three size fractions of the surface and subsurface materials. The pH of the material at equilibrium was determined using deionised water without acid or base addition and is referred to as the material pH. Preliminary acid neutralisation experiments were carried out to determine the approximate volume and strength of nitric acid (1-10 mol L^{-1}) or sodium hydroxide (1-5 mol L^{-1}) required to reach specific target pH values (between pH 2 and pH 13) for the batch experiments. Triplicate samples (4g) were mixed with 40ml deionised water (18 MΩ, *Millipore X500XX*) in 50ml polyethylene tubes, and the pre-determined volumes of acid (HNO_3) or base (NaOH) were added to each suspension. Samples were agitated on an orbital shaker (70 ± 2 RPM), and further acid/base additions were made as

required following measurement of the solution pH (suspensions were allowed to settle for 10 minutes prior to measurement). In some cases, several pH adjustments were required, and the experiments were run for either 7 or 8 days (the samples were equilibrated for at least a day after the last pH correction). Atmospheric CO_2 was not controlled for the experiments.

4.2.3 Analytical methods

Solution pH was measured using a Thermo Fisher Sure-Flow Electrode and Orion 3 Star pH meter, which was calibrated daily using pH buffers 4, 7, 10 and 12.5. At the end of testing, 10 mL of solution was taken from all replicates and filtered using a 0.22 µm polyethersulfone syringe filters. 1 mL of filtered solution was acidified with 2% HNO_3 (9 mL) for analysis of elements Ca, Si, Al, Mg, Fe, and S using a Thermo iCAP 7400 radial ion-coupled plasma optical emission spectrometer and Pb, Cr, V, Mn and Cu using a Thermo iCAP Qc ion-coupled plasma mass spectrometer (ICP-MS), and the remainder of the filtered sample was stored without acid addition for anion analysis (Cl^-) by ion chromatography on a Thermo Scientific ICS5000. Samples were kept refrigerated at 4°C before analysis. Data that were below the LOD or limit of quantification (LOQ) are reported at the respective LOD or LOQ value. LODs and uncertainty (%) are reported in Appendix Section A Table A1 and A2.

4.3 Results

4.3.1 Characterisation of crushed concrete

The x-ray diffractograms from the sand and fine fractions (Figure 4.2) have multiple large peaks at 2θ values characteristic of quartz, multiple clear peaks at 2θ values characteristic of calcite, and small peaks at 2θ values characteristic of dolomite, barite, muscovite and microcline. The identification of quartz and calcite as the major minerals present in both surface and subsurface samples is supported by the major element XRF analysis (Table 4.1), where Si and Ca were the most abundant elements detected in all fractions, followed by Al, Fe, Ti, Mg, S, K, Mn and P. There were only minor compositional differences between the size fractions and between the surface and subsurface samples although Ti was higher in the subsurface fractions.

Trace element concentrations (Cl, V, Cr, Sr, Ag, Sn, Sb, Hg, Pb, Th, U) were greater in the subsurface fractions than in the surface fractions but were generally comparable across the size fractions of the same samples (Table 4.2). Although, in the surface samples, there was higher chloride concentrations in the sand and fines fractions

(Table 4.2). V concentrations were highest (and also exhibited the most scatter), followed by Sr, Cl, Pb, Cr, Sn, Zn, Sb, Y, Rb, and Cu. Elements Cu, Zn, As, Rb and Y were comparable across the surface and subsurface samples. Some elements (Co, Mo, Ag, Sn, Sb, Hg, Th and U) were only detected in some replicates across both samples.

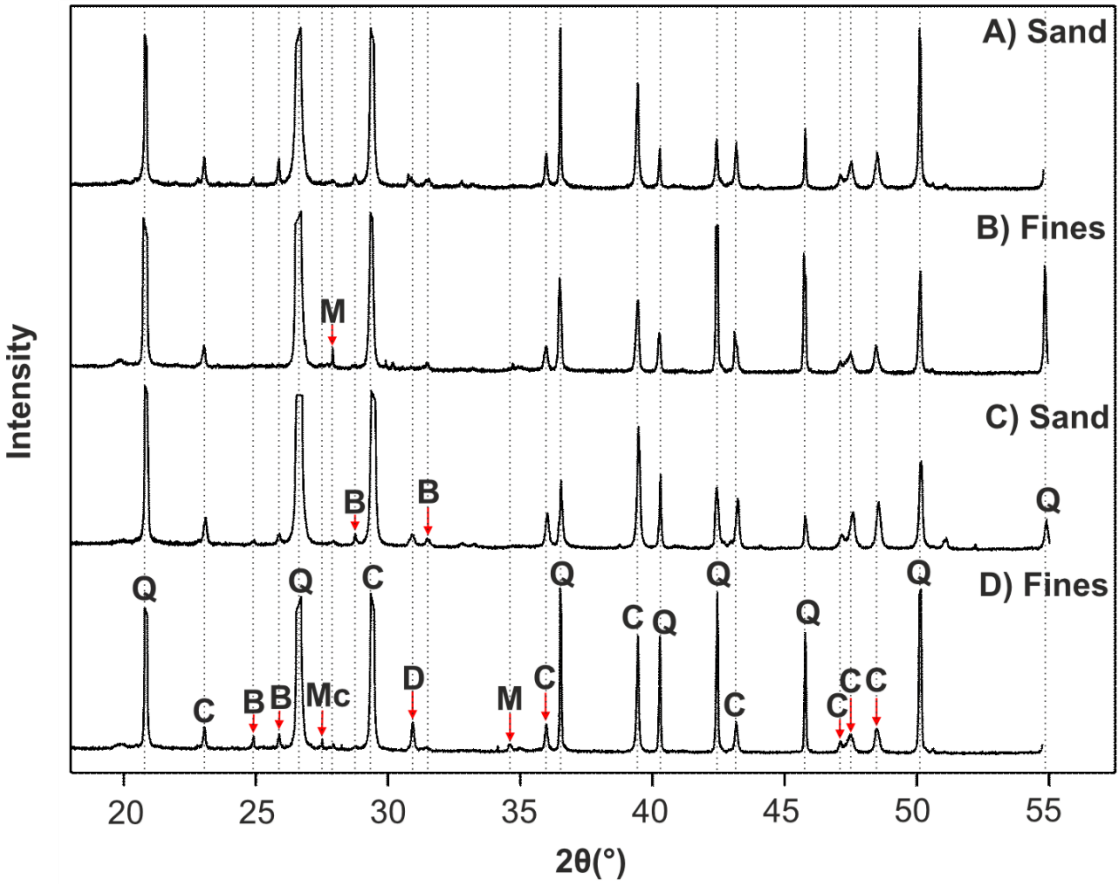

Figure 4.2 Selected XRD patterns of sand (0.6 – 6.3 mm) and fines (<0.6 mm) fractions of crushed concrete materials; Figure 4.2 A) and B) are from subsurface (2.5 – 2.7 m) and C) and D) are from the surface 0 – 0.1 m of trial pit RS4 from stockpile 1. Labelled minerals detected are quartz (Q), calcite (C), dolomite (D), barite (B), microcline (Mc) and muscovite (M). The major quartz and calcite peaks have been truncated to allow minor peaks from other phases to be discernible. The dotted lines are used to show the peak positions in the different samples.

Table 4.1 Major element composition (wt%) of gravel, sand and fines fractions from surface 0 – 0.1 m (Surface) and subsurface 2.5 - 2.7 m (Sub-S.) samples in trial pits RS1 and RS4 from stockpile 1 (Chapter 3 Section 3.1 Figure 3.1) given as mean (n=6) ±1σ of 6 replicates. Obtained from XRF analysis.

	Mg	Al	Si	P	S	K	Ca	Ti	Mn	Fe
Gravel (6.3 – 20 mm)										
Surface	0.6 ±0.2	1.2 ±0.4	24.2 ±1.1	<0.1	0.2 ±0.1	0.3 ±0.0	9.5 ±0.8	0.3 ±0.2	<0.1	1.3 ±0.3
Sub-S.	0.6 ±0.2	1.3 ±0.3	25.0 ±2.0	<0.1	0.9 ±0.4	0.3 ±0.1	9.0 ±1.6	2.0. ±1.1	0.1 ±0.05	1.0 ±0.3
Sand (0.6 – 6.3 mm)										
Surface	0.6 ±0.2	1.7 ±0.8	23.6 ±1.0	<0.1	0.2 ±0.1	0.4 ±0.1	8.4 ±1.1	0.4 ±0.2	<0.1	1.2 ±0.2
Sub-S.	0.6 ±0.2	1.6 ±0.5	24.2 ±1.5	<0.1	0.6 ±0.4	0.4 ±0.1	8.3 ±1.4	1.6 ±1.1	0.1±0.05	1.0 ±0.2
Fines (< 0.6 mm)										
Surface	0.6 ±0.2	2.2 ±0.5	23.3 ±1.8	<0.1	0.2 ±0.1	0.5 ±0.1	7.7. ±1.4	0.5 ±0.1	<0.1	1.3 ±0.2
Sub-S.	0.5 ±0.2	1.9 ±0.4	23.2 ±1.8	<0.1	0.4 ±0.2	0.4 ±0.05	7.8 ±1.3	1.1 ±0.8	0.1 ±0.05	1.0 ±0.2

Table 4.2 Trace element concentrations (ppm) in gravel (6.3 – 20 mm), sand (0.6 – 6.3 mm) and fines (<0.6 mm) sized fractions recovered from the surface 0 – 0.1 m and subsurface 2.5 – 2.7 m in trial pits RS1 and RS4 from stockpile 1 (Chapter 3 Section 3.1 Figure 3.1) given as the mean (n=6) ±1SD of 6 replicates. Ni, Se, Cd, Bi, W were all not detected (n.d) and therefore not shown. Obtained from XRF analysis.

	Cl	**V**	**Cr**	**Co**	**Cu**	**Zn**	**As**	**Rb**	**Sr**	**Y**
Surface										
Gravel	n.d	130±170	23±14	59	n.d	31±18	7±3	10±6	239±85	13±5
Sand	142	183±155	31±15	n.d	10±1	46±22	8±2	12±6	228±24	12±1
Fines	158±10	230±110	40±3	n.d	12±4	60±15	10±4	16±5	261±58	16±3
Subsurface										
Gravel	260±46	1800±1100	110 ±50	n.d	11±1	36±14	7±0.3	10±6	677±232	11±3
Sand	280±113	1400±1200	89±59	n.d	12±5	49±31	10±5	13±5	624±386	14±3
Fines	210±33	830 ±840	67±44	n.d	12±1	58±23	8*	15±4	440±309	13±3
	Mo	**Ag**	**Sn**	**Sb**	**Hg**	**Pb**	**Th**	**U**	**Mo**	**Ag**
Surface										
Gravel	n.d	n.d	n.d	n.d	n.d	30±27	n.d	n.d	n.d	n.d
Sand	n.d	n.d	n.d	n.d	n.d	44±26	n.d	n.d	n.d	n.d
Fines	n.d	n.d	20	37	n.d	60±7	n.d	n.d	n.d	n.d
Subsurface										
Gravel	5	13±2	66±18	18±4	7	123±89	17	18±1	5	13±2
Sand	n.d	12±3	59±30	19±0	7	129±111	n.d	18	n.d	12±3
Fines	n.d	10±0.3	57±12	19±7	n.d	138±125	15	n.d	n.d	10±0.3

SEM-EDS analysis identified several distinct phases within the CCW particles. Phases dominated by either Si and O, or Ca and O, were consistent with the quartz and calcite phases detected by XRD. The most common particles seem in SEM micrographs were individual quartz grains, followed by particles consisting of a mixture of quartz and calcite particles within a matrix material that was dominated by Ca, Si and O but with sub-regions of varying chemical composition. The BSE and EDS maps (Figure 4.3) collected from representative composite particles from the surface and subsurface samples show that quartz and calcite are often encased within a matrix material (containing Ca, Si and O with minor amounts of Al, S, Mg and Fe) with poorly defined margins and a variable Ca/Si composition, with local sub-regions that are Al-, S- or Ti-rich in the subsurface samples, and Al-, Mg-, Fe- or S- rich in the surface samples. Point counting analysis, averaged across 5 false colour SEM-EDS images, revealed that by volume the surface particles contained 22 ±3 % quartz, 30 ±3% calcite and 49 ±4% matrix material, whilst subsurface particles contained 18 ±3% quartz, 12 ±3% calcite and 70 ±4% matrix material. Calcite is commonly present as thick surface coatings on the surface sample particles, which are thinner or absent on the subsurface sample particles.

Both surface and subsurface particles are predominantly composed of a Ca- and Si-rich matrix that differs in composition between the surface and subsurface samples. In the subsurface samples, the majority of EDS spot analyses (Figure 4.4a) were clustered close to that of an idealised C-(A)-S-H phase indicating that the predominant matrix phase is likely to be a mixture of amorphous C-(A)-S-H gel phases, which although abundant, are not detected by XRD. The Ca/Si ratio of the C-(A)-S-H matrix phase (using a cut-off to separate the intermixed phases and clinker phases, see method section 3.2.4.1) was 0.90 ± 0.34 in the subsurface samples and 0.53 ± 0.34 in the surface samples. Other cement phases such as AFt and hemicarbonate/monocarbonate (Hc/Mc) (Figure 4.4b) were also identified, and some compositions close to the C-S-H phase jennite were also observed. There were some phases close in composition to AFm and AFt in both samples in Figure 4.4a, but there were only subsurface spot analyses clustered around AFt in Figure 4.4b. In the surface samples, there were some spot analyses close to AFm although the spot analyses had higher Al/Ca ratios. In the surface samples, the majority of EDS spot analyses were concentrated close to calcite at the axis origin. Overall, the surface spot analyses have a much greater spread in values and appear to spread away from the Al/Ca and Si/Ca ratios expected for C-(A)-S-H phases and towards progressively more Ca-depleted Si-

and Al-rich phases. There were a few points from the surface and subsurface that plotted above the graph range (up to Al/Ca = 6 and Si/Ca =6.5) but these are not shown, so that the general trend of the data can be better seen as most of the data is concentrated within the axis range on Figure 4.4.

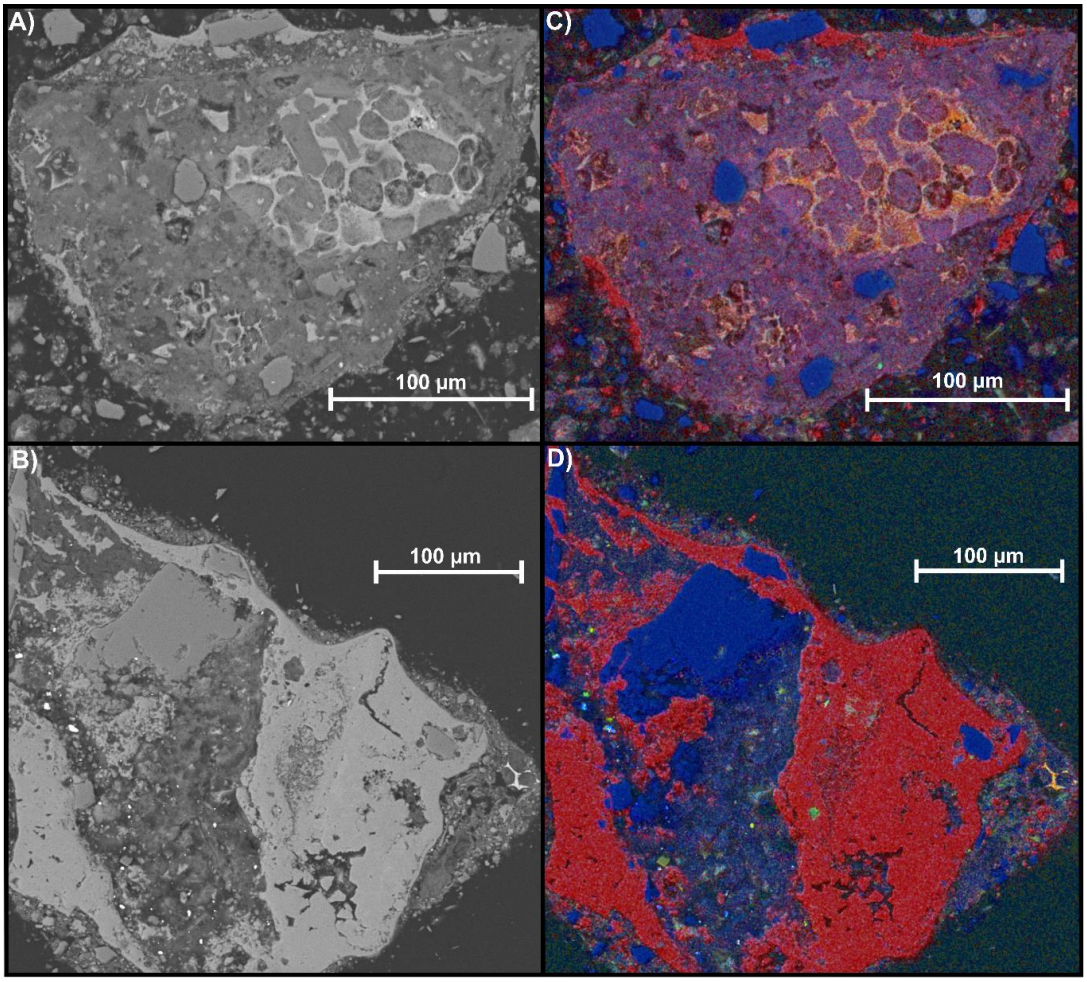

Figure 4.3 SEM BSE images of sand-sized fraction (0.6 – 6.3 mm) of crushed concrete particles collected from trial pit RS4 from the A) subsurface 2.5 - 2.7 m below surface and B) surface 0 – 0.1 m of stockpile 1. C) and D) show corresponding subsurface and surface false colour SEM-EDS elemental maps collected from the same locations where; Blue = Si, Red = Ca, Green = Fe, Orange = Mg, Yellow = S, Gold = Al, Magenta = Na (subsurface only).

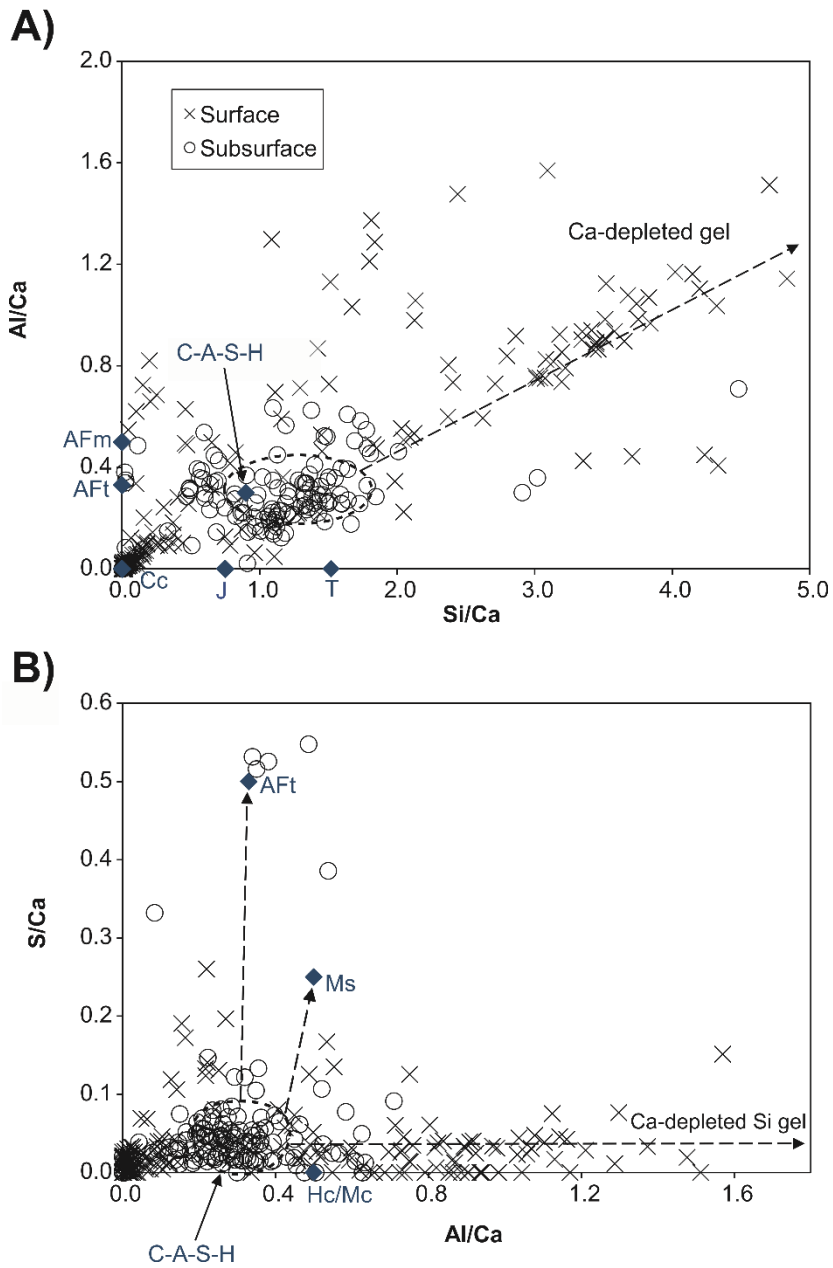

Figure 4.4 Elemental ratios determined by SEM-EDS spot analysis of the matrix of sand-sized (0.6 – 6.3 mm) particles recovered from the surface (0 – 0.1 m) and subsurface (2.5 – 2.7 m) layers of trial pit RS4 in stockpile 1. A) Elemental ratios Si/Ca against Al/Ca, and B) elemental ratios Al/Ca against S/Ca. Also plotted are the elemental ratios of selected phases from Rossen et al. (2017) including; calcium aluminate silicate hydrate (C-(A)-S-H), calcite (Cc), jennite (J), tobermorite (T), calcium aluminate monosulphate (AFm), calcium monosulphate (Ms), calcium hemi-carbonate/mono-carbonate (Hc/Mc), and calcium aluminate trisulphate (AFt). Oval represents the average C-(A)-S-H matrix composition of the subsurface samples ± 1σ; dotted arrows represent potential mixing lines between selected phases.

4.3.2 Material pH and acid neutralisation behaviour

After suspension in deionised water for 7 days the aqueous pH was between 10 and 11.3 for the subsurface material and between 8 and 9.6 for the surface material, with a slight increase in pH observed with increasing size-fraction (Table 4.3). This pH value is hereafter denoted as the material pH and is equivalent to the short-term (1 week) equilibrium pH for these materials. The acid neutralising capacity (ANC) was similar in both subsurface and surface samples (Figure 4.5) and was greatest for the sand and fines fractions. Approximately 0.1-0.7 mmol g^{-1} of acid was required to produce pH 7 (± 0.3) in experiments using both the subsurface and surface samples (Figure 4.5) with the sands and fines fractions falling at the upper end of the range. Larger differences between the size fractions were apparent in the volume of acid needed to reach pH 4 (± 0.3) with 3-4.8 mmol g^{-1} required for the sand and fines fraction, whilst the gravel fraction required 1.4 to 2.6 mmol g^{-1}. In contrast, there was no discernible difference in base buffering capacity between the subsurface and surface samples for any of the size fractions tested, with only 0.3 mmol/g of NaOH required to raise pH >12 in both materials, indicating a low base buffering capacity.

Table 4.3 Mean and range of pH values of water in contact with gravel, sand and fines sized fractions of crushed concrete materials recovered from surface (0 – 0.1 m) and subsurface (2.5 – 2.7 m) layer from trial pits RS1 and RS4 in stockpile 1 after suspension in deionised water for 7 days. The values in brackets indicate the range. The ranges are given in brackets.

Size fraction	Surface	Subsurface
Gravel (6.3 - 20 mm)	9.1 (8.7 – 9.6)	10.6 (10.0 – 11.3)
Sand (0.6 – 6.3 mm)	8.7 (8.4 – 9.0)	10.4 (10.2 – 10.7)
Fines (< 0.6 mm)	8.3 (8.0 – 8.5)	10.2 (9.9 – 10.5)

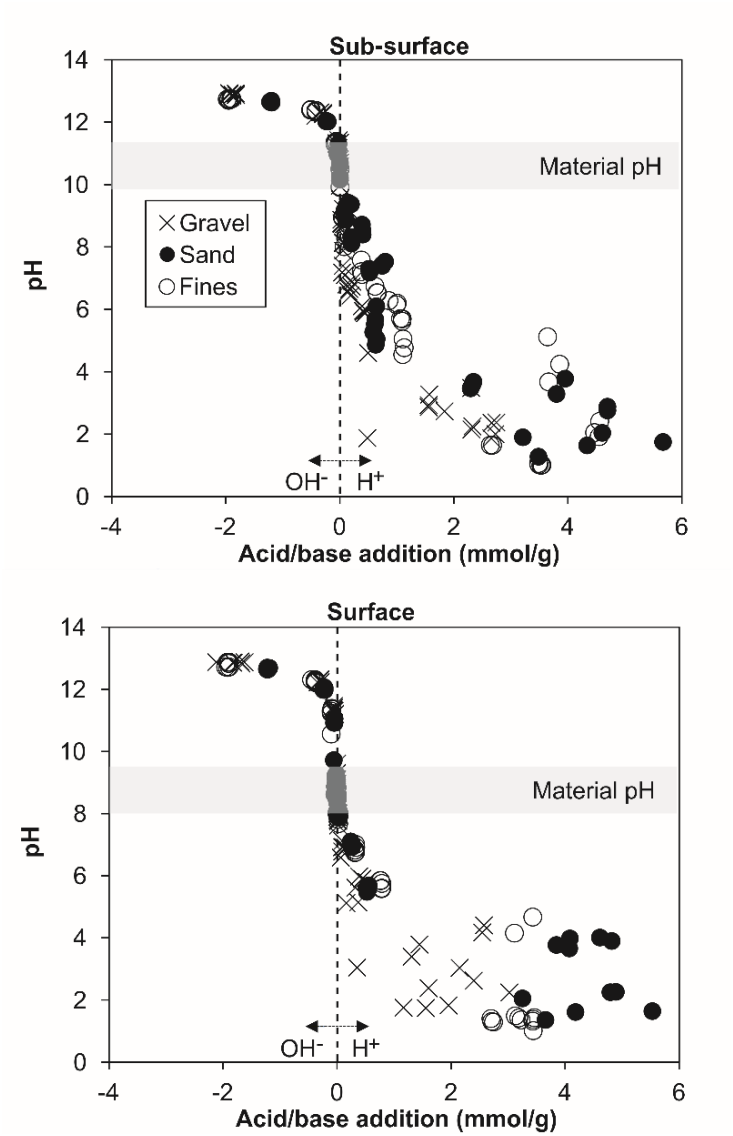

Figure 4.5 Acid neutralising capacity of different crushed concrete size fractions recovered from the subsurface (2.5 – 2.7 m) and surface (0 – 0.1 m) layers of trial pits RS1 and RS4 from stockpile 1 (Figure 3.1, Chapter 3 Section 3.1). Data from gravel (6.3 – 20 mm), sand (0.6 – 6.3 mm) and fines (< 0.6 mm) sized fractions are shown.

4.3.3 Major element leaching as function of pH

At the material pH, the major elements leached from the subsurface (Figure 4.6; Table 4.4) and surface (Figure 4.7) samples were (in order of concentration): Ca, Si, S, Al, Fe and Mg. Leaching behaviour was similar for both subsurface and surface samples, although Ca and Si were slightly higher in the subsurface. This similarity was also apparent as pH was altered outside the material pH range with the exception that Ca

leaching from the subsurface fractions was an order of magnitude higher than from the surface fractions over the pH range 8-9 (the unadjusted pH of the surface fraction).

Table 4.4 Mean and range of aqueous elemental concentrations for all size fractions from surface (0 – 0.1 m) and subsurface (2.5 – 2.7 m) samples of trial pits RS1 and RS4 from stockpile 1 in leaching experiments after 7 days equilibrium with deionised water. The ranges are given in brackets.

Determinand	Units	Surface	Subsurface
pH	-	8.7 (8.0 – 9.6)	10.4 (9.9 – 11.3)
Ca	(mg L^{-1})	40 (16.8 - 66.0)	56.4 (25.8 - 102)
Si	(mg L^{-1})	10.1 (3.3 - 16.7)	23.7 (15.8 - 36.1)
Fe	(mg L^{-1})	0.5 (0.3 - 0.6)	0.5 (0.3 - 0.6)
Al	(mg L^{-1})	2.5 (0.4 - 4.5)	3.1 (0.4 - 4.3)
Mg	(mg L^{-1})	0.7 (0.3 - 1.2)	0.3 (0.2 - 0.6)
S	(mg L^{-1})	8.6 (1.7 - 31.4)	20.6 (7.8 - 40.6)
Cl^-	(mg L^{-1})	6.1 (2.9 - 19.7)	4.7 (2.1 - 8.1)
Pb	(µg L^{-1})	2.5 (1.5 - 4.3)	2.3 (0.8 - 3.5)
Cr	(µg L^{-1})	7.0 (4 - 21.4)	25.0 (9 - 129)
V	(µg L^{-1})	6.9 (3.2 - 9.6)	27.5 (7.3 - 46.1)
Cu	(µg L^{-1})	10.4 (8.5 – 12.1)	13.5 (9.1 – 19.5)
Mn	(µg L^{-1})	6.6 (2.9 – 9.6)	6.3 (2.9 – 9.6)

As pH was increased above the material pH range, Ca leaching progressively declined, Mg and Fe leaching remained at a minimum, and S release remained fairly constant for all size fractions (although there is scatter in the S concentration from both gravel fractions). The leaching of Si and Al increased as pH was raised above the material

pH. The concentration at which Al, Mg and Fe release are at a minimum varies between the size fractions because of the different LOD and LOQ for each ICP batch. When pH was lowered below the material pH, leaching of Ca and Mg increased by several orders of magnitude as pH became increasingly acidic. Leaching of Fe was not observed until pH was <5, while S release increased gradually as pH was lowered. All elements measured reached the greatest concentrations at pH ≤ 2. Although there is greater sample variability in the behaviour of the gravel-sized material (especially for S), there appears to be no systematic differences in the leaching behaviour between the size fractions of either the subsurface or surface materials.

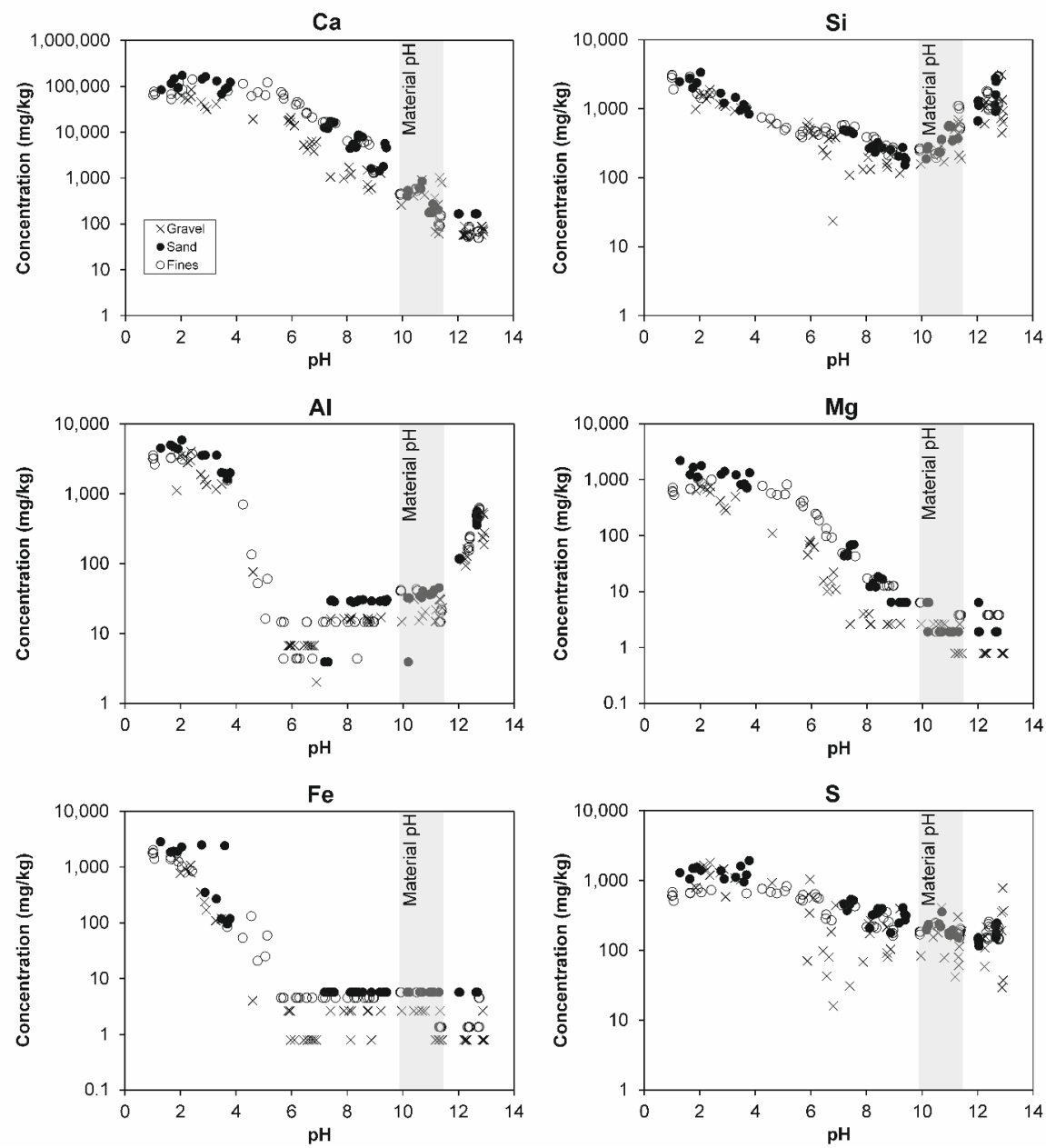

Figure 4.6 Leaching of major elements Ca, Si, Al, Mg, Fe and S from the subsurface (2.5 – 2.7 m) crushed concrete gravel, sand and fines sized fractions from trial pit RS1 and RS4 of stockpile 1 as a function of pH. Material pH denotes the range of aqueous pH values measured after suspension in deionised water for 7 days.

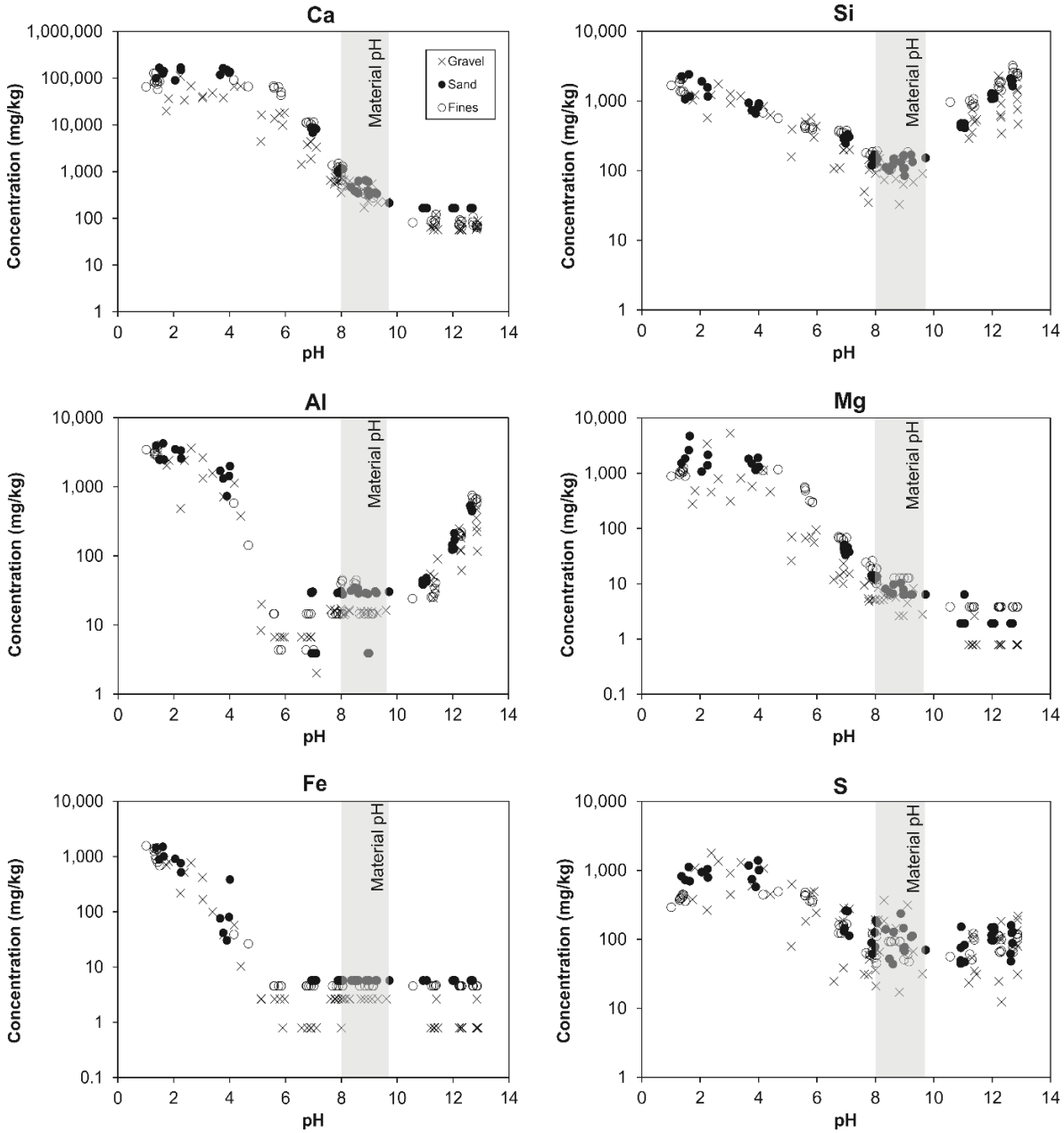

Figure 4.7 Leaching of major elements Ca, Si, Al, Mg, Fe and S from the surface (0 – 0.1 m) crushed concrete gravel, sand and fines fractions from trial pit RS1 and RS4 as a function of pH. Material pH denotes the range of aqueous pH values measured after suspension in deionised water for 7 days.

4.3.4 The pH-dependent release of trace elements

At the material pH values, the trace element leaching concentrations were similar in the size fractions of both subsurface (Figure 4.8) and surface (Figure 4.9) samples for Cl^-, Pb, Cu, and Mn despite the subsurface samples having higher concentrations for the former two elements in the solid (Table 4.2). Moreover, the average concentration for Cr, V and S were slightly higher (Table 4.4) in the subsurface samples, with scatter apparent from the gravel fraction in both surface and subsurface samples (Figure 4.8 and 4.9). When the pH was adjusted outside the material pH range, there were generally only modest differences in the leaching of trace metals between the subsurface and surface samples and between the different size fractions, although scatter is apparent for Cr, V, Cl^-, Cu and Mn release from the gravel fraction across several pH values.

For all fractions, Pb and Mn leaching was at a minimum between pH 6-11 and pH 7-13 respectively and typically rose by several orders of magnitude as pH was adjusted above and below this range for Pb, and below this range for Mn, with greatest release at pH ≤ 4. The minimum reported Pb and Mn concentration varies between the size fractions because of the different LODs and LOQs for the respective ICP run. Cu release was at a minimum between pH 6-10 but rose as pH was adjusted below or above this range. As pH was raised above pH 10, the surface fractions leached slightly higher Cu than the subsurface at pH 11 only, with the fines and sand leaching higher Cu. Between pH 6 and pH >12, Cr release was relatively constant (except for gravel samples), whilst V release was similarly constant between pH 6-9, and gradually increased as pH rose. Between pH 4 and 5, V and Cr release was at a minimum, but as pH was lowered below <4, leaching progressively rose by two orders of magnitude. In contrast, Cl^- showed no pH-dependent leaching pattern and generally remained relatively consistent across all pH values.

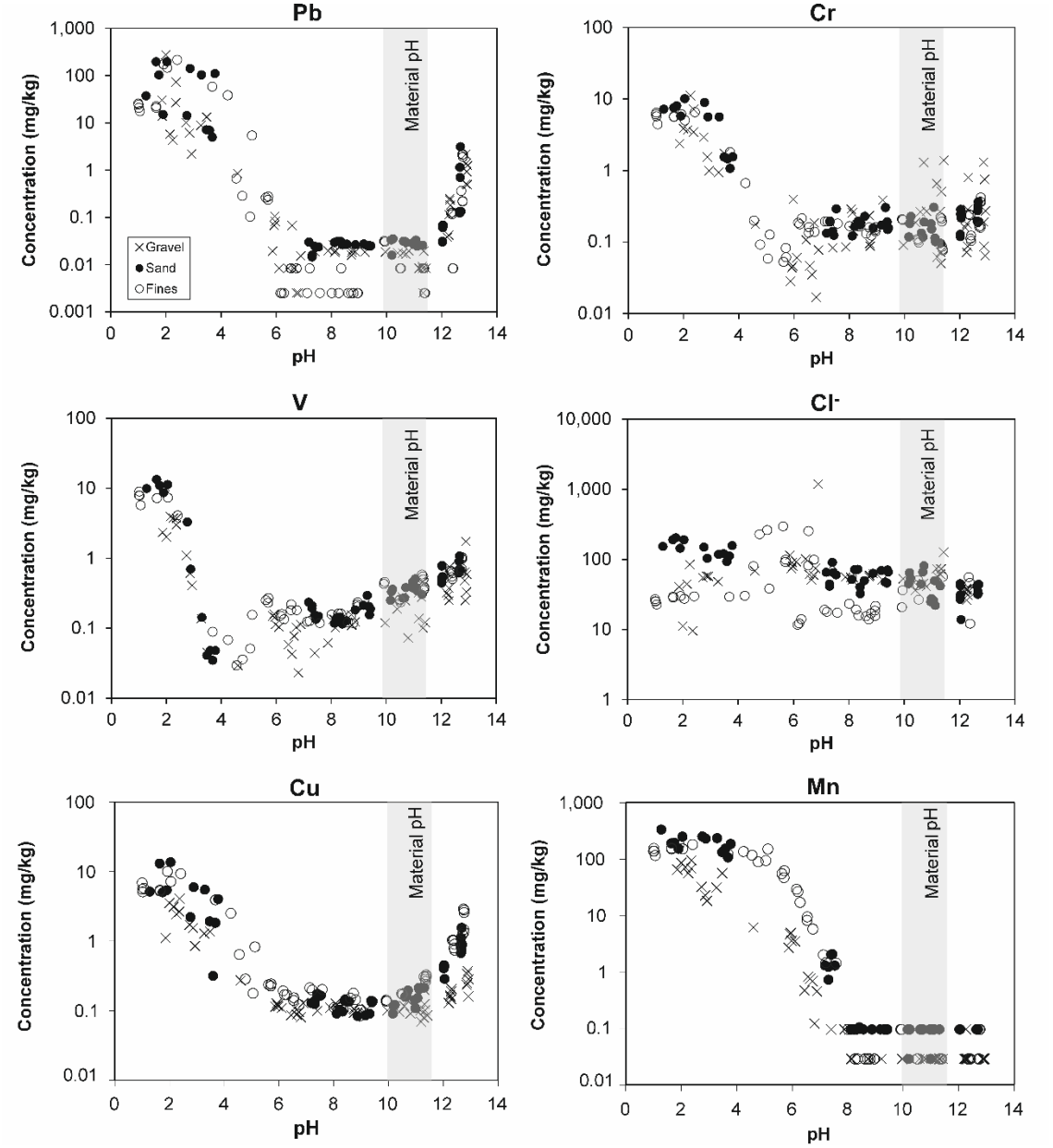

Figure 4.8 Leaching of trace elements Pb, Cr, V, Cl^-, Cu and Mn from the subsurface (2.5 – 2.7 m) crushed concrete gravel, sand and fines sized fractions from trial pit RS1 and RS4 of stockpile 1 as a function of pH. Material pH denotes the range of aqueous pH values measured after suspension in deionised water for 7 days.

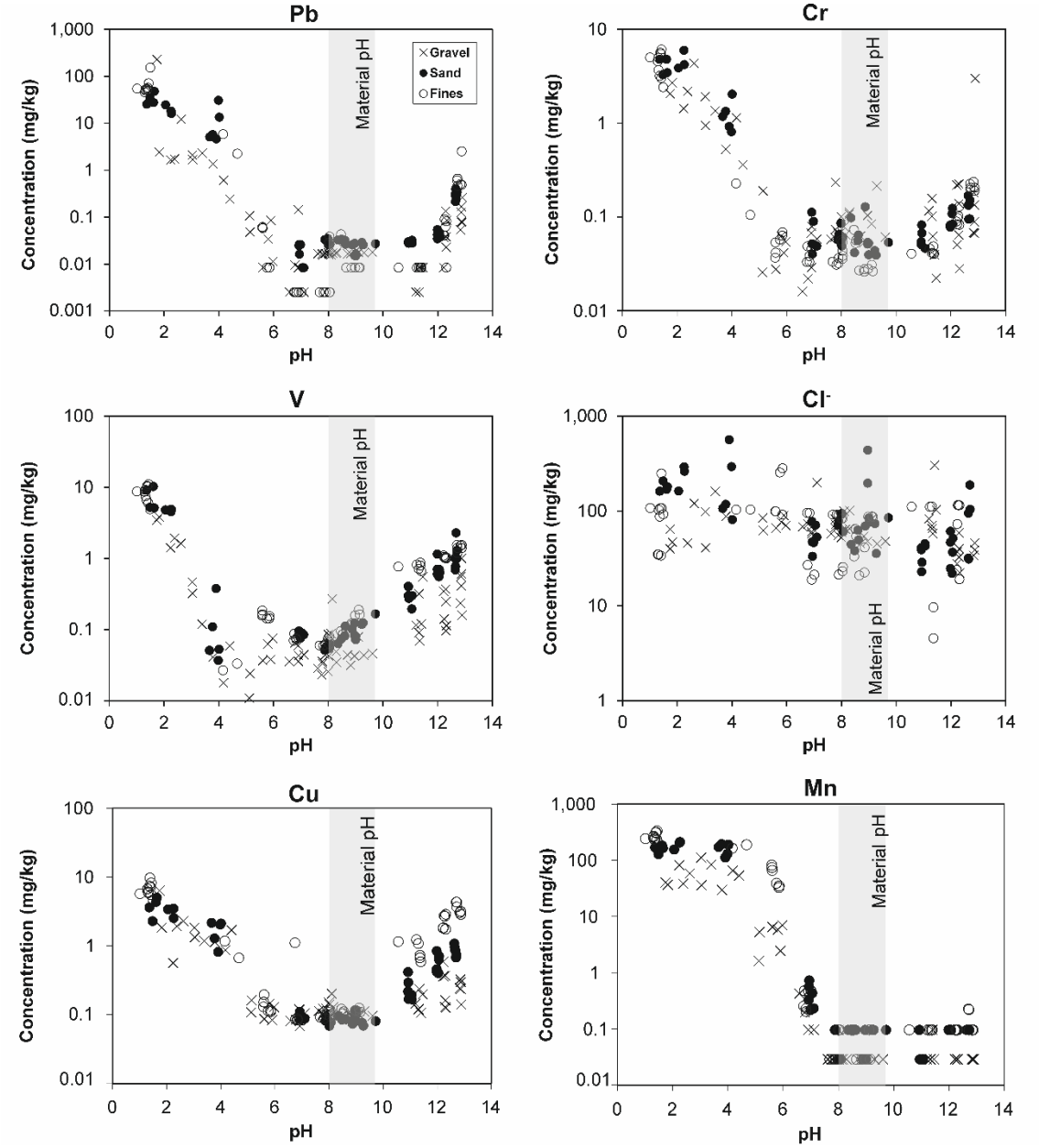

Figure 4.9 Leaching of trace elements Pb, Cr, V, Cl^-, Cu and Mn from the surface (0 – 0.1 m) crushed concrete gravel, sand and fines fractions from trial pit RS1 and RS4 as a function of pH. Material pH denotes the range of aqueous pH values measured after suspension in deionised water for 7 days.

4.4 Discussion

4.4.1 Composition and characterisation of crushed concrete

The crushed concrete material sourced from the subsurface (2.5 – 2.7 m) and the surface (0 – 0.1 m) of the stockpile at this site was found to consist primarily of silica grains (quartz sand) and calcite in a C-(A)-S-H matrix, containing some phases close in

composition to pure phase Hc/Mc, AFm and jennite (Figure 4.4). Whilst there were some surface EDS spot analyses close to AFm in composition, they were generally richer in Al relative to Ca, which indicates they are Ca-poor relative to AFm phases, and that Ca has leached out (Figure 4.4a). This is similar to the general trend of the spot analyses for the surface samples, showing many points tend toward a Ca-depleted gel (Figure 4.4a). There were typically only AFt phases present in the subsurface samples (Figure 4.4b), which suggests that AFt phases in the surface samples have weathered and carbonated and so are no longer present. This indicates greater weathering in the surface samples with respect to AFt. Evidence of weathering is apparent in both subsurface and surface samples; no portlandite was detected in X-ray diffraction patterns (Figure 4.2), which indicates that both samples have been leached by rainwater during stockpile storage, removing more soluble cement phases. Calcite is a common product of cement carbonation involving reaction with atmospheric CO_2 (Chen, J. et al., 2013; Šavija and Luković, 2016). Although both materials contain carbonate phases (calcite, dolomite), the particles in the surface samples have a more distinct calcium carbonate layer and greater proportion of calcite measured by point counting and EDS (Figure 4.3; 4.4).

The material pH values for the subsurface (pH 10 – 11.3) and surface (pH 8 – 9.6) samples are consistent with that of hardened cement paste that has undergone weathering and carbonation (i.e. pH is below the portlandite equilibrium pH of 12.4; Table 4.3) (Garrabrants et al., 2004). As carbonation results in the progressive neutralisation of the pore solution to < pH 9 (Garrabrants et al., 2004), the lower material pH of the surface samples are evidence of a greater degree of both weathering and carbonation relative to the subsurface samples. Indeed, the lower material pH values of the surface material are consistent with leaching of calcium carbonate phases (e.g. at log PCO_2 = -3.5 the equilibrium pH of calcite in water is 8.3; (Langmuir, 1997)), whilst the higher material pH values found for the subsurface materials are attributed to leaching of the C-(A)-S-H gel. The substantially lower Ca/Si ratio of the C-(A)-S-H gel in surface particles (Ca/Si = 0.53 ± 0.34) relative to subsurface particles (Ca/Si = 0.90 ± 0.34) provides further evidence of extensive decalcification that has occurred in the surface samples, and is consistent with the lower surface material pH values (Lagerblad, 2001; Glasser et al., 2008; Šavija and Luković, 2016). Leaching of the surface material may for a time, therefore, be controlled by carbonate dissolution, although the material at the stockpile surface only represents a minor portion of concrete rubble for disposal.

The C-(A)-S-H phases in a hardened cement paste is typically a C-S-H matrix with some alumina bonding between the Si chains and sheets (i.e. a mixed C-(A)-S-H / C-S-H phase), therefore the leaching behaviour of C-(A)-S-H can be compared directly to that of C-S-H. The material pH and Ca/Si ratio of C-(A)-S-H in the subsurface samples are consistent with leaching of C-S-H phases with Ca/Si ratios of 0.85-1.0, which dissolve incongruently and commonly buffers cement waters to pH values between 10 and 11 (Atkinson, 1985; Walker et al., 2016). Higher Ca/Si ratio C-S-H phases are shown to preferentially leach Ca into solution relative to Si (Harris et al., 2002), and are associated with higher pH values, so it is likely that the leaching of the subsurface material during in-situ disposal will initially reflect the relatively high Ca/Si ratio C-(A)-S-H phases, until they are exhausted, producing an equilibrium pH between 10 and 11. This reaffirms that partially carbonated CCW can still produce a high pH eluate in leaching tests (Engelsen et al., 2009; Foy et al., 2019; Mahedi and Cetin, 2020).

4.4.2 Chemical stability and leaching of crushed concrete

If crushed concrete wastes are ultimately used as site infill within existing below ground structures, the material may come in contact with water from surface infiltration and groundwater ingress. The equilibrium test results are therefore beneficial for understanding how the CCW could behave when saturated with water.

In terms of size fraction, the consensus in the nuclear (and CDW) sector is to avoid the use of fines from freshly crushed concrete, due to the potential production of high pH leachates (Foy et al., 2019). Although this generally applies for fines from freshly crushed concrete (as uncarbonated surfaces are exposed), this is not observed in the present study; long-term (10 to >20 years) stockpiling of crushed concrete has resulted in lower material pH for the fines fraction relative to larger size fractions (Table 4.3). This trend of pH reducing with size fraction of CCW was also observed by Chen et al (2012) who used similar size fractions (gravel 4.75 – 75 mm, sand 0.075 – 4.75 mm and fines, <0.075 mm) and was attributed to a higher degree of carbonation during storage due to an increased reactive surface area in smaller particles. There are also concerns with the potential for enhanced leaching from fines, due to increased surface area. Although crushed concrete fines have higher surface area relative to larger particles, which theoretically would increase leaching, no substantial differences were observed in this study, besides a higher chloride content in the sand and fines fractions in the surface samples which suggests chloride ingress. Similarities in leachate composition between the size fractions after 1 week suggests that leaching was

independent of surface area and may be under equilibrium control. This indicates an overall beneficial impact of long-term stockpiling after crushing CCW before eventual on-site use as fill. The lower material pH of the stockpiled fines implies no need for their deliberate removal and if desired the fines for stockpiled CCW could even be suitable for reuse as fine aggregate in cement grouts (Foy et al., 2019).

An approximate calculation of the volume of alkaline leachate that will be generated by onsite disposal of CDW can be made using the ANC test results. If rainwater or acidic groundwater with a pH value of 5 ($[H^+] = 1 \times 10^{-5}$ mol L^{-1}) were to infiltrate CCW backfill material, it would require approximately 10-70 x 10^3 L of water per kg of the backfill material to lower the pH to 7. However, surface infiltration is expected to be minimal at nuclear sites due to use of engineered caps with low permeability and the rate of groundwater ingress through existing concrete structures (wall and floors) is also expected to be low. It is therefore more likely that the pore waters within the disposal volume will equilibrate with the CCW producing aqueous compositions similar to batch leaching tests using the subsurface materials (Table 4.4). This composition can be expected to be stable over long time scales (provided that groundwater flow rates remain low). Egress of water from the disposal structure will also be low and may produce a small alkaline plume downstream of the structure, the scale of which will depend on the alkaline buffering capacity of the surrounding soils. However, if the CCW is used for landscaping purposes in unlined structures, then leachate will be released more readily into the surrounding soils. If local soil waters are acidic in nature, unacceptable leaching of contaminant metals such as Al, Cr, Pb, V, Mn and Cu that are much more mobile at low pH (Figures 4.6-4.9) may also occur. Therefore, the use of fine size fractions of CCW as fill in situations where contact with low pH soil waters is expected is not advised, assuming a worse case scenario where the ANC is exceeded.

The elemental concentrations in the subsurface are nearly all higher than in the surface leachates (Table 4.4). This suggests limited weathering and carbonation of the subsurface samples relative to the surface samples. This is also supported by the location of the carbonate layer, as the surface samples are extensively carbonated on the surface and throughout the particle, whilst in the subsurface there is only a thin carbonate layer on the particle surface (Figure 4.3). In reference to the EQS (Table 2.4, Chapter 2 Section 2.7), at material pH the average Cr, Pb and Cu release is above the EQS-AA for freshwater in both surface and subsurface samples, whilst the average V release is just above the EQS-AA for subsurface samples (although Cr, Pb and V are

all generally below the DWS). This indicates another positive effect of weathering and carbonation in the surface samples where concentrations are slightly lower (Cr, V, S; Table 4.4). Mn is also below the DWS and was mostly below the LOD/Q at material pH. However, any leachate produced from either surface or subsurface samples in the field would be diluted and attenuated to some degree when the leachate reaches surface or groundwaters and this effect would need to be considered.

4.4.3 Implications for management of void-filling

The priority for management of void-filling is to reduce the potential for the generation and egress of alkaline leachate and associated contaminant metals or radionuclides. While some water ingress is inevitable, reducing the volume of groundwater ingress through the grouting of internal voids is a potential solution. Grouting reduces the pore volume and particularly surface area of material in contact with any pore water, restricting contact with CCW to cracks in the grout. However, the use of a conventional ordinary Portland cement grout should be avoided, as the high pH of fresh cement pore water (pH > 13) could be problematic as the CCW has a low base buffering capacity, therefore, metals that are mobile at high pH such as Al, V, Pb and Cu could be released into solution.

It is recommended that the appropriate chemical composition is assumed for the CCW when modelling in-situ disposal as part of any site-specific risk assessment. Otherwise, the modelling results will be overly conservative, as freshly crushed concrete typically contains portlandite which can generate leachate with pH values >12, whereas the stockpiled CCW material analysed in this study was devoid of portlandite and the subsequent leaching behaviour was dominated by C-(A)-S-H phases. However, it will be important to account for any weathering of CCW after it has been crushed. The Ca/Si ratio of the C-(A)-S-H phases in the CCW varied with post-crushing weathering, with more weathered material dominated by C-(A)-S-H phases with a lower Ca/Si ratio, and abundant calcite from carbonation, producing a more benign leachate. Thus, it may be appropriate in a conservative model to assume that leaching is dominated by C-(A)-S-H with a Ca/Si ratio between 0.8 and 1.0 and a tobermorite-like structure, unless extensive weathering and carbonation has been confirmed.

4.5 Conclusion

The crushed concrete samples from the subsurface (2.5 – 2.7 m) and surface (0 – 0.1 m) locations consisted mainly of silica and calcite grains encased in a C-(A)-S-H matrix

of varying composition. Research objectives 1 and 2 were achieved in this chapter. The alkalinity generating potential of CCW from the surface and subsurface of two stockpiles was determined as a function of size fraction (gravel, sand and fines), which answered objective 1. Calcite, which was more abundant in the surface samples, was present mainly on particle surfaces and resulted from carbonation of cement phases during weathering. More highly weathered surface materials contained C-(A)-S-H gel phases with a Ca/Si ratio of 0.53 ± 0.34 and produced less alkaline leachate in leaching tests (pH 8 – 9.6). Whereas less weathered subsurface materials contained C-(A)-S-H gel phases with a Ca/Si ratio of 0.90 ± 0.34 and produced a more alkaline leachate (pH 10 – 11.3). Research objective 2 was achieved using batch equilibrium experiments conducted at different pH values, and the release of major and trace elements from the gravel, sand and fines fraction of stockpiled CCW was determined. Dissolution of major elements, such as Ca and Si, and leaching of trace contaminants, such as Al, Pb, Cr, V, Cu and Mn was generally minimised in the pH range produced by equilibrium with either surface or subsurface samples but increased by several orders of magnitude as pH was either raised above pH 12 or lowered below pH 5. Above pH 11, leaching of Cu was greater in the surface fines fraction. At material pH, release of S, Cr and V was slightly lower in the surface samples, indicating a positive effect of weathering during stockpiling. Despite the pH-difference at the material pH, the two materials produced leachate with generally similar elemental compositions from all size fractions (with scatter from the gravel fraction), suggesting that fines removal is not required prior to the use of stockpiled CCW as a fill material. Although the release of Cu from both surface and subsurface samples and the release of Cr, Pb and V in subsurface samples were above the freshwater EQS-AA (but below the DWS) in the field the small volume of leachate expected would be subject to dilution processes meaning the leachate could still be considered benign under these circumstances.

4.6 References

Atkinson, A. 1985. *The time dependence of pH within a repository for radioactive waste disposal.* UKAEA Atomic Energy Research Establishment.

Bath, A., Deissmann, G. and Jefferis, S. 2003. *Radioactive Contamination of Concrete: Uptake and Release of Radionuclides.*

Berner, U.R. 1992. Evolution of pore water chemistry during degradation of cement in a radioactive waste repository environment. *Waste Management.* **12**(2), pp.201-219.

Chen, J., Tinjum, J. and Edil, T. 2013. Leaching of Alkaline Substances and Heavy Metals from Recycled Concrete Aggregate Used as Unbound Base Course. *Transportation Research Record: Journal of the Transportation Research Board.* **2349**, pp.81-90.

Cornelis, G., Johnson, C.A., Gerven, T.V. and Vandecasteele, C. 2008. Leaching mechanisms of oxyanionic metalloid and metal species in alkaline solid wastes: A review. *Applied Geochemistry.* **23**(5), pp.955-976.

Coudray, C., Amant, V., Cantegrit, L., Le Bocq, A., Thery, F., Denot, A. and Eisenlohr, L. 2017. Influence of Crushing Conditions on Recycled Concrete Aggregates (RCA) Leaching Behaviour. *Waste and Biomass Valorization.* **8**(8), pp.2867-2880.

Deissmann, G., Bath, A., Jefferis, S., Thierfeldt, S. and Wörlen, S. 2006. Development and application of knowledge-based source-term models for radionuclide mobilisation from contaminated concrete. *MRS Online Proceedings Library.* **932**(991).

Ekström, T. 2001. *Leaching of concrete : experiments and modelling.* Lund University.

Engelsen, C.J. 2020. Leaching performance of recycled aggregates. In: Pacheco-Torgal, F., et al. eds. *Advances in Construction and Demolition Waste Recycling.* Woodhead Publishing, pp.439-451.

Engelsen, C.J., van der Sloot, H.A., Wibetoe, G., Justnes, H., Lund, W. and Stoltenberg-Hansson, E. 2010. Leaching characterisation and geochemical modelling of minor and trace elements released from recycled concrete aggregates. *Cement and Concrete Research.* **40**(12), pp.1639-1649.

Engelsen, C.J., van der Sloot, H.A., Wibetoe, G., Petkovic, G., Stoltenberg-Hansson, E. and Lund, W. 2009. Release of major elements from recycled concrete aggregates and geochemical modelling. *Cement and Concrete Research.* **39**(5), pp.446-459.

Faucon, P., Adenot, F., Jacquinot, J.F., Petit, J.C., Cabrillac, R. and Jorda, M. 1998. Long-term behaviour of cement pastes used for nuclear waste disposal: review of physico-chemical mechanisms of water degradation. *Cement and Concrete Research.* **28**(6), pp.847-857.

Faucon, P., Le Bescop, P., Adenot, F., Bonville, P., Jacquinot, J.F., Pineau, F. and Felix, B. 1996. Leaching of cement: Study of the surface layer. *Cement and Concrete Research.* **26**(11), pp.1707-1715.

Foy, J., Jones, G., Sephton, M. and Gaitonde, R. 2019. *Managing On-site Stockpiling and Use of High Volumes of Concrete-based Demolition Material.* Cumbria, UK: AECOM on behalf of the Nuclear Decommissioning Authority.

Garrabrants, A.C., Sanchez, F. and Kosson, D.S. 2004. Changes in constituent equilibrium leaching and pore water characteristics of a Portland cement mortar as a result of carbonation. *Waste Management.* **24**(1), pp.19-36.

Gérard, B., Le Bellego, C. and Bernard, O. 2002. Simplified modelling of calcium leaching of concrete in various environments. *Materials and Structures.* **35**(10), pp.632-640.

Glasser, F.P., Marchand, J. and Samson, E. 2008. Durability of concrete — Degradation phenomena involving detrimental chemical reactions. *Cement and Concrete Research.* **38**(2), pp.226-246.

Gomes, H.I., Mares, W.M., Rogerson, M., Stewart, D.I. and Burke, I.T. 2016. Alkaline residues and the environment: a review of impacts, management practices and opportunities. *Journal of Cleaner Production.* **112**, pp.3571-3582.

GRR. 2018. *Management of Radioactive Waste from Decommissioning of Nuclear Sites: Guidance on Requirements for Release from Radioactive Substances Regulation Version 1.0.* [Online]. [Accessed 20/05/2023]. Available from: https://www.sepa.org.uk/media/365893/2018-07-17-grr-publication-v1-0.pdf

Harris, A.W., Manning, M.C., Tearle, W.M. and Tweed, C.J. 2002. Testing of models of the dissolution of cements—leaching of synthetic CSH gels. *Cement and Concrete Research.* **32**(5), pp.731-746.

International Atomic Energy Agency (IAEA). 2008. *Managing Low Radioactivity Material from the Decommissioning of Nuclear Facilities.* Vienna, Austraia: IAEA.

Jacques, D., Perko, J., Seetharam, S.C. and Mallants, D. 2014. A cement degradation model for evaluating the evolution of retardation factors in radionuclide leaching models. *Applied Geochemistry.* **49**, pp.143-158.

Jefferson, P. 2009. The risks of reclamation. *Professional Broking.* p16.

L'Hôpital, E., Lothenbach, B., Scrivener, K. and Kulik, D.A. 2016a. Alkali uptake in calcium alumina silicate hydrate (C-A-S-H). *Cement and Concrete Research.* **85**, pp.122-136.

L'Hôpital, E., Lothenbach, B., Kulik, D.A. and Scrivener, K. 2016b. Influence of calcium to silica ratio on aluminium uptake in calcium silicate hydrate. *Cement and Concrete Research.* **85**, pp.111-121.

L'Hôpital, E., Lothenbach, B., Le Saout, G., Kulik, D. and Scrivener, K. 2015. Incorporation of aluminium in calcium-silicate-hydrates. *Cement and Concrete Research.* **75**, pp.91-103.

Lagerblad, B. 2001. *Leaching performance of concrete based on studies of samples from old concrete constructions.* Svensk Kärnbränslehantering AB.

Langmuir, D. 1997. *Aqueous environmental geochemistry.* Upper Saddle River, N.J: Prentice Hall.

Mahedi, M. and Cetin, B. 2020. Carbonation based leaching assessment of recycled concrete aggregates. *Chemosphere.* **250**, p126307.

NDA. 2010. *UK Strategy for the Management of Solid Low Level Radioactive Waste from the Nuclear Industry.*

NDA. 2016. *UK Strategy for the Management of Solid Low Level Waste from the Nuclear Industry.* [Online]. Department of Energy & Climate Change. [Accessed 10/05/2023]. Available from: https://www.gov.uk/government/consultations/consultation-on-an-update-of-the-uk-strategy-for-the-management-of-solid-low-level-radioactive-waste-from-the-nuclear-industry

NDA. 2020. *Concrete example of dealing with decommissioning rubble.* [Online]. [Accessed 05/07/21]. Available from: https://www.gov.uk/government/case-studies/concrete-example-of-dealing-with-decommissioning-rubble

Nuclear Energy Agency. 2017. *Reycling and Re-use of Materials Arising From the Decommissioning of Nuclear Facilities.* Co-operative Programme on Decommissioning.

Richardson, I.G. 1999. The nature of C-S-H in hardened cements. *Cement and Concrete Research.* **29**(8), pp.1131-1147.

Sanger, M., Natarajan, B.M., Wang, B., Edil, T. and Ginder-Vogel, M. 2020. Recycled concrete aggregate in base course applications: Review of field and laboratory investigations of leachate pH. *J Hazard Mater.* **385**, p121562.

Šavija, B. and Luković, M. 2016. Carbonation of cement paste: Understanding, challenges, and opportunities. *Construction and Building Materials.* **117**, pp.285-301.

Segura, I., Molero, M., Aparicio, S., Anaya, J.J. and Moragues, A. 2013. Decalcification of cement mortars: Characterisation and modelling. *Cement and Concrete Composites.* **35**(1), pp.136-150.

van der Sloot, H.A. 2000. Comparison of the characteristic leaching behavior of cements using standard (EN 196-1) cement mortar and an assessment of their long-term environmental behavior in construction products during service life and recycling. *Cement and Concrete Research.* **30**(7), pp.1079-1096.

van der Sloot, H.A., Meeussen, J.C.L., Garrabrants, A.C. and Kosson, D.S. 2009. *Review of the Physical and Chemical Aspects of Leaching Assessment.* IAEA.

Van Gerven, T., Cornelis, G., Vandoren, E., Vandecasteele, C., Garrabrants, A.C., Sanchez, F. and Kosson, D.S. 2006. Effects of progressive carbonation on heavy metal leaching from cement-bound waste. *AIChE Journal.* **52**(2), pp.826-837.

Vollpracht, A. and Brameshuber, W. 2016. Binding and leaching of trace elements in Portland cement pastes. *Cement and Concrete Research.* **79**, pp.76-92.

Walker, C.S., Sutou, S., Oda, C., Mihara, M. and Honda, A. 2016. Calcium silicate hydrate (C-S-H) gel solubility data and a discrete solid phase model at 25 °C based on two binary non-ideal solid solutions. *Cement and Concrete Research.* **79**, pp.1-30.

Chapter 5 Dissolution kinetics of crushed concrete waste: effect of pH on leaching behaviour

Summary

Reuse of crushed cementitious construction and demolition wastes as a fill material can lead to leaching of reactive cement phases. The short-term dissolution kinetics of a CCW, produced at a UK nuclear site, were studied by calculating the pseudo-steady state leaching rates of major and trace element constituents as a function of leachate pH using deionised water (DIW), acidic (HCl, acetic acid) and alkaline (NaOH) leachant solutions. At alkaline pH (>10), Ca and Si leaching rates were similar (2-6 x 10^{-11} mol m^{-2} s^{-1}) producing leachates with Ca/Si ratios (1.1 ±0.4) suggesting congruent leaching of the C-(A)-S-H phases in the CCW (pre-leached Ca/Si = 0.9 ±0.3). At pH <10, Ca leaching rates progressively increased relative to Si and produced leachates with high Ca/Si ratios, indicating leaching processes dominated by initial rapid carbonate dissolution and incongruent dissolution of C-(A)-S-H phases producing Ca-depleted solids with overall higher rates of mass loss relative to alkali-leached solids. The leaching rates of Mg, Fe and Mn were pH-dependent (with higher leaching rates at low pH) and solubility-controlled whilst the leaching rates of Cr, V, Pb, As, K and Zn were mostly pH independent and mainly mass-transport-limited or availability-limited. Trace element leaching rates along with Al and Si were generally low relative to Ca or below detection between pH 3-13. This information can be used to help predict the long-term leaching behaviour of CCW disposed in scenarios where meteoric or groundwater flow through the waste is expected.

5.1 Introduction

A potential waste management option under consideration for the significant volumes of CCW generated during the decommissioning of UK nuclear facilities is on-site disposal as void-fill, either in landscaping or as backfill in larger basements (GRR, 2018; Foy et al., 2019; NDA, 2020). Non-radioactive crushed concrete materials resemble conventional CDW that are commonly reused as unbound aggregate in shallow environments such as road sub-base or pavements (van der Sloot, 2000; Engelsen et al., 2012; 2017; Chen, J. et al., 2013; Engelsen et al., 2017; Natarajan et al., 2019; Sanger et al., 2020). As CCW deposited in the subsurface will likely encounter water from surface infiltration (e.g. rainfall) or ingress of soil waters and/or groundwater, there are two concerns with the use of CCW in subsurface disposals: firstly, the generation of a high pH, alkaline leachate which may be detrimental to local

water receptors and vegetation (Steffes, 1999), and secondly, the leaching of trace and heavy metal constituents that are typically found in cement phases (e.g. As, Ba, Cd, Co, Cr, Cu, Mn, Mo, Ni, Pb, Sb, Se, Ti, V and Zn) which originate from the raw materials used in cement production (Engelsen et al., 2010; Chen, J. et al., 2013; Butera et al., 2014; Galvín et al., 2014; Vollpracht and Brameshuber, 2016; Foy et al., 2019; Natarajan et al., 2019; Sanger et al., 2020).

Concrete consists predominantly of natural coarse and fine inert aggregate (e.g. gravel and sand) and hardened cement paste, the latter is usually more reactive in water and causes high pH leachates (Ekström, 2001; Smith and Collis, 2001; Hidalgo et al., 2007; Ochs et al., 2015; Foy et al., 2019; Daiber, 2022). Hydrated cement paste is predominantly composed of nonstoichiometric calcium silicate hydrate gel (C-S-H), which accounts for at least 60% of fully hydrated cement paste and is the main binding phase in Portland cements (Richardson, 1999; Trapote-Barreira et al., 2014). C-S-H is hereafter referred to as a calcium aluminate silicate hydrate gel (C-(A)-S-H) as it is not phase pure in concrete and is of variable composition that can be described in terms of Ca/Si and Al/Si ratios (Richardson, 1999; L'Hôpital et al., 2016). Other hydrated phases include portlandite (CH), monosulphate aluminate and trisulphate aluminate (respectively AFm and AFt), minor hydroxides (e.g., KOH, NaOH) and a pore solution (Berner, 1992). Unhydrated Portland cement particles (clinker grains) also remain in hydrated cement paste unless extensive leaching has occurred (Diamond, 2004).

When water is in contact with CCW, diffusion-transport processes and chemical reactions cause the dissolution and leaching of alkaline cementitious phases, which are responsible for high pH leachates (Faucon et al., 1998). In fresh, non-carbonated cement pastes leachates can reach over pH >13 where Na and K alkalis along with portlandite are present and control leachate pH (Faucon et al., 1998; Berner, 1992). However, CCW has typically been weathered and carbonated either during the service life of the concrete or during stockpiling after crushing (Lagerblad, 2005; Abbaspour et al., 2016) (Chapter 4). Weathering leaches out soluble alkalis and carbonation consumes cement phases by reaction with atmospheric CO_2 to form calcium carbonate, which progressively reduces the pH of cement leachates with time to <10 (Faucon et al., 1998; Lagerblad, 2005). Carbonation also reduces the Ca/Si ratio of C-(A)-S-H phases, eventually forming an amorphous silica gel (Faucon et al., 1998; Garrabrants et al., 2004; Šavija and Luković, 2016; Walker et al., 2016). Carbonated CCW has a positive impact on the pH of leachates formed, but the extent of carbonation will vary across CCW as the material is naturally heterogeneous (Mahedi

and Cetin, 2020). In Chapter 4 using CCW that had been stockpiled from 1997 to 2012, no portlandite was detected by XRD and was presumed leached out and the equilibrium pH results (pH <11.3) were consistent with C-(A)-S-H phases dominating leaching. Therefore, it is important to consider how the composition of C-(A)-S-H phases, which dominate the composition of cement paste, evolve with leaching conditions.

Water in contact with carbonated and weathered CCW produces lower pH leachates (pH <8 to 11), which is favourable when assessing the environmental risk of CCW for on-site disposal (Chapter 4 Section 4.3.2). However, oxyanion-forming elements (e.g., As, Cr, Mo, Sb, Se and V) are reported to have an increased solubility in carbonated cement leachates relative to non-carbonated cement leachates when leached by deionised water (Mulugeta et al., 2011; Mahedi and Cetin, 2020). For example, in Mulugeta et al (2011), the release of Cr oxyanions were 8-12 times higher in carbonated CCW leachates (pH between 10.3 and 11.9) relative to non-carbonated cements (pH between 12.4 and 12.5), and similarly Mahedi and Cetin (2020) reported higher Cr release in carbonated cement leachates (pH between 11.1 and 12.6) which was correlated with higher Ca concentrations. Both studies are in agreement with the pH-dependent release of oxyanions (CrO_4^{2-}, MoO_4^{2-}, VO_4^{3-}) reported by van der Sloot (2000; 2002) where maximum release is at neutral to mild alkaline pH, and below pH 5 (van der Sloot, 2000). This behaviour is attributed to the dissolution and degradation of cement hydrate phases such as ettringite which have been shown to incorporate Cr and Mo oxyanions in solid solutions by substitution of sulphate ions (Gougar et al., 1996; van der Sloot, 2002; Leisinger et al., 2010; Mulugeta et al., 2011; Mahedi and Cetin, 2020), and sorption to or incorporation into the C-S-H matrix by possible substitution of silicate (Omotoso et al., 1995; Halim et al., 2004; Mulugeta et al., 2011; Leisinger et al., 2014)**.** As CCW used in void fill applications will likely encounter waters of different chemical composition (e.g. ground water, rainfall, acid soil waters), it is essential to investigate leaching at different pH values (Engelsen et al., 2010).

Leaching is a strongly pH-controlled process and chemical factors such as dissolution, sorption and availability determine the release of metal ions to solution (van der Sloot and Dijkstra, 2004). As trace metals may be incorporated within the structure of, or sorbed to hydrated cement phases such as C-(A)-S-H or hydrated calcium aluminates, dissolution of these phases may release trace metal ions into solution (Garrabrants and Kosson, 2004). As the leachability of metals is most important when assessing the

environmental risk of using CCW, rather than total metal composition (van der Sloot, 2000), it is important to study leaching behaviour under different release conditions.

Leaching tests which investigate different leaching mechanisms are necessary to understand the leaching of CCW and address various field scenarios. The release of metals by leaching is typically described in terms of equilibrium control or mass-transport control (Garrabrants et al., 2004; Engelsen et al., 2017). Batch equilibrium tests on stockpiled CCW were conducted in Chapter 4 and these tests are relevant for conditions of slow percolation and slow flow rates, such as in-situ disposal in lined structures where expected water ingress is low. CCW disposed of in shallower voids, however, may encounter faster flow conditions where mass-transport processes such as diffusion, advection and surface wash-off may dominate metal release and dissolution of CCW (van der Sloot and Dijkstra, 2004). Flow-through experiments are best suited to approximate faster flow conditions and to investigate mass transport leaching mechanisms.

Flow-through leaching experiments involve continuous leachant renewal and either use monoliths to study flow through a sample (Poon and Chen, 1999) or granular materials to study dissolution kinetics (Trapote-Barreira et al., 2014; Marty et al., 2017). Sometimes column experiments are referred to as flow-through experiments, but column experiments typically use crushed and compacted material and measure leaching as a function of the liquid to solid ratio (Lopez Meza et al., 2008; Butera et al., 2015). As the crushing of materials can overestimate metal leaching expected in the field by increasing particle surface area and exposing non-carbonated cement phases (van der Sloot, 2000; Chen, J. et al., 2013; Butera et al., 2015; Sanger et al., 2020), using non-crushed materials better simulates disposal of hydraulically unbound concrete rubble in the field where no crushing is expected prior to use in void-filling. Moreover, in flow-through conditions leaching will either be under equilibrium control (slow-flow conditions) or mass-transport control (faster flow conditions), depending on the flow-rate (Garrabrants and Kosson, 2004). However, there is a gap in knowledge on CCW leaching using flow-through reactors under high flow conditions, and as a function of leachant solution pH.

To address this gap, this study used sand to fine gravel sized (0.6 – 6.3 mm) fractions from CCW stockpiled at a nuclear licensed site to investigate leaching behaviour in flow-through leaching reactors at far-from-equilibrium conditions (Research objective 3). The leaching rates of major (Ca, Si, Al) and trace (As, Cr, Cu, Fe, K, Mg, Mn, Pb, S, V, Zn) constituents were calculated to measure CCW dissolution kinetics at different

pH values (Research objective 4). The leached materials were characterised using SEM-EDS and BET. The data produced are valuable for understanding short-term dissolution kinetics of CCW relevant to the use of stockpiled CCW as void-fill in unlined structures.

5.2 Methods

5.2.1 Sample Information

Crushed concrete was recovered from 2.5 – 2.7 m below the surface of an above ground CCW stockpile at a UK nuclear site. This study used the sand-fine gravel sized fraction of the CCW sample (0.6 – 6.3 mm). This size fraction represents around 20% of the mass of the total stockpiled material sampled. As no substantial grain size dependant difference in the leaching behaviour of CCW was observed in Chapter 4, this size fraction was chosen to maximise the particle surface area associated with the volume of material used in the flow-through reactor. The material was not further crushed to avoid the production of new surfaces (leading to overestimation of element release).

The size fraction 0.6 – 6.3 mm had individual quartz (aggregate) grains as the most common particle, followed by composite particles consisting of a matrix material (containing Ca, Si and O) with varying composition around quartz and calcite particles (Chapter 4 Section 4.3.1). The composite particles are composed of 18 ± 3% quartz, 12 ± 3% calcite and 70 ± 4% matrix material (Chapter 4 Section 4.3.1). The matrix material is predominantly composed of a mix of amorphous C-(A)-S-H phases and has Fe, Mn, Ti, Mg and K rich regions (full characterisation is reported in Chapter 4 Section 4.3.1). The Ca/Si ratio of the C-(A)-S-H phases (calculated as reported in Chapter 3 Section 3.2.4.1) in the matrix material was 0.9 ± 0.3 (Chapter 4 Section 4.3.1).

5.2.2 Leaching experiments

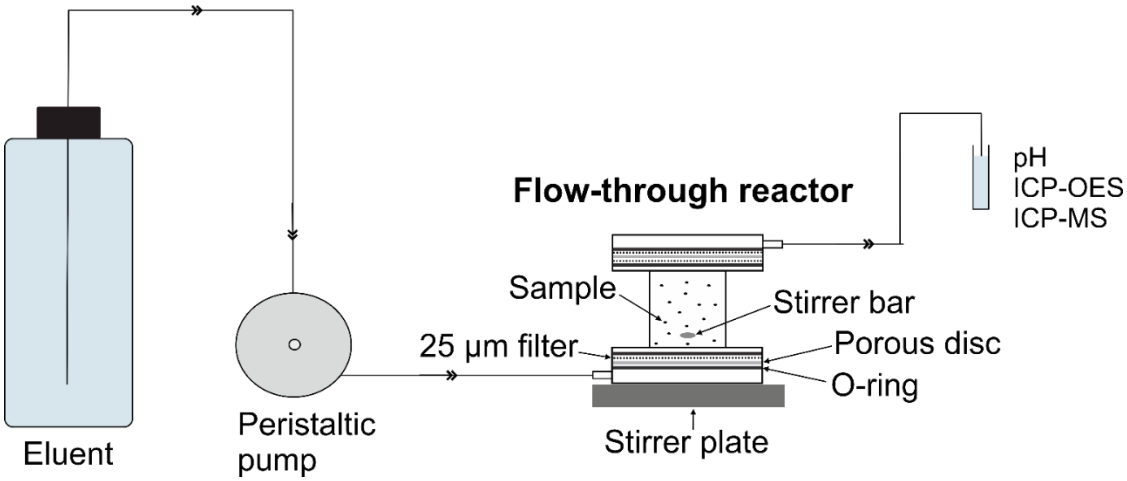

Figure 5.1 Diagram of flow-through leaching experiments. Diagram adapted from Marty et al (2015).

Flow-through leaching experiments (Figure 5.1, diagram adapted from Marty et al (2015)) were conducted to study the leaching kinetics of crushed concrete as a function of pH. The samples (typically 4g, but 2g when leaching with DIW) were contained within the reactor using 25 µm polypropylene filters at each end. Three different reactors were used and the volume ranged between 74 and 86 mL. A magnetic stirrer bar was inside the reactor and the leachant was passed through the reactor using peristaltic pumps. The average leachant flow rate was 0.47 ± 0.08 mL/min producing one complete reactor volume exchange every 3.0 ± 0.6 hours. Ten different leachants were used (DIW, and 0.5-5 mM HCl, 1 mM acetic acid and 1-100 mM NaOH; see Table 5.1). The experiments were run for between 1 and 6 days for all acid and alkali leachants, and 8 to 14 days for DIW. The leachate was collected 1 to 5 times per day, with more samples taken more frequently for the acid leaching experiments as pH changed faster than that for DIW or alkaline leachant samples. As the goal was to gather measurements at steady state conditions (i.e. a relatively stable pH), once pH had dropped the experiment was ended, so usually only one or two measurements were taken on the final day of the experiment. Experiments were carried out under room temperature conditions (19.6 ± 2.4°C measured at the time of sampling) and CO_2 was not controlled.

Table 5.1 Leachant solution composition and pH. The experimental duration is written in the numerical order of the replicates.

Leachant	**Leachant pH**	**Number of Replicates**	**Experiment duration (days)**
100 mM NaOH	12.8 ± 0.1	3	3, 3, 2
10 mM NaOH	11.9 ± 0.1	3	3, 3, 3
1 mM NaOH	10.9 ± 0.1	2	4, 4, 4
0.5 mM HCl	3.3 ± 0.0	3	3, 3, 3
1 mM HCl	3.0 ± 0.0	3	6, 5, 4
1 mM HOAc	4.0 ± 0.1	3	5, 5, 2
2 mM HCl	2.8 ± 0.1	2	4, 3
3 mM HCl	2.6 ± 0.1	3	2, 1, 2
5 mM HCl	2.3 ± 0.0	2	3, 3
DIW	5.8 ± 0.3	2	14, 8

5.2.3 Solution analysis

9 mL of sample was collected for sampling. The leachate was stirred for ~2 minutes using a magnetic stirrer bar. 1 mL of the stirred leachate was filtered using 0.22 µm polyethersulfone syringe filters, and the pH of the remainder was measured using a Thermo Fisher Sure-Flow Electrode and Orion 3 Star pH meter. The pH meter was calibrated daily using pH buffers 4.01, 7.00, 10.01. When the leachate was alkaline the meter was further calibrated at pH 12.5 and the measurement was made within 30 minutes of elution. The filtered leachate was added to tubes containing 2% HNO_3 (9 mL) and refrigerated at 4°C prior to elemental analysis. The elements Ca, Si, Al, Mg, K, S were analysed using a Thermo Fisher iCAP 7400 Radial ion-coupled optical emission spectrometer and As, Cr, Cu, Fe, Mn, Pb, V and Zn were measured using a

Thermo Fisher iCAP Qc ion-coupled plasma mass spectrometer. A matrix correction was undertaken on sample data for most elements due to high background concentrations in the acid used (Chapter 3 Section 3.4.1). The average of the matrix blanks was subtracted from the samples and values were only accepted as valid if they were above the average plus 3xSD of the matrix blanks. The LOD values and uncertainty (%) for different sample runs are shown in the Appendix Section B (Table B1 and B2). Only values that were ten times above the LOD were accepted because of the dilution used to prepare the samples.

5.2.4 Material analysis

After the flow-through leaching experiments, the solution was allowed to settle for approximately 30-60 minutes before retrieving the leached materials from the reactors by filtering the solution using Whatmann No1 papers. The recovered solid materials on the filter were dried at 100 °C or 105 °C overnight and weighed. The dried samples were double-bagged and stored in air-tight glass jars.

5.2.5 SEM

Six samples (DIW, 0.5-1 mM HCl, 3 mM HCl, 1 mM HOAc, 100 mM NaOH) were selected for SEM analysis to look for alteration by leaching and to determine the change in Ca/Si ratio of the C-(A)-S-H phases that remained after leaching by SEM-EDS spot analysis. The samples were prepared as explained in Chapter 3 Section 3.2.4. EDS spot analysis was undertaken using a Tescan VEGA3XM equipped with an Oxford instruments X-max 150 SDD EDS using Aztec 3.3 software. A beam energy of 15 keV was used, with counts set to 600,000 and the working distance was 15mm. Spot analysis was performed randomly across several grains for each leached sample to identify the composition of the phases. Points where spectra were collected included carbonated layers but avoided aggregates. The total number of spectral points on the matrix material was 166 for acid leached samples (24 particles), 87 for DIW (12 particles) and 32 for the alkaline leached sample (6 particles). The Al/Si of the pre-leached material is reported in the results.

The Ca/Si ratios of the cement matrix were estimated from the EDS spot analysis, but data from spots that fell below the belite threshold values (Georget et al., 2021) were excluded from further analysis (as reported in Chapter 3 Section 3.2.4.1). The results are reported by leachant composition (acid, alkaline or DIW) for a general comparison between leachants.

5.2.6 BET

The specific surface area (m^2/g) of the pre-leached and leached material were determined by measurement of a 10-point N_2 absorption isotherm between 0.05 and 0.30 p/p_0 (equilibrium pressure/saturation pressure) using a Micromeritics Gemini VII 2390 analyser. The samples were degassed using N_2 at 105 °C between ~19 and ~26 hours. The whole sample for each individual replicate was analysed, and the data are presented as the average ± 1 SD of the replicates for each leachant (displayed in Table 5.1 in Section 5.2.1).

5.3 Results

5.3.1 The pH of the leachate from the flow-through reactor

The leaching behaviour of CCW was different in the acid leachants from either DIW or the alkaline leachants (Figure 5.2). When either DIW or NaOH (1-100 mM) was used as the leachant, the leachate pH was alkaline (pH = 9.7 – 13) and remained steady over time, despite the increasing cumulative elution volume. The pH values of the NaOH leachants were unchanged by contact with the CCW, but DIW with an initial pH of 5.8 (due to equilibration with atmospheric CO_2) was buffered consistently to ~9.9 ±0.1 for up to 340 hours (not shown on Figure 5.2) due to contact with the cementitious phases. In contrast, when HCl or HOAc was used as the leachant solution, the pH of the leachate was initially buffered upwards to $9.7 \leq pH \leq 6.4$, depending on the pH of the leachant, but then progressively decreased with increasing leachate volume. Typically, leachants with a lower H^+ concentration (e.g. 0.5-2 mM HCl) had a greater buffering ability relative to the leachant pH (Table 5.1) by around one pH unit. After the initial buffering period and up to 100 hours, the pH of subsequent leachates varied by around 0.5 to 3.7 units when leached by all acidic leachants, with the greatest decline in pH generally seen for leachants with a higher H^+ concentration. There was no substantial difference in pH trends for experiments using HOAc or HCl at the same concentration over the same period of time despite the one pH unit difference in leachant pH (Table 5.1).

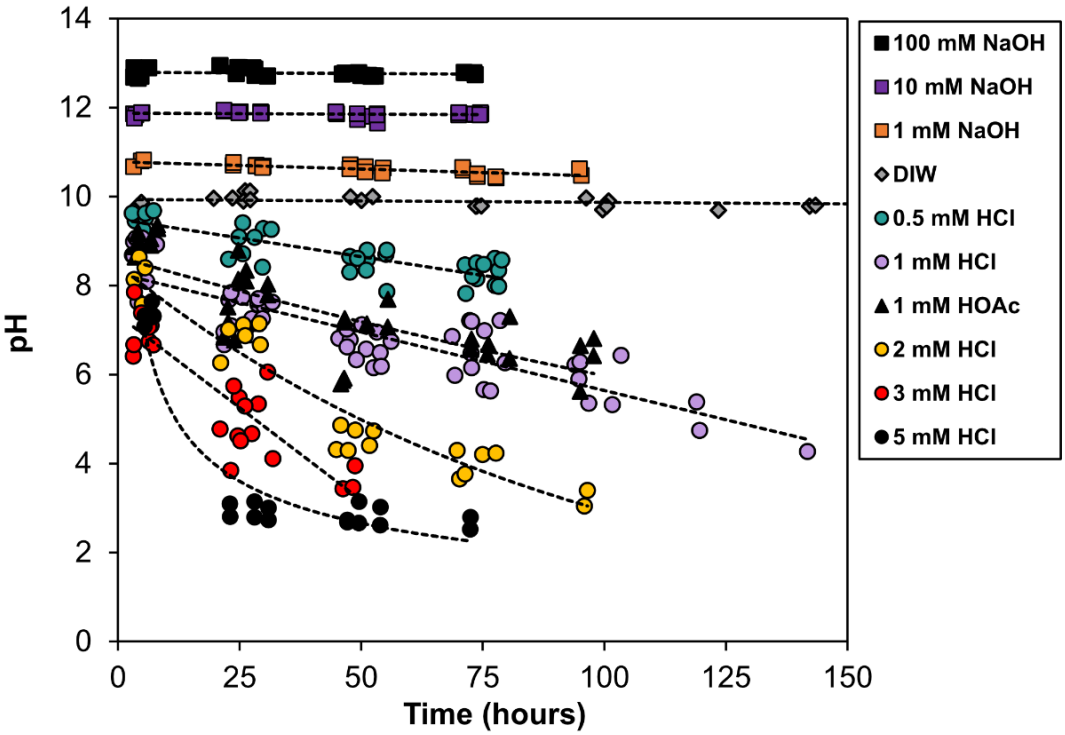

Figure 5.2 pH evolution of crushed concrete leachate measured in flow-through experiments using DIW, 0.5-5 mM HCl, 1-100 mM NaOH and 1 mM acetic acid (HOAc). Individual data points represent the leachate fraction measured within 30 minutes of elution. Trend lines have been added to guide the eye only.

5.3.2 Example flow-through reactor data sets.

The Ca, Si and Al concentrations, the Ca/Si and Al/Si ratios and the pH of the leachate are shown as a function of hours since experiment start time from example acidic and basic reaction conditions. In the 5 mM HCl experiment (Figure 5.3), the initial pH (up to 7 hours) was 7.3 ±0.2 and Ca and Si concentrations were 135 ± 8 mg L^{-1} and 11 ±1 mg L^{-1}, but the pH decreased to 2.7 ±0.2 from 23 hours and the Ca and Si concentrations decreased to 54 ±14 mg L^{-1} and 6 ± 2 mg L^{-1}, respectively. Thus, the initial Ca/Si ratio in solution was 14 ±1 but this declined to 11 ±1 after 23 hours. Conversely, Al concentrations were initially below detection but increased to 3.2 ±0.5 mg L^{-1} after 7 hours. The Al/Si ratio between 23 and 31 hours was 0.46 ± 0.03, which then rose to 0.68 ± 0.17 after 31 hours.

In the 10 mM NaOH experiment, the pH and Ca concentrations remained at 11.7-11.9 and 4.7 ± 1 mg L^{-1} respectively throughout the experiments, but Si concentration decreased from 10.1 ± 1.4 mg L^{-1} during the first 5 hours to 5.1 ± 1.1 mg L^{-1} after 22

hours. Thus, the initial Ca/Si ratio up to 5 hours was initially 0.45 ± 0.07 but rose to 0.80 ± 0.07 after 22 hours. Al concentrations and the Al/Si ratio also remained at 1.3 ± 0.31 mg L^{-1} and 0.12 ± 0.03 respectively until 53 hours, after which Al concentrations decreased to below detection.

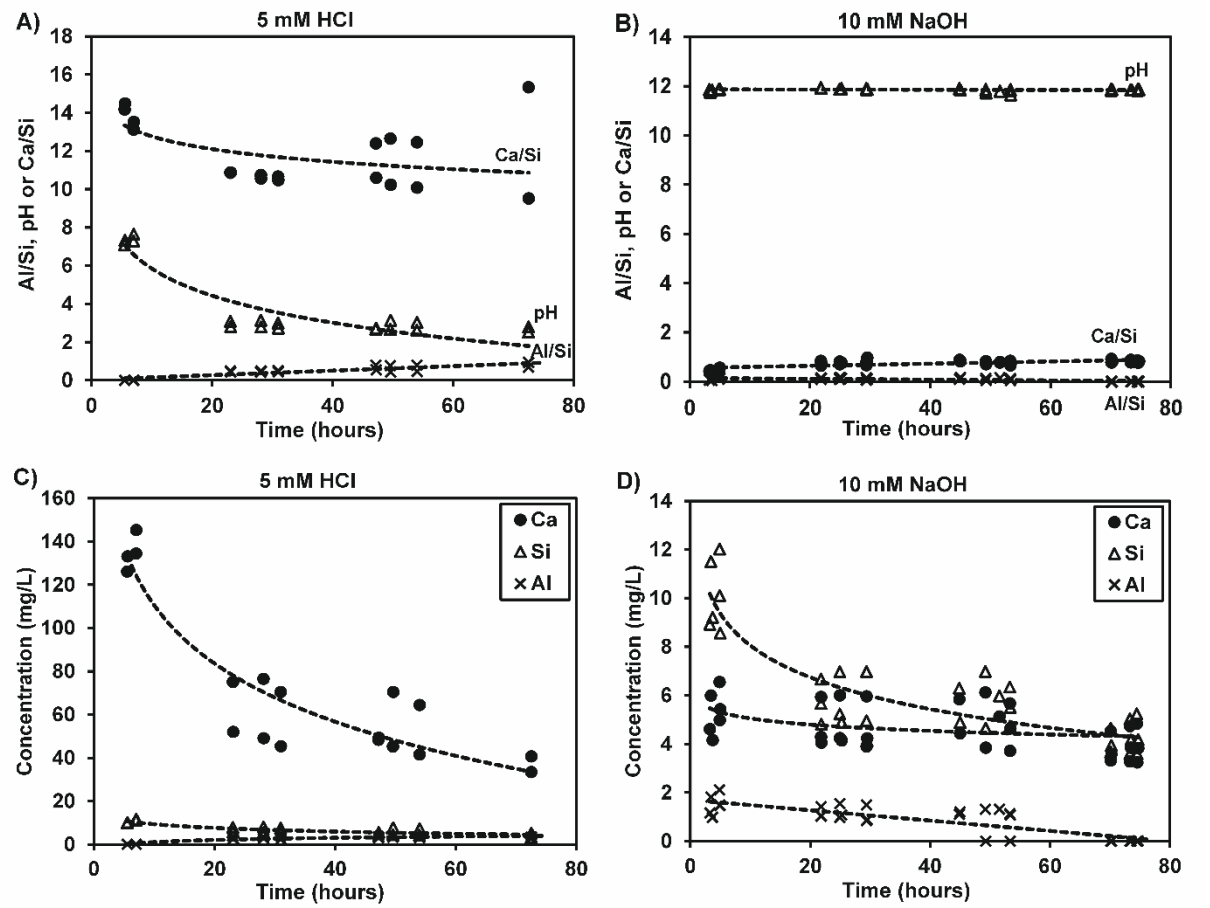

Figure 5.3 Evolution of leachate chemistry measured in flow-through experiments. Top two (A and B) panels show pH, Ca/Si and Al/Si from 5 mM HCl and 10 mM NaOH experiments. Bottom two panels (C and D) show Ca, Si and Al concentrations (mg/L). Individual data points represent leachate fraction from individual collection periods (plotted at the endpoint of the periods). Trend lines have been added to guide the eye only. 5 mM HCl consists of two replicates and 10 mM NaOH consists of three replicates (Table 5.1, Section 5.2.1).

5.3.3 Leaching rate calculations

The flow-through leaching experiments investigated how the leachant pH controls the rate of element release from CCW at far-from-equilibrium conditions (i.e., under high solution to solid ratio and with relatively short contact times). At steady state (i.e., when

the output concentrations of elements of interest are constant over time), the mass-normalised rate of release of element i (in mol g^{-1} s^{-1}) is:

$$R_i = q_v \times (C_i - C^o_i) / mass$$

Where; q_v is the flow rate through the reactor in L s^{-1}, C_i and C^o_i are the leachant and leachate concentrations of the element of interest in mol L^{-1} over the steady period (which is reported in the following paragraphs), and the mass of the solids in g. Similarly, a surface area normalised rate (in mol m^{-2} s^{-1}) is:

$$R_i' = q_v \times (C_i - C^o_i) / (mass \times SA)$$

Where SA is the BET surface area of the solids in m^2 g^{-1}.

In experiments using single phase pure minerals R_i is also often adjusted for the stoichiometry of the element of interest in the mineral being studied (Trapote-Barreira et al., 2014; Bray et al., 2015). However, for waste materials such as the CCW used in this study the exact stoichiometry of the reactive phase(s) is not known *a priori* and this adjustment was therefore omitted. The initial mass of each sample to be leached and the average BET surface area of the pre-leached CCW were used in rate calculations as this is useful to understand how the bulk material will behave during disposal, although it should be acknowledged that the rates produced will underestimate the reaction rates of the phases likely to be controlling element release (e.g., reactive C-(A)-S-H phases) due to their abundance being less than 100% of the CCW.

Where acid leachant solutions were used, the leachate Ca concentration was initially high for the first 7 hours and then decreased (Figure 5.3c) possibly due to the rapid dissolution of calcite from the partially carbonated CCW. With alkaline leachant solutions, the leachate Si concentration was initially high and decreased after 7 hours (Figure 5.3d), and the leachate Al concentration decreased after 53 hours (possibly due to exhaustion of reactive phases). However, with both the acid and alkaline leachants and DIW, the leachate Ca, Si and Al concentrations are relatively stable from 21 hours to 56 hours, indicating a relatively steady state. This applies to all experiments apart from 2 mM HCl, where the steady period ran from 45 hours to 71 hours since the experiment began. Therefore, steady-state rate calculations instead used the average (± 1σ) of elemental concentrations in the leachate between 21 hours and 56 hours for all experiments except 2 mM HCl, which used 45-71 hours.

Within this time range, the relative standard deviation (RSD, %) for the major elemental concentrations (Ca, Si, Al) in each leachant set was typically <23%, except for Al which

had an RSD of <51%. Where Al was below the LOD or LOQ, it was not included in leaching calculations, and this applied to four out of ten of the leachants used in this study. The RSD for the trace element concentrations generally ranged from >30% to over 100%, which reflected the error bars on the leaching graphs (Figure 5.5), although the RSD for V, Mg and Mn concentrations were <40% in the majority of experiments. This range for RSD during the period where steady state is assumed is higher than reported for studies of single mineral phases (5-15%; Bray et al. (2015); Trapote-Barreira et al. (2014)), but this is attributed to CCW sample heterogeneity. When calculating the leaching rate, a minimum of three measurements were used. Any samples missing from figures are those with less than 3 measurements above the LOD or LOQ. Data below the LOQ were excluded from leaching rate calculations.

5.3.3.1 Leaching rates of major elements over the pseudo-steady state period

The rate of Ca leaching was pH-dependent and decreased with increasing pH (Figure 5.4). The Ca leaching rate was one order of magnitude greater at pH ~3 ($3.7 \pm 0.84 \times 10^{-10}$ mol m^{-2} s^{-1}) than at pH ~13 ($3.7 \pm 0.65 \times 10^{-11}$ mol m^{-2} s^{-1}). The Si leaching rate (also shown in Figure 5.4) was around threefold greater at pH ~3 and ~5 ($5.7 \pm 1.3 \times 10^{-11}$ mol m^{-2} s^{-1} and $6.5 \pm 0.72 \times 10^{-11}$ mol m^{-2} s^{-1} respectively) and twofold greater at ~pH 13 ($4.8 \pm 1.1 \times 10^{-11}$ mol m^{-2} s^{-}1) compared to the leaching rate at pH ~8.7 ± 0.4 where it was lowest ($2.4 \pm 0.51 \times 10^{-11}$ mol m^{-2} s^{-1}). The leaching rates of Si were lower than those of Ca between pH ~3 to pH 10 but were at similar magnitudes above pH 10 (2-6.4 x 10^{-11} mol m^{-2} s^{-1}). The leaching rate of Al was similar to Si with higher rates at pH 3 ($3.1 \pm 0.46 \times 10^{-11}$ mol m^{-2} s^{-1}) and pH 13 ($1.5 \pm 0.53 \times 10^{-11}$ mol m^{-2} s^{-1}), however Al was not detected from $5.5 \leq pH \leq 6.5$ and $8 \leq pH \leq 10$. The Al leaching rates at low and high pH were an order of magnitude above the lowest leaching rates at pH 7.3 ± 0.8 ($2.2 \pm 0.13 \times 10^{-12}$ mol m^{-2} s^{-1}).

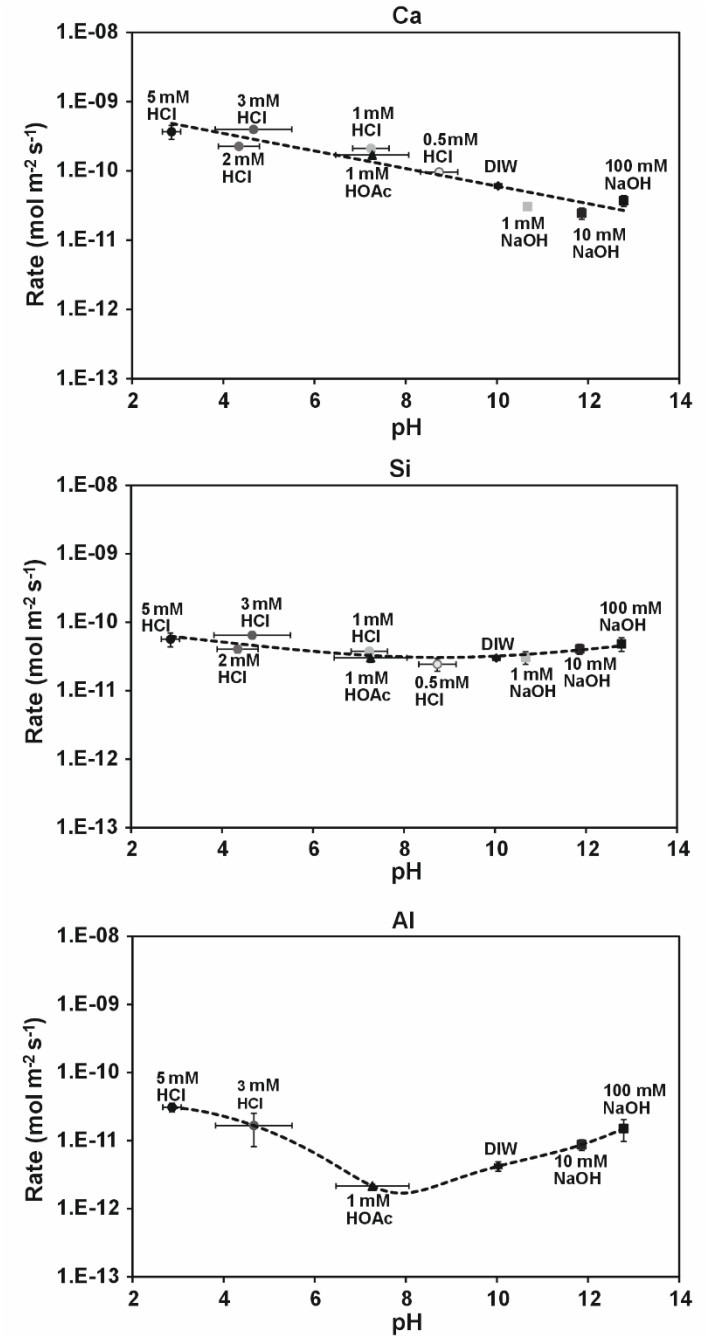

Figure 5.4 Variation of the leaching rate (mol m^{-2} s^{-1}) of Ca, Si and Al as a function of average pH calculated over the steady period (21 to 56 hours for all experiments except 2 mM HCl which was over 45-71 hours). Symbols represent the average of replicates, and the error bars represent one standard deviation. Error bars that are not visible are so small that they are within the symbol size. Missing leachants indicate samples were below the LOQ/D and were therefore not included in leaching rate calculations. Only samples with a minimum of three samples above the detection limit were used in calculating average leaching rates. Dashed trend lines are added as a guide to the eye only.

5.3.3.2 Leaching rates of trace elements over the pseudo-steady state period

The leaching rates of Mg, Fe and Mn all exhibited a similar pattern of decreasing rate with increasing pH (Figure 5.5). The leaching rate for Mg and Fe declined from 1.3 ± 0.37 x 10^{-11} mol m^{-2} s^{-1} and 3.7 ± 3.9 x 10^{-11} mol m^{-2} s^{-1} at pH ~3 by around two orders of magnitude to 1.7 ± 0.32 x 10^{-13} mol m^{-2} s^{-1} and three orders of magnitude to 5.8 ± 0.76 x 10^{-14} mol m^{-2} s^{-1} at pH ~10 respectively. Above pH ~10, Mg and Fe were generally below the detection limit. Mn was also leached in a similar pattern with respect to pH and varied by around two orders of magnitude from 6.2 ± 1.9 x 10^{-13} mol m^{-2} s^{-1} at pH ~3 to around 7.1 ± 1.5 x 10^{-15} mol m^{-2} s^{-1} at pH 13.

Cr and V leaching rates (Figure 5.5) did not vary as strongly with pH although leaching was typically greatest at pH ~3 for all elements. The V leaching rates from pH 4 to 13 were around 4.2 ± 2.1 x 10^{-15} mol m^{-2} s^{-1}, with greatest rates at pH 3 (2.0 ± 1.4 x 10^{-14} mol m^{-2} s^{-1}) and lowest rates when leached by 2 mM HCl at pH 4.3 ± 0.4 (1.7 ± 0.41 x 10^{-15} mol m^{-2} s^{-1}). Cr leaching rates were typically similar to V across pH 4 to 13 (7.0 ± 4.5 x 10^{-15} mol m^{-2} s^{-1}), but were around an order of magnitude greater when leached by 1 mM HOAc (3.2 ± 3.9 x 10^{-14} mol m^{-2} s^{-1}) and 5 mM HCl (4.0 ± 3.4 x 10^{-14} mol m^{-2} s^{-1}). Pb leaching rates were similar to those of Cr and V at low and high pH values (1.9 ± 0.55 x 10^{-14} mol m^{-2} s^{-1} at pH ~3 and 4.7 ± 0.88 x 10^{-15} mol m^{-2} s^{-1} at pH ~13) but the Pb concentration was generally below the detection limit from $5 \leq pH \leq 9$ and $11 \leq pH \leq 12$.

Several elements measured (K, As, Zn, Cu, S) leached in only a few experiments or were below detection over the pseudo-steady state period. In three experiments within the pH range 6-13, K leaching rates were around 8.2 ± 3.4 x 10^{-12} mol m^{-2} s^{-1}. As was only detected when leached by 1 mM HOAc (pH 7.3 ± 0.8) and DIW (pH ~10) and leaching rates were around 2.7 ± 1.1 x 10^{-15} mol m^{-2} s^{-1}. Zn was only present above detection when leached by DIW with rates around 2.2 ± 1.5 x 10^{-14} mol m^{-2} s^{-1}. No Cu or S was detected in any samples.

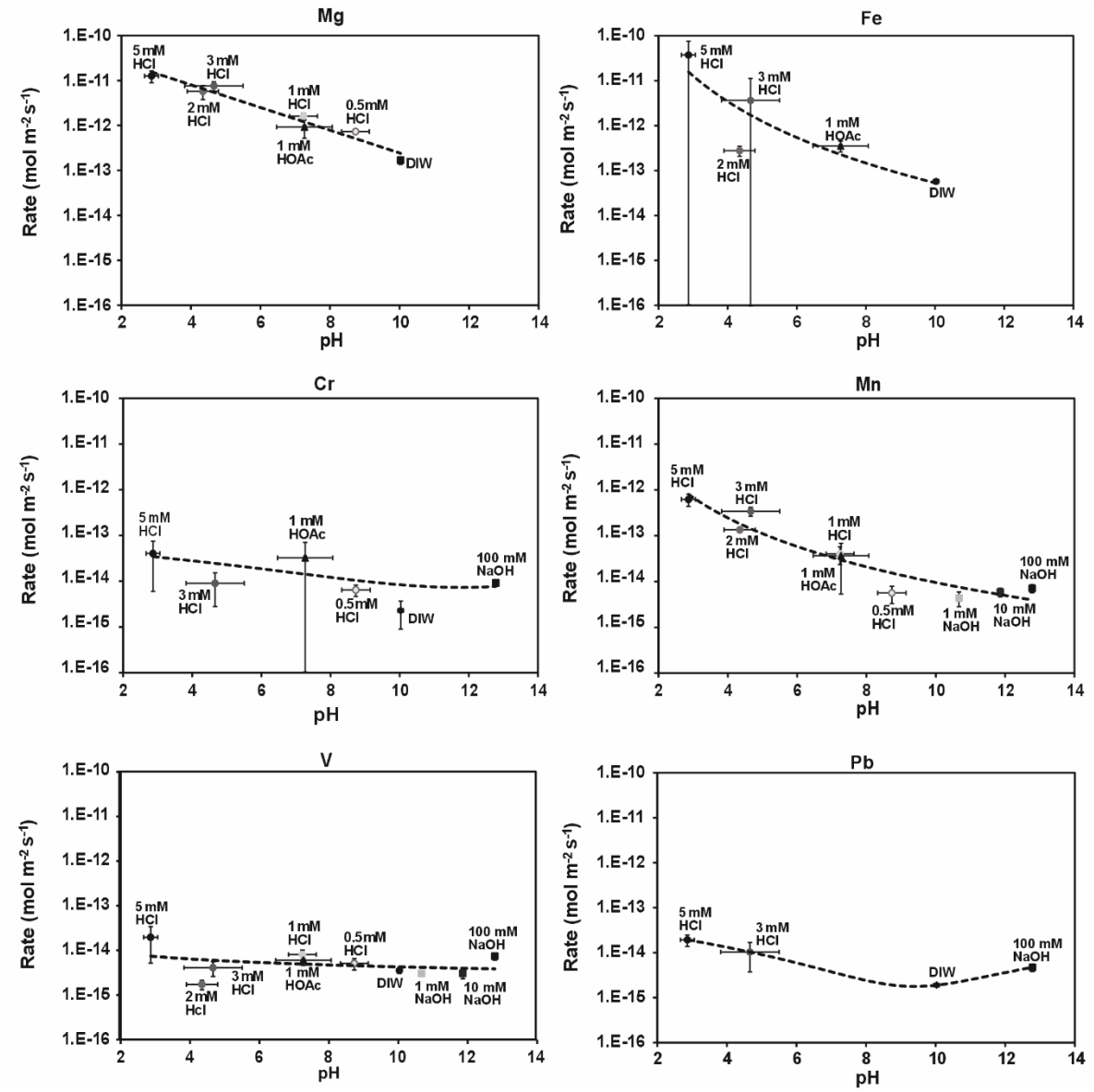

Figure 5.5 Variation of the **l**eaching rate (mol m^{-2} s^{-1}) of Mg, Fe, Cr, Mn, V and Pb as a function of average pH calculated over the steady period (21 to 56 hours for all experiments except 2 mM HCl which was over 45-71 hours). Symbols represent the average of replicates and the error bars represent one standard deviation. Error bars that are not visible are so small that they are within the symbol size, and error bars reaching the axis indicate a non-normal distribution of element concentrations in the sample replicates. Missing leachants indicate samples were below the LOQ/D and were therefore not included in leaching rate calculations. Only samples with a minimum of three samples above the detection limit were used in calculating average leaching rates. Dashed trend lines are added as a guide to the eye only.

5.3.4 Variation in Ca/Si and Al/Si as a function of pH

The Ca/Si ratio of the leachate decreased with increasing pH from about 9 ± 0.5 at pH ~3 to around 1.2 ± 0.4 when the pH >11 (Figure 5.6a). In contrast, the Al/Si ratio at 4≤pH≤5.5, and pH 13 was about the same as the pre-leached C-(A)-S-H phases (Al/Si = 0.28 ± 0.15). At 10≤pH≤12, the Al/Si ratio was just below the average but generally within the range of the stoichiometric ratio (Figure 5.6b). However, Al concentrations were typically below the LOD from 5.5≤pH≤9 and pH 11, except when the leachant was 1 mM HOAc where they were just above the LOD, giving the lowest Al/Si ratio. The Al/Si ratio at pH ~3 (Al/Si = 0.55 ± 0.12) was just above the pre-leached solid value.

5.3.5 Characterisation of leached material

5.3.5.1 SEM-EDS analysis

SEM analysis indicates that the most common particles in the leached CCW were quartz grains (fine aggregate), calcium carbonate phases (calcite), and a fine-grained heterogeneous matrix composed predominantly of Ca, Si and Al in variable stoichiometry (Figure 5.7 and Table 5.2) which is essentially the same as the pre-leached materials (Chapter 4 Section 4.2.1). Calcium carbonate was present in all samples, including those leached with acidic leachant solutions (e.g. Figure 5.7). Like in the pre-leached material (Figure 5.7a), residual unhydrated clinker relics were seen in some of the leached particle interiors (e.g. Figure 5.7c;f) that resembled SEM images of clinker relics in Frýbort et al. (2020) and clinker phases belite, aluminate and/or ferrite in Stutzman et al. (2015). CCW particles recovered from leaching tests contained evidence of leaching artefacts such as relatively smooth edges, leached surface areas and pitting as dark regions depleted in all elements. However, these features are also present in the pre-leached materials.

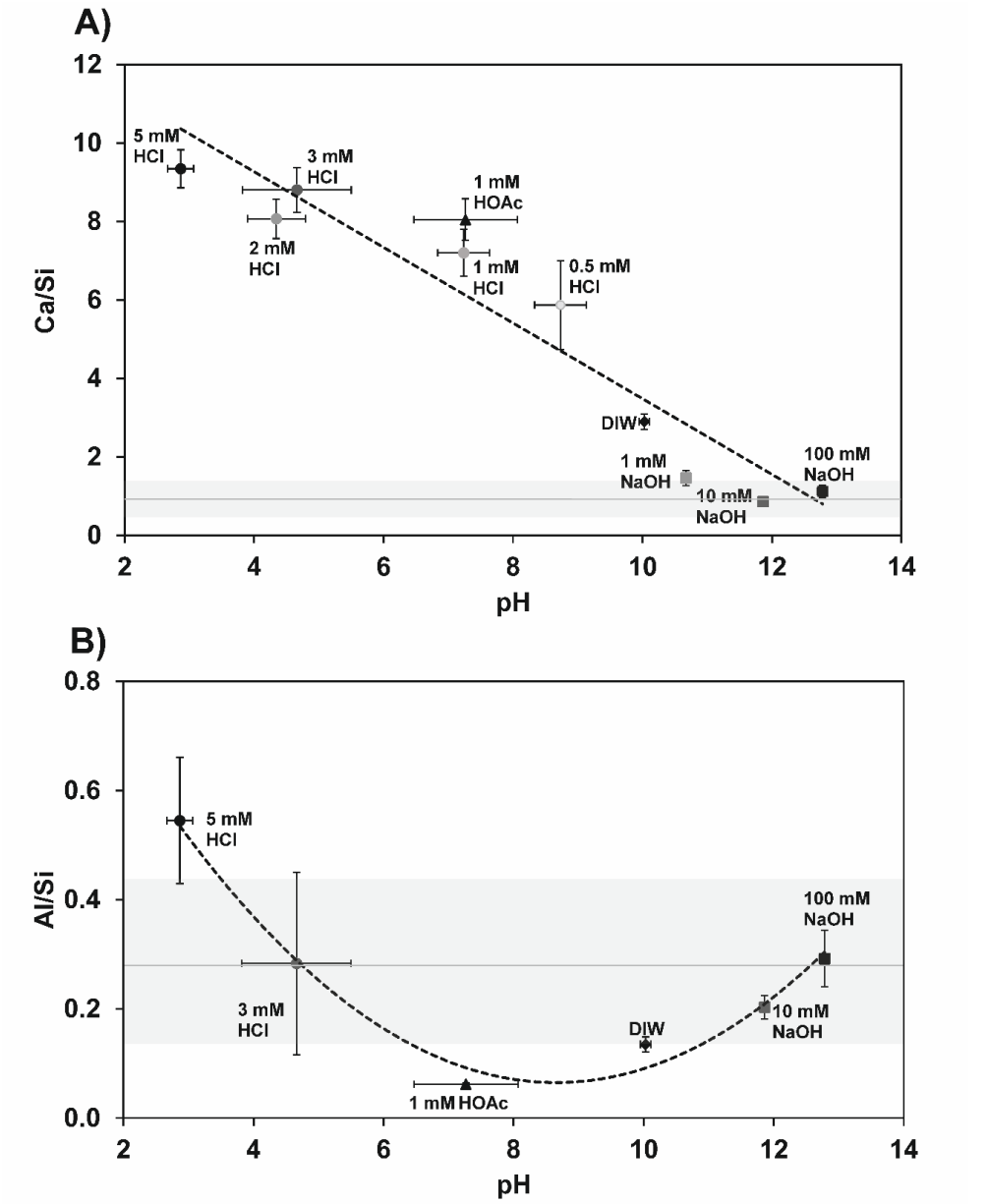

Figure 5.6 Average Ca/Si (A) and Al/Si (B) ratio in leachates plotted against the average pH over the steady period (21 to 56 hours in all flow-through experiments except for 2 mM HCl which was over 45-71 hours) using DIW, 0.5-5 mM HCl, 1-100 mM NaOH and 1 mM Acetic acid (HOAc). Points represent average of replicates and error bars represent one standard deviation. Missing samples are where the Al concentration (mg L^{-1}) was below the LOD. Trend line is to guide the eyes only. The average Ca/Si and Al/Si of the pre-leached C-(A)-S-H phases is shown as a solid line with 1 SD represented by the shaded regions.

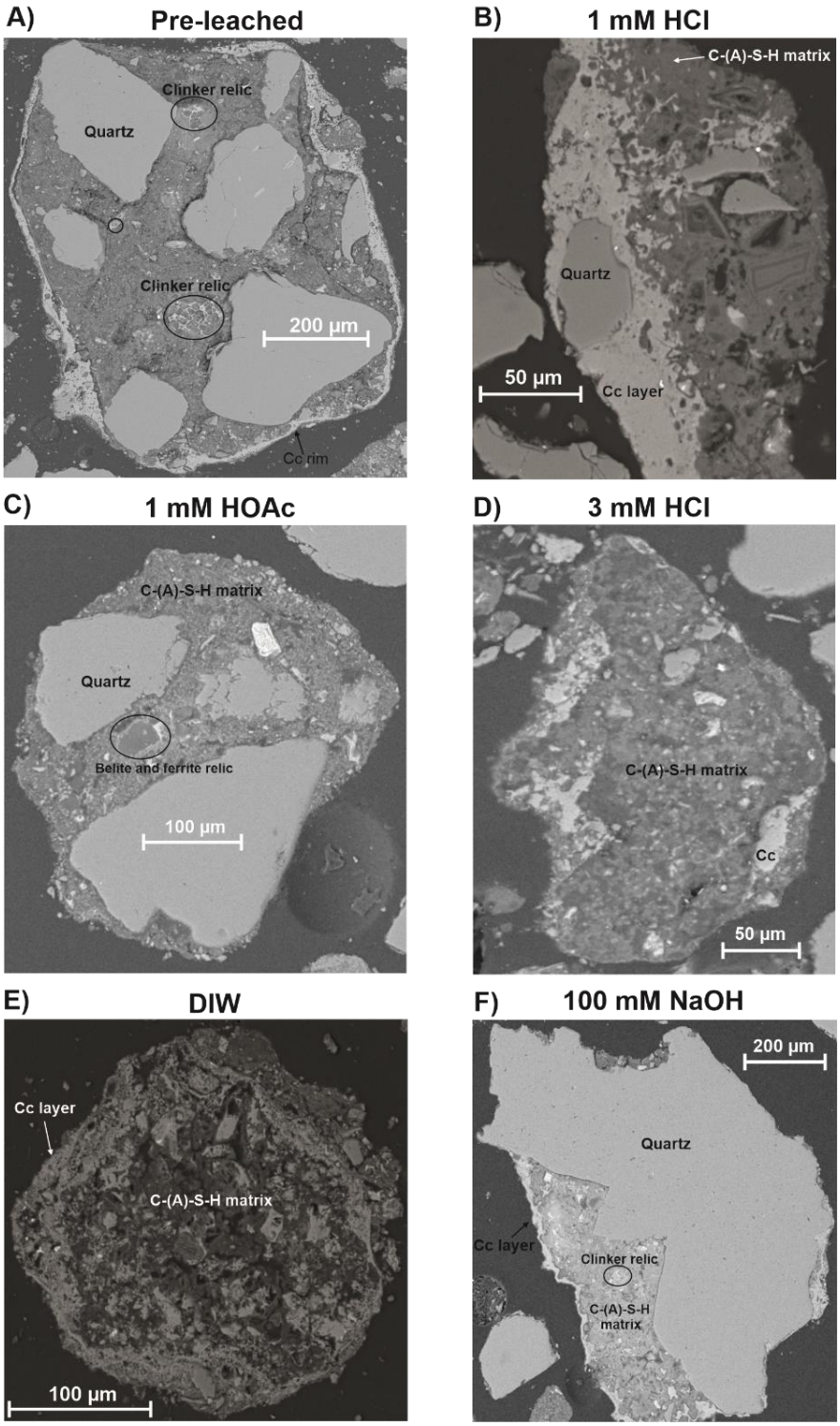

Figure 5.7 Backscattered electron (BSE) images of sand-sized particles before leaching (A) and after leaching by), 1 mM HCl (B), 1 mM HOAc (C), 3 mM HCl (D), DIW (E) and 100 mM NaOH (F). Quartz grains are labelled, the C-(A)-S-H matrix is in the grey 'glue' that binds the aggregates together and carbonate (Cc) is present as rims on A and F, as a layer on B and throughout D and E. Clinker relics, including belite and ferrite, are labelled as black circles.

Table 5.2 Chemical composition (atomic %) and assigned phase for quartz, calcium carbonate (Cc) and C-(A)-S-H matrix of a particle leached by 1 mM HCl labelled on Figure 5.7b.

	Assigned phase		
Element	**Quartz**	**Calcium carbonate (Cc)**	**C-(A)-S-H matrix**
Ca	0.08	25.1	7.76
Si	34.44	0.94	17.26
O	65.48	73.34	66.98
Al	-	-	5.15
Mg	-	-	1.74
Fe	-	-	0.40
Cl	-	-	0.41
Ti	-	-	0.07
P	-	-	0.23
S	-	0.31	-

The SEM-EDS spot analysis of the matrix phase of leached samples (Figure 5.8) shows that the alkaline leached samples cluster around the pure phase C-(A)-S-H composition, whilst the acid- and DIW-leached samples are typically more Al and Si rich. Two distinct mixing lines emerge from the data (a result of two phases in varying proportions present in the EDS excitation volume of ~1-2 μm^3): (1) between compositions consistent with the C-(A)-S-H phases and AFm and; (2) between C-(A)-S-H and $CaCO_3$ at the origin. Although $CaCO_3$ and $Ca(OH)_2$ will both plot at the origin in Fig. 5.8, $Ca(OH)_2$ is presumed unlikely to be present in these samples as portlandite was not detected in XRD analysis of the pre-leached material (Chapter 4 Section 4.3.1). The average Ca/Si ratio (±1σ) of the C-(A)-S-H matrix (using a threshold cut-off

described in Chapter 4 Section 3.2.4.1) of the leached particles was lower when leached by acids (0.7 ±0.4) and DIW (0.6 ±0.5) than when leached by alkaline solutions (1.1 ±0.3). For the acid or DIW leached particles there is also a distinct trend of compositions with higher Si/Ca and Al/Ca ratios, indicating a relative depletion in Ca. Some EDS spots (8 for DIW, 2 for acid and 1 for alkaline) plotted above the range of the graph (up to Si/Ca = 10 and Al/Ca = 5) and so are included in the Ca/Si ratio calculation but are not shown.

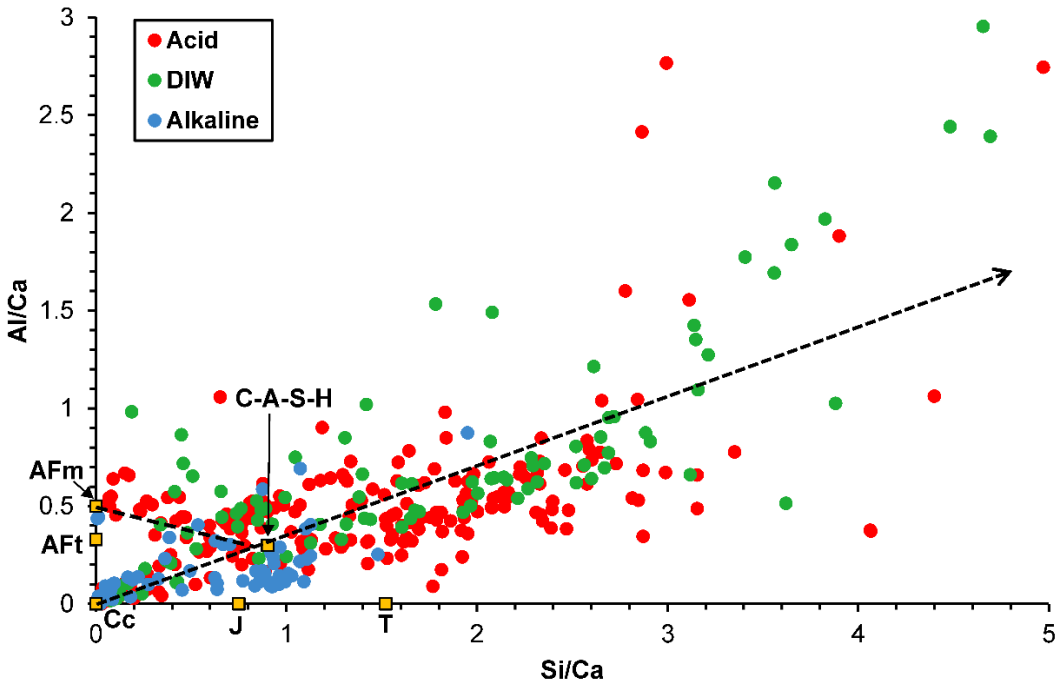

Figure 5.8 Elemental ratios determined by SEM-EDS spot analysis of the matrix of crushed concrete particles leached by acid (0.5-1 mM HCl, 3 mM HCl, 1 mM HOAc), alkaline (100 mM NaOH) and DIW leachants. Plotted in yellow are ideal phase compositions from Rossen and Scrivener (2017) of calcium monosulfoaluminate (AFm), ettringite (AFt), calcium aluminate silicate hydrate (C-A-S-H), calcite (Cc), jennite (J) and tobermorite (T). The dotted lines represent mixing lines apparent between C-A-S-H and AFm compositions, and C-A-S-H and Cc at the origin.

5.3.5.2 Change in surface area and mass

The mass loss during leaching (Table 5.3) was slightly higher in the acidic and DIW leaching tests than the alkaline leaching tests. The BET surface area of the leached material (also in Table 5.3) was similar in all tests, and ~25% lower than the initial material (5.6 – 6.2 versus 7.8 m^2 g^{-1}).

Table 5.3 Mass loss (%) and BET ($m^2\ g^{-1}$) measurements of the initial pre-leached material and the sample material leached by DIW, acidic and alkaline leachant solutions, shown as the average (±1σ) of 2 (*) or 3 replicates. The mass loss and surface area data for each experiment are included in Appendix C.

Sample	Mass Loss (%)	Average surface area ($m^2\ g^{-1}$)
Initial	n.a	7.8 ±0.3
DIW	13 ± 2	5.6 ±0.7*
Acid	11 ±2	6.2 ±1
Alkaline	8 ±2	5.7 ±1

5.4 Discussion

5.4.1 pH-dependent leaching of CCW

The pH of the leachant caused substantially different changes in the pH of the CCW leachate over time, and these changes are reflected by the lines of best fit chosen in Figure 5.2. When leached under acidic conditions, there was a short initial buffering period that then dropped by several pH units depending on the acidity of the leachant. As such, the trendlines for the acidic leachants reflect the significant loss of alkaline buffering capacity from dissolution of cement phases and depletion of the CCW. On the other hand, when the pH was high (pH ≥10) there was minimal change in leachate pH because the cement phases were stable under these conditions, and this is reflected in the straight trendline used for DIW and alkaline leachants.

When CCW was leached by alkaline leachants, the Ca/Si ratio of the leachate was about the same as the alkaline leached C-(A)-S-H phases and was similar to the C-(A)-S-H phases in the unleached CCW. Ca leaching rates were the lowest observed and the Al/Si ratio (where measurable) was about the same or slightly below the C-(A)-S-H phases in the unleached CCW indicating slightly more Si leaching relative to Al. Congruent dissolution is evidenced by a constant ratio of constituents that have the same stoichiometry as the solid phase (Berner, 1992; Harris et al., 2002). For example, in Trapote-Barreira et al. (2014), congruent dissolution of C-S-H by DIW under steady-state conditions was observed when the Ca/Si of the solution was similar to that of

tobermorite (Ca/Si = 0.83), which is also in agreement with Harris et al. (2002). Therefore, it may be assumed that the aqueous Ca, Si and Al concentrations were controlled by congruent leaching of C-(A)-S-H phases in the CCW at alkaline pH, as both the Ca/Si and Al/Si ratio of the leachate were about the same as the unleached C-(A)-S-H phases.

The leaching rates of Si at pH >10 (2-6.4 x 10^{-11} mol m^{-2} s^{-1}) were on the same order of magnitude as those reported in Trapote-Barreira et al. (2014), when C-S-H dissolution was congruent under steady-state conditions, and pH was around 10. In Trapote-Barreira et al. (2014), C-S-H dissolution was calculated based on steady-state Si release. Si leaching rates in their study ranged from 4 x 10^{-13} mol m^{-2} s^{-1} to 3.6 x 10^{-11} mol m^{-2} s^{-1}, with faster flow experiments (average flow rate 0.12 mL min^{-1}) typically producing higher leaching rates (i.e., above 1 x 10^{-11} mol m^{-2} s^{-1}; Trapote-Barreira et al., 2014). Thus, the Si leaching rates from CCW in this study (average flow rate of 0.47 ± 0.08 mL) are consistent with Si leaching rates from the faster flow experiments in Trapote-Barreira et al. (2014). In addition, the Si leaching rates are on the same order of magnitude as quartz dissolution rates across pH 10-12 under far-from-equilibrium conditions (~10^{-11} mol m^{-2} s^{-1}; Schott et al., 2009). This suggests Si leaching may also be from quartz aggregate in the CCW, as well as from C-(A)-S-H. Above pH 10, Ca leaching rates are also low, especially in comparison to calcite dissolution rates under far-from-equilibrium conditions, which are on the order of 10^{-6} mol m^{-2} s^{-1} (Brantley, 2008), indicating Ca leaching rates are low at high pH.

In the range 3≤ pH≤10, Ca leaching rates were higher than in the alkaline tests, which is consistent with the higher mass loss observed. As there were only small differences in the Si leaching rate, this resulted in higher Ca/Si ratios in the leachate than in the alkaline tests. The higher rate of Ca leaching could potentially be due to the dissolution of a range of calcium-containing phases, including carbonates, C-(A)-S-H phases and other Ca-containing phases (e.g. AFt and AFm, Fig. 8). Meanwhile, the Al/Si ratio was generally similar in the pH range 4≤pH≤13, but higher at pH 3 due to greater Al leaching.

The initial, non-steady state phase of the acid leaching tests were characterised by a pH between 6.4 and 9.7 and high Ca leaching rates, without similar increases in Si or Al leaching (e.g. Fig. 3) that are indicative of rapid calcium carbonate dissolution, and subsequently both the pH and Ca leaching rate decreased as a steady state was established. Thus, calcium carbonate dissolution was probably not important when the steady state had been reached. Instead, it is likely that C-(A)-S-H phases (and

potentially AFt and AFm phases, where present) dominated steady-state leaching as Si/Ca and Al/Ca compositions typically trended higher (i.e. lower Ca/Si ratio) than the alkaline leached CCW (Fig. 8). Between pH 3.4 and 10, the leached solid matrix phase had higher Si/Ca and Al/Ca compositions suggesting incongruent leaching of Ca relative to Si and Al from C-(A)-S-H phases.

5.4.2 Leaching of trace elements

When the CCW is leached, dissolution processes will release trace constituents that may be of concern to nearby surface water receptors. The results showed that, overall, leaching was low for all trace elements and Al (on the order of $< 1 \times 10^{-10}$ mol m^{-2} s^{-1}) under pseudo-steady state conditions, which is environmentally favourable. Whilst only Fe and Mg leached at rates similar to Ca and Si at acidic pH, the leaching rates for Cr, Mn, V, Pb were several orders of magnitude lower at near neutral and alkaline pH. Above pH 4, leaching rates for all trace elements were $<1 \times 10^{-11}$ mol m^{-2} s^{-1}. Leaching rates were even lower above pH 6 for Fe, Cr, Mn, V, and Pb and were on the order of $< 3 \times 10^{-13}$ mol m^{-2} s^{-1}), especially in comparison to the Ca and Si leaching rates ($>1 \times 10^{-11}$ mol m^{-2} s^{-1}). The trace element leaching rates are also very low in comparison to the dissolution kinetics of calcite and quartz at far-from-equilibrium conditions above pH 6. Compared to the dissolution kinetics of calcite (~10^{-6} mol m^{-2} s^{-1} at pH 5-11; Brantley, 2008), the leaching rates of trace elements from CCW (Figure 5.5) are approximately 4-8 orders of magnitude lower. In addition, trace element leaching rates are several orders of magnitude below the dissolution kinetics of quartz, which varies from 10^{-13} mol m^{-2} s^{-1} at pH 4-7, 10^{-12} mol m^{-2} s^{-1} at pH 8-9 and 10^{-11} mol m^{-2} s^{-1} above pH 10 (Schott et al. 2009). Therefore, leaching of trace elements from CCW may be regarded as low, especially in comparison to quartz which is known to be poorly soluble (Langmuir, 1997).

The phases controlling trace element release to solution appear to be different for different trace elements, with some pH-dependent and others more pH-independent. As the leaching rates of Mg, Fe and Mn were similar and highly pH-dependent, it is likely Mg-, Fe(III)- and Mn(II)-oxides or hydroxides were the main phases controlling release, and leaching was heavily influenced by phase solubility, with greater leaching rates at acidic pH and low or below detection concentrations at high pH (>10).

On the other hand, the leaching rates of Cr, V and Pb (and K, As, and Zn where present) were only slightly pH-dependent. Pb concentrations were below detection between pH ~6 and 10, which may indicate Pb oxides and hydroxides as the solubility

controlling phase as these phases are insoluble across this pH range (Stumm and Morgan 1996). The leaching patterns of V and Cr were generally similar to Si indicating C-(A)-S-H phases as the main source. These elements were likely controlled by the slow dissolution of C-(A)-S-H phases and were released during dissolution or desorption reactions (Garrabrants and Kosson, 2004; Vollpracht and Brameshuber, 2016).

The leaching pattern differs between the flow-through leaching experiments and the equilibrium experiments carried out in the previous chapter (Chapter 4 Section 4.3.4) at corresponding pH values. The constant replenishment of solution in flow-through experiments at the prevailing infiltration rate prevents the establishment of equilibrium and leads to a slow and steady dissolution of CCW. When the leaching solution is not replenished, element concentrations are typically far greater (Drinčić et al., 2017). For example, the leaching of trace elements Cr, V and Pb was typically lower during the far-from-equilibrium pseudo-steady state leaching than during corresponding batch equilibrium experiments at different pH values (Chapter 4 Section 4.3.4). Although the pH of the leachant solution or leachate controls the leachability of elements (Hartwich and Vollpracht, 2017), the limited variation in Cr, V and Pb leaching indicates that leaching at far-from-equilibrium conditions is mass-transport-controlled and availability-limited (Garrabrants and Kosson, 2004). Cu was detected in the batch experiments, but not in the flow-through leaching experiments, meaning Cu release may only occur under equilibrium-controlled conditions, or is availability-limited. On the other hand, the pattern of Mn leaching was similar to the batch experiments and is similarly solubility-controlled.

When comparing the total contents of trace elements measured by XRF in Table 4.1 and 4.2 (Chapter 4 Section 4.3.1), the leaching of trace elements is not correlated with the total composition measured in the pre-leached material, which was similar to the results in the batch experiments (Section 4.3.3 and 4.3.4). For example, As, Cu, S and Zn were present in the subsurface sand fraction but rarely detected (As, Zn) or consistently below detection (S, Cu) in the flow-through leaching experiments. This result of total content not correlating with leaching is in line with many studies (van der Sloot, 2000; van der Sloot and Dijkstra, 2004; Chen, J. et al., 2012; Bestgen et al., 2016; Zhang, Y. et al., 2018; Eckbo et al., 2022).

5.4.3 Implications for disposal

Flow-through experiments have provided insight into short-term CCW dissolution kinetics and the leachate composition at a pseudo-steady state far-from-equilibrium condition in response to a range of different pH solutions. This condition is relevant to the waste disposal scenario of direct disposal into an unlined void and approximates the leachate composition under high flow, saturated conditions (e.g., from high surface water infiltration and/or groundwater flow through the subsurface). In the field, the pH of any infiltrating surface or groundwater is likely to be slightly acidic to slightly alkaline (Shand et al., 2007). Under pseudo-steady state conditions, acidic leachants (from ~pH 2.3 to 4, Table 5.1) resulted in the buffering of pH to moderately acidic (pH ~3), slightly acidic (~4-6) and neutral to slightly basic (8-9) pH conditions, dependent on the proton concentration of the leachant solution. Leaching with DIW produced a moderately basic pH of ~10, similar to the material pH measured in batch equilibrium experiments (Chapter 4 Section 4.3.2) but in the field infiltrating surface and groundwater will contain solutes such as carbonate, sulphate, chloride and/or magnesium (Walker et al. 2016), which will result in a less aggressive (relative to DIW) leaching environment as DIW has a very low ion concentration that drives leaching by dissolution and diffusion (Hartwich and Vollpracht, 2017). Assuming the CCW leachate is buffered between pH 4 and 9 at a pseudo-steady state, the leaching rates are low (from 3 to 5 orders of magnitude lower than Ca leaching rates) for many trace elements (Fe, Mn, Cr, V, Pb from pH ~3-5.5) or mostly below detection (Pb from pH 6 to 10, As, Zn, S), but slightly elevated for Mn, Fe (and Cr for leaching by HOAc only) as pH is lowered. At high pH, the pH was the same as the leachant solution as CCW has no alkaline buffering capacity, but leaching rates for all elements were generally even lower. Moreover, the use of stirrer bars in laboratory leach tests can cause particle abrasion, impacting reactive surface area so that the derived leach rates will slightly overestimate leaching expected in the field. Overall, the low leaching rates observed indicate the CCW leachate is benign where far-from-equilibrium conditions are established, which is beneficial for field applications of CCW as void fill.

In Chapter 4, from the results of the batch equilibrium experiments it was advised that the use of CCW in unlined voids should not be encouraged if local soil waters were acidic in nature due to higher levels of leaching of contaminant metals Al, Cr, Pb, V, Mn and Cu at acidic pH. This would occur during equilibration of CCW at acidic pH values buffered by undissociated humic acids in a very acidic groundwater. For similar reasons, van der Sloot (2000) recommends that fine construction material debris

should not be applied where soils are peaty or acidic (around pH ~4) in nature. A scenario such as this could be a concern if sealed subsurface structures containing CCW had an ingress of acidic soil water which caused the rising of internal water levels leading to overtopping of the structure (a worse-case scenario) and movement of the leachate downstream raising environmental concerns. However, this is an unlikely scenario because even very acidic water would not overcome the buffering capacity of CCW until many volumes of water are passed. Alternatively, if the equilibrated pH of the internal water was alkaline there could be concerns with the generation of alkaline plumes downstream (from a flux of high pH water generated from an overtopping scenario), which are dependent on the alkaline buffering capacity of surrounding soils. However, if the water was able to flow-through the structure, either by leaving existing penetrations (such as pipes and drains) unsealed, or purposefully creating holes in the structure, then the flow-through results are relevant and provide a different conclusion. With increasing volumes of water in contact with the CCW, any residual contamination levels are also unlikely to be problematic. The dilution of high pH CCW leachates from underground structures would also occur in the field (Gupta et al., 2018) which is beneficial when considering the potential environmental concerns with metal leaching and high pH alkaline plumes. Therefore, it may be beneficial for site managers to take advantage of the slow dissolution kinetics observed for CCW and consider designs that allow free water flow through subsurface structures.

5.5 Conclusion

Research objectives 3 and 4 were achieved in this chapter through the establishment of far-from-equilibrium, pseudo-steady state flow-through leaching conditions using stockpiled CCW. Under such leaching conditions, leaching by alkali solutions was consistent with the congruent leaching of C-(A)-S-H phases. Leaching of CCW by acidic or DIW leachant produced leachates with high Ca/Si ratios and Ca-depleted solids, which was consistent with the incongruent leaching of C-(A)-S-H phases and the dissolution of carbonates. Ca leaching rates and overall mass loss were lower when leached by alkali solutions relative to acidic or DIW leachants, which had preferential leaching of Ca relative to Si and Al as well as greater mass loss. There was generally no preferential leaching of Si or Al at $4 \leq pH \leq 5.5$, and pH 13, where leaching was about the same as the pre-leached C-(A)-S-H phases, and Al release was low or below detection between pH 5.5 and 11. The leaching of Mg, Fe and Mn was pH-dependent (higher leaching at acidic pH) and solubility-controlled but pH-independent for Cr, V, Pb, As, K and Zn. Leaching was mass-transport controlled for all trace

elements, as well as availability-limited. Research objective 4 was answered in this chapter from determining the dissolution kinetics of CCW using different pH leachants. The data suggest that disposal of CCW in unlined voids under high water infiltration rates at pseudo-steady state far-from-equilibrium conditions buffered above pH 4 will dissolve CCW slowly and produce a benign leachate with below detection or low leaching rates (<1 x 10^{-10} mol m^{-2} s^{-1}) for contaminant metals Al, Cr, Pb, V, Mn, As and Cu.

5.6 References

Abbaspour, A., Tanyu, B. and Cetin, B. 2016. Impact of aging on leaching characteristics of recycled concrete aggregate. **23**.

Berner, U.R. 1992. Evolution of pore water chemistry during degradation of cement in a radioactive waste repository environment. *Waste Management.* **12**(2), pp.201-219.

Bestgen, J.O., Cetin, B. and Tanyu, B.F. 2016. Effects of extraction methods and factors on leaching of metals from recycled concrete aggregates. *Environmental Science and Pollution Research.* **23**(13), pp.12983-13002.

Brantley, S.L., Kubicki, J.D. and White, A.F. 2008. Kinetics of mineral dissolution. *Kinetics of water-rock interaction.* New York: Springer Verlag.

Bray, A.W., Oelkers, E.H., Bonneville, S., Wolff-Boenisch, D., Potts, N.J., Fones, G. and Benning, L.G. 2015. The effect of pH, grain size, and organic ligands on biotite weathering rates. *Geochimica et Cosmochimica Acta.* **164**, pp.127-145.

Butera, S., Christensen, T.H. and Astrup, T.F. 2014. Composition and leaching of construction and demolition waste: Inorganic elements and organic compounds. *Journal of Hazardous Materials.* **276**, pp.302-311.

Butera, S., Hyks, J., Christensen, T.H. and Astrup, T.F. 2015. Construction and demolition waste: Comparison of standard up-flow column and down-flow lysimeter leaching tests. *Waste Management.* **43**, pp.386-397.

Chen, J., Tinjum, J.M. and Edil, T.B. 2013. Leaching of Alkaline Substances and Heavy Metals from Recycled Concrete Aggregate Used as Unbound Base Course. *Transportation Research Record.* **2349**(1), pp.81-90.

Chen, J., Bradshaw, S., Benson, C.H., Tinjum, J.M. and Edil, T.B. 2012. pH-Dependent Leaching of Trace Elements from Recycled Concrete Aggregate. *GeoCongress 2012.* pp.3729-3738.

Daiber, E. 2022. *Recycled Concrete Aggregate Leachate: A Literature Review.* Publication 22-03-003 ed. [Online]. Olympia: Washington State Department of Ecology. [Accessed 16/05/2023]. Available from: https://apps.ecology.wa.gov/publications/SummaryPages/2203003.html

Diamond, S. 2004. The microstructure of cement paste and concrete—a visual primer. *Cement and Concrete Composites.* **26**(8), pp.919-933.

Drinčić, A., Nikolić, I., Zuliani, T., Milačič, R. and Ščančar, J. 2017. Long-term environmental impacts of building composites containing waste materials: Evaluation of the leaching protocols. *Waste Management.* **59**, pp.340-349.

Eckbo, C., Okkenhaug, G. and Hale, S.E. 2022. The effects of soil organic matter on leaching of hexavalent chromium from concrete waste: Batch and column experiments. *Journal of Environmental Management.* **309**, p114708.

Ekström, T. 2001. *Leaching of concrete : experiments and modelling.* Lund University.

Engelsen, C.J., van der Sloot, H.A. and Petkovic, G. 2017. Long-term leaching from recycled concrete aggregates applied as sub-base material in road construction. *Science of The Total Environment.* **587-588**, pp.94-101.

Engelsen, C.J., van der Sloot, H.A., Wibetoe, G., Justnes, H., Lund, W. and Stoltenberg-Hansson, E. 2010. Leaching characterisation and geochemical modelling of minor and trace elements released from recycled concrete aggregates. *Cement and Concrete Research.* **40**(12), pp.1639-1649.

Engelsen, C.J., Wibetoe, G., van der Sloot, H.A., Lund, W. and Petkovic, G. 2012. Field site leaching from recycled concrete aggregates applied as sub-base material in road construction. *Science of The Total Environment.* **427-428**, pp.86-97.

Faucon, P., Adenot, F., Jacquinot, J.F., Petit, J.C., Cabrillac, R. and Jorda, M. 1998. Long-term behaviour of cement pastes used for nuclear waste disposal: review of physico-chemical mechanisms of water degradation. *Cement and Concrete Research.* **28**(6), pp.847-857.

Foy, J., Jones, G., Sephton, M. and Gaitonde, R. 2019. *Managing On-site Stockpiling and Use of High Volumes of Concrete-based Demolition Material.* Cumbria, UK: AECOM on behalf of the Nuclear Decommissioning Authority.

Frýbort, A., Štulířová, J. and Grošek, J.J.M.W.C. 2020. Complementary analyses of concrete characteristics performed on cores taken from concrete pavements. *MATEC Web of Conferences.* **310**, p00036.

Galvín, A.P., Agrela, F., Ayuso, J., Beltrán, M.G. and Barbudo, A. 2014. Leaching assessment of concrete made of recycled coarse aggregate: Physical and environmental characterisation of aggregates and hardened concrete. *Waste Management.* **34**(9), pp.1693-1704.

Garrabrants, A.C. and Kosson, D.S. 2004. *Leaching Processes and Evaluation Tests for Inorganic Constituent Release from Cement-Based Matrices.* Boca Raton: CRC Press.

Garrabrants, A.C., Sanchez, F. and Kosson, D.S. 2004. Changes in constituent equilibrium leaching and pore water characteristics of a Portland cement mortar as a result of carbonation. *Waste Management.* **24**(1), pp.19-36.

Georget, F., Wilson, W. and Scrivener, K.L. 2021. edxia: Microstructure characterisation from quantified SEM-EDS hypermaps. *Cement and Concrete Research.* **141**, p106327.

Gougar, M.L.D., Scheetz, B.E. and Roy, D.M. 1996. Ettringite and C-S-H Portland cement phases for waste ion immobilization: A review. *Waste Management.* **16**(4), pp.295-303.

GRR. 2018. *Management of Radioactive Waste from Decommissioning of Nuclear Sites: Guidance on Requirements for Release from Radioactive Substances Regulation Version 1.0.* [Online]. [Accessed 20/05/2023]. Available from: https://www.sepa.org.uk/media/365893/2018-07-17-grr-publication-v1-0.pdf

Halim, C.E., Amal, R., Beydoun, D., Scott, J.A. and Low, G. 2004. Implications of the structure of cementitious wastes containing Pb(II), Cd(II), As(V), and Cr(VI) on the leaching of metals. *Cement and Concrete Research.* **34**(7), pp.1093-1102.

Harris, A.W., Manning, M.C., Tearle, W.M. and Tweed, C.J. 2002. Testing of models of the dissolution of cements—leaching of synthetic CSH gels. *Cement and Concrete Research.* **32**(5), pp.731-746.

Hartwich, P. and Vollpracht, A. 2017. Influence of leachate composition on the leaching behaviour of concrete. *Cement and Concrete Research.* **100**, pp.423-434.

Hidalgo, A., Petit, S., Domingo, C., Alonso, C. and Andrade, C. 2007. Microstructural characterization of leaching effects in cement pastes due to neutralisation of their alkaline nature: Part I: Portland cement pastes. *Cement and Concrete Research.* **37**(1), pp.63-70.

L'Hôpital, E., Lothenbach, B., Scrivener, K. and Kulik, D.A. 2016. Alkali uptake in calcium alumina silicate hydrate (C-A-S-H). *Cement and Concrete Research.* **85**, pp.122-136.

Lagerblad, B. 2005. *Carbon dioxide uptake during concrete life cycle - State of the art.* [Online]. Stockholm, Sweden: Swedish Cement and Concrete Research Institute.

Langmuir, D. 1997. *Aqueous environmental geochemistry.* Upper Saddle River, N.J: Prentice Hall.

Leisinger, S.M., Bhatnagar, A., Lothenbach, B. and Johnson, C.A. 2014. Solubility of chromate in a hydrated OPC. *Applied Geochemistry.* **48**, pp.132-140.

Leisinger, S.M., Lothenbach, B., Le Saout, G., Kagi, H., Wehrli, B. and Johnson, C.A. 2010. Solid Solutions between CrO4- and SO4-Ettringite Ca-6(Al(OH)(6))(2)-(CrO4)(x)(SO4)(1-x) (3)*26 H2O. *Environmental Science & Technology.* **44**(23), pp.8983-8988.

Lopez Meza, S., Garrabrants, A.C., van der Sloot, H. and Kosson, D.S. 2008. Comparison of the release of constituents from granular materials under batch and column testing. *Waste Management.* **28**(10), pp.1853-1867.

Mahedi, M. and Cetin, B. 2020. Carbonation based leaching assessment of recycled concrete aggregates. *Chemosphere.* **250**, p126307.

Marty, N.C.M., Grangeon, S., Lerouge, C., Warmont, F., Rozenbaum, O., Conte, T. and Claret, F. 2017. Dissolution kinetics of hydrated calcium aluminates (AFm-Cl) as a function of pH and at room temperature. *Mineralogical Magazine.* **81**(5), pp.1245-1259.

Mulugeta, M., Engelsen, C.J., Wibetoe, G. and Lund, W. 2011. Charge-based fractionation of oxyanion-forming metals and metalloids leached from recycled concrete aggregates of different degrees of carbonation: A comparison of laboratory and field leaching tests. *Waste Management.* **31**(2), pp.253-258.

Natarajan, B.M., Kanavas, Z., Sanger, M., Rudolph, J., Ginder-Vogel, M., Edil, T., Chen, J. and Tuncer. 2019. *Characterization of Recycled Concrete Aggregate after Eight Years of Field Deployment.*

NDA. 2020. *Concrete example of dealing with decommissioning rubble.* [Online]. [Accessed 05/07/21]. Available from: https://www.gov.uk/government/case-studies/concrete-example-of-dealing-with-decommissioning-rubble

Ochs, M., Mallants, D. and Wang, L. 2015. Cementitious Materials and Their Sorption Properties. *Radionuclide and Metal Sorption on Cement and Concrete. Topics in Safety, Risk, Reliability and Quality.* [Online]. Springer, Cham.

Omotoso, O.E., Ivey, D.G. and Mikula, R. 1995. CHARACTERIZATION OF CHROMIUM-DOPED TRICALCIUM SILICATE USING SEM/EDS, XRD AND FTIR. *Journal of Hazardous Materials.* **42**(1), pp.87-102.

Poon, C.-S. and Chen, Z.Q. 1999. Comparison of the characteristics of flow-through and flow-around leaching tests of solidified heavy metal wastes. *Chemosphere.* **38**(3), pp.663-680.

Richardson, I.G. 1999. The nature of C-S-H in hardened cements. *Cement and Concrete Research.* **29**(8), pp.1131-1147.

Rossen, J.E. and Scrivener, K.L. 2017. Optimization of SEM-EDS to determine the C–A–S–H composition in matured cement paste samples. *Materials Characterization.* **123**, pp.294-306.

Sanger, M., Natarajan, B.M., Wang, B., Edil, T. and Ginder-Vogel, M. 2020. Recycled concrete aggregate in base course applications: Review of field and laboratory investigations of leachate pH. *J Hazard Mater.* **385**, p121562.

Šavija, B. and Luković, M. 2016. Carbonation of cement paste: Understanding, challenges, and opportunities. *Construction and Building Materials.* **117**, pp.285-301.

Schott, J., Pokrovsky, O.S. and Oelkers, E.H. 2009. 6. The Link Between Mineral Dissolution/Precipitation Kinetics and Solution Chemistry. In: Eric, H.O. and Jacques, S. eds. *Thermodynamics and Kinetics of Water-Rock Interaction.* Berlin, Boston: De Gruyter, pp.207-258.

Scrivener, K., Bazzoni, A., Mota, B. and Rossen, J.E. 2017. Electron Microscopy In: Scrivener, K., et al. eds. *A Practical Guide to Microstructural Analysis of Cementitious Materials.* [Online]. 1sts ed. Boca Raton: CRC Press. [Accessed 7/07/2023].

Shand, P., Edmunds, W.M., Lawrence, A.R., Smedley, P. and Burke, S. 2007. *The natural (baseline) quality of groundwater in England and Wales.* Environment Agency.

Smith, M.R. and Collis, L. 2001. 8. Aggregates for concrete. *Aggregates: Sand, gravel and crushed rock aggregates for construction purposes.* Geological Society of London, p.0.

Steffes, R. 1999. *Laboratory Study of the Leachate From Crushed Portland Cement Concrete Base Material.* Iowa: Iowa Department of Transportation.

Stumm, W. and Morgan, J.J. 1996. *Aquatic chemistry: chemical equilibria and rates in natural waters.* Third edition. ed. New York: Wiley.

Stutzman, P.E., Bullard, J.W. and Feng, P. 2015. *Quantitative Imaging of Clinker and Cement Microstructure.* National Institute of Standards and Technology.

Trapote-Barreira, A., Cama, J. and Soler, J.M. 2014. Dissolution kinetics of C-S-H gel: Flow-through experiments. **70**, pp.17-31.

van der Sloot, H.A. 2000. Comparison of the characteristic leaching behavior of cements using standard (EN 196-1) cement mortar and an assessment of their long-term environmental behavior in construction products during service life and recycling. *Cement and Concrete Research.* **30**(7), pp.1079-1096.

van der Sloot, H.A. 2002. Characterization of the leaching behaviour of concrete mortars and of cement–stabilized wastes with different waste loading for long term environmental assessment. *Waste Management.* **22**(2), pp.181-186.

van der Sloot, H.A. and Dijkstra, J.J. 2004. *Development of horizontally standardized leaching tests for construction materials: a material based or release based approach? Identical leaching mechanisms for different materials.* Energy Research Center of the Netherland.

Vollpracht, A. and Brameshuber, W. 2016. Binding and leaching of trace elements in Portland cement pastes. *Cement and Concrete Research.* **79**, pp.76-92.

Walker, C.S., Sutou, S., Oda, C., Mihara, M. and Honda, A. 2016. Calcium silicate hydrate (C-S-H) gel solubility data and a discrete solid phase model at 25 °C based on two binary non-ideal solid solutions. *Cement and Concrete Research.* **79**, pp.1-30.

Zhang, Y., Chen, J., Ginder-Vogel, M. and Edil, T. 2018. Effect of pH and Grain Size on the Leaching Mechanism of Elements from Recycled Concrete Aggregate. pp.325-334.

Chapter 6 Summary, implications and further work

6.1 Summary

The aim of this research was to establish the alkalinity generating potential and mechanisms controlling contaminant and constituent release from stockpiled crushed concrete wastes which have been weathered. This contribution to technical understanding of CCW leachate evolution is beneficial for the on-site reuse of CCW as void fill or backfill on UK nuclear sites. Research objectives 1 and 2 were answered in Chapter 4. The alkalinity generating potential (research objective 1) of gravel, sand and fines fractions of stockpiled CCW was determined in Chapter 4 through batch equilibrium experiments. In addition, batch equilibrium experiments determined the potential for release of major and trace elements with changes in pH and at the material pH (research objective 2). It was shown that metal leaching potential was generally similar between the surface (more weathered) and subsurface stockpiled CCW, with a slightly lower release of Cr, V and S in the surface samples. Along with the lower material pH (pH 8-9.6) of the surface material relative to the subsurface (pH 10-11.3), carbonation has had a positive effect on the production of high pH leachates and low metal leaching potential at pH values relevant to field conditions (pH 4-13). A positive effect of carbonation reducing leachate pH with decreasing size fraction was also found. This study was useful for approximating the composition of the leachate under continuously saturated and stagnant conditions where reactions may tend toward chemical equilibrium. In Chapter 5, research objectives 3 and 4 were answered using flow-through leaching experiments which investigated contaminant release mechanisms (research objective 3) and determined the dissolution kinetics of CCW (research objective 4). The flow-through experiments demonstrated the low metal leaching potential of CCW using the sand (0.6-6.3 mm) size fraction, which is relevant for scenarios of shallow below-ground voids. In this chapter, a summary of the major findings from the two data chapters are provided with reference to the research objectives stated in Chapter 1 and the implications of the research are discussed, along with a discussion of future work that may extend this study. This has useful implications for the reuse of CCW as backfill or void fill in underground voids on nuclear sites undergoing decommissioning.

6.2 Major findings and implications

CCW will form a significant portion of decommissioning wastes produced in the coming decades, requiring a sustainable management approach in line with the waste

hierarchy that avoids unnecessary disposal to landfill. As such, research on the leaching behaviour of CCW under conditions relevant to field conditions is essential to support this process. The results presented in this thesis are the first studies to use CCW obtained from a nuclear site that have been stockpiled over the long-term (10 to >20 years). This thesis presents the composition of CCW derived from a representative UK nuclear site along with a characterisation of leaching behaviour with results relevant to safety assessments for the in-situ disposal of crushed concrete as void fill. Previous laboratory studies on CCW have used crushed material in laboratory tests which produce an overestimation of contaminant release and therefore unrealistic conditions expected in the field. This may limit reuse as void fill by being overly conservative. Therefore, this study did not crush any samples for the leaching experiments and thus provided more realistic results relevant to safety assessments.

All four research objectives were answered in this thesis, and the summary of the results are presented in line with each individual objective. The research objectives from Chapter 1 are repeated below, with the chapter number in brackets to indicate where the objective was answered:

1. Determine the alkalinity generating potential of stockpiled crushed concrete wastes from a representative UK nuclear site as a function of size fraction and weathering after long-term stockpiling (Chapter 4)
2. Determine the potential for release of major elements and trace contaminants from stockpiled crushed concrete wastes as a function of pH and size fraction under batch equilibrium conditions (Chapter 4)
3. Investigate the release mechanisms of major elements and trace contaminants from stockpiled CCW under far-from-equilibrium conditions (Chapter 5)
4. Determine the short-term dissolution kinetics of CCW as a function of pH under far-from-equilibrium conditions (Chapter 5)

Research objective 1 was answered in Chapter 4. CCW was first characterised to understand the material composition responsible for the alkalinity generating potential. This was necessary to determine the effect of weathering from long-term stockpiling on leachate pH. Using XRD, XRF and SEM, the composition of the sand size fraction (0.6-6.3 mm) of CCW was found to be dominated by silica and calcite grains in a matrix of C-(A)-S-H phases with average Ca/Si ratios (defined using a boundary threshold minimum as described in Chapter 3 Section 3.2.4.1 to exclude cement clinker phases still present and intermixed phases) of 0.5 ± 0.3 in the surface samples and 0.9 ± 0.3 in

the subsurface samples. Phases similar to Hc/Mc, AFm and jennite were also present (Chapter 4.4 Figure 4.4) and no portlandite was detected by XRD in any of the surface or subsurface samples and was therefore presumed leached out during the period of stockpiling. AFt was present in subsurface samples but not surface samples and thus was also presumed leached out and weathered. In CCW the most reactive (least inert) fraction is the cement paste, which is dominated by C-(A)-S-H phases. Weathering occurring after stockpiling occurred most strongly in CCW from the stockpile surface (0-0.1m), resulting in decalcified C-(A)-S-H phases, increased calcite content and lower leachate pH. In terms of size fraction, it was found that CCW from the surface of the stockpiles had a lower material pH leachate (pH 8-9.6) relative to CCW from the subsurface (pH 10-11.3) (Chapter 4 Table 4.3 Section 4.3.2), attributed to carbonation and weathering. This supports long-term stockpiling to reduce concerns over high pH leachate generation. Although, no substantial difference in ANC was observed between the two samples. Furthermore, a positive effect of carbonation was also identified with particle size, with the lowest pH values associated with decreasing particle size (Chapter 4 Table 4.3 Section 4.3.2), an effect also found in other studies (Chen, J. et al., 2012; Zhang, Y. et al., 2018; Natarajan et al., 2019). This is due to carbonation that occurred on a higher number of reactive surfaces on the fine particles during stockpiling (Chen, J. et al., 2012; Zhang, Y. et al., 2018; Natarajan et al., 2019).

Research objective 2 was answered in Chapter 4. The release potential of major elements and trace contaminants was determined in batch equilibrium experiments using gravel, sand and fines fractions of stockpiled CCW. It was found that there was generally no difference between the size fractions in terms of contaminant release, especially at material pH. However, there were two minor exceptions as pH was altered outside the material pH range, with higher Cu leaching from the surface finer fractions above pH 11 only, and the larger gravel fraction exhibited the most scatter across most pH values for all trace elements. Generally, this conclusion of no clear particle size effect is similar to Bestgen et al. (2016) who instead suggested the material composition was more important. This is especially relevant at the material pH and within the range of expected pH conditions in the field, as leachate composition will depend on the material composition. The general similarities in leaching behaviour with variation in pH in the batch tests indicate that leaching may be under equilibrium control. The pH-dependent leaching patterns generally indicate the lowest levels of leaching at the material pH and provide information on leaching across the pH range relevant for field conditions (i.e. slightly acidic, neutral and slightly alkaline pH). As the

fines fraction had the lowest pH, they may even be suitable for reuse in as fine aggregate in cement grouts (Foy et al., 2019). Usually, concern is on the finer fraction of CCWs in relation to reuse because of the reported enhanced contaminant release as a function of increased surface area (e.g. Molla et al. (2021) recommends disposal of fines (<4.75 mm) to landfill), however this effect was not observed in the batch equilibrium experiments.

Whilst carbonation and weathering has been shown to produce lower pH leachates (and therefore a lower alkalinity generating potential; objective 1), studies have found increased solubility of oxyanion-forming elements in carbonated cement leachates (e.g. Mulugeta et al. (2011)) or cement leachates in line with the pH range (neutral to mildly alkaline) of carbonated cements (e.g. van der Sloot (2000; 2002)). However, this was not observed when comparing the surface and subsurface samples. Instead, a slightly greater concentration of Cr, V and S was observed in the subsurface samples which have a higher material pH than the surface samples (Chapter 4 Table 4.4 Section 4.3.3), suggesting a low metal leaching potential for carbonated CCW (research objective 2). As the surface samples will only form a minor proportion of the total CCW available for disposal, the subsurface samples were used for the flow-through experiments as they are representative of the bulk of material available for on-site disposal.

Research objectives 3 and 4 were achieved in Chapter 5 using flow-through experiments to study leaching from long-term stockpiled CCW under far-from-equilibrium conditions as a function of pH and to provide technical information on leaching behaviour and dissolution kinetics. Research objective 3 was achieved by investigating the release behaviour of major elements and trace contaminants from the sand-sized fraction (0.6-6.3 mm) of CCW obtained from the subsurface of the stockpile. The dissolution of CCW proceeds slowly, with the highest rates attributed to Ca which originated from the rapid dissolution of carbonates and incongruent leaching of C-(A)-S-H phases. Si and Al leaching was lower than Ca and typically did not preferentially leach. The leaching of Mg, Fe and Mn was pH-dependent and solubility-controlled but pH-independent for trace elements Cr, V, Pb, As, K and Zn. All elements had the highest leaching at acidic pH, but release was relatively low across pH 4-13, which is relevant for field conditions. The leaching of trace elements was mass transport controlled and availability-limited. Cu was not detected in any flow-through leachates however it was leached in the batch experiments, indicating Cu leaching may only

leach under slow-flow conditions that tend toward equilibrium, rather than at far-from-equilibrium conditions.

Research objective 4 was achieved through the calculation of the dissolution kinetics of CCW by different pH leachants under far-from-equilibrium conditions. The flow-through experiments showed that under pseudo-steady state conditions, trace element leaching was below detection or low ($<1 \times 10^{-10}$ mol m^{-2} s^{-1}) across all pH values for contaminant metals Al, Cr, Pb, V, Mn, As and Cu. In the field, the leaching rates will also be lower as the experiments used stirrer bars which increase reaction rates. From this study it is concluded that CCW leachates are benign due to slow dissolution kinetics, especially in the pH ranges relevant to field conditions. This information is valuable for understanding leaching under continuously saturated conditions and is relevant to the disposal of CCW in unlined shallow voids where high water infiltration rates (surface water and/or groundwater) are expected. Overall, it may be concluded that the CCW leachate produced by the batch and flow-through experiments may be regarded as benign and suitable for reuse in the field.

As all four objectives have been addressed, the aim of this thesis – to contribute to the technical understanding of the evolution in CCW leachate composition – has been achieved, and the findings have value in on-site reuse of CCW as void fill or backfill on UK nuclear sites. The major findings from the leaching experiments are beneficial for determining what site designs (e.g. Figure 2.2 (GRR, 2018) in Chapter 2 Section 2.1) may be suitable when using CCW either as backfill in lined subsurface structures (e.g. repositories) or in unlined shallow voids. If designs preventing free water flow are used, the leachate may resemble that observed in the batch leaching studies (Chapter 4) if groundwater leaching rates remain low, allowing leaching to be under equilibrium control rather than mass transport control.

The results of this study on CCW leaching behaviour and mechanisms of contaminant release have implications in the site design options for on-site reuse of CCW as backfill or void fill. When using CCW on-site in lined structures, the site design options may vary between reducing water flow (by blocking up existing penetrations and/or grouting void space) or encouraging free water flow through existing penetrations (or creating new ones). When restricting water flow, any leachate would be likely be small and resemble that obtained from the subsurface fractions during the batch tests, where leaching was likely under equilibrium control. If grout is used to reduce pore volume space, this could lead to high pH leachates (>13) and high contaminant metal (Al, Cr, V, Pb, Cu) concentrations if leaching is under equilibrium control. Moreover, at material

pH (10-11.3) and near-neutral pH, the subsurface CCW leachate had trace elements (Cr, V, Pb, S, Cu) above the EQS-AA, but they were generally still below the DWS. As a small volume of leachate would likely be produced under this scenario, it would be diluted when mixing with surface or ground waters. In addition, neutralisation and attenuation processes would occur and these could be investigated later in future work. Therefore, the leachate could still be regarded as benign when factoring in these environmental processes.

If site designs utilise free flow of water then the flowing water will disperse contaminants to insignificantly low concentrations, prevent build-up and immediately dilute CCW leachates. This is also relevant to direct disposal of CCW into unlined voids. Under this scenario, the leachate may resemble the leachate in the flow-through leaching experiments, the results of which suggest that it may not be necessary to restrict groundwater ingress so that designs can take advantage of the slow dissolution kinetics and generally low metal leaching potential of CCW (Chapter 5).

Under either scenario (unlined void fill or backfilling lined subsurface structures), the leachate produced will most likely be neutralized, attenuated and diluted (Gupta et al., 2018). Although these environmental processes occurring in the field were not the subject of this study, future work should identify these processes relevant to the subsurface soil environment specific to in-situ disposal environment as studies have found that CCW leachates can be neutralised and attenuated in the field by soil acidity, organic matter content and clay content of soils (Gupta et al., 2018; Chen, J. et al., 2019; Oliveira, F.D. et al., 2020).

6.3 Further work

This study used short-term leaching experiments to characterise the release behaviour of selected contaminants. Firstly, this work may be extended using flow-through experiments incorporating intermittent wetting periods, as intermittent leaching is common in field conditions (Sanchez et al., 2002). Flow-through reactors could be drained, the material allowed to dry for a specified period of time and then the experiments repeated. The effects of carbonation during the longer-term leaching periods could be incorporated into work under oxic and anoxic conditions or accelerated carbonation. Anoxic conditions would represent conditions within larger/deeper backfilled subsurface soils and would be relevant to characterising the evolution of leachates. Moreover, an extended range of inorganic and organic contaminants that could be present in CCW leachates (discussed in Chapter 2

Literature review) could be included in future leaching studies, as CCW is naturally heterogeneous. Real groundwater leachates could also be used for site specific studies to determine contaminant leaching relevant to a particular site. Geochemical speciation modelling could be used to identify phases controlling leaching at equilibrium (like in Engelsen et al. (2009; 2010)).

This work may be extended through the characterisation of CCW leachate interactions in the surrounding subsurface soil environment relevant to the in-situ disposal site of interest. Future work could characterise the nature of the neutralisation and attenuation processes through reacting real CCW leachates (obtained from batch, column or flow-through leaching experiments) with representative soil samples. It would also be beneficial to use radioactively contaminated material that is likely to be present in larger subsurface structures and defining the interaction of contaminated leachates with the CCW backfill material in larger backfilled structures.

6.4 References

Bestgen, J.O., Cetin, B. and Tanyu, B.F. 2016. Effects of extraction methods and factors on leaching of metals from recycled concrete aggregates. *Environmental Science and Pollution Research.* **23**(13), pp.12983-13002.

Chen, J., Sanger, M., Ritchey, R., Edil, T. and Ginder-Vogel, M. 2019. Neutralization of High pH and Alkalinity Effluent from Recycled Concrete Aggregate (RCA) by Common Subgrade Soil. *Journal of Environmental Quality.*

Chen, J.C., Bradshaw, S., Benson, C.H., Tinjum, J.M. and Edil, T.B. 2012. pH-Dependent Leaching of Trace Elements from Recycled Concrete Aggregate. *GeoCongress 2012.* pp.3729-3738.

Engelsen, C.J., van der Sloot, H.A., Wibetoe, G., Justnes, H., Lund, W. and Stoltenberg-Hansson, E. 2010. Leaching characterisation and geochemical modelling of minor and trace elements released from recycled concrete aggregates. *Cement and Concrete Research.* **40**(12), pp.1639-1649.

Engelsen, C.J., van der Sloot, H.A., Wibetoe, G., Petkovic, G., Stoltenberg-Hansson, E. and Lund, W. 2009. Release of major elements from recycled concrete aggregates and geochemical modelling. *Cement and Concrete Research.* **39**(5), pp.446-459.

Foy, J., Jones, G., Sephton, M. and Gaitonde, R. 2019. *Managing On-site Stockpiling and Use of High Volumes of Concrete-based Demolition Material.* Cumbria, UK: AECOM on behalf of the Nuclear Decommissioning Authority.

GRR. 2018. *Management of Radioactive Waste from Decommissioning of Nuclear Sites: Guidance on Requirements for Release from Radioactive Substances Regulation Version 1.0.* [Online]. [Accessed 20/05/2023]. Available from: https://www.sepa.org.uk/media/365893/2018-07-17-grr-publication-v1-0.pdf

Gupta, N., Kluge, M., Chadik, P.A. and Townsend, T.G. 2018. Recycled concrete aggregate as road base: Leaching constituents and neutralization by soil Interactions and dilution. *Waste Management.* **72**, pp.354-361.

Molla, A.S., Tang, P., Sher, W. and Bekele, D.N. 2021. Chemicals of concern in construction and demolition waste fine residues: A systematic literature review. *Journal of Environmental Management.* **299**, p113654.

Mulugeta, M., Engelsen, C.J., Wibetoe, G. and Lund, W. 2011. Charge-based fractionation of oxyanion-forming metals and metalloids leached from recycled concrete aggregates of different degrees of carbonation: A comparison of laboratory and field leaching tests. *Waste Management.* **31**(2), pp.253-258.

Natarajan, B.M., Kanavas, Z., Sanger, M., Rudolph, J., Ginder-Vogel, M., Edil, T., Chen, J. and Tuncer. 2019. *Characterization of Recycled Concrete Aggregate after Eight Years of Field Deployment.*

Oliveira, F.D., Gupta, N., Kluge, M., Finizio, C.M., Spreadbury, C.J., Chadik, P., Laux, S.J. and Townsend, T.G. 2020. pH attenuation by soils underlying recycled concrete aggregate road base. *Resources, Conservation and Recycling.* **161**, p104987.

Sanchez, F., Gervais, C., Garrabrants, A.C., Barna, R. and Kosson, D.S. 2002. Leaching of inorganic contaminants from cement-based waste materials as a result of carbonation during intermittent wetting. *Waste Management.* **22**(2), pp.249-260.

van der Sloot, H.A. 2000. Comparison of the characteristic leaching behavior of cements using standard (EN 196-1) cement mortar and an assessment of their long-term environmental behavior in construction products during service life and recycling. *Cement and Concrete Research.* **30**(7), pp.1079-1096.

van der Sloot, H.A. 2002. Characterization of the leaching behaviour of concrete mortars and of cement–stabilized wastes with different waste loading for long term environmental assessment. *Waste Management.* **22**(2), pp.181-186.

Zhang, Y., Chen, J., Ginder-Vogel, M. and Edil, T. 2018. Effect of pH and Grain Size on the Leaching Mechanism of Elements from Recycled Concrete Aggregate. pp.325-334.

Appendix

The LOD and Uncertainty (%) of the ICP-OES and ICP-MS measurements presented in Chapters 4 and 5 are presented in Section A and Section B respectively. The uncertainty was calculated at the 95% confidence interval of 6 replicate sample measurements and is related to the mean as a percentage.

Section A LOD for batch experiments in Chapter 4

Table A1 LOD for elements Al, Ca, Fe, Mg, S and Si measured by ICP-OES for gravel, sand and fines fractions sample runs. As a dilution of 1:10 was used (1 mL sample in a matrix of 9mL 2% nitric acid), the data presented are corrected (multiplied by 10) to account for this. This is so that the LOD relevant to the elemental concentrations presented in Table 4.4 (in mg L^{-1}) and Figures 4.6-4.9 (in mg/kg) can be easily compared.

	mg L^{-1}					
	Al	**Ca**	**Fe**	**Mg**	**S**	**Si**
Gravel	0.20	1.71	0.08	0.08	0.17	0.36
Sand	0.39	4.99	0.17	0.19	0.15	0.16
Fines	0.44	1.50	0.14	0.38	0.13	0.83

The uncertainty (%) at the 95% confidence interval was between 3 and 6% for all major elements across the size fractions.

Table A2 LOD for elements Cr, Pb, V, Cu, Mn (measured by ICP-MS) and Cl- (measured by ion chromatography) in all sample batches with dilution factor applied as explained in Table A1.

µg L^{-1}					**ppb**
V	**Cr**	**Pb**	**Cu**	**Mn**	**Cl**
0.116	0.153	0.252	0.89	2.9	100

Uncertainty at the 95% confidence interval was 1-3% for V, Cr, Pb, Cu and Mn measured using ICP-MS.

Section B LOD for flow-through experiments in Chapter 5

Table B1 LOD for major elements (ICP-OES) from three separate sample runs.

	mg L^{-1}					
	Al	**Ca**	**K**	**Mg**	**S**	**Si**
DIW	0.001	0.002	0.017	0.001	0.014	0.016
Bulk	0.010	0.017	0.029	0.001	0.034	0.011
$HOAc_{(1+2)}$	0.009	0.011	0.059	0.002	0.054	0.007

Table B2 LOD for trace elements (ICP-MS) from three separate sample runs.

	µg L^{-1}							
	As	**Cu**	**Cr**	**Fe**	**Mn**	**Pb**	**V**	**Zn**
DIW	0.003	0.0018	0.0021	0.0286	0.0052	0.0103	0.0008	0.059
Bulk*	0.1177	0.0276	0.0106	0.1998	0.0151	0.0265	0.0022	0.265
$HOAc_{(1+2)}$	0.0079	0.0047	0.0022	0.0419	0.0106	0.0012	0.0045	0.0159

*Bulk includes all acid (0.5-5 mM HCl, and one HOAc replicate) and alkaline (1-100 mM NaOH) leachants. $HOAc_{(1+2)}$ includes two replicates.

Uncertainty at 95% confidence interval (%)

DIW uncertainty was between 1 and 8% for major elements and between 1 and 4% for trace elements. Bulk uncertainty was between 1 and 5% for major elements and between 2 and 4% for trace elements. HOAc uncertainty was between 1 and 2% for major elements and between 0.5 and 1% for trace elements

Section C Additional data for Table 5.3 in Chapter 5

Table C1 Full list of mass loss (%) and surface area (m^2/g) data for all experiments in Chapter 5. The replicate number is in brackets. DIW1 for surface area is missing as the sample was lost. Data for 5 mM HCl (replicate 1) is excluded due to an operational problem with the oven for that individual sample.

Sample leachant (replicate number)	Mass loss (%)	BET surface area (m^2/g)
DIW (1)	14	
DIW (2)	11	5.1
DIW (3)	15	6.1
0.5 mM HCl (1)	9	6.3
0.5 mM HCl (2)	10	5.2
0.5 mM HCl (3)	10	5.8
1 mM HCl (1)	13	6.6
1 mM HCl (2)	12	7.1
1 mM HCl (3)	13	4.7
1 mM HOAc (1)	12	7.9
1 mM HOAc (2)	12	5.5
1 mM HOAc (3)	9	6.9
2 mM HCl (1)	14	5.6
2 mM HCl (2)	12	7.9
3 mM HCl (1)	12	5.7
3 mM HCl (2)	8	5.9
3 mM HCl (3)	14	6.1
5 mM HCl (2)	12	6.2
100 mM NaOH (1)	10	5.9
100 mM NaOH (2)	6	6.1
100 mM NaOH (3)	8	4.4
10 mM NaOH (1)	10	4.7
10 mM NaOH (2)	7	7.0
10 mM NaOH (3)	10	4.8
1 mM NaOH (1)	9	6.4
1 mM NaOH (2)	6	6.6
Unleached (1)		8.2
Unleached (2)		7.6
Unleached (3)		7.6